P-04-312

Forsmark site investigation

Rock stress measurements with hydraulic fracturing and hydraulic testing of pre-existing fractures in borehole KFM01A, KFM01B, KFM02A and KFM04A

Laboratory Core Investigations

F Rummel, U Weber
MeSy GmbH Bochum

Svensk Kärnbränslehantering AB
Swedish Nuclear Fuel
and Waste Management Co
Box 5864
SE-102 40 Stockholm Sweden
Tel 08-459 84 00
+46 8 459 84 00
Fax 08-661 57 19
+46 8 661 57 19

ISSN 1651-4416
SKB P-04-312

Forsmark site investigation

Rock stress measurements with hydraulic fracturing and hydraulic testing of pre-existing fractures in borehole KFM01A, KFM01B, KFM02A and KFM04A

Laboratory Core Investigations

F Rummel, U Weber
MeSy GmbH Bochum

November 2004

Keywords: Density, Ultrasonic velocities, Dynamic elasticity parameters, Hydraulic tensile strength, Hydrofrac coefficient, Hydrofrac simulation calculations, AP PF 400-04-023.

This report concerns a study which was conducted for SKB. The conclusions and viewpoints presented in the report are those of the authors and do not necessarily coincide with those of the client.

A pdf version of this document can be downloaded from www.skb.se

Abstract

In April/May 2004 a total of 85 hydraulic fracturing/hydraulic tests on pre-existing fractures were conducted in 4 boreholes, KFM01A, KFM01B, KFM02A and KFM04A, to a depth of almost 1,000 m at the Forsmark test site. The results of these in-situ tests are presented in the MeSy Final Report No 28.04A (SKB P-04-311). During in-situ testing approximately 12 m of core material of the drillholes were selected for laboratory testing at MeSy Bochum. The core material consisted of 36 core pieces of approximately 34 cm length and 50 mm diameter each. The laboratory test program consisted of rock density determination (buoyancy method in water, geometric density method on dry samples), ultrasonic tests to measure ultrasonic P- and S-velocities and to derive dynamic elasticity parameters (Young's modulus E, Poisson's ratio ν), fracture toughness tests by the 3-point bending method on Chevron-notched samples to determine the fracture toughness K_{IC} for fracture mechanics analysis of hydrofrac tests, and of hydrofrac tests on samples with axial injection holes, subjected to confining pressures to simulate in-situ stress conditions. Density and ultrasonic tests primarily served for rock characterization (homogeneity, isotropy), fracture toughness and the hydrofrac tests on cores were used to characterize the effect of the rock microfractures on hydraulic fracturing in-situ tests, and to conduct fracture mechanics hydrofrac simulation calculations as a quality control of the in-situ hydraulic fracturing records.

This report describes the testing methods used (Chapter 3), the core material selected and the test sample preparation (Chapter 4), and the test results obtained (Chapter 5). Finally, we present the fracture mechanics analysis with the physical interpretation of hydraulic fracturing tensile strength and hydrofrac simulation plots for comparison with in-situ observed hydrofrac records.

A total of 12 hydrofrac simulation calculations were conducted for 12 test sections in the 4 boreholes, using the experimental parameters of the in-situ tests (borehole radius, test depth, injection rate, system stiffness), stress and permeability data derived from the in-situ tests, and rock physical properties determined during laboratory testing. Uncertain input variables like initial microcrack size, fracture width, or the fluid pressure gradient within the activated fractures had to be varied within acceptable limits to match both the breakdown pressure value as well as the pumping pressure during the initial fracturing cycle of the in-situ tests. Therefore, the simulation may be regarded as a quality control of the results of in-situ testing.

Sammanfattning

Under våren 2004 utfördes totalt 85 hydrauliska in-situ tester, dels hydraulisk spräckning och dels hydrauliska tester av existerande sprickor (HTPF), i borrhålen KFM01A, KFM01B, KFM02A och KFM04A. Resultaten av utförda in-situ tester redovisas i rapport SKB P-04-311.

Utöver in-situ testerna utfördes laboratorietester på borrkärnor. Sammanlagt togs ca 12 meter borrkärna (36 stycken prover á 34 cm med en diameter på 50 mm) från de fyra borrhålen. Laboratorietesterna utfördes vid Mesy's laboratorium i Bochum, Tyskland. Denna rapport redovisar resultaten av utförda laboratorietester.

Följande tester utfördes; densitet (vägning av provet i luft respektive under vatten), densitet (beräkning med hänsyn till provets uppmätta volym), ultraljudtester (för mätning av hastigheten på skjuvvåg och kompressionsvåg för beräkning av dynamiska värden på elasticitetsmodul och Poissons tal), trepunkts böjtest (för att mäta brottseghet, KIC) samt hydraulisk spräckning i axiella hål i borrkärnorna för olika omgivande tryck för att härigenom simulera in-situ spänningar.

Densitets- och ultraljudtesterna utfördes primärt för att karaktärisera berget (homogenitet och isotropi). Mätning av brottseghet och hydrauliska spräckningar av borrkärnorna utfördes dels för att karaktärisera effekten av mikrosprickor vid in-situ testerna och dels för att använda resultaten som indata i brottmekaniska simuleringar av hydraulisk spräckning som en kvalitetskontroll av in-situ testerna.

Denna rapport är indelad i följande kapitel och innehåll; kapitel 3 (beskrivning av laboratorietesterna), kapitel 4 (beskrivning av borrkärnornas egenskaper och deras beredning före laboratorietesterna), kapitel 5 (resultaten från laboratorietesterna) samt kapitel 6 (jämförelse mellan sprickmekaniska analyser och in-situ tester).

Brottmekaniska simuleringar av spräckningar inom tolv av de aktuella borrhålssektionerna har utförts. Indata till simuleringarna har utgjorts av: primärdata från in-situ testerna (borrhålsradie, testdjup, injektionsflöde och systemets styvhet), analysresultat från in-situ testerna (bergsspänningar och permeabilitet) samt bergparametrar från laboratorietesterna.

Vissa erforderliga, men ej mätbara, indata till den brottmekaniska analysen, såsom storleken på mikrosprickor, sprickvidd och tryckgradienten i sprickan, har varierats inom rimliga gränser för att erhålla en god passning mellan simulerade och uppmätta spräck- och injektionstryck.

De brottmekaniska simuleringarna anses vara en kvalitetskontroll av de genomförda in-situ testerna.

Contents

1 Introduction

This document reports results gained by hydrofrac related laboratory tests on the core material of the boreholes KFM01A+B, KFM02A and KFM04A which were drilled within the site investigation program at Forsmark. The work was carried out in accordance with the activity plan AP-PF 400-04-023. In Table 1-1 controlling documents for performing this activity are listed. Both activity plan and method descriptions are SKB's internal controlling documents.

Table 1-1. Controlling documents for performance of the activity.

Activity plan	Number	Version
	AP PF 400 04 023	1.0
Method descriptions	**Number**	**Version**
	SKB MD 600.004e	1.0 (relevant only for the in-situ tests)
	SKB MD 620.010e	1.0 (relevant only for the in-situ tests)
	SKB MD 182.003e	1.0 (relevant only for the in-situ tests)

- The laboratory tests on the core material of the 4 boreholes were conducted to contribute to the interpretation of the in-situ results of the hydraulic fracturing and hydraulic injection tests in the 4 boreholes at Forsmark carried out during 27.04 to 21.05.2004. The test program consisted of detailed density measurements on both the core pieces and on samples prepared for further testing of ultrasonic velocity measurements to determine rock dynamic elasticity parameters, fracture toughness tests by the 3-point loading method on Chevron-notched samples, and of hydraulic fracturing tests on samples subjected to confining pressures up to 30 MPa. The core material was selected by the MeSy staff in collaboration with SKB personnel during the in-situ test work, was brought back to MeSy Bochum together with the in-situ tests equipment on 23.05.2004, was prepared for testing during June 2004, and was tested at MeSy Bochum during July/August 2004.
- The results of the in-situ hydraulic fracturing and hydraulic injections tests on "pre-existing" fractures are presented in the Final MeSy Report No 28.04 A. All 4 core-drilled boreholes are located at the Forsmark investigation site. Three of the boreholes (KFM01A/02A/04A) had a drill length of approximately 1,000 m, borehole KFM01B a length of approximately 500 m. All four boreholes penetrate an essentially homogeneous granitic rock. The core pieces selected had a diameter of 50 mm.
- The laboratory tests were conducted in close agreement with existing ISRM standards or with published references given in Table 1-2. Reference is also given to the hydrofrac model used to apply the results of laboratory tests to in-situ hydrofrac tests.

Table 1-2. Data references.

Subactivity	Standards	Reference
Ultrasonic tests	ISRM No 4	/Rummel and van Heerden, 1978/ Int.J. Rock Mech, 15, 53–58
Fracture toughness tests	ISRM	/Ouchterlony et al. 1988/ Int. J. Rock Mech, 25, 71–96, 1988
Laboratory hydrofrac tests	–	/Rummel, 1987/ Fracture Mech. of Rock (Atkinson editor), Academic Press Geol. Ser, 6, 217–239
Hydrofrac modelling	–	/Rummel and Hansen, 1989/ Int. J. Rock Mech, 26, 661–671

2 Objective and scope

Apparently, both overcoring stress measurements and observed core discing have suggested the existence of anomalous high horizontal stresses for the Forsmark area. Therefore, the Forsmark Site Investigation program has included a comprehensive in-situ hydraulic fracturing and hydraulic test program on pre-existing fractures in 4 deep boreholes to determine constraints on the horizontal stress regime (AP PF 400-04-023, Section 2). In order to support the results derived from the in-situ tests, in particular from the hydraulic fracturing tests, core material from the boreholes was selected (AP PF 400-04-023, Section 4.2) for laboratory tests relevant to hydraulic fracturing.

The laboratory tests should provide data on the tensile strength of the rock on the laboratory scale, on the dependence of breakdown pressure upon confining pressure (frac coefficient), and data for numerical simulation calculation to generate hydrofrac records for comparison with observed in-situ hydrofrac pressure records. The laboratory tensile strength p_{co} will be compared with the in-situ tensile strength $P_{co} = P_c - P_r$ using a fracture mechanics scaling relation, which also allows to determine the intrinsic crack size of both the in-situ rock and the laboratory samples. The simulation calculation by the MeSy code FRAC requires physical property data as input, such as density, porosity, permeability, elasticity and fracture mechanics properties.

3 Equipment and methodology

3.1 Density measurements

Density measurements were carried out by the buoyancy method in water (core pieces), and by the buoyancy method and determination of sample volume and weight (core samples). The experimental set-up for the buoyancy method density determination is shown in Figure 3-1. The density is determined by the relation

$$\rho = \frac{m_{air}}{m_{air} - m_{fluid} - m_{syst}} \cdot \rho_{fluid}$$

where m_{air} and m_{fluid} are the sample mass in air and water, m_{syst} is the system buoyancy mass, and ρ_{fluid} is the water density (1 g/cm^3). The geometric density determination consisted of mass, diameter and length measurements of samples with flat endplanes. The weight measurements are conducted with electronic balances of 0.4 kg/4 kg range and 0.01/0.1 g accuracy, type OHAUS. Diameter and length were measured with a sliding caliper. In this case the sample density is given by the relation

$$\rho = \frac{m_{air}}{r^2 \cdot \pi \cdot h}$$

where r is the sample radius and h is the sample height.

Figure 3-1. *Experimental set-up for density measurements by the buoyancy method.*

3.2 Ultrasonic velocities and elasticity parameter testing

The ultrasonic tests were conducted in close agreement with the ISRM standard no 4, (1978). The ultrasonic apparatus is shown schematically in Figure 3-2 and in photo by Figure 3-3. The transmitter signal is a 1 MHz pulse with an amplitude of 40 Volts. The transmitter/receiver are of type Krautkrämer B1s. The measurements were conducted by axial pulse transmission on samples with flat parallel endplanes. The seismograms were recorded on a 4-channel digital oscilloscope via the MeSy data acquisition system Seismo.

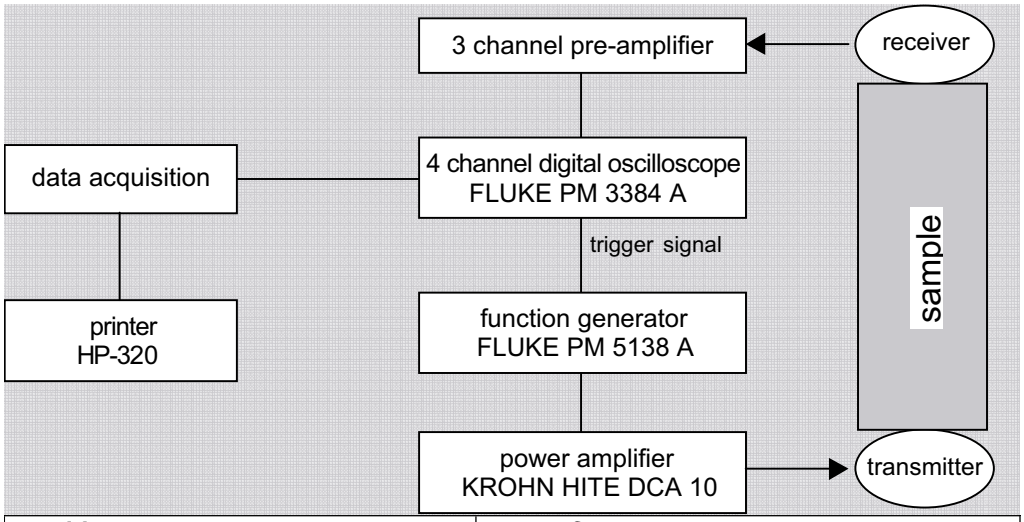

position	manufacturer
transmitter / receiver	Krautkrämer / B1s, 1 MHz
4 - channel digital oscilloscope	FLUKE TYP PM 3384 A
function generator	FLUKE TYP PM 5138 A
3 - channel pre-amplifier	MeSy Geo-Meßsysteme
power amplifier	KRHOHN HITE TYP DCA 10
data acquisition	PC-486-100-8 with program SEISMO

Figure 3-2. *Schematic of ultrasonic testing.*

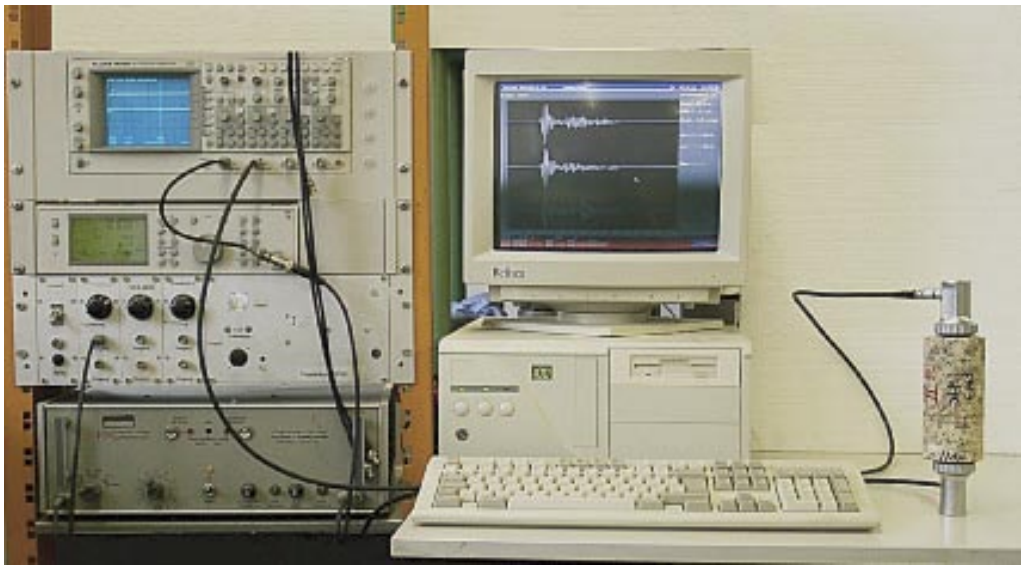

Figure 3-3. *Experimental set-up for ultrasonic velocity testing.*

The onset of P- and S-wave arrivals were marked on the seismograms manually, and the dynamic elastic parameters Young's modulus E and Poisson's ratio ν were calculated from the P- and S-wave velocities by the relations

$$E = 2v_s^{\,2}\rho\left(1+\nu\right)$$

$$\nu = \frac{1}{2}\cdot\frac{2-\left(v_p/v_s\right)^2}{1-\left(v_p/v_s\right)^2}$$

The standard deviation of the velocity determination is approximately

$$\frac{\Delta v_p}{v_p} = 1\%\ for\ P-wave\ velocity$$

$$\frac{\Delta v_s}{v_s} = 5\%\ for\ \ S-wave\ velocity$$

Position	Manufacturer
Transmitter/receiver	Krautkrämer/B1s, 1 MHz
4 – channel digital oscilloscope	FLUKE TYP PM 3384 A
Function generator	FLUKE TYP PM 5138 A
3 – channel pre-amplifier	MeSy Geo-Meßsysteme
Power amplifier	KRHOHN HITE TYP DCA 10
Data acquisition	PC-486-100-8 with program SEISMO

3.3 Fracture toughness testing

Fracture toughness K_{IC} was measured by the three-point-bending method of cylindrical core samples of approximately 50 mm diameter and approximately 150 mm test length, containing a Chevron notch of approximately 8 mm depth and 1 mm width, in close accordance with the ISRM standard, (1988). The test set-up is shown schematically in Figure 3-4 and in photo in Figure 3-5. The Chevron notch was made by diamond sawing with water as cooling agent. The bending load was measured with a load cell type Burster of 5 kN range. The piston displacement was measured with a displacement transducer type Burster of ±6.35 mm range. The constant piston displacement rate was approximately 10^{-6} m/s. The bending load was recorded with the digital data acquisition system SILVI (0.07 s/16 bit). From the maximum bending load F_{max} and from the geometrical parameters (sample diameter D, notch depth a_o) the fracture toughness can be calculated by the formula;

$$K_{IC} = A_{\min}\cdot\frac{F_{\max}}{D^{1.5}}$$

$$A_{\min} = 3.33\left[1.835 + 7.15\frac{a_o}{D} + 9.85\left(\frac{a_o}{D}\right)^2\right]$$

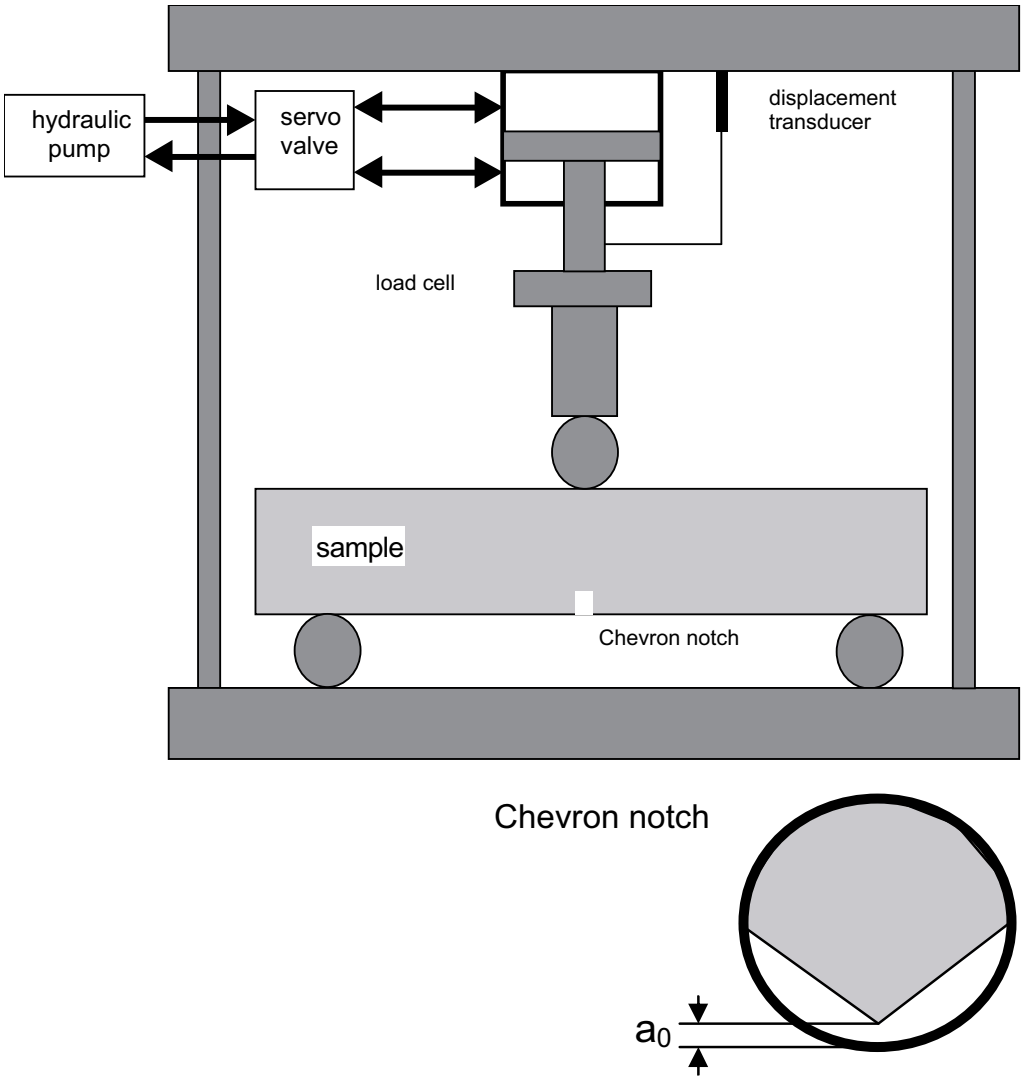

Figure 3-4. *Schematic of fracture toughness testing.*

Figure 3-5. *Experimental set-up for fracture toughness testing.*

3.4 Hydrofrac testing

The hydrofrac tests were conducted on core samples of approximately 50 mm diameter which contained a 3 mm diameter axial injection hole which was diamond core drilled with water as cooling agent. The samples' circumferential surface was protected against confining pressure penetration by a spray varnish. The samples were then triaxially loaded with a constant confining pressure (Tellus 32 oil) and a constant axial stress within a 400 MPa pressure vessel and a 60-ton loading machine. The axial stress was about 10% higher than the confining pressure to prevent the confining pressure medium to enter between the sample and the axial loading piston. The axial load was measured by a 500 kN load cell type MeSy, and the confining pressure by a HBM pressure transducer of range 200 MPa. The fracturing fluid (Tellus 32 oil, viscosity 25 cPoise) was injected into the coaxial 3 mm diameter hole of the sample via a hydraulic pressure amplifier cylinder. The piston movement of the cylinder piston was displacement servo-controlled by a HBM displacement transducer of ± 100 mm range. The injection system provided a constant injection rate of approximately 1 ml/s. Axial stress σ_1, injection pressure p_i, confining pressure p_m, and amplifier piston displacement were recorded by the MeSy digital data acquisition system SILVI (0.14 s/16 bit). The pressure vessel is shown in Figure 3-6, the total set-up in the loading machine in Figure 3-7.

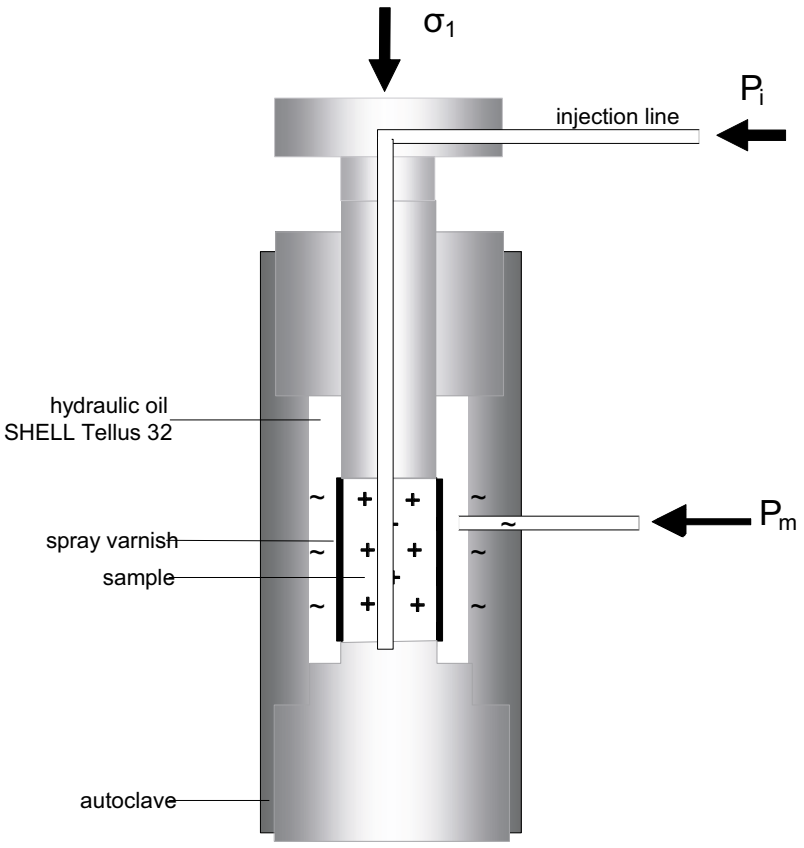

Figure 3-6. *Pressure vessel for hydrofrac testing on samples with axial drillholes (Pi fluid injection pressure, Pm fluid confining pressure, note: rubber sleeve was replaced by spray varnish).*

Figure 3-7. *Set-up for hydrofrac testing.*

The experimental procedure was as follows:

- triaxial loading the sample to constant values of p_m and σ_1,
- injection pressure increase at constant injection rate until fracturing occurred which was observed by equilibration of p_m, p_i and σ_1.

Tests were conducted under confining pressures up to approximately 30 MPa. The fracturing pressure p_c then is plotted versus the confining pressure p_m which in general leads to a linear relationship

$$p_c = p_{co} + k \cdot p_m$$

where p_{co} is the sample hydraulic tensile strength and k is the hydrofrac coefficient.

3.5 Equipment calibration

Laboratory pressure transducers, load cells, and displacement transducers were calibrated in April 2004. The calibrations were partly documented in the MeSy Quality Plan (MeSy Report No 22.04, test protocols C1 to C4). Additional calibration checks prior to each test series are a routine procedure as part of MeSy's quality management. In general, pressure transducers are tested against load cells, displacement transducers by a special caliper set-up (Figure 3-8). Both calibration and experimental testing were carried out by experienced MeSy personnel.

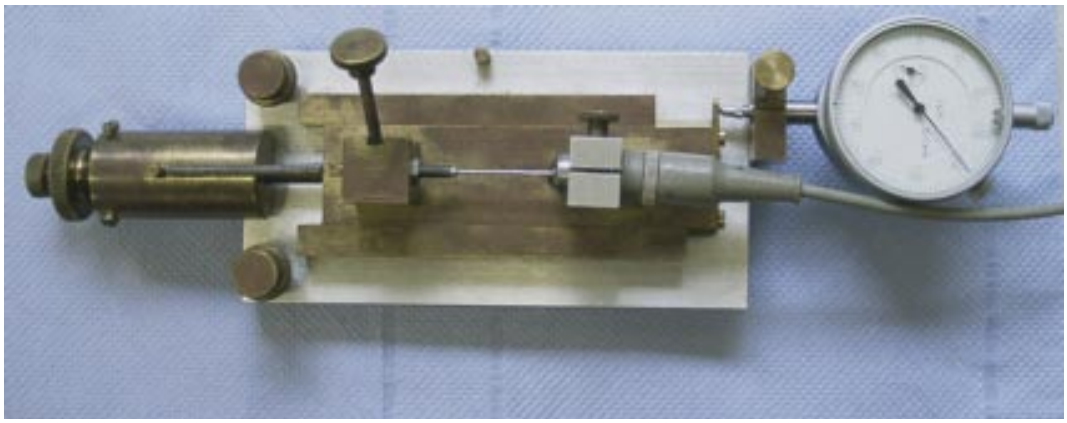

Figure 3-8. *Set-up for displacement transducer calibration.*

4 Execution

4.1 General

The testing methodology has already been described in Section 3. As mentioned, existing ISRM standards (velocity, fracture toughness) were considered. In the case of laboratory hydrofracturing, a long-time experience exists at RUBochum and MeSy Bochum, documented by numerous theses and publications /e.g. Rummel, 1987/.

4.2 Preparations

- Each test series (density ultrasonic, fracture toughness, hydrofracturing) required the preparation of the apparatus, function tests and calibrations of the test sensors (see Section 3.5).
- Most of the preparation effort was applied to core and sample documentation and to sample preparation by diamond sawing, diamond drilling and end plane grinding.
- For **core piece documentation, data sheets** were prepared for each core piece, containing information on its origin (borehole number, depth), its dimensions (length, diameter), on its lithology, and a photo. The data are in agreement with the data list obtained from the SKB project manager on 26.06.04. The data sheets are given in Appendix A. A summary of the core material is given in Table 4-1. Note that MeSy has issued core piece numbers, the first symbols of which relate to the borehole (e.g. 1A for a core piece of borehole KFM01A), the third symbol to the core piece. These core piece numbers are further used.
- Sample preparation (sawing, drilling, grinding) was documented on **sample preparation sheets** poviding information of which type of preparation was carried out on which sample, for which tests, on which date, by which operator. These data sheets remain within the MeSy Forsmark documentation file at MeSy Bochum.
- As can be seen from Table 4-1, a total of 36 core pieces of approximately 34 cm length was available for laboratory testing. From these core pieces a total of 143 samples were prepared for density, ultrasonic, fracture toughness and hydrofrac testing.
- For each single test a **work sheet** was prepared which contains information on the sample, the test performed, the equipment used, the operators, the test date, and the measured data. These data sheets remain within the MeSy Forsmark documentation file at MeSy Bochum.

Table 4-1. Core list with lithology.

Project:	SKB Forsmark				
Operator:	Taringer (SKB), Weber (MeSy)				
Date:	23.06.04				
Borehole no	Depth range from	to	Mean depth m	MeSy core-no	Rock type
KFM01A	423.00	423.34	423.17	1A-1	Granite to granodiorite, metamorphic, medium-grained
KFM01A	424.66	425.00	424.83	1A-2	Granite to granodiorite, metamorphic, medium-grained
KFM01A	428.00	428.34	428.17	1A-3	Granite to granodiorite, metamorphic, medium-grained
KFM01A	484.42	484.76	484.59	1A-4	Granite to granodiorite, metamorphic, medium-grained
KFM01A	499.78	490.12	489.95	1A-5	Granite, granodiorite and tonalite, metamorphic, fine- to medium-grained or Granite to granodiorite, metamorphic, medium-grained
KFM01A	504.52	504.86	504.69	1A-6	Granite, granodiorite and tonalite, metamorphic, fine- to medium-grained
KFM01A	687.96	688.30	688.13	1A-7	Granite to granodiorite, metamorphic, medium-grained
KFM01A	949.83	950.17	950.00	1A-8	Granite to granodiorite, metamorphic, medium-grained
KFM01A	971.40	971.74	971.57	1A-9	Granite, granodiorite and tonalite, metamorphic, fine- to medium-grained
KFM01A	978.36	978.70	978.53	1A-10	Granite to granodiorite, metamorphic, medium-grained
KFM01B	420.86	421.20	421.03	1B-1	Granite to granodiorite, metamorphic, medium-grained
KFM01B	421.43	421.77	421.60	1B-2	Granite to granodiorite, metamorphic, medium-grained
KFM01B	427.92	428.26	428.09	1B-3	Granite to granodiorite, metamorphic, medium-grained
KFM01B	429.80	430.14	429.97	1B-4	Granite to granodiorite, metamorphic, medium-grained
KFM01B	430.26	430.60	430.43	1B-5	Granite to granodiorite, metamorphic, medium-grained
KFM01B	454.96	455.30	455.13	1B-6	Granite to granodiorite, metamorphic, medium-grained
KFM01B	456.03	456.37	456.20	1B-7	Granite to granodiorite, metamorphic, medium-grained
KFM02A	220.68	221.00	220.84	2A-1	Granite to granodiorite, metamorphic, medium-grained
KFM02A	225.87	226.20	226.04	2A-2	Granite to granodiorite, metamorphic, medium-grained
KFM02A	395.88	396.20	396.04	2A-3	Granite to granodiorite, metamorphic, medium-grained
KFM02A	413.90	414.24	414.07	2A-4	Granite to granodiorite, metamorphic, medium-grained
KFM02A	451.13	451.50	451.32	2A-5	Granite to granodiorite, metamorphic, medium-grained
KFM02A	554.22	554.56	554.39	2A-6	Granite, granodiorite and tonalite, metamorphic, fine- to medium-grained
KFM02A	594.21	594.55	594.38	2A-7	Granite to granodiorite, metamorphic, medium-grained
KFM02A	602.75	603.09	602.92	2A-8	Granite, granodiorite and tonalite, metamorphic, fine- to medium-grained
KFM02A	699.66	700.00	699.83	2A-9	Granite to granodiorite, metamorphic, medium-grained
KFM02A	702.64	703.00	702.82	2A-10	Granite to granodiorite, metamorphic, medium-grained
KFM04A	192.11	192.45	192.28	4A-1	Granite to granodiorite, metamorphic, medium-grained
KFM04A	192.45	192.77	192.61	4A-2	Granite to granodiorite, metamorphic, medium-grained
KFM04A	260.14	260.48	260.31	4A-3	Granite to granodiorite, metamorphic, medium-grained
KFM04A	527.46	527.80	527.63	4A-4	Granite to granodiorite, metamorphic, medium-grained
KFM04A	527.80	528.14	527.97	4A-5	Granite to granodiorite, metamorphic, medium-grained
KFM04A	528.21	528.55	528.38	4A-6	Granite to granodiorite, metamorphic, medium-grained
KFM04A	528.62	528.96	528.79	4A-7	Granite to granodiorite, metamorphic, medium-grained
KFM04A	528.96	529.30	529.13	4A-8	Granite to granodiorite, metamorphic, medium-grained
KFM04A	529.30	529.64	529.47	4A-9	Granite to granodiorite, metamorphic, medium-grained

5 Results

5.1 Density

The densities of the 36 core pieces are listed in Table 5-1. The density values range between 2.626 (core piece no 2A-8) and 2.684 g/cm^3 (core piece no 1A-6). From the lithology known to us, no obvious relation between density and lithology of the granite exists. The over-all mean density is (2.655 ± 0.009) g/cm^3. The mean values for the 4 boreholes are:

KFM01A 2.661 ± 0.014 g/cm^3

KFM01B 2.652 ± 0.003 g/cm^3

KFM02A 2.653 ± 0.012 g/cm^3

KFM04A 2.655 ± 0.003 g/cm^3

mean 2.655 ± 0.009 g/cm^3

Sample densities were measured on 72 samples prepared for ultrasonic and hydrofrac testing. The values are given in Table 5.2. The sample density values range between 2.628 (sample no 2A-8A/C) and 2.692 g/cm^3 (sample no 1A-6A) determined by the buoyancy method, and between 2.609 and 2.680 g/cm^3 for mass and volume measurements. The over-all mean values are 2.659 g/cm^3 and 2.644 g/cm^3, respectively. The geometric density values are systematically about 0.5 per cent lower than the buoyancy values, which can be explained by the fact that the sample diameter generally is measured on the higher side. The mean values for the 4 boreholes are:

	Buoyancy g/cm^3	**Geometric g/cm^3**
KFM01A	2.663 ± 0.016	2.651 ± 0.014
KFM01B	2.656 ± 0.007	2.637 ± 0.011
KFM02A	2.658 ± 0.012	2.642 ± 0.016
KFM04a	2.659 ± 0.004	2.645 ± 0.010
Mean	2.659 ± 0.011	2.644 ± 0.014

By comparison of the core and sample densities we observe an almost perfect agreement. Variations in densities must be explained by the petrographic investigations.

Table 5-1. Core densities derived from test by the buoyancy method.

Core piece no	Mean depth m	Density ρ g/cm³
1A-1	423.17	2.645
1A-2	424.83	2.663
1A-3	428.17	2.664
1A-4	484.59	2.656
1A-5	489.95	2.666
1A-6	504.69	2.684
1A-7	688.13	2.658
1A-8	950.00	2.659
1A-9	971.57	2.641
1A-10	978.53	2.657
mean		2.661 ± .014
1B-1	421.03	2.649
1B-2	421.60	2.649
1B-3	428.09	2.649
1B-4	429.97	2.655
1B-5	430.43	2.652
1B-6	455.13	2.656
1B-7	456.20	2.656
mean		2.652 ± .003
2A-1	220.84	2.655
2A-2	226.04	2.656
2A-3	396.04	2.656
2A-4	414.07	2.673
2A-5	451.32	2.656
2A-6	554.39	2.649
2A-7	594.38	2.653
2A-8	602.92	2.626
2A-9	699.83	2.657
2A-10	702.82	2.651
mean		2.653 ± .012
4A-1	192.28	2.650
4A-2	192.61	2.655
4A-3	260.31	2.652
4A-4	527.63	2.659
4A-5	527.97	2.656
4A-6	528.38	2.657
4A-7	528.79	2.656
4A-8	529.13	2.657
4A-9	529.47	2.657
mean		2.655 ± .003

Table 5-2. Sample densities derived from tests by the buoyancy method and by volume and mass determination.

Sample	Mean depth m	Density bouyancy g/cm^3	Density geometric g/cm^3
1A-1a	423.17	2.637	2.631
1A-1c		2.635	2.632
1A-2a	424.83	2.654	2.652
1A-2c		2.661	2.659
1A-3a	428.17	2.664	2.657
1A-3c		2.665	2.659
1A-4a	484.59	2.662	2.655
1A-4c		2.660	2.653
1A-5a	489.95	2.663	2.656
1A-5c		2.679	2.668
1A-6a	504.69	2.692	2.680
1A-6c		2.689	2.675
1A-7a	688.13	2.665	2.651
1A-7c		2.664	2.648
1A-8a	950.00	2.692	2.644
1A-8c		2.661	2.646
1A-9a	971.57	2.647	2.633
1A-9c		2.647	2.628
1A-10a	978.53	2.656	2.644
1A-10c		2.668	2.657
mean		2.663 ± .016	2.651 ± .014
1B-1a	421.03	2.650	2.605
1B-1c		2.658	2.642
1B-2a	421.60	2.653	2.638
1B-2c		2.656	2.644
1B-3a	428.09	2.656	2.630
1B-3c		2.655	2.643
1b-4a	429.97	2.648	2.638
1B-4c		2.661	2.647
1b-5a	430.43	2.644	2.622
1b-5c		2.666	2.640
1b-6a	455.13	2.657	2.638
1b-6c		2.652	2.638
1b-7a	456.20	2.665	2.648
1b-7c		2.666	2.645
mean		2.656 ± .007	2.637 ± .011
2A-1a	220.84	2.658	2.636
2A-1c		2.670	2.655
2A-2a	226.04	2.659	2.650
2A-2c		2.661	2.651
2A-3a	396.04	2.659	2.645
2A-3c		2.660	2.648
2A-4a	414.07	2.673	2.663
2A-4c		2.672	2.660
2A-5a	451.32	2.666	2.646
2A-5c		2.660	2.645
2A-6a	554.39	2.651	2.632
2A-6c		2.650	2.638
2A-7a	594.38	2.661	2.656

Sample	Mean depth m	Density bouyancy g/cm³	Density geometric g/cm³
2A-7c		2.663	2.646
2A-8a	602.92	2.628	2.609
2A-8c		2.630	2.609
2A-9a	699.83	2.663	2.645
2A-9c		2.662	2.612
2A-10a	702.82	2.661	2.659
2A-10c		2.651	2.637
mean		2.658 ± .012	2.642 ± .016
4A-1a	192.28	2.661	2.654
4A-1c		2.654	2.637
4A-2a	192.61	2.663	2.646
4A-2c		2.657	2.641
4A-3a	260.31	2.660	2.637
4A-3c		2.659	2.645
4A-4a	527.63	2.664	2.650
4A-4c		2.654	2.642
4A-5a	527.97	2.661	2.649
4A-5c		2.662	2.652
4A-6a	528.38	2.656	2.647
4A-6c		2.662	2.653
4A-7a	528.79	2.663	2.655
4A-7c		2.657	2.652
4A-8a	529.13	2.660	2.645
4A-8c		2.662	2.646
4A-9a	529.47	2.665	2.649
4A-9c		2.649	2.610
mean		2.659 ± .004	2.645 ± .010

5.2 Ultrasonic velocities and elasticity parameters

The measured velocity data are listed in Table 5-3 together with the derived elasticity parameters Young's modulus and Poisson's ratio. The measured seismograms are given in Appendix B. The velocity measurements were conducted on core specimens of approximately 50 mm diameter and approximately 75 mm length by axial pulse transmission from flat sample ends. The P-wave velocities range between 5.70 km/s and 4.96 km/s, the S-wave velocities between 3.26 km/s and 2.78 km/s, with mean values of 5.44 km/s and 3.07 km/s for all 72 samples tested. The Young's moduli range between 71 and 52 GPa, with an overall mean value of 64 GPa. The mean Poisson's ratio is 0.27. For the 4 boreholes the situation may be summarized as:

Borehole	v_p km/s	v_s km/s	E GPa	v
KFM01A	5.4 ± 0.2	3.0 ± 0.1	62 ± 6	0.27
KFM01B	5.6 ± 0.1	3.2 ± 0.1	67 ± 2	0.27
KFM02a	5.5 ± 0.1	3.1 ± 0.1	66 ± 3	0.26
KFM04a	5.3 ± 0.2	3.0 ± 0.1	60 ± 4	0.27
Mean	5.4 ± 0.2	3.1 ± 0.1	64 ± 5	0.27

Table 5-3. Ultrasonic velocities v_p and v_s and elastic parameters Young's modulus E and Poisson's ratio.

Sample no	v_p km/s	v_s km/s	E_{dyn} GPa	v_{dyn}
1A-1A	5.58	3.17	67	0.26
1A-1C	5.45	3.11	67	0.26
1A-2A	5.62	3.17	67	0.27
1A-2C	5.61	3.16	67	0.27
1A-3A	5.52	3.14	66	0.26
1A-3C	5.50	3.07	69	0.27
1A-4A	5.58	3.18	68	0.26
1A-4C	5.53	3.05	64	0.28
1A-5A	5.23	2.98	59	0.26
1A-5C	5.20	2.89	57	0.28
1A-6A	5.62	3.18	69	0.27
1A-6C	5.61	3.11	66	0.28
1A-7A	5.36	3.03	62	0.27
1A-7C	5.46	3.05	63	0.27
1A-8A	5.03	2.83	55	0.27
1A-8C	4.96	2.78	52	0.27
1A-9A	5.12	2.86	55	0.27
1A-9C	5.12	2.91	57	0.26
1A-10A	5.32	3.01	61	0.26
1A-10C	5.16	2.84	55	0.28
mean	5.38 ± .22	3.03 ± .13	62 ± 6	0.27 ± .01
1B-1A	5.76	3.24	71	0.27
1B-1C	5.63	3.20	69	0.26
1B-2A	5.62	3.15	67	0.27
1B-2C	5.67	3.23	70	0.26
1B-3A	5.65	3.17	68	0.27
1B-3C	5.63	3.18	68	0.26
1B-4A	5.44	3.09	64	0.26
1B-4C	5.48	3.06	63	0.27
1B-5A	5.50	3.12	65	0.26
1B-5C	5.52	3.11	65	0.27
1B-6A	5.65	3.25	70	0.25
1B-6C	5.59	3.19	68	0.26
1B-7A	5.53	3.12	66	0.27
1B-7C	5.57	3.08	65	0.28
mean	5.59 ± .09	3.16 ± .06	67 ± 2	0.27 ± .01
2A-1A	5.43	3.04	62	0.27
2A-1C	5.43	3.02	62	0.28
2A-2A	5.48	3.10	65	0.26
2A-2C	5.52	3.14	66	0.26
2A-3A	5.47	3.14	66	0.25
2A-3C	5.46	3.08	64	0.27
2A-4A	5.43	3.06	64	0.27
2A-4C	5.53	3.15	67	0.26
2A-5A	5.53	3.21	69	0.25
2A-5C	5.55	3.22	69	0.25
2A-6A	5.60	3.26	70	0.24
2A-6C	5.54	3.10	65	0.27
2A-7A	5.34	3.00	61	0.27
2A-7C	5.27	3.00	60	0.26

Sample no	v_p km/s	v_s km/s	E_{dyn} GPa	v_{dyn}
2A-8A	5.64	3.15	67	0.27
2A-8C	5.59	3.15	66	0.27
2A-9A	5.53	3.16	67	0.26
2A-9C	5.70	3.17	68	0.28
2A-10A	5.60	3.19	68	0.26
2A-10C	5.57	3.12	66	0.27
mean	5.51 ± .10	3.12 ± .07	66 ± 3	0.26 ± .01
4A-1A	5.57	3.20	68	0.25
4A-1C	5.55	3.04	63	0.29
4A-2A	5.55	3.07	64	0.28
4A-2C	5.61	3.10	65	0.28
4A-3A	5.27	2.99	60	0.26
4A-3C	5.39	3.02	62	0.27
4A-4A	5.17	2.93	58	0.26
4A-4C	5.28	2.97	59	0.27
4A-5A	5.09	2.89	56	0.26
4A-5C	5.02	2.83	54	0.27
4A-6A	5.16	2.94	58	0.26
4A-6C	5.16	2.87	56	0.28
4A-7A	5.19	2.94	58	0.26
4A-7C	5.10	2.87	56	0.27
4A-8A	5.31	3.06	62	0.25
4A-8C	5.24	2.93	58	0.27
4A-9A	5.13	2.88	56	0.27
4A-9C	5.55	3.18	67	0.26
mean	5.30 ± .19	2.98 ± .11	60 ± 4	0.27 ± .01
overall mean	5.44 ± .19	3.07 ± .12	64 ± 5	0.27 ± 0.01

5.3 Fracture toughness K_{IC}

A total of 71 fracture toughness tests could successfully be carried out. The test plots are given in Appendix C together with photos of the fracture plane. The K_{IC}-data are listed in Table 5-4. The fracture toughness data range between 0.71 and 2.76 MPa/$m^{1/2}$ with an overall mean value of 2.04 MPa/$m^{1/2}$. For the 4 boreholes the mean values are

Borehole	K_{IC} MPa/$m^{1/2}$
KFM01A	1.92 ± 0.34
KFM01B	2.12 ± 0.24
KFM02A	2.19 ± 0.12
KFM04A	1.97 ± 0.26
Overall mean	2.04 ± 0.27

Such values are typical for competent granites /Atkinson and Meredith, 1987/. They compare with values measured for the Stripa or the Bohus granites /e.g. Ouchterlony and Sun, 1983/, the Finnsjön granodiorite /Olofsson, 1978/, or the US Westerly granite /Ingraffea et al. 1984/. The standard deviation of approximately 0.3 MPa/$m^{1/2}$ is almost

negligible, and the low value of 0.7 MPa/$m^{1/2}$ is singular and may be neglected. The difference in the mean values for the 4 boreholes may also be neglected since the differences are small. Any further consideration of singular data requires a detailed petrographic rock analysis and a detailed analysis of the fracture surfaces. It may be noted that the mean values of K_{IC} correlate with the mean values of Young's moduli for the 4 boreholes, which may be an indication for microcrack density in the rock, although the singular sample data do not obviously support this hypothesis.

Table 5-4. Fracture toughness K_{IC}, D sample diameter, a_0 Chevron notch depth, F_{max} maximum bending force.

Sample no	D mm	a_o mm	F_{max} kN	K_{IC} MPa/$m^{1/2}$
1A-1AB	50.6	7.6	2.40	2.20
1A-1BC	50.6	6.7	2.66	2.30
1A-2AB	50.5	7.2	2.23	2.00
1A-2BC	50.6	7.0	2.55	2.25
1A-3AB	50.7	7.1	2.53	2.24
1A-3BC	50.7	6.7	2.26	1.95
1A-4AB	50.6	6.9	2.20	1.93
1A-4BC	50.6	7.1	2.21	1.96
1A-5AB	50.8	7.1	2.23	1.96
1A-5BC	50.9	7.3	0.80	0.71
1A-6AB	50.8	7.1	2.35	2.07
1A-6BC	50.7	7.2	2.42	2.15
1A-7AB	51.0	7.3	1.94	1.72
1A-7BC	51.0	7.3	2.35	2.08
1A-8AB	50.8	7.2	1.95	1.73
1A-8BC	50.9	7.3	1.94	1.72
1A-9AB	50.8	6.7	2.15	1.84
1A-9BC	50.8	7.0	2.07	1.81
1A-10AB	50.7	6.9	2.12	1.85
1A-10BC	50.8	7.4	2.15	1.93
mean				1.92 ± 0.34
1B-1AB	50.7	7.0	2.46	2.16
1B-1BC	50.7	7.4	2.49	2.24
1B-2AB	50.7	7.4	2.54	2.29
1B-2BC	50.7	7.4	2.23	2.01
1B-3AB	50.8	7.3	2.64	2.35
1B-3BC	50.8	7.0	2.24	1.96
1B-4AB	50.8	6.8	2.12	1.83
1B-4BC	50.8	6.8	2.22	1.92
1B-5AB	50.8	7.5	3.06	2.76
1B-5BC	50.8	6.9	2.21	1.92
1B-6AB	50.8	6.5	2.48	2.10
1B-6BC	50.8	7.0	2.30	2.01
1B-7AB	50.7	7.3	2.24	2.01
1B-7BC	50.7	7.4	2.37	2.14
mean				2.12 ± .24
2A-1AB	50.9	7.3	2.39	2.12
2A-1BC	50.9	7.5	2.60	2.34
2A-2AB	50.9	7.2	2.70	2.38
2A-2BC	50.9	7.6	2.53	2.29

Sample no	D mm	a_o mm	F_{max} kN	K_{IC} MPa/m$^{1/2}$
2A-3AB	50.8	6.8	2.48	2.14
2A-3BC	50.7	7.3	2.43	2.18
2A-4AB	50.8	7.2	2.55	2.26
2A-4BC	50.8	7.1	2.19	1.93
2A-5AB	50.7	7.2	2.60	2.31
2A-5BC	50.7	7.0	2.34	2.05
2A-6AB	50.6	7.4	2.59	2.34
2A-6BC	50.8	6.5	-	-
2A-7AB	50.9	7.0	2.50	2.18
2A-7BC	50.8	6.9	2.40	2.09
2A-8AB	51.0	6.7	2.53	2.15
2A-8BC	51.0	7.3	2.59	2.29
2A-9AB	50.8	7.0	2.53	2.21
2A-9BC	50.8	7.0	2.47	2.16
2A-10AB	50.8	6.8	2.46	2.12
2A-10BC	50.8	7.0	2.41	2.11
mean				2.19 ± .12
4A-1AB	50.8	6.7	2.62	2.25
4A-1BC	50.8	6.6	2.61	2.22
4A-2AB	50.8	6.9	2.73	2.37
4A-2BC	50.7	7.0	2.64	2.32
4A-3AB	50.7	6.7	2.55	2.24
4A-3BC	50.7	0	2.68	1.43
4A-4AB	50.7	6.6	2.10	1.80
4A-4BC	50.6	7.2	2.14	1.91
4A-5AB	50.6	7.2	2.24	2.00
4A-5BC	50.6	7.0	1.99	1.75
4A-6AB	50.6	7.2	2.30	2.05
4A-6BC	50.7	7.4	2.10	1.89
4A-7AB	50.6	7.2	2.41	2.15
4A-7BC	50.7	7.0	2.19	1.92
4A-8AB	50.7	7.0	2.12	1.86
4A-8BC	50.7	6.7	1.81	1.56
4A-9AB	50.7	6.9	2.14	1.87
4A-9BC	50.8	7.0	2.07	1.81
mean				1.97± .26
Overall mean				2.04 ± 0.27

5.4 Laboratory hydrofrac results

Laboratory hydrofrac tests were conducted on a total of 71 samples under confining pressures up to 30 MPa. The test plots are given in Appendix D. The data are listed in Table 5-5 and are graphically presented in Figures 5-1 to 5-4 separately for the 4 boreholes in the form of plots of fracture initiation pressure (maximum injection pressure) p_c versus confining pressure p_m. The p_c-value for $p_m = 0$ is the hydraulic tensile strength p_{co}, the slope yields the frac coefficient k. For the 4 boreholes and for the total test series we obtain the following mean values:

Borehole	p_{co}, MPa	k
KFM01A	27.1 ± 3.1	1.39 ± .15
KFM01B	24.7 ± 8.2	1.60 ± .46
KFM02A	23.0 ± 2.9	1.61 ± .15
KFM04A	30.2 ± 3.6	1.46 ± .17
Mean	25.9 ± 2.1	1.53 ± .11

In most of the tests axial fractures were initiated. Induced inclined fractures are steeply inclined and do not alter the general result of a linear relationship between p_c and p_m. For some reasons the tests on samples from borehole KFM01B show a higher scatter. The overall mean tensile rock sample strength is approximately 26 MPa, whereas the overall mean frac coefficient k is approximately 1.5 (Figure 5-5).

Table 5-5. Fracture initiation pressure p_c, and applied axial stress σ_1 and confining pressure p_m.

Injection rate, ml s^{-1}	: 1				
Sample no	σ_1 MPa	p_m MPa	p_c MPa	Frac	Remark
1A-1A	20.82	18.21	52.01	axial	
1A-1C	21.29	14.14	46.25	dto.	
1A-2A	23.88	10.02	44.13	dto.	
1A-2C	13.18	3.96	34.11	dto.	
1A-3A	37.20	29.98	62.28	dto.	
1A-3C	30.44	25.54	63.95	axial, inclined	
1A-4A	34.59	22.58	56.46	axial	
1A-4C	25.18	11.50	39.87	inclined	
1A-5A	28.37	22.23	50.51	axial, inclined	see photo
1A-5C	35.71	24.68	66.34	axial, inclined	see photo
1A-6A	29.39	23.89	62.71	dto.	see photo
1A-6C	31.06	26.82	68.32	dto.	see photo
1A-7A	37.64	28.82	57.24	axial	
1A-7C	14.55	8.28	32.12	dto.	
1A-8A	24.28	20.80	62.61	dto.	
1A-8C	30.94	21.63	64.36	dto.	
1A-9A	24.06	17.94	57.73	dto.	
1A-9C	16.11	12.49	42.08	dto.	
1A-10A	18.82	16.45	69.07	dto.	
1A-10C	19.23	15.97	49.35	dto.	
1B-1A	31.41	29.75	42.88	axial	not used for linear regression
1B-1C	11.49	7.55	24.22	axial + inclined	see photo
1B-2A	13.86	10.21	50.93	axial	
1B-2C	29.85	23.41	56.39	inclined	
1B-3A	13.85	8.37	28.03	axial	
1B-3C	36.26	28.18	59.40	dto.	
1B-4A	22.43	16.12	40.84	dto.	
1B-4C	40.89	29.96	132.42	dto.	not used for linear regression
1B-5A	32.41	25.42	81.55	axial, inclined	see photo
1B-5C	10.97	5.62	51.54	axial	
1B-6A	55.52	25.02	72.63	axial, inclined	see photo
1B-6C	15.36	12.24	42.06	axial	
1B-7A	22.33	16.92	50.81	dto.	
1B-7C	21.70	20.16	30.74	inclined	not used for linear regression

Injection rate, ml s^{-1} : 1					
Sample no	**σ_1 MPa**	**p_m MPa**	**p_c MPa**	**Frac**	**Remark**
2A-1A	22.85	20.07	53.67	axial	
2A-1C	15.46	10.04	43.36	dto.	
2A-2B	34.87	30.51	44.98	dto.	not used for linear regression
2A-2C	29.70	25.01	61.56	dto.	
2A-3A	45.00	17.74	44.99	dto.	
2A-3C	23.11	17.38	50.34	dto.	
2A-4A	49.49	29.52	79.64	dto.	
2A-4C	28.76	22.49	58.15	axial, inclined	see photo
2A-5A	12.08	7.64	39.20	axial	
2A-5C	11.37	5.60	29.34	dto.	
2A-6A	19.25	6.42	35.62	dto.	
2A-6C	36.22	28.67	77.43	dto.	
2A-7A	40.23	29.39	60.80	axial, inclined	see photo
2A-7C	23.05	15.38	47.14	axial	
2A-8A	23.41	18.78	53.29	dto.	
2A-8C	38.59	27.33	64.95	dto.	
2A-9A	20.55	12.42	40.98	dto.	
2A-9C	19.07	13.71	44.34	dto.	
2A-10A	31.94	29.84	54.40	dto.	not used for linear regression
4A-1A	22.91	19.80	57.57	axial	
4A-1C	48.80	24.19	68.36	axial, inclined	see photo
4A-2A	26.95	22.19	63.64	axial	
4A-2C	25.66	17.87	57.07	dto.	
4A-3A	34.83	25.95	69.55	dto.	
4A-3C	21.50	16.02	57.41	dto.	
4A-4A	61.09	28.30	72.71	axial, inclined	see photo
4A-4C	27.40	14.66	66.69	axial	
4A-5A	29.11	12.06	43.05	dto.	
4A-5C	18.35	9.80	43.68	dto.	
4A-6A	61.09	28.30	72.71	axial, inclined	see photo
4A-6C	34.46	29.84	73.02	axial	
4A-7A	14.34	8.43	35.31	dto.	not used for linear regression
4A-7C	16.79	6.85	36.41	dto.	
4A-8A	23.45	20.09	51.21	axial, inclined	see photo
4A-8C	35.98	32.81	75.26	axial	
4A-9A	23.75	20.56	59.33	dto.	
4A-9C	16.20	13.45	49.64	axial, inclined	see photo

*): see photo in Appendix D

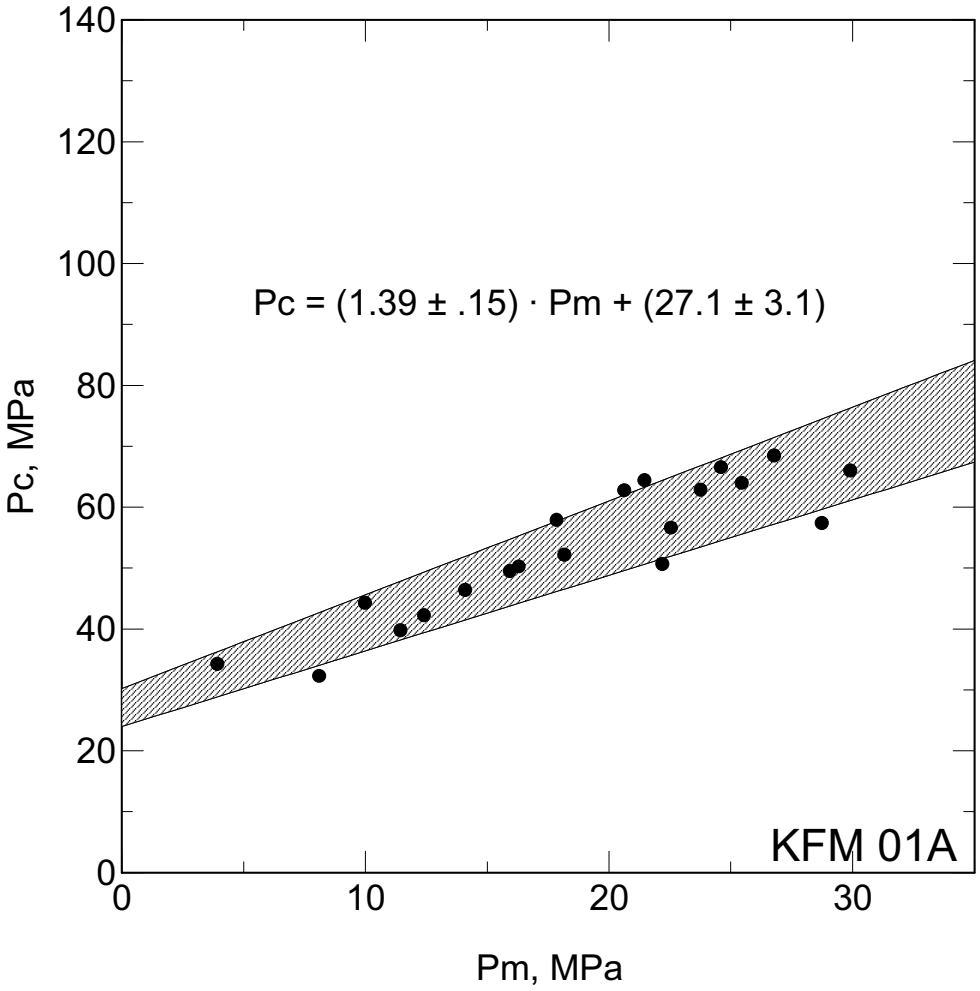

Figure 5-1. *Fracture initiation pressure p_c versus confining pressure p_m for samples from borehole KFM01A.*

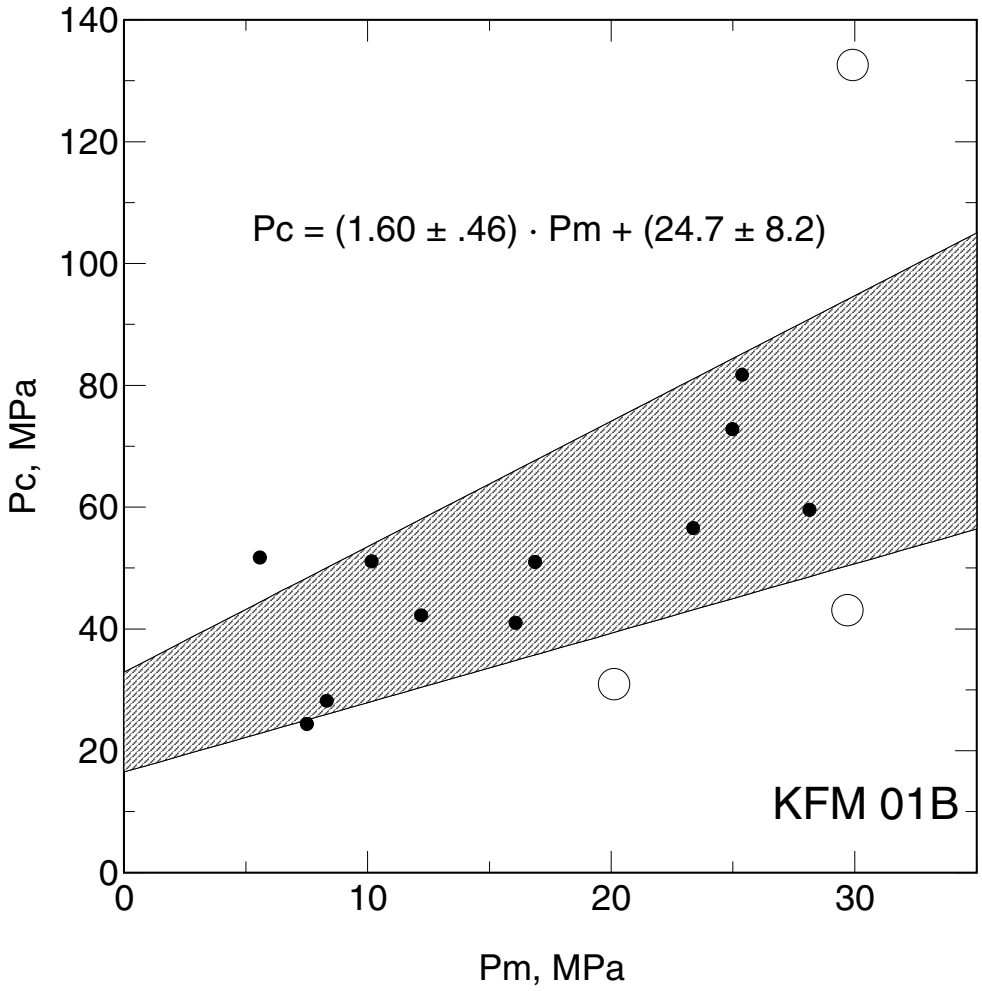

Figure 5-2. *Fracture initiation pressure p_c versus confining pressure p_m for samples from borehole KFM01B (open circles: not used for linear regression for p_c – relation).*

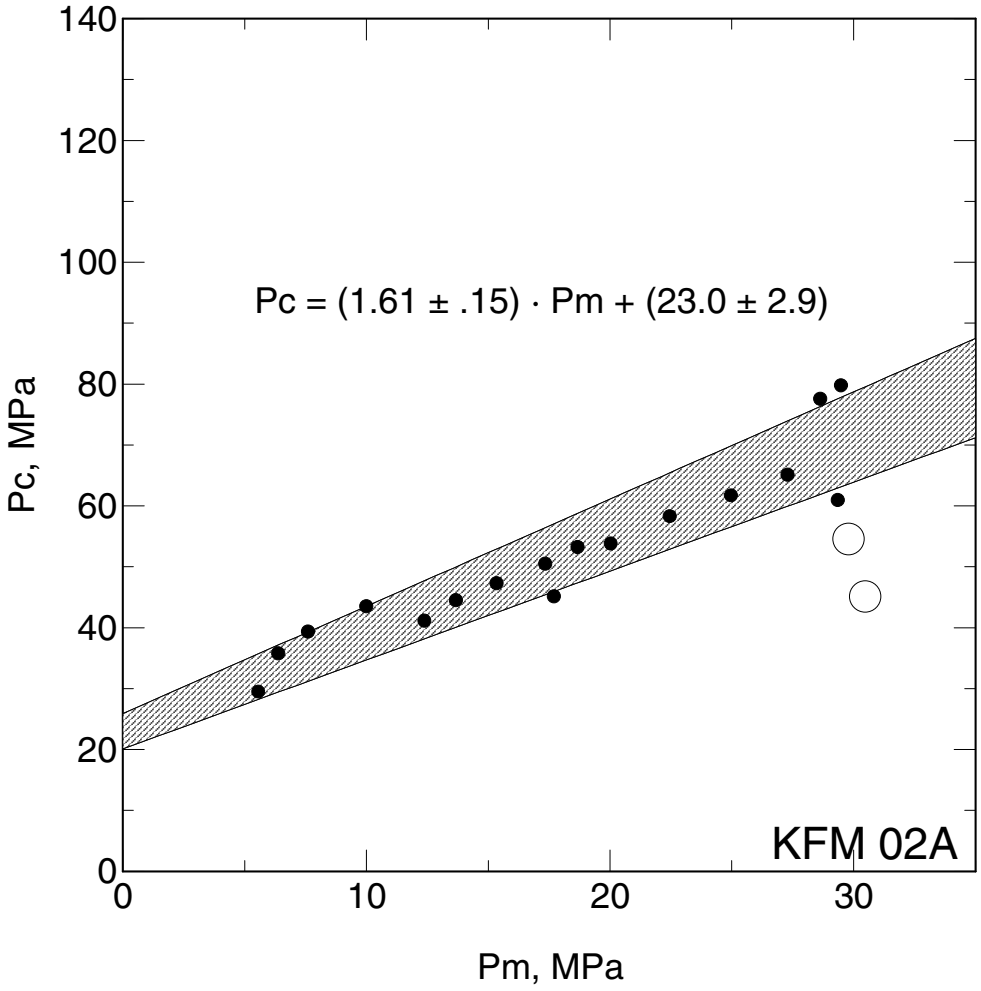

Figure 5-3. *Fracture initiation pressure p_c versus confining pressure p_m for samples from borehole KFM02A (open circles: not used for linear regression for p_c – relation).*

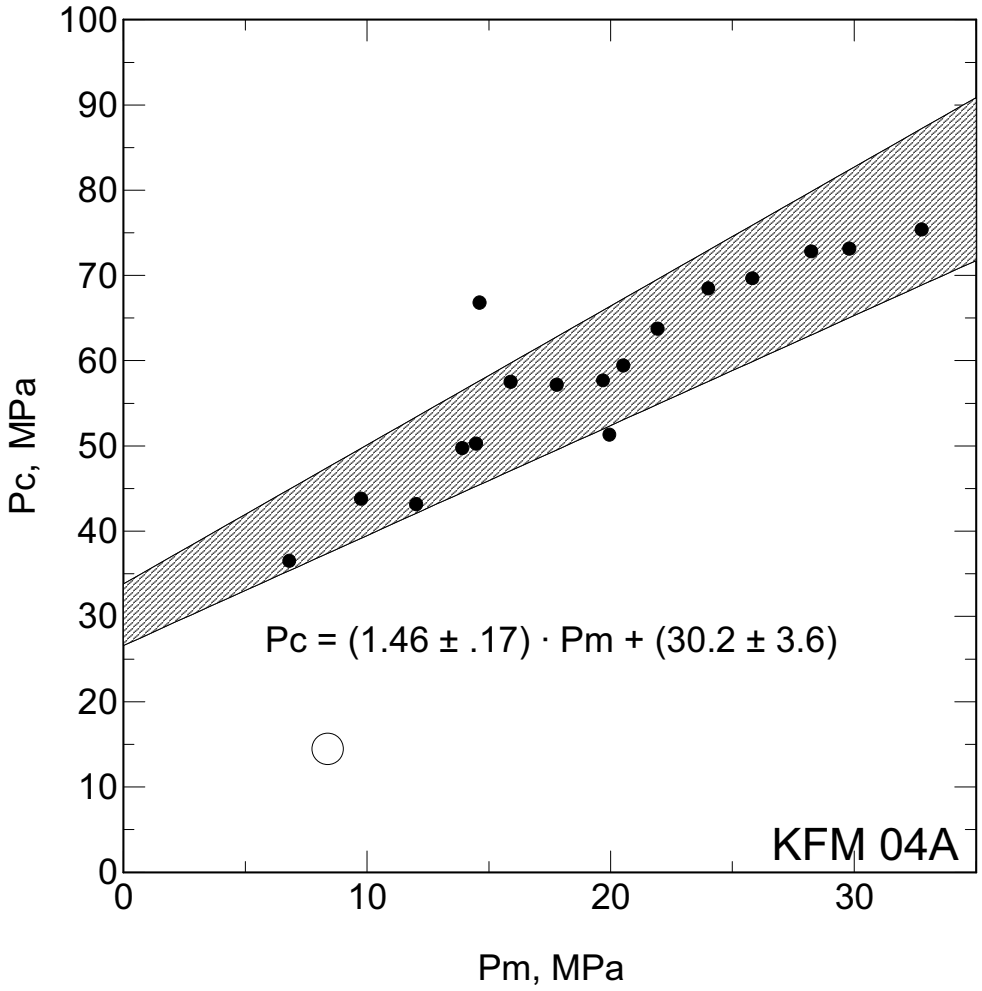

Figure 5-4. *Fracture initiation pressure p_c versus confining pressure p_m for samples from borehole KFM04A (open circles: not used for linear regression for p_c – relation).*

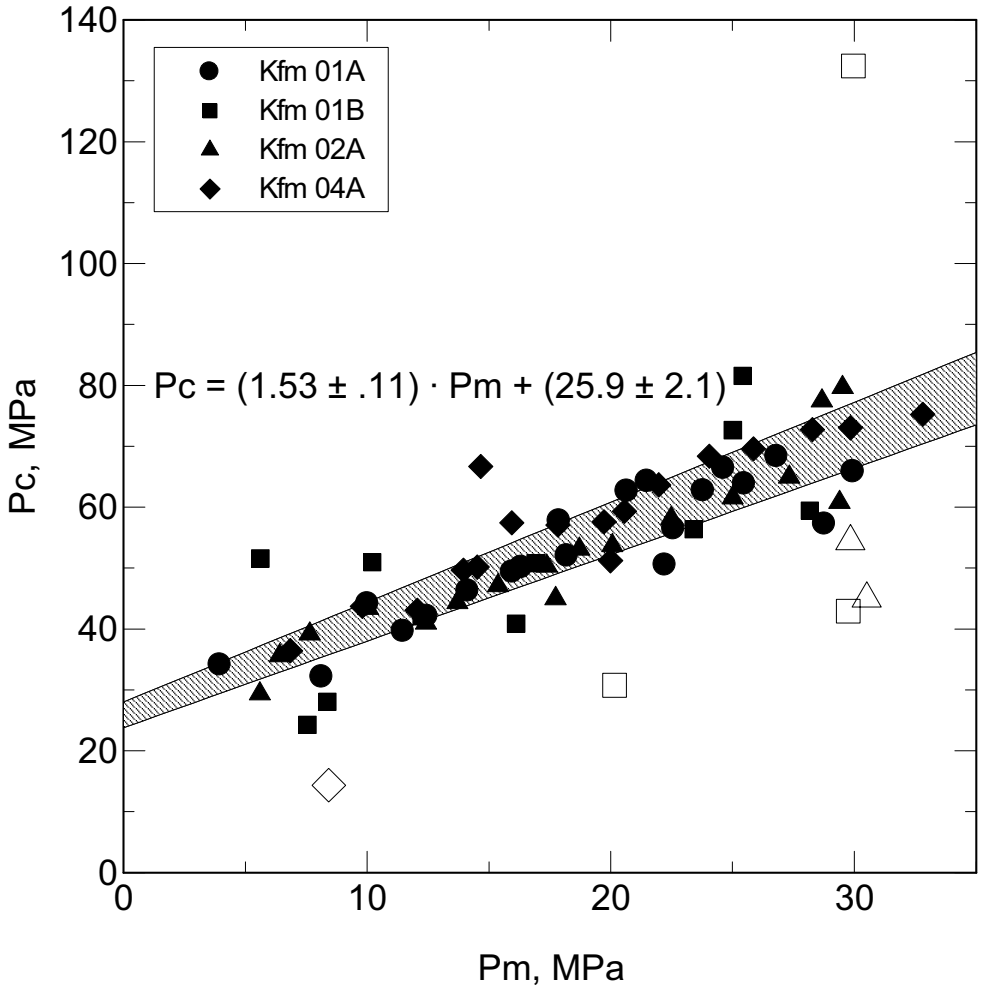

Figure 5-5. *Fracture initiation pressure p_c versus confining pressure p_m for samples from boreholes KFM01A, KFM01B, KFM02A and KFM04A (open circles: not used for linear regression for p_c – relation).*

6 Summary and discussions

6.1 Discussion of laboratory rock sample data

For an overview the mean data of the measured laboratory rock properties are summarized (without standard deviations):

Borehole no	1A	1B	2A	4A	Mean
ρ_{core} g/cm^3	2.661	2.652	2.653	2.665	2.655±0.009
ρ_{sample} g/cm^3	2.663	2.656	2.658	2.659	2.659±0.011
v_p, km/s	5.38	5.59	5.51	5.30	5.4±0.2
v_s, km/s	3.03	3.16	3.12	2.98	3.1±0.2
K_{IC}, MPa/m$^{1/2}$	1.92	2.12	2.19	1.97	2.04±0.27
p_{co}, MPa	27.1	24.7	23.0	30.2	25.9±2.1
k	1.39	1.60	1.61	1.46	1.53±.11
E, GPa	62	67	66	60	64±5
v	0.27	0.27	0.26	0.27	0.27

The variation in density, Young's modulus and fracture toughness are shown in Figure 6-1. The frequency distributions are displayed in Figure 6-2. Cross plots between K_{IC} and Young's moduli E and between densities and Young's moduli are given in Figure 6-3. As mentioned in Section 5.3, there exists a vague relation between K_{IC} and E, while the E vs. ρ plot shows random scatter. As a conclusion, the rock may be characterized as rather homogeneous with respect to ρ, E and K_{IC}.

As mentioned in Section 5.4 axial fractures were induced in most cases, an expression that weakness planes in the rock samples do not play an important role. As shown in Figure 5-5 the hydrofrac data demonstrate a clear linear relationship between p_c and the confining pressure p_m with only small scatter and independent on the rock from the different boreholes. Therefore, it is justified to accept the mean values for the tensile strength, p_{co}, and for the frac coefficient k as representative for the rock of the 4 boreholes in the Forsmark area.

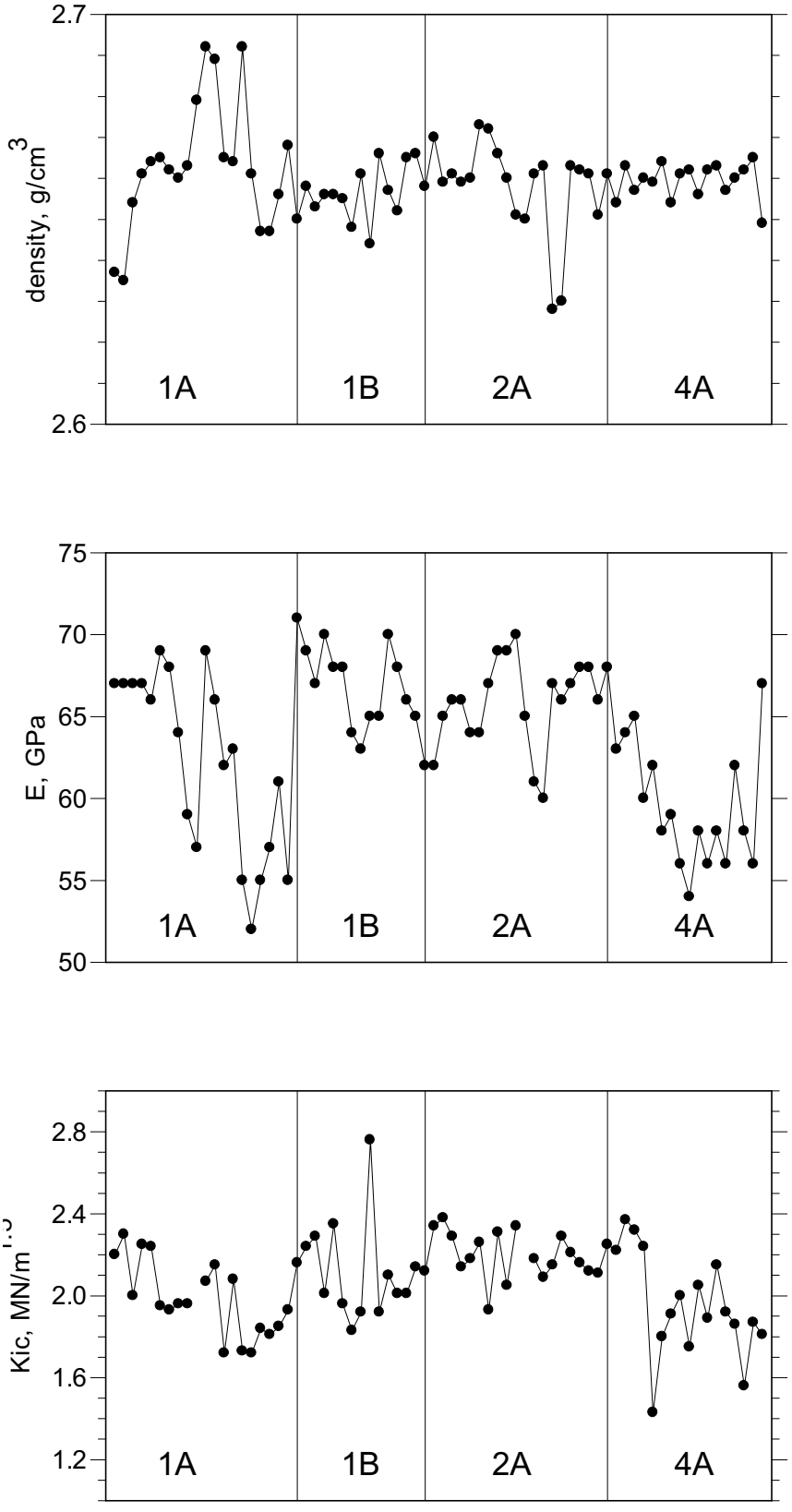

Figure 6-1. *Variation in density (sample density), Young's modulus and* K_{IC}.

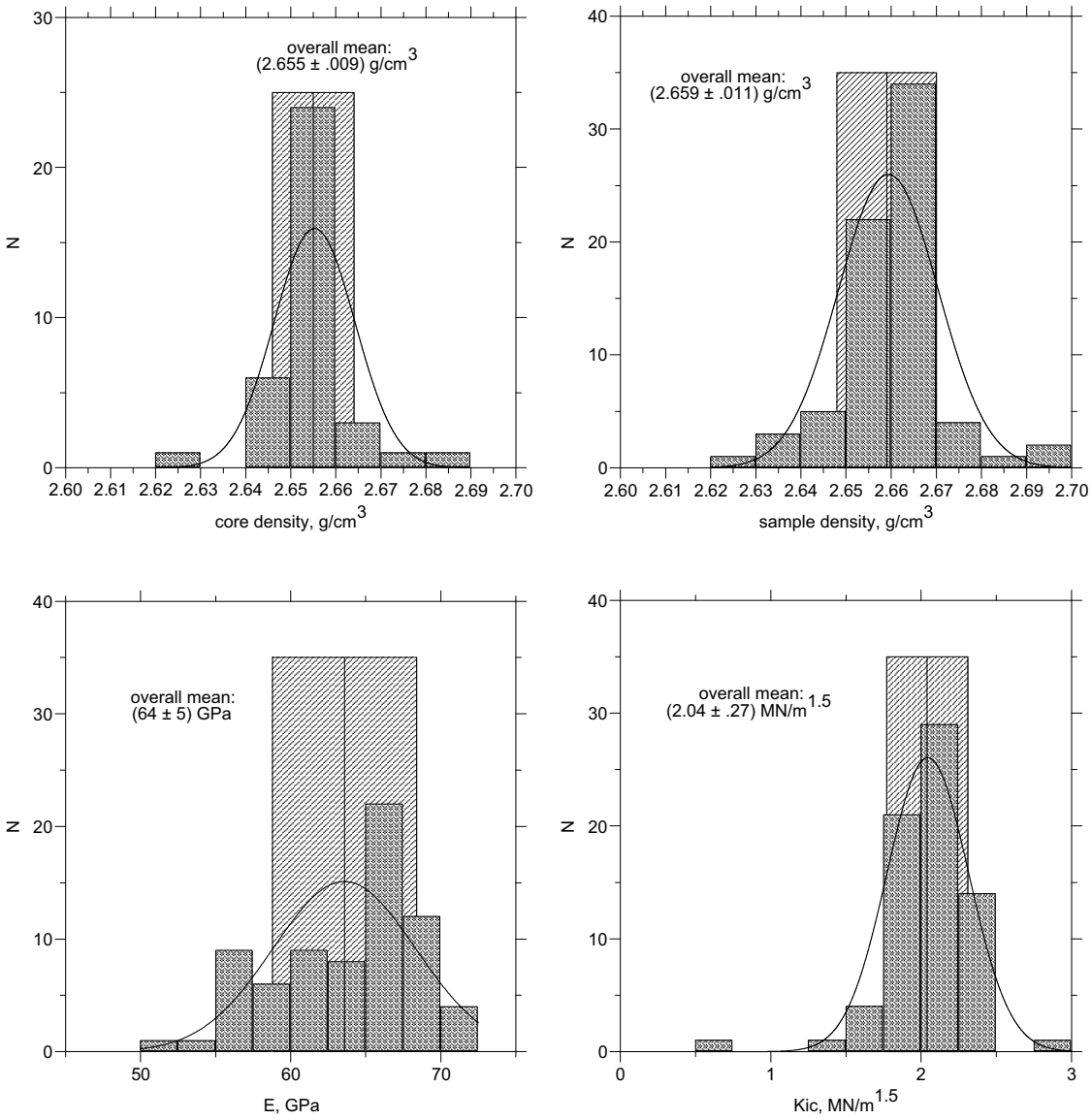

Figure 6-2. *Frequency distribution for density, Young's modulus and fracture toughness* K_{IC}.

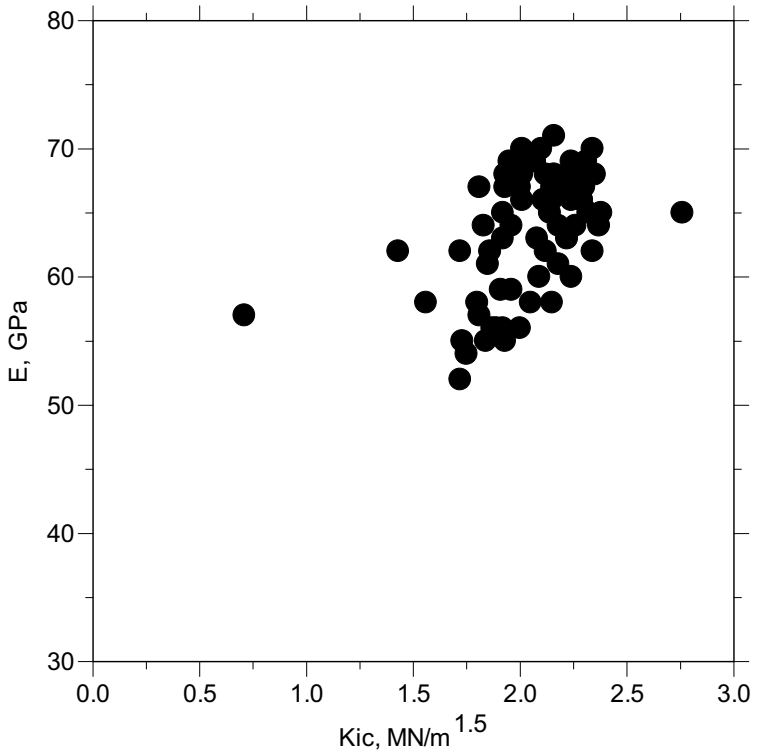

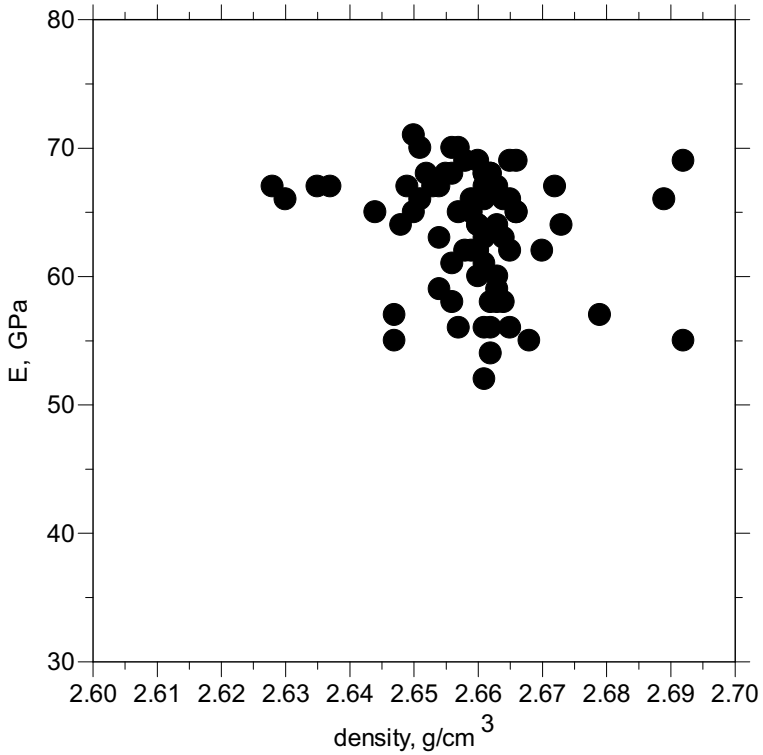

Figure 6-3. *Cross plots between E, ρ (sample density) and K_{IC}.*

6.2 Fracture mechanics analysis

The fracture mechanics analysis relates the fracture initiation pressure p_c to the confining pressure p_m and to the intrinsic crack length a_o of the sample /Rummel, 1987/ by the relations

$$p_c = \frac{K_{IC}}{(h_o + h_a)\sqrt{R}} + kp_m$$

$$k = \frac{f + g}{h_o + h_a}$$

$$p_{co} = \frac{K_{IC}}{(h_o + h_a)\sqrt{r}}$$

where f, g, h_o and h_a are dimensionless stress intensity functions for the effect of the far-field stress p_m (f and g), the pressure acting within the borehole of radius r (h_o), and the pressure acting within an existing microcrack prior to its instability (h_a). Thus, the laboratory hydraulic tensile strength p_{co} may be compared with the observed in-situ hydraulic tensile strength $P_{co} = P_c - P_r$ by the simple relation

$$p_{co} \cdot (h_o + h_a) \cdot \sqrt{r} = P_{co} \cdot (H_o + H_a) \cdot \sqrt{R}$$

where capital letters refer to the in-situ case. The relation assumes that K_{IC} is not size dependent and is valid for both the laboratory rock samples and the in-situ rock. The dimensionless stress intensity factors are only dependent on the existing crack size in the sample (a_o) and the in-situ rock (A_o). Thus, the relations allow to speculate from the laboratory tests on both the in-situ hydraulic tensile strength P_{co} and the characteristic crack size of the rock samples and the in-situ rock.

Neglecting the difference in the stress intensity function values for the laboratory and the in-situ cases, the laboratory tensile strength values p_{co} suggest in-situ tensile strength values P_{co} of approximately 5.6 MPa, compared to observed strength values of approximately 9.2 MPa (see Final Report No 28.04 A). The data for the different boreholes are as follows:

Borehole	p_{co} MPa	P_{co} (observed) MPa	P_{co} (calculated) MPa
KFM01A	27.1 ± 3.1 (20)	10.8 ± 3.8 (20)	4.8 to 6.1
KFM01B	24.7 ± 8.2 (11)	8.7 ± 3.5 (7)	3.3 to 6.5
KFM02A	23.0 ± 2.9 (17)	8.4 ± 4.0 (26)	4.0 to 5.1
KFM04A	30.2 ± 3.6 (17)	6.2 ± 1.9 (3)	5.2 to 6.1
mean	25.9 ± 2.1 (65)	9.2 ± 4.0 (56)	5.6 ± 0.4

( ) number of tests

The result clearly demonstrates the size effect, and the comparison shows that the measured in-situ tensile strength values of approximately 9.2 MPa may be considered as realistic for the in-situ rock for the case of hydraulic fracturing.

When solving above given relations for ($h_o + h_a$) and ($H_o + H_a$), respectively, and considering the dependence of the stress intensity functions on the crack size a_o for the laboratory scale and A_o for the in-situ case, we obtain the following data using the appropriate data for the fracture toughness K_{IC}:

Borehole	K_{IC} MN/3/2	$h_o + h_a$	a_o mm	$H_o + H_a$	A_o mm
KFM01A	1.92 (20)	1.89	0.95	1.15	7.9
KFM01B	2.12 (14)	2.59	2.7	1.56	18.4
KFM02A	2.19 (19)	2.52	1.9	1.76	27.7
KFM04A	1.97 (18)	1.74	0.7	1.86	26.9
Mean	2.04 (71)	2.07	1.1	1.22	17.2

( ) number of tests

The result again is an expression of the size effect with an intrinsic crack size a_o of the laboratory samples in the mm-range, while due to the larger rock surface exposed at the pressurization during the in-situ tests, the intrinsic crack-size A_o of the rock is more than 10 times larger. The small crack size of the rock samples is also supported by the rather high value of the frac coefficient k = 1.5. The result also suggests that the Hubbert and Willis concept for in-situ stress evaluation is appropriate, since fluid penetration into the rock prior to fracturing can be neglected.

6.3 Fracture mechanics hydrofrac simulation

The simulation calculations were carried out by the MeSy fracture mechanics simulation code FRAC /e.g. Weber and Rummel, 1995; Rummel et al. 1995; Rummel and Hansen, 1989/. It is assumed that the vertical stress is the intermediate principal stress, the most critical microcrack of the test interval aligned with the major horizontal stress S_H is activated, and propagates in the direction perpendicular to the least principal stress S_h. Crack growth will occur whenever the stress intensity at the crack tip exceeds the fracture toughness of the rock. The stress intensity is controlled by the far field stresses S_H and S_h, the fluid pressure in the test interval, p, and the fluid pressure distribution within the fracture, p_a, which is expressed by the pressure gradient coefficient c_2. The model further assumes that the fracture height is equivalent to the length of the test interval (0.8 m) and remains constant, the injected fluid is water with a viscosity of 1 cPoise. For fracture toughness K_{IC}, we take the mean values determined for each borehole, the same for the mean elasticity parameters E and ν, and for the crack length B ($B = 1 + A_o/R$) derived from the observed hydraulic mean strength P_{co} for each borehole.

A total of 12 simulation calculations were carried out for 3 HF-tests in borehole KFM01A, for 3 HF-tests in borehole KFM01B, for 4 HF-tests in borehole KFM02A, and for 2 HF-tests in borehole KFM04A. Input parameters were the following:

- MD measured depth, in m,
- TVD true vertical depth, in m,
- borehole radius R, 0.04 m (constant),

- test section length L, 0.8 m (constant),
- effective rock density ρ, in kg /m^3 (derived from S_v to guarantee consistency with in-situ report),
- rock permeability K, in µDarcy (from in-situ P-test),
- rock strength P_{co}, in MPa (from in-situ tests),
- fracture toughness K_{IC}, in MN/m^2 (from lab tests),
- normalized initial crack length B from fracture mechanics analysis of P_{co}),
- fluid viscosity, cPoise (1 cP for water),
- injection rate, in m^3/s (see in-situ tests),
- system compressibility, in m^2/N (from in-situ test pressurization cycle),
- crack width w, in mm (simulation parameter),
- pressure loss coefficient c_1 at crack inlet (c_1 = 1, i.e. no pressure loss),
- pressure gradient coefficient c_2 within a microcrack (simulation parameter),
- S_H/S_V ratio from in-situ test Report,
- S_h/S_H ration (from in-situ test Report).

Further input parameters are the acceptable overpressure limit (some Pa), the acceptable accuracy for input energy (10 Joule), the number of iteration steps, or the definition of final crack length (end of stimulation). The used numbers for all input parameters are listed in Table 6-1 for the 4 boreholes. The simulation results are shown in Figure 6-4 in the form of pressure-time plots in comparison with the specific observed in-situ plot, and in the form of crack length B versus time plots (normalized crack length B = 1 + A/R, A crack length, R borehole radius).

As can be seen from Figures 6-4a to 6-4l, the frac cycle of each test can be well matched using the in-situ experimental parameters (test interval length for fracture height, injection rate q, system compressibility, test depth), the stress ratios derived from the in-situ tests (MeSy Report 28.04 A), the rock permeability derived from the in-situ P-tests (MeSy Report 28.04 A), and the fracture toughness K_{IC} determined during laboratory testing. For final matching only the model parameters fracture width w, the initial microcrack length A_o, and the fluid pressure gradient coefficient c_2 had to be varied within reasonable limits. Most attention was paid to match the magnitude of the in-situ observed breakdown pressure, but in most cases even the pumping pressure after fracture growth initiation is well simulated, which may be taken as an indication that those fractures propagated in a direction perpendicular to S_h. As one can see from the plots fracture length versus time, the fractures grow to a length of approximately ten times the borehole radius during the fracture cycle, a result which seems acceptable by assuming a constant fracture height of 0.8 m (test interval length). Thus, the simulation supports the results of the in-situ stress evaluation and may be regarded as an independent quality control.

Table 6-1. Input parameters for hydrofrac simulation in boreholes KFM01A, KFM01B, KFM02A and KFM04A.

Borehole		KFM 01A			KFM 01B			KFM 02A				KFM 04A	
Test depth MD, m		456.26	502.0	975.5	187.9	237.0	410.5	220.7	551.6	626.19	704.3	196.91	553.90
Depth of measuring interval: TVD, m		453.	498.	960.	183.	231.	397.	214	549.	624.	701.	173.	173.
Radius of borehole: R, m		0.04	0.04	0.04	0.04	0.04	0.04	0.04	0.04	0.04	0.04	0.04	0.04
Radius of hydraulic-hose : r_{hyd}, mm		4	4	4	4	4	4	4	4	4	4	4	4
Fracture toughness: K_{IC}, $MN/m^{3/2}$		1.92	1.92	1.92	2.12	2.36	2.12	2.19	2.19	2.19	2.19	1.97	1.97
Average rock density: ρ, kg/m^3		2,836	2,839	2,846	2,811	2,821	2,834	2,409	2,677	2,697	2,713	3,220	3,311
Rock permeability: perm, µDarcy		1	1	12	7	13	4.00	43	1	20	2	5	3
S_H/S_v: X		1.63	1.59	1.37	2.36	2.10	1.70	2.33	1.57	1.52	1.47	2.49	1.12
S_h/S_H: Y		0.62	0.62	0.63	0.59	0.60	0.62	0.48	0.72	0.75	0.77	0.38	0.75
P_{c0}, MPa		10.6	10.6	10.6	8.7	8.7	8.7	8.4	8.4	8.4	8.4	6.2	6.2
Pre-existing fracture length : $B_0=1+A_0/R$		1.100	1.130	2.100	1.910	1.085	1.900	1.120	3.800	2.000	3.300	7.000	1.090
End of fracture simulation: B_{end}	(1)	30	8	10	15	20	20	10	20	20	20	40	40
Crack width: w, mm		0.8	2.5	2	1.5	0.5	1.5	0.9	2	0.5	.5	0.2	0.5
Crack height: h, m		0.80	0.80	0.80	0.80	0.80	0.80	0.80	0.80	0.80	0.80	0.80	0.80
Pressure decay at crack inlet: c_1		1.00	1.00	1.00	1.00	1.00	1.00	1.00	1.00	1.00	1.00	1.00	1.00
Coefficient for pressure drop along crack: c_2		0.220	0.500	0.700	0.400	0.012	0.400	0.52	0.600	0.900	0.800	0.100	0.010
System stiffness: κ, $\cdot 10^{-9} m^2/N$		0.85	1.15	0.53	1.50	0.90	0.70	0.50	1.10	0.55	0.25	1.15	0.10
Pumping rate: q, $\cdot 10^{-5}$ m^3/s		1.33	1.67	1.08	1.83	1.33	1.83	0.75	2.50	1.00	1.00	1.00	0.83
Accuracy for energy determination: eps, J	(2)	100	10	10	10	10	10	10	10	10	10	10	10
Limit of iteration steps : n_{end}	(2)	200	200	200	200	400	400	400	400	400	400	400	400
Pressure over p_c : p_{opc}, Pa	(2)	10	10	10	10	5	5	5	5	5	5	5	5

(1): B_{end} only determines numerically simulation duration and minimizes the data file
(2): P_{opc}, n_{end} and eps are only numerical parameters for fracture growth stability

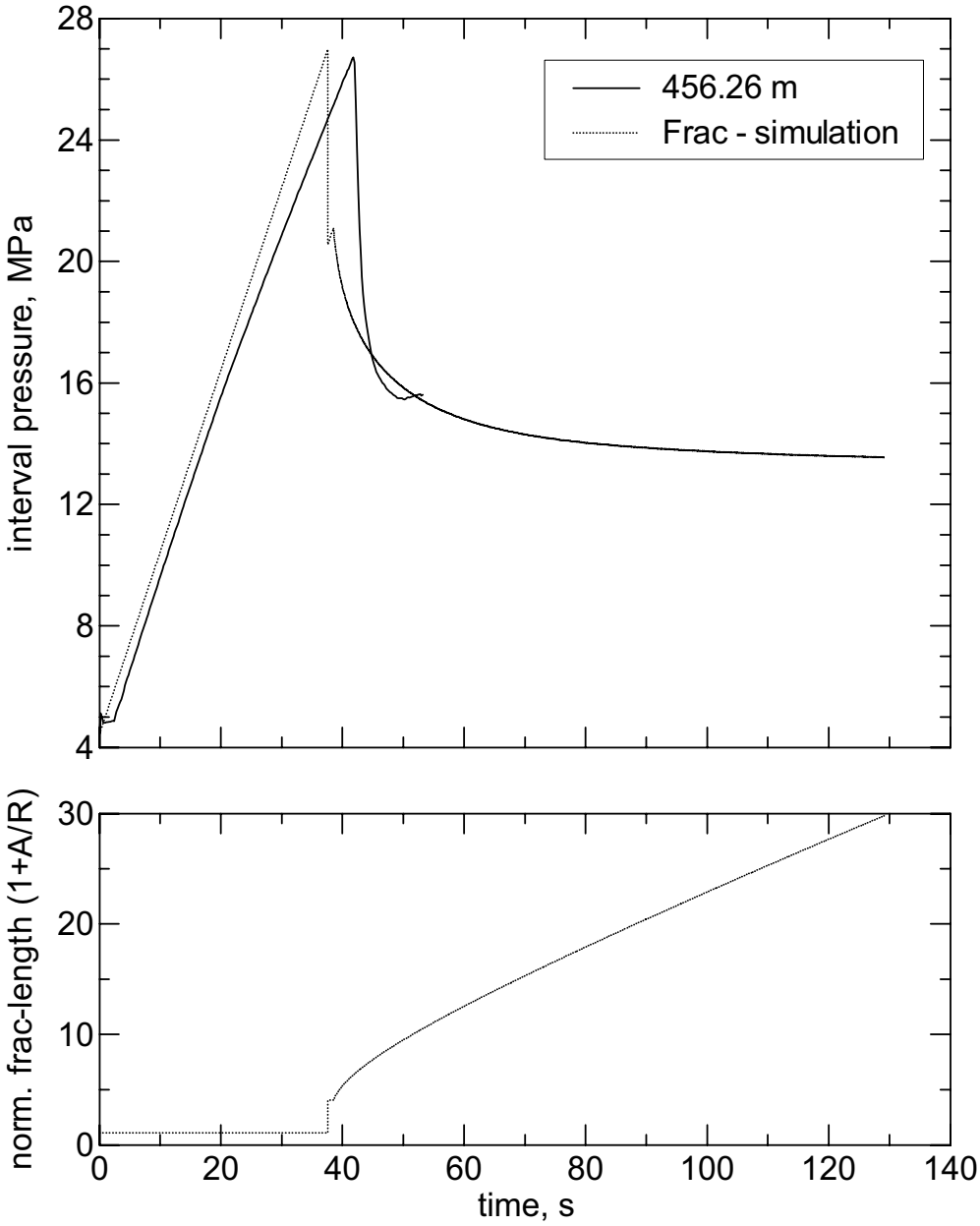

Figure 6-4a. *Hydrofrac simulation for test 8 at 456 m depth in borehole KFM01A.*

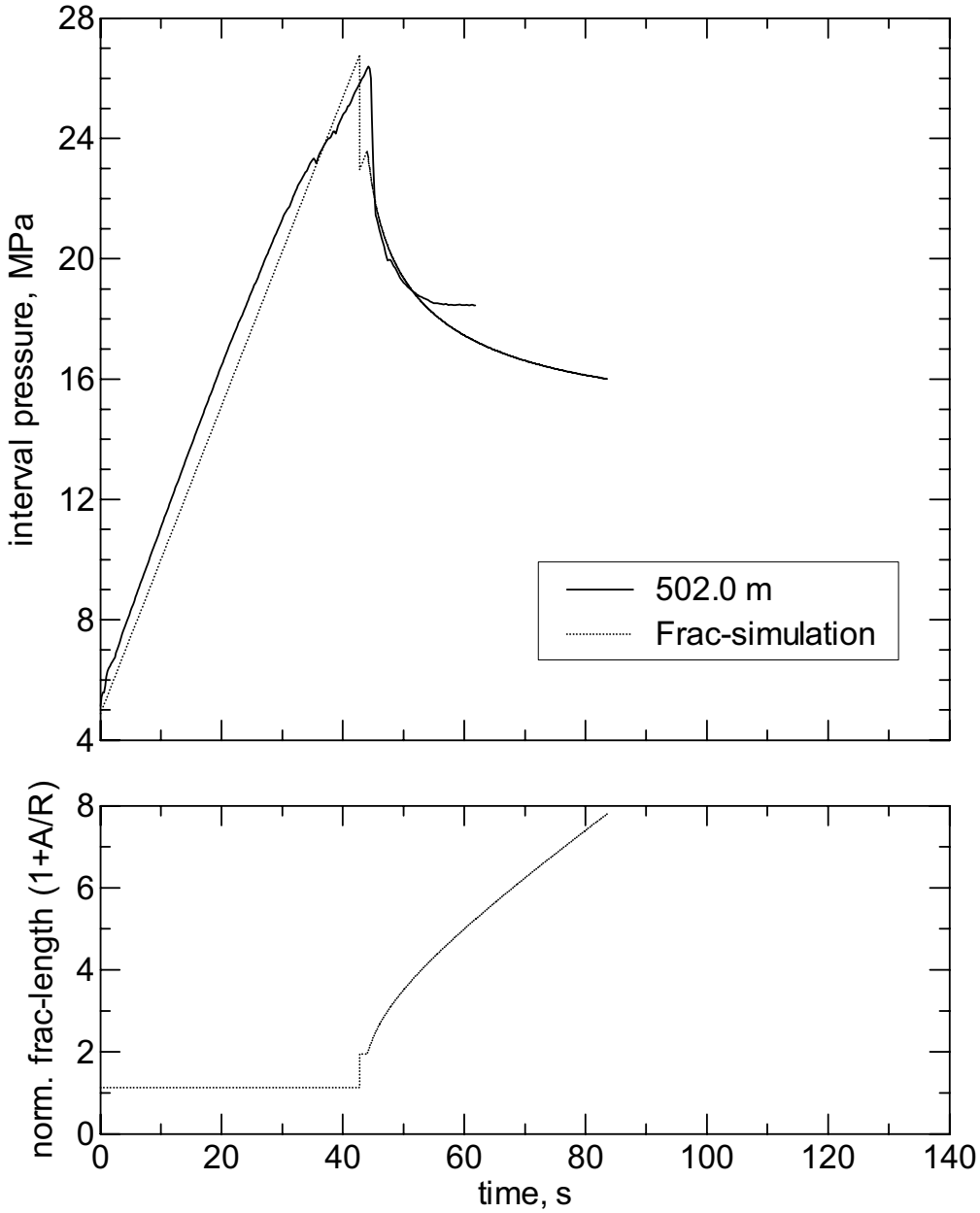

Figure 6-4b. *Hydrofrac simulation for test 2 at 502 m depth in borehole KFM01A.*

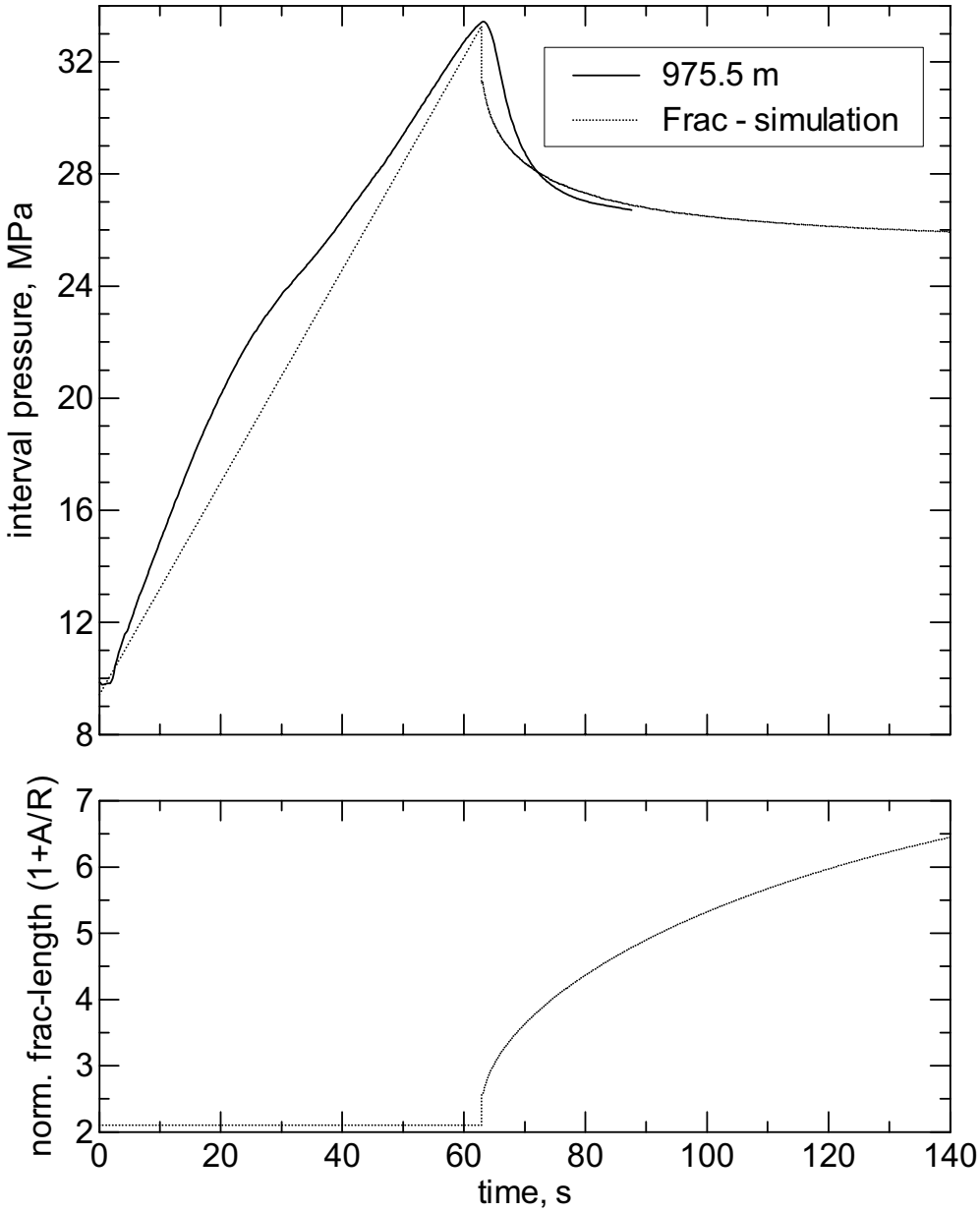

Figure 6-4c. *Hydrofrac simulation for test 10 at 975.5 m depth in borehole KFM01A.*

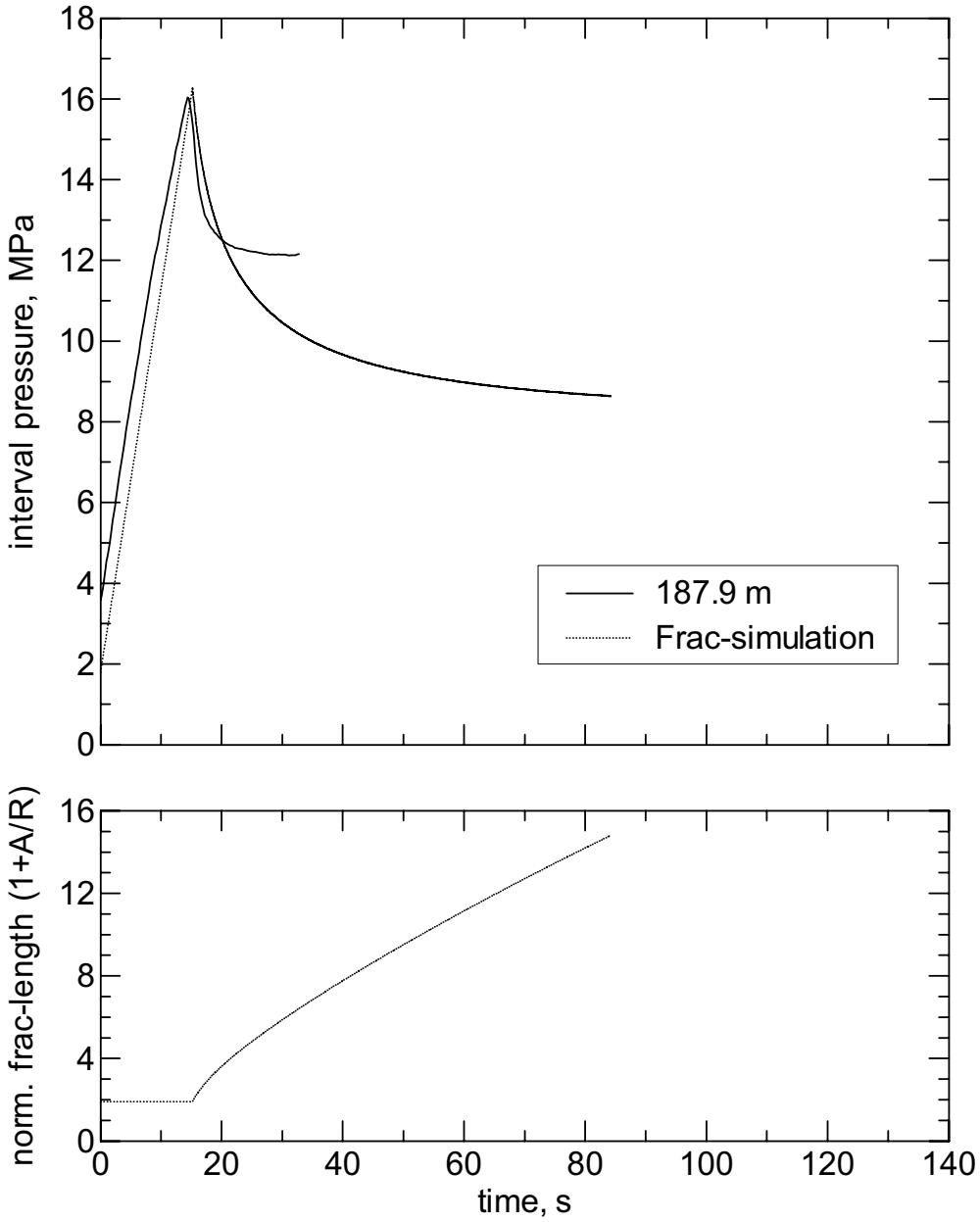

Figure 6-4d. *Hydrofrac simulation for test 2 at 188 m depth in borehole KFM01B.*

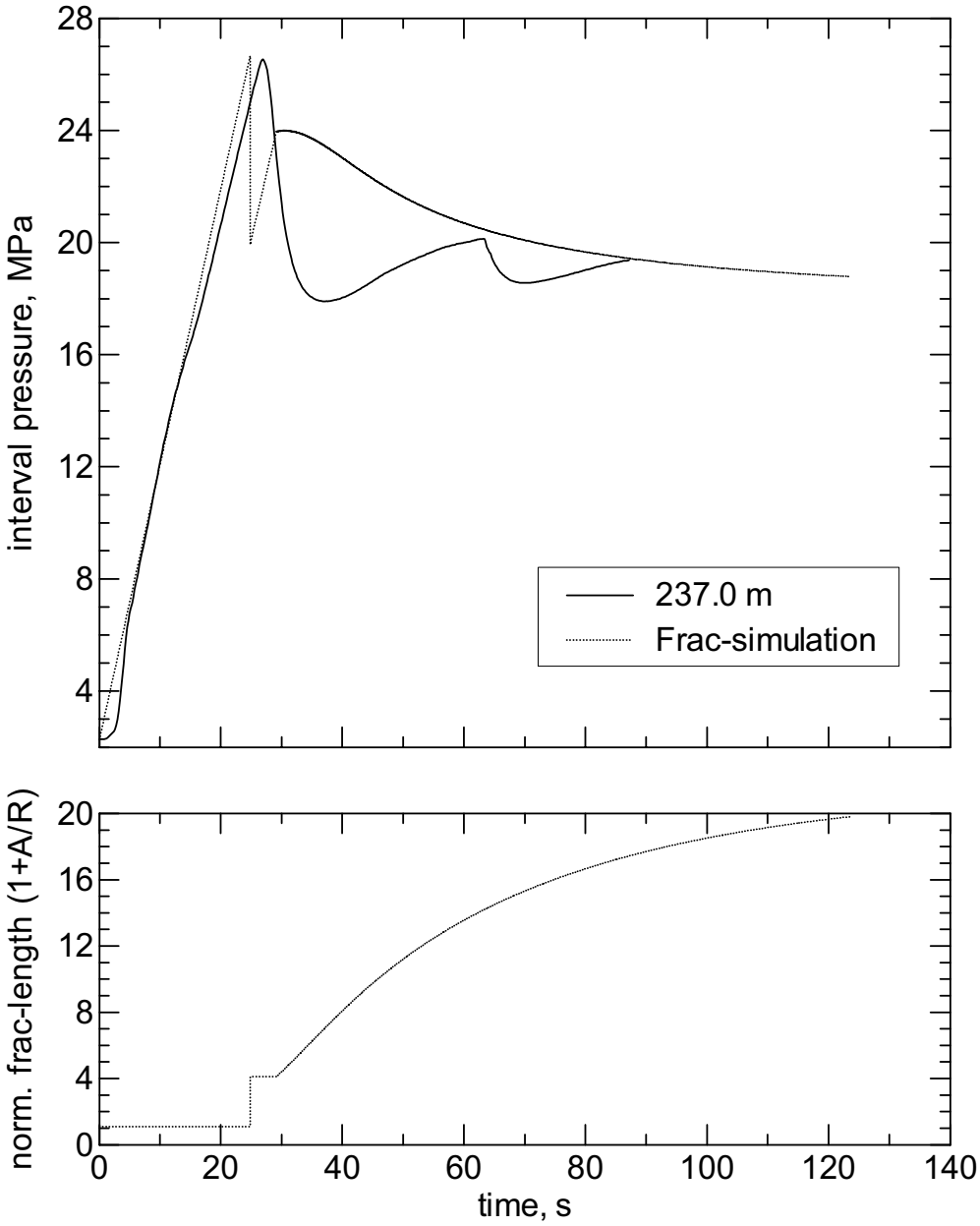

Figure 6-4e. *Hydrofrac simulation for test 10 at 237 m depth in borehole KFM01B.*

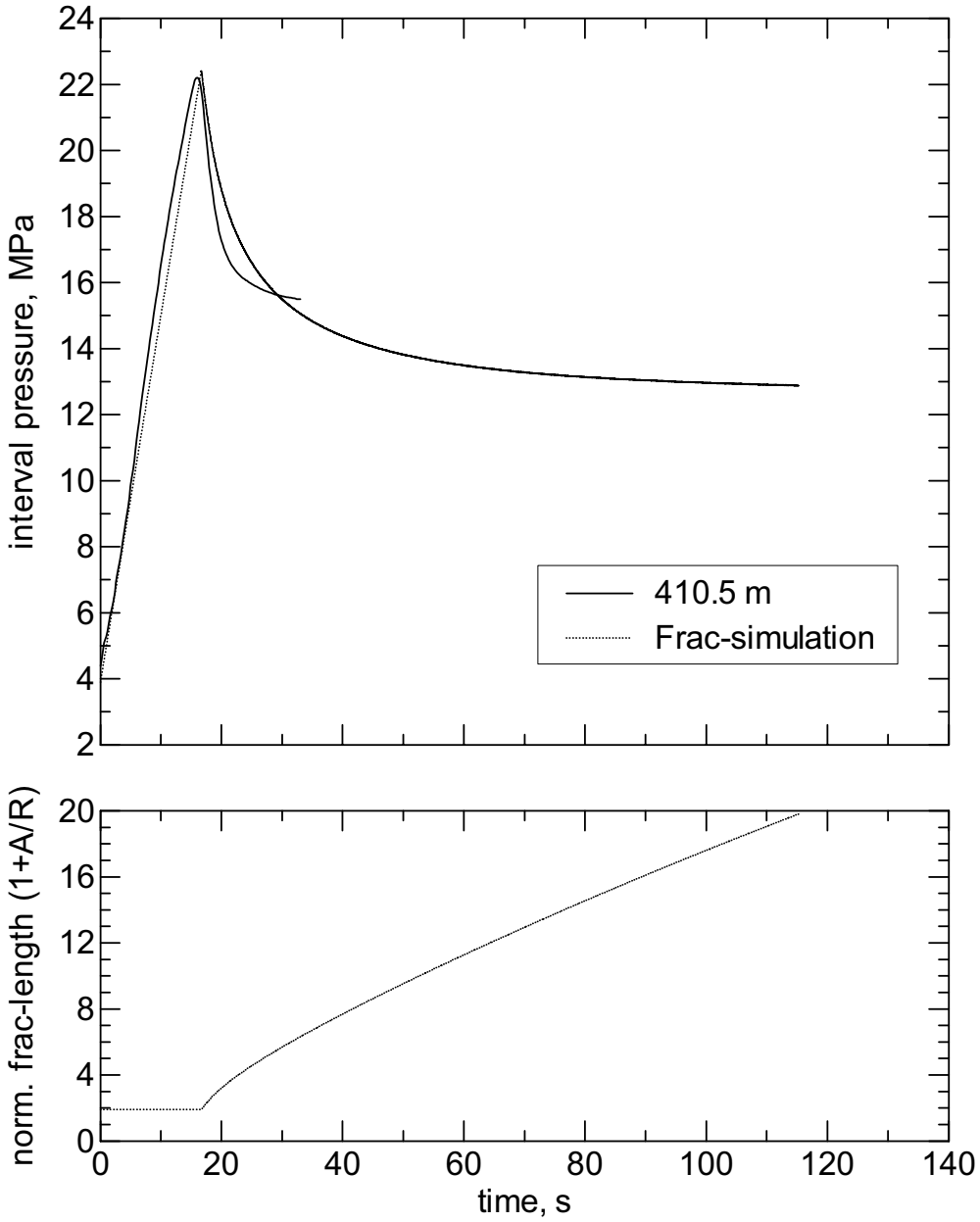

Figure 6-4f. *Hydrofrac simulation for test 8 at 410.5 m depth in borehole KFM01B.*

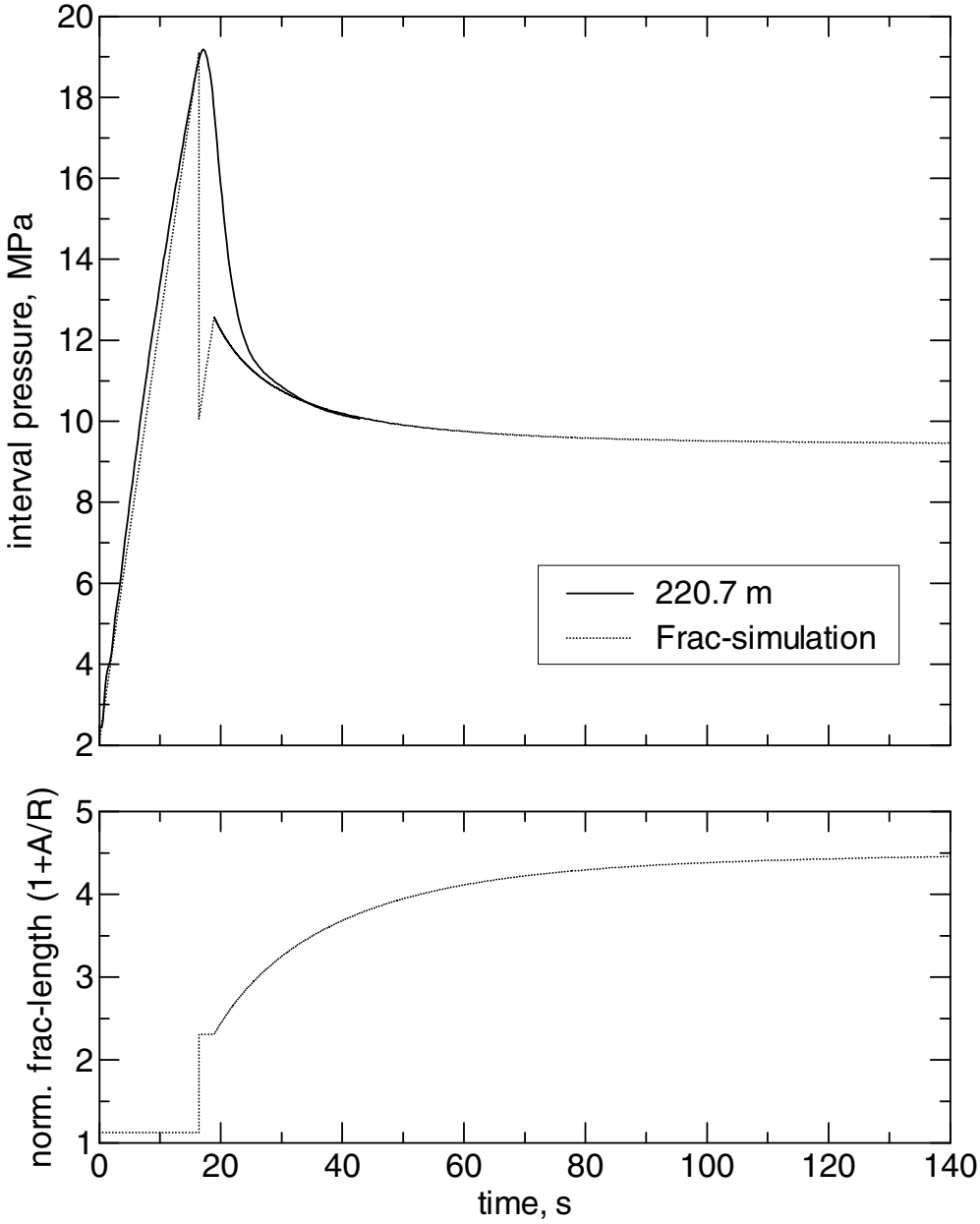

Figure 6-4g. *Hydrofrac simulation for test 35 at 221 m depth in borehole KFM02A.*

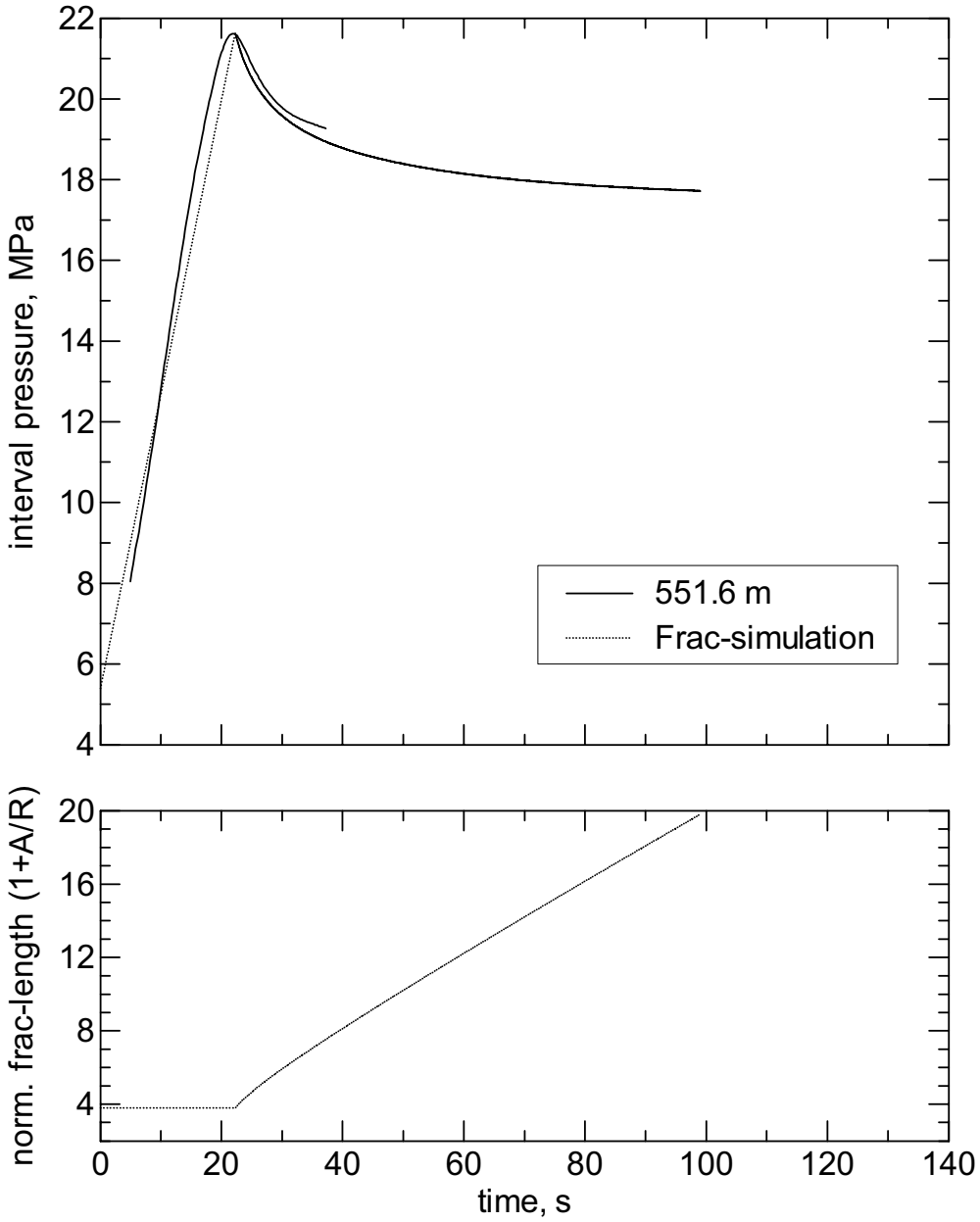

Figure 6-4h. *Hydrofrac simulation for test 20 at 551.6 m depth in borehole KFM02A.*

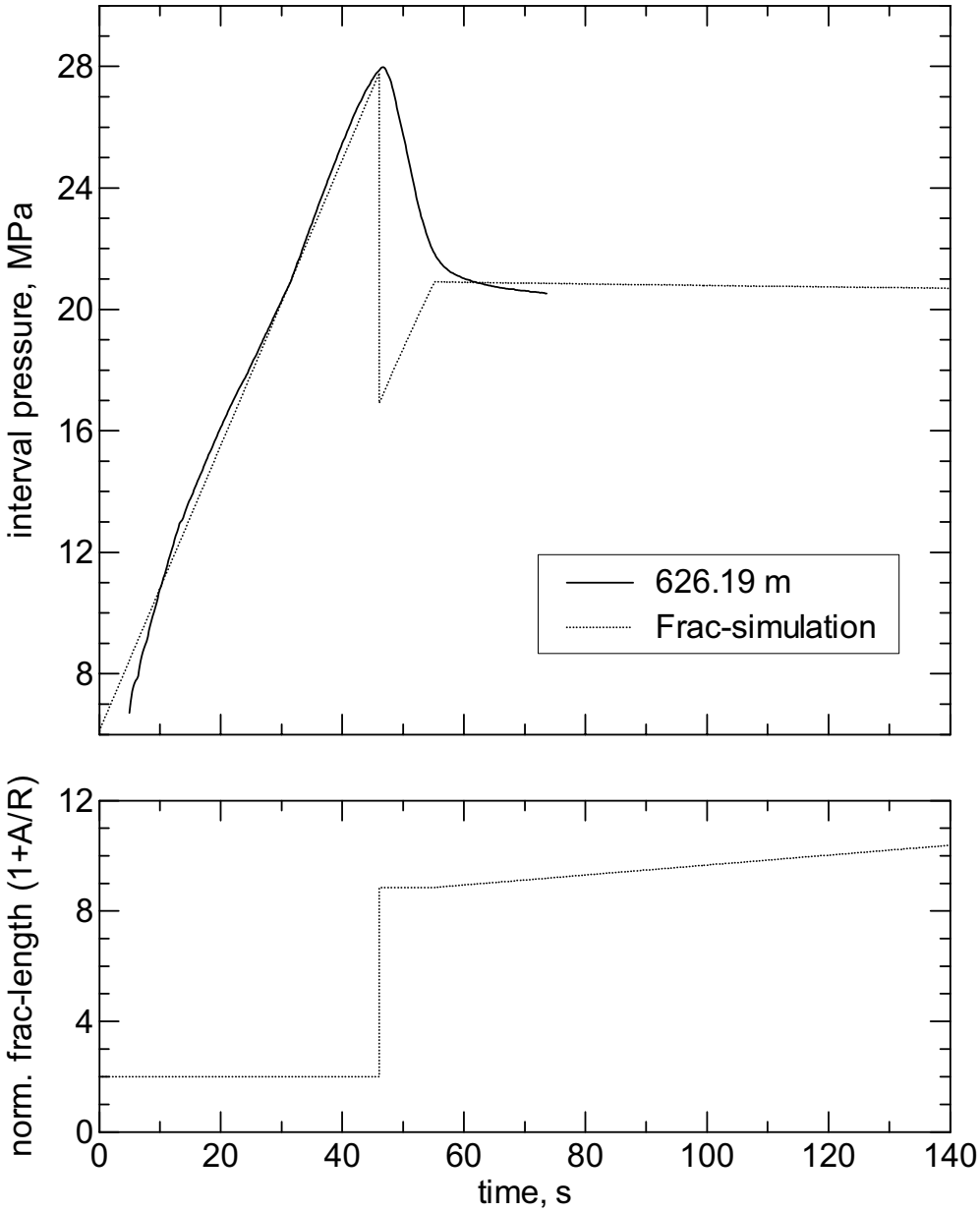

Figure 6-4i. *Hydrofrac simulation for test 9 at 626.2 m depth in borehole KFM02A.*

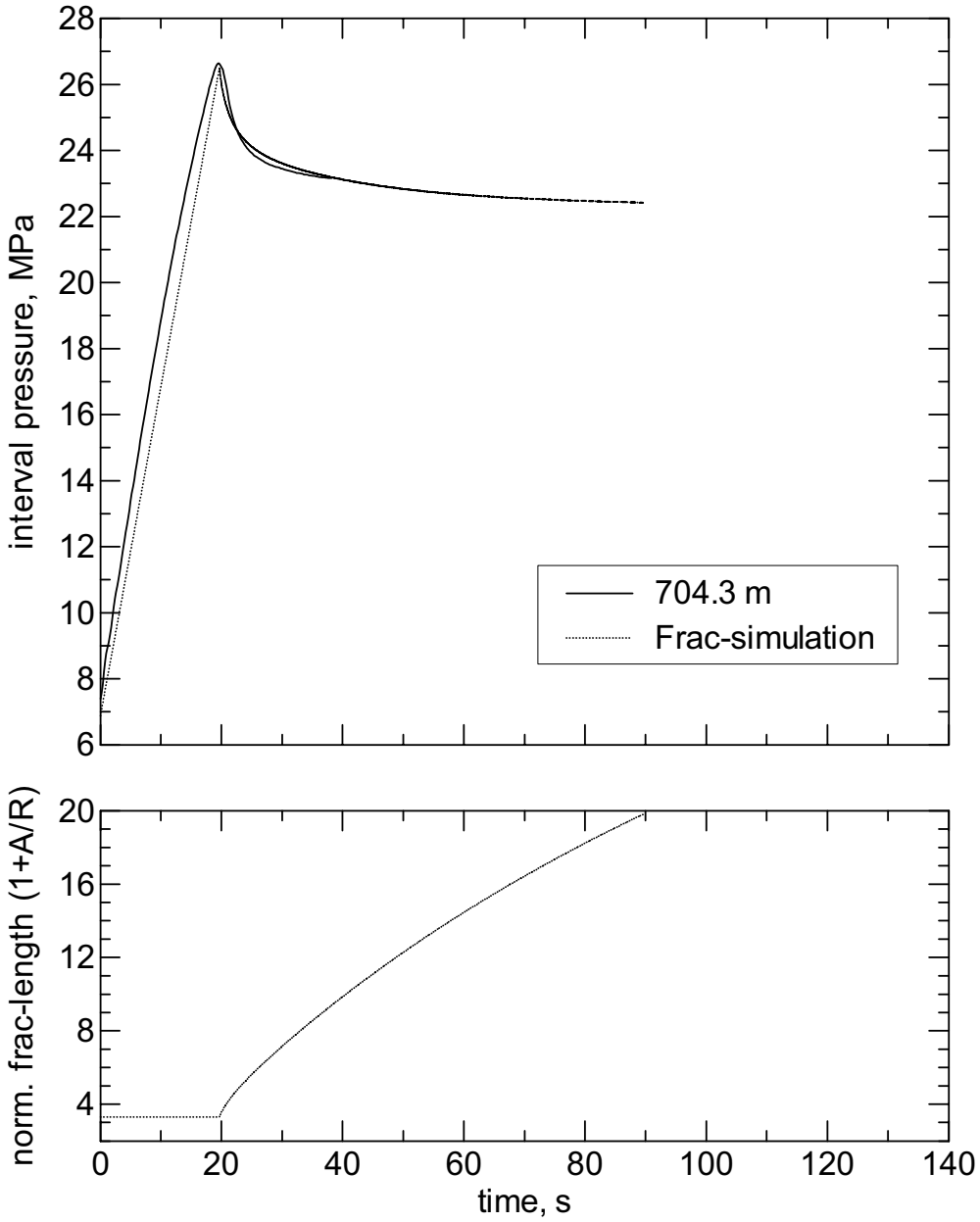

Figure 6-4j. *Hydrofrac simulation for test 3 at 704.3 m depth in borehole KFM02A.*

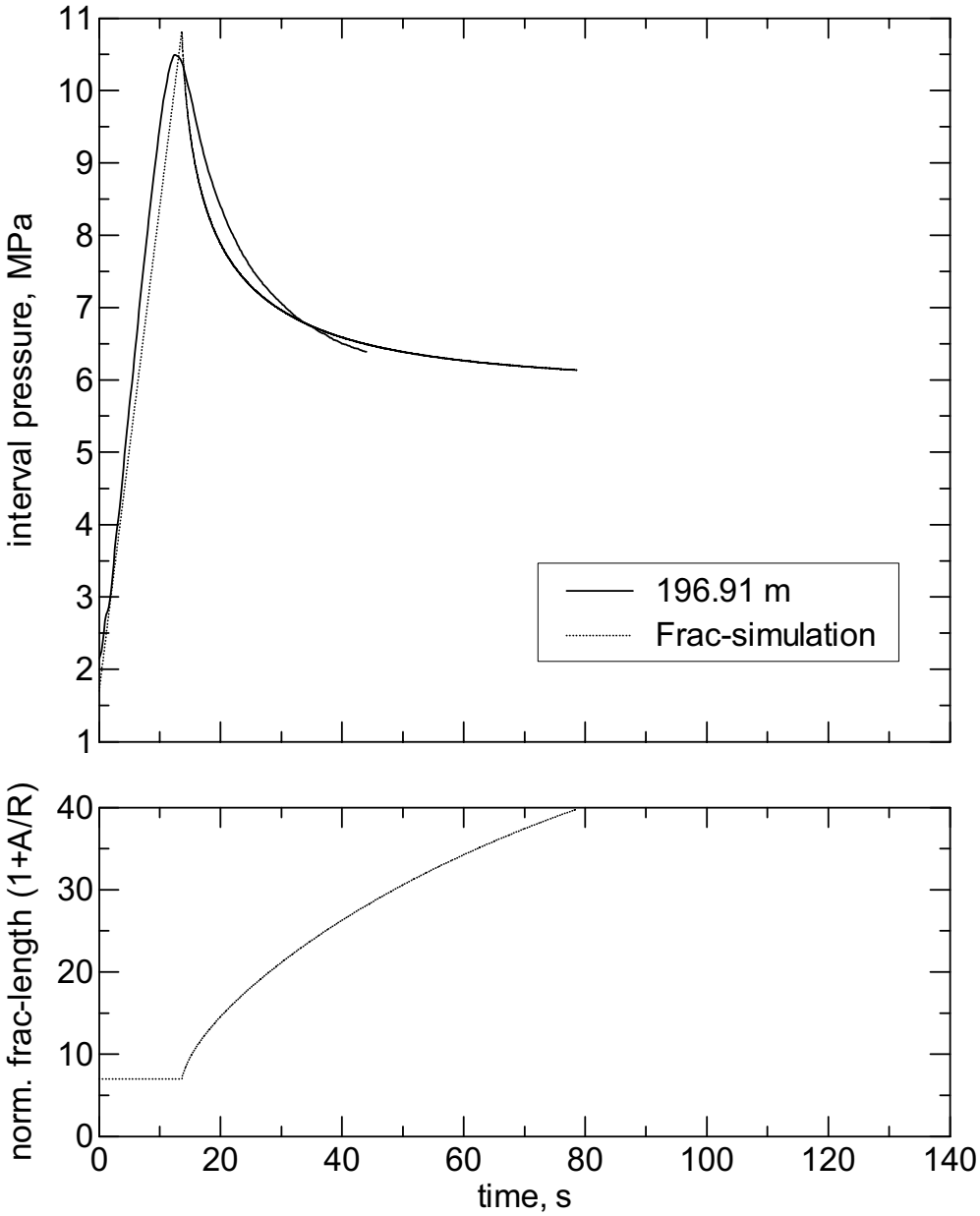

Figure 6-4k. *Hydrofrac simulation for test 10 at 196.9 m depth in borehole KFM04A.*

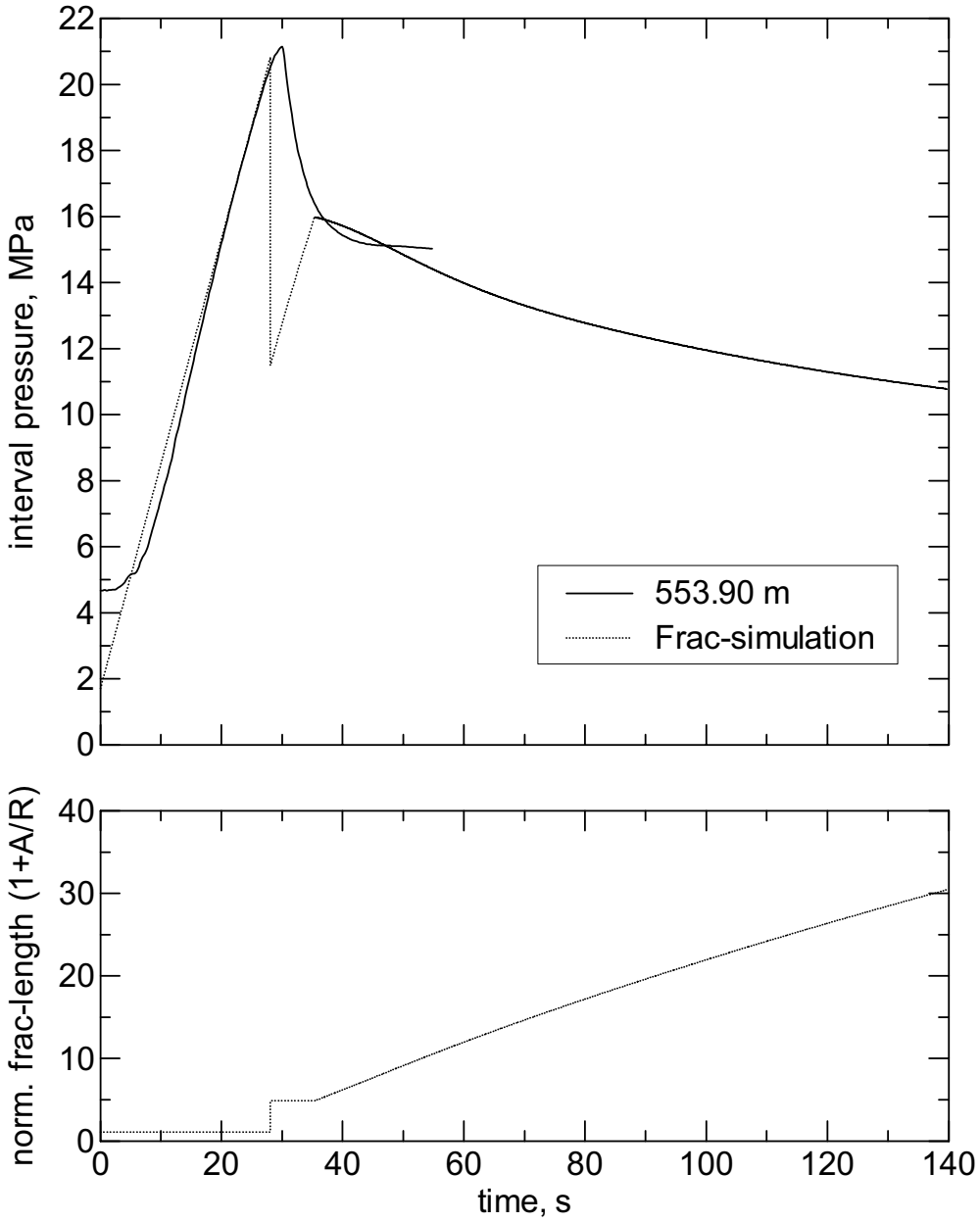

Figure 6-4l. *Hydrofrac simulation for test 4 at 553.9 m depth in borehole KFM04A.*

References

Atkinson BK, Meredith PG, 1987. Experimental fracture mechanic data for rocks and minerals. In: Fracture Mechanics of Rock (ed. Atkinson), Ch. 11, 477–525, Acad. Press Geol. Ser.

Ingraffea AR, Gunsallus KL, Beech JF, Nelson PP, 1984. Chevron-notched specimen: testing and analysis. ASTM, STP 855, 152–156.

Olofsson T, 1978. Rep. 195 E, Univ. Lulea.

Ouchterlony F, Sun Z, 1983. New methods of measuring fracture toughness of cores. Svedefo Rep. DS 1983:10.

Ouchterlony F et al. 1988. ISRM suggested methods for determining fracture toughness of rock. Int. J. Rock Mech, 25, 71–96.

Rummel F, van Heerden WL, 1978. ISRM suggested methods for determining sound velocity. Int. J. Rock Mech, 15, 53–58.

Rummel F, 1987. Fracture mechanics approach to hydraulic fracturing stress measurements. In: Fracture Mechanics of Rock (ed. Atkinson), Ch. 6, 217–239, Acad. Press Geol. Ser.

Rummel F, Hansen J, 1989. Interpretation of hydrofrac pressure recordings using a simple fracture mechanics simulation model. Int. J. Rock. Mech, 26/6, 483–488.

Rummel F, Klee G, Weber U, 1995. Hydraulic versus pneumatic fracturing for in-situ stress determination in rock salt. Int. J. Rock Mech, 32/4, 337–342.

Weber U, Rummel F, 1995. Fracture mechanics models for sensitivity analysis of hydraulic fracturing model parameters. Proc. world Geothermal Congress Florence, Vol. 4, 2563–2564.

Acknowledgement

This report is part of the Final Report for SKB order no 10485 dated 5.3.2004 on "Hydraulic fracturing technique during SKB's site investigations for the location Forsmark". We are grateful to Mr. Rolf Christiansson for contract negotiations, numerous scientific discussions during on-site work and suggestions for the preparations of the Final Report. We are also grateful to Mr Roger Taringer (Swepro) acting as project coordinator and responsible for control of activities and quality management. The core material for laboratory testing was selected with R Christiansson and R Taringer. The laboratory tests were conducted by the following MeSy personnel: U Weber, H Vogt, F Seebald, M Witthaus and L Küperkoch, the data interpretation was in the responsibility of U Weber and F Rummel.

Appendix A

Core Piece Data Sheet

client:		SKB AB	
project:		SKB, Forsmark	
operator:		Seebald, Weber	
date:		04.06.04	
borehole:		KFM 01A	
core piece number:		1A-1	
depth (min, max), m:		423.00-423.34	
core dimensions:			
length (min), mm:	342	diameter (min), mm:	50.6
length (max), mm:	342	diameter (max), mm:	50.6
core piece mass, g		1821.3	
remarks and observations:			

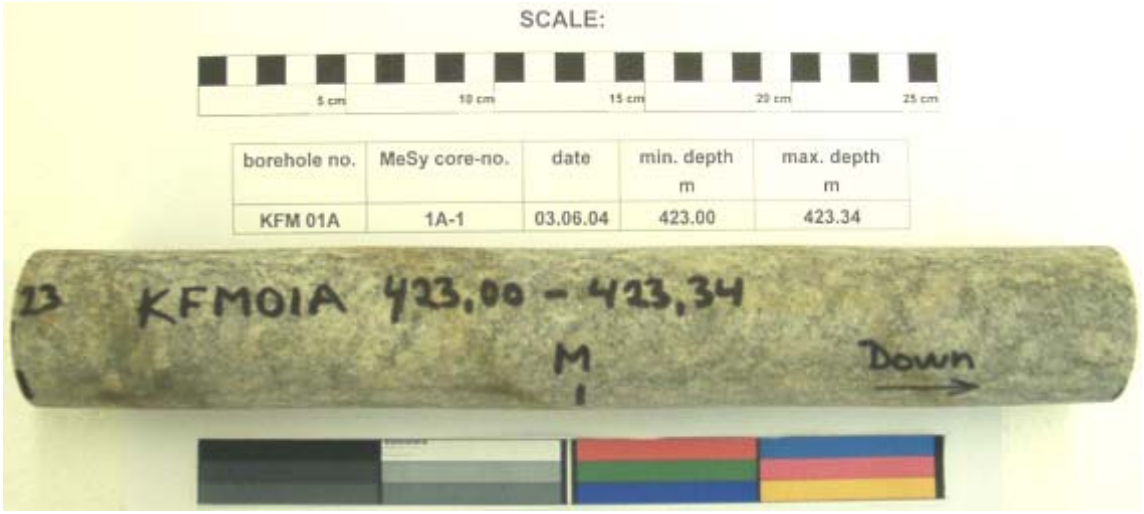

client:		SKB AB	
project:		SKB, Forsmark	
operator:		Seebald, Weber	
date:		04.06.04	
borehole:		KFM 01A	
core piece(s) number(s):		1A-2	
depth (min, max), m:		424.66 - 425.00	
core dimensions:			
length (min), mm:	339	diameter (min), mm:	50.7
length (max), mm:	341	diameter (max), mm:	50.7
core piece mass, g		1816.8	
remarks and observations:			

client:		SKB AB	
project:		SKB, Forsmark	
operator:		Seebald, Weber	
date:		04.06.04	
borehole:		KFM 01A	
core piece(s) number(s):		1A-3	
depth (min, max), m:		428.00 - 428.34	
core dimensions:			
length (min), mm:	338	diameter (min), mm:	50.8
length (max), mm:	339	diameter (max), mm:	50.8
core piece mass, g		1818.6	
remarks and observations:			

client:		SKB AB	
project:		SKB, Forsmark	
operator:		Seebald, Weber	
date:		04.06.04	
borehole:		KFM 01A	
core piece(s) number(s):		1A-4	
depth (min, max), m:		484.42 - 484.76	
core dimensions:			
length (min), mm:	338	diameter (min), mm:	50.7
length (max), mm:	338	diameter (max), mm:	50.7
core piece mass, g		1809.9	
remarks and observations:			

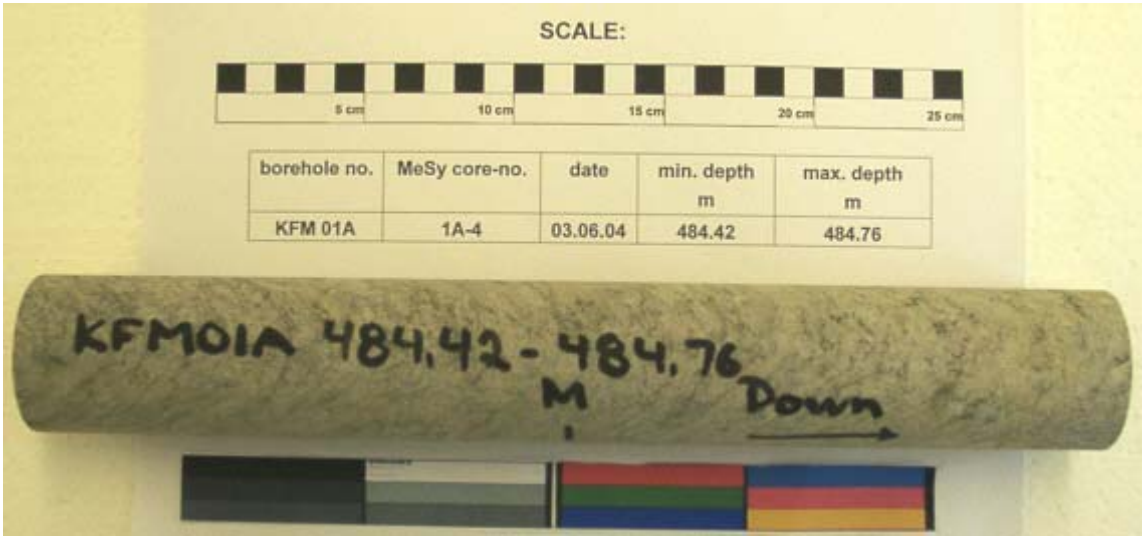

client:		SKB AB	
project:		SKB, Forsmark	
operator:		Seebald, Weber	
date:		04.06.04	
borehole:		KFM 01A	
core piece(s) number(s):		1A-5	
depth (min, max), m:		489.78 - 490.12	
core dimensions:			
length (min), mm:	341	diameter (min), mm:	51.0
length (max), mm:	341	diameter (max), mm:	51.0
core piece mass, g		1845.2	
remarks and observations:			

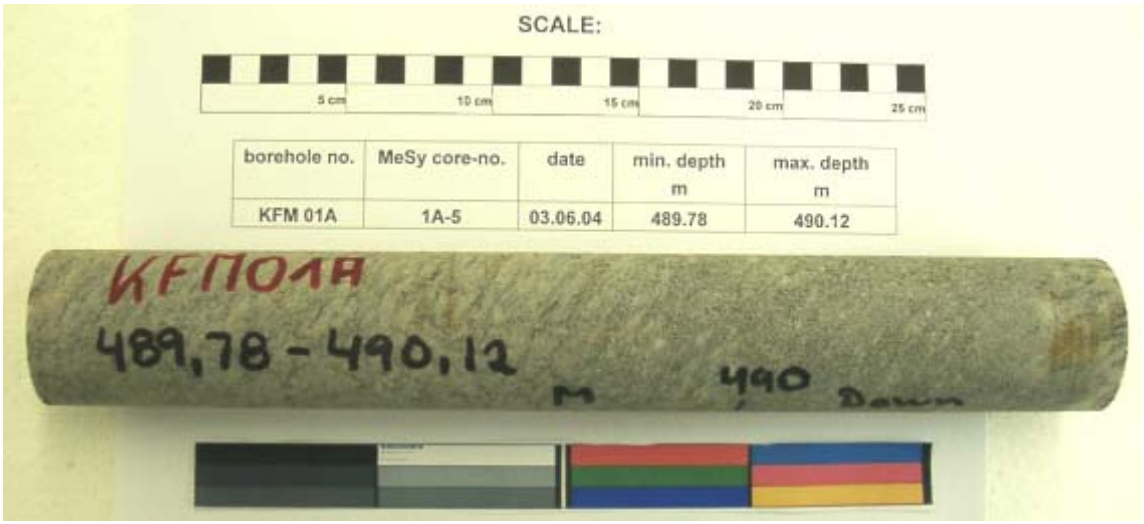

client:		SKB AB	
project:		SKB, Forsmark	
operator:		Seebald, Weber	
date:		04.06.04	
borehole:		KFM 01A	
core piece(s) number(s):		1A-6	
depth (min, max), m:		504.52 - 504.86	
core dimensions:			
length (min), mm:	337	diameter (min), mm:	50.9
length (max), mm:	337	diameter (max), mm:	50.8
core piece mass, g		1827.2	
remarks and observations:			

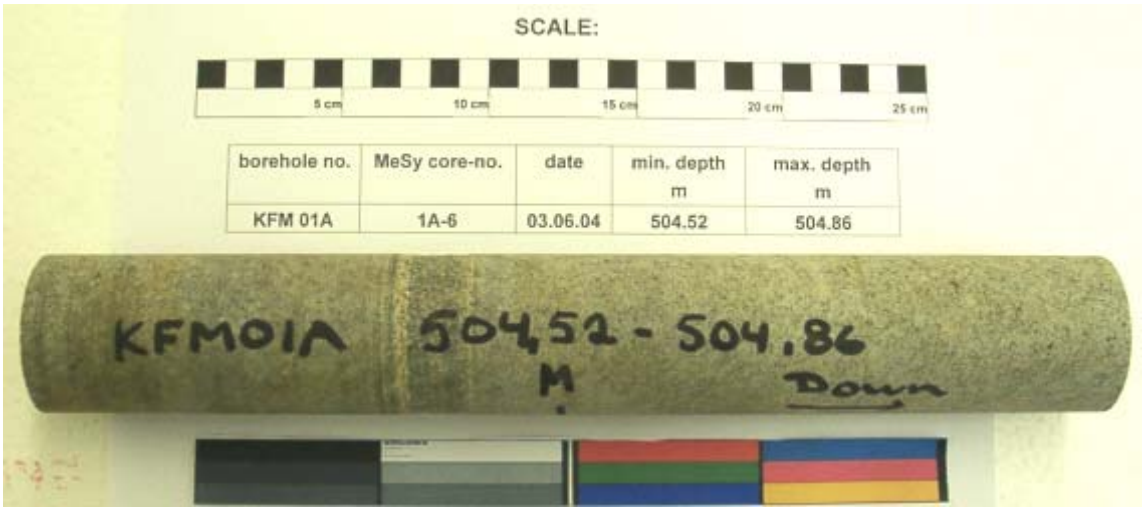

client:		SKB AB	
project:		SKB, Forsmark	
operator:		Seebald, Weber	
date:		04.06.04	
borehole:		KFM 01A	
core piece(s) number(s):		1A-7	
depth (min, max), m:		687.96 - 688.30	
core dimensions:			
length (min), mm:	337	diameter (min), mm:	51.1
length (max), mm:	337	diameter (max), mm:	51.0
core piece mass, g		1831.3	
remarks and observations:			

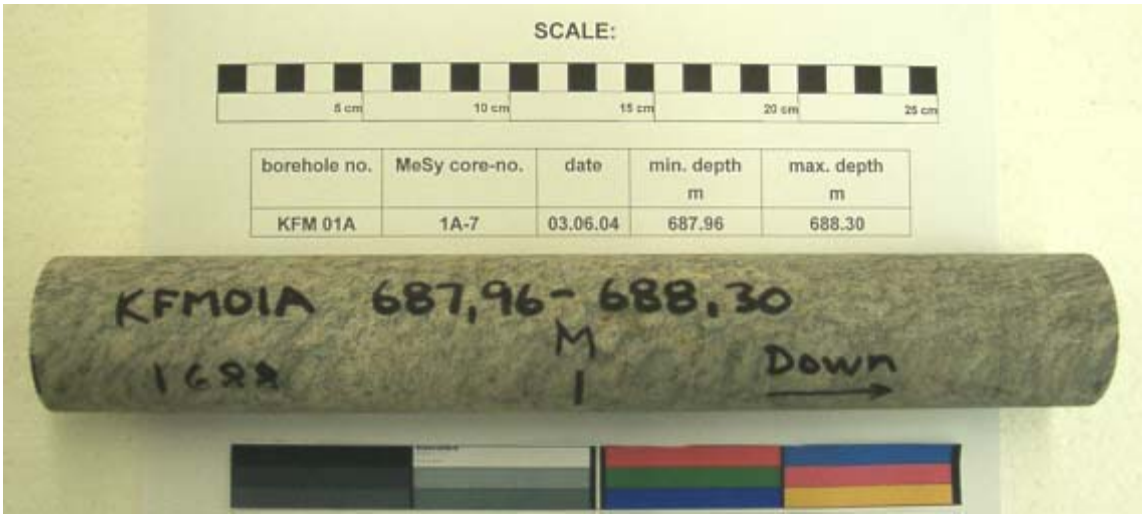

client:		SKB AB	
project:		SKB, Forsmark	
operator:		Seebald, Weber	
date:		04.06.04	
borehole:		KFM 01A	
core piece(s) number(s):		1A-8	
depth (min, max), m:		949.83 - 950.17	
core dimensions:			
length (min), mm:	338	diameter (min), mm:	51.0
length (max), mm:	338	diameter (max), mm:	51.0
core piece mass, g		1828.3	
remarks and observations:			

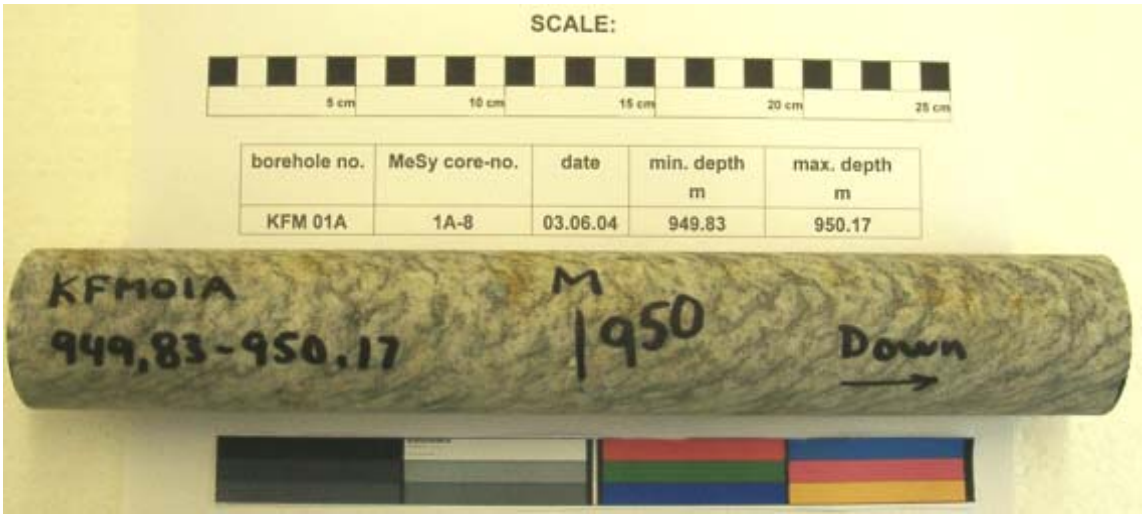

client:		SKB AB	
project:		SKB, Forsmark	
operator:		Seebald, Weber	
date:		04.06.04	
borehole:		KFM 01A	
core piece(s) number(s):		1A-9	
depth (min, max), m:		971.40 - 971.74	
core dimensions:			
length (min), mm:	340	diameter (min), mm:	50.9
length (max), mm:	340	diameter (max), mm:	50.8
core piece mass, g		1817.4	
remarks and observations:			

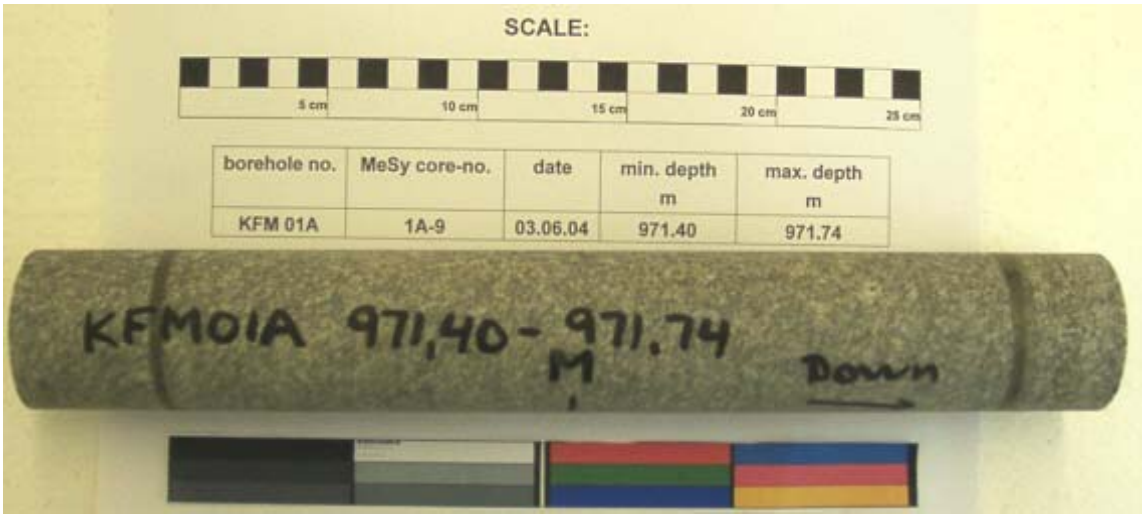

client:		SKB AB	
project:		SKB, Forsmark	
operator:		Seebald, Weber	
date:		04.06.04	
borehole:		KFM 01A	
core piece(s) number(s):		1A-10	
depth (min, max), m:		978.36 - 978.70	
core dimensions:			
length (min), mm:	341	diameter (min), mm:	50.8
length (max), mm:	342	diameter (max), mm:	50.8
core piece mass, g		1837.8	
remarks and observations:			

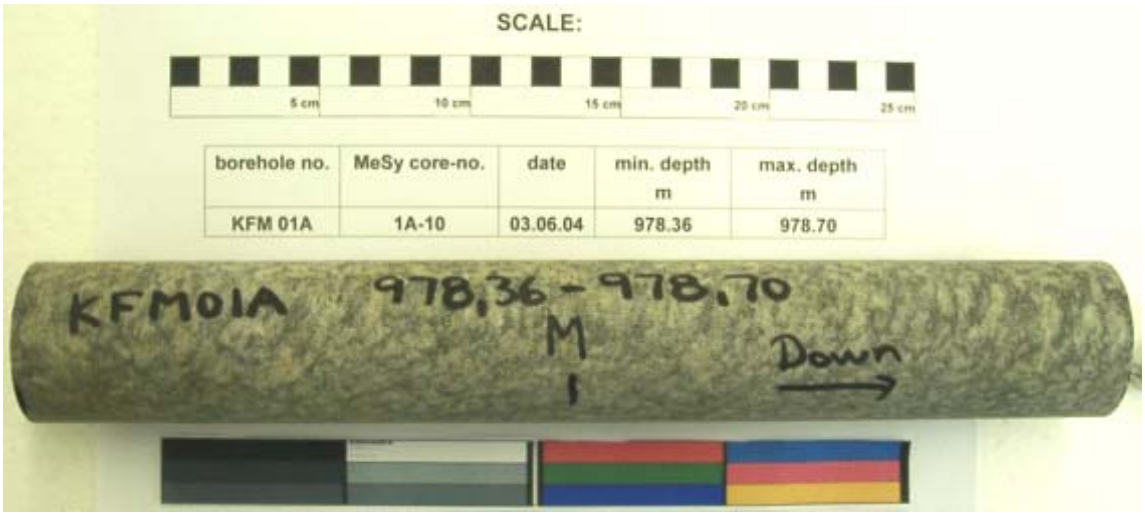

client:		SKB AB	
project:		SKB, Forsmark	
operator:		Seebald, Weber	
date:		04.06.04	
borehole:		KFM 01B	
core piece(s) number(s):		1B-1	
depth (min, max), m:		420.86 - 421.20	
core dimensions:			
length (min), mm:	337	diameter (min), mm:	50.7
length (max), mm:	338	diameter (max), mm:	50.7
core piece mass, g		1804.4	
remarks and observations:			

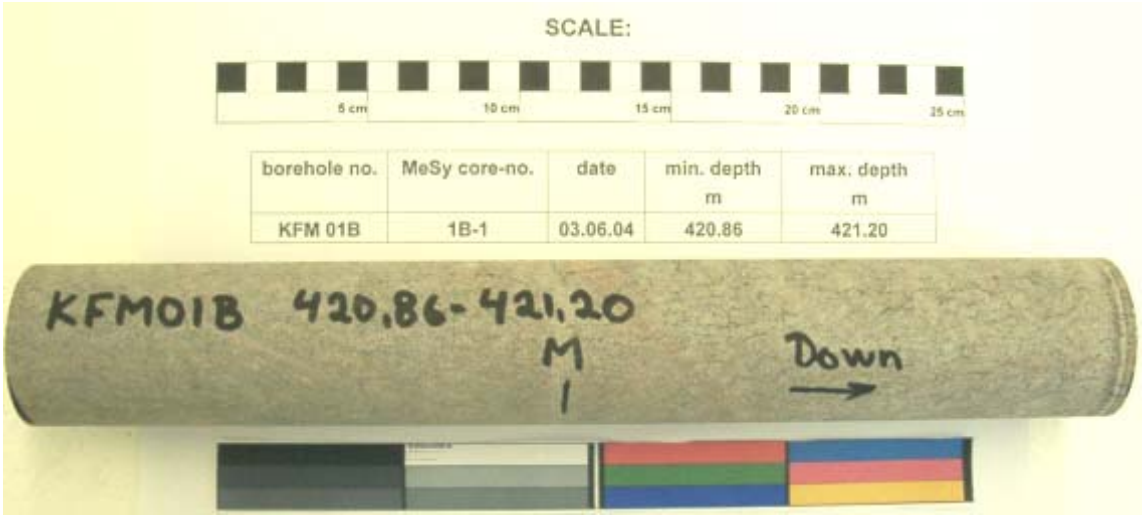

client:		SKB AB	
project:		SKB, Forsmark	
operator:		Seebald, Weber	
date:		04.06.04	
borehole:		KFM 01B	
core piece(s) number(s):		1B-2	
depth (min, max), m:		421.43-421.77	
core dimensions:			
length (min), mm:	340	diameter (min), mm:	50.8
length (max), mm:	340	diameter (max), mm:	50.8
core piece mass, g		1818.0	
remarks and observations:			

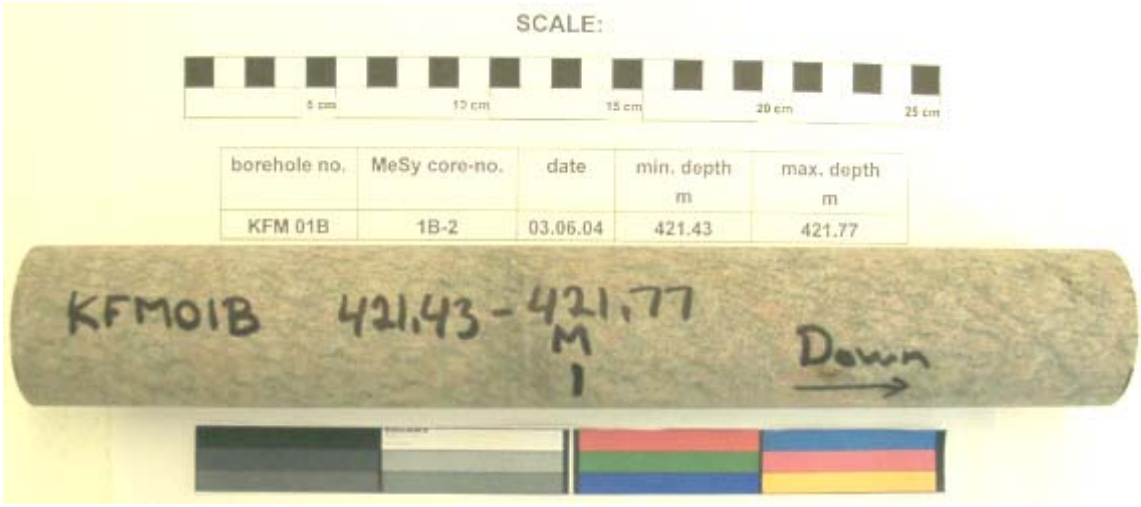

client:		SKB AB	
project:		SKB, Forsmark	
operator:		Seebald, Weber	
date:		04.06.04	
borehole:		KFM 01B	
core piece(s) number(s):		1B-3	
depth (min, max), m:		427.92 - 428.26	
core dimensions:			
length (min), mm:	341	diameter (min), mm:	50.9
length (max), mm:	341	diameter (max), mm:	50.9
core piece mass, g		1834.2	
remarks and observations:			

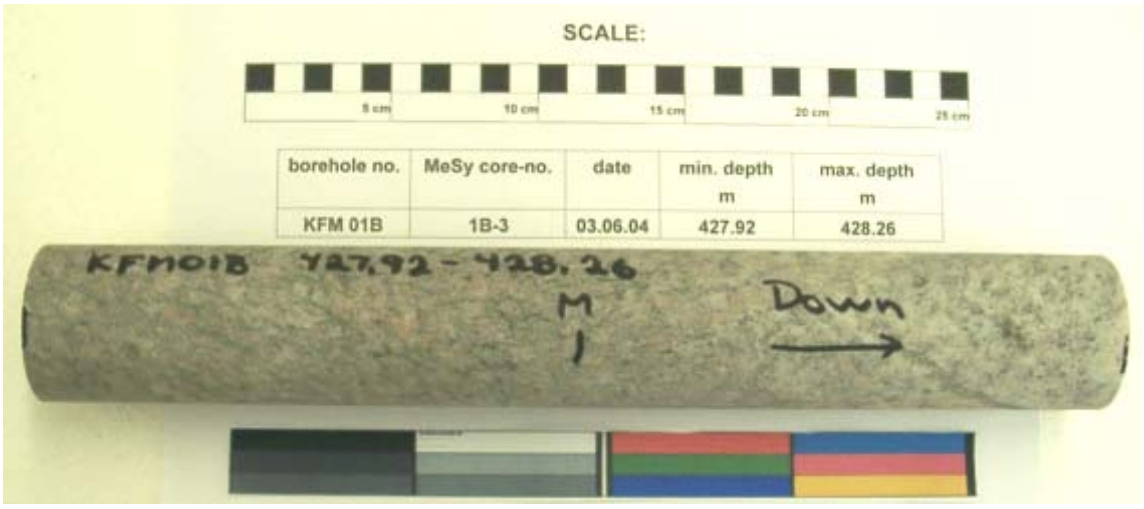

client:		SKB AB	
project:		SKB, Forsmark	
operator:		Seebald, Weber	
date:		04.06.04	
borehole:		KFM 01A	
core piece(s) number(s):		1B-4	
depth (min, max), m:		429.80-430.14	
core dimensions:			
length (min), mm:	338	diameter (min), mm:	51.0
length (max), mm:	339	diameter (max), mm:	51.0
core piece mass, g		1820.2	
remarks and observations:			

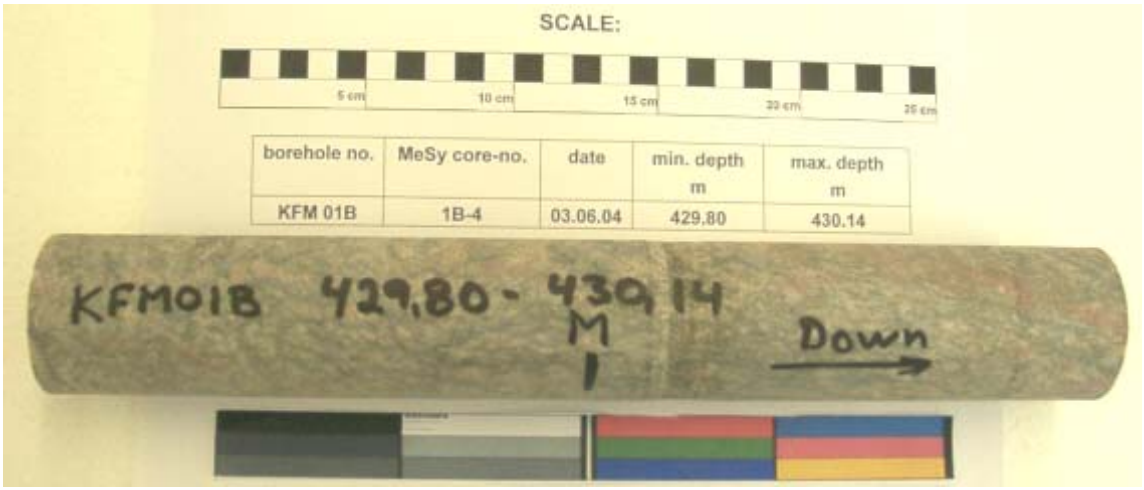

client:		SKB AB	
project:		SKB, Forsmark	
operator:		Seebald, Weber	
date:		04.06.04	
borehole:		KFM 01B	
core piece(s) number(s):		1B-5	
depth (min, max), m:		430.26-430.60	
core dimensions:			
length (min), mm:	340	diameter (min), mm:	50.9
length (max), mm:	341	diameter (max), mm:	50.8
core piece mass, g		1826.4	
remarks and observations:			

client:		SKB AB	
project:		SKB, Forsmark	
operator:		Seebald, Weber	
date:		04.06.04	
borehole:		KFM 01B	
core piece(s) number(s):		1B-6	
depth (min, max), m:		454.96-455.30	
core dimensions:			
length (min), mm:	342	diameter (min), mm:	50.8
length (max), mm:	342	diameter (max), mm:	50.8
core piece mass, g		1834.8	
remarks and observations:			

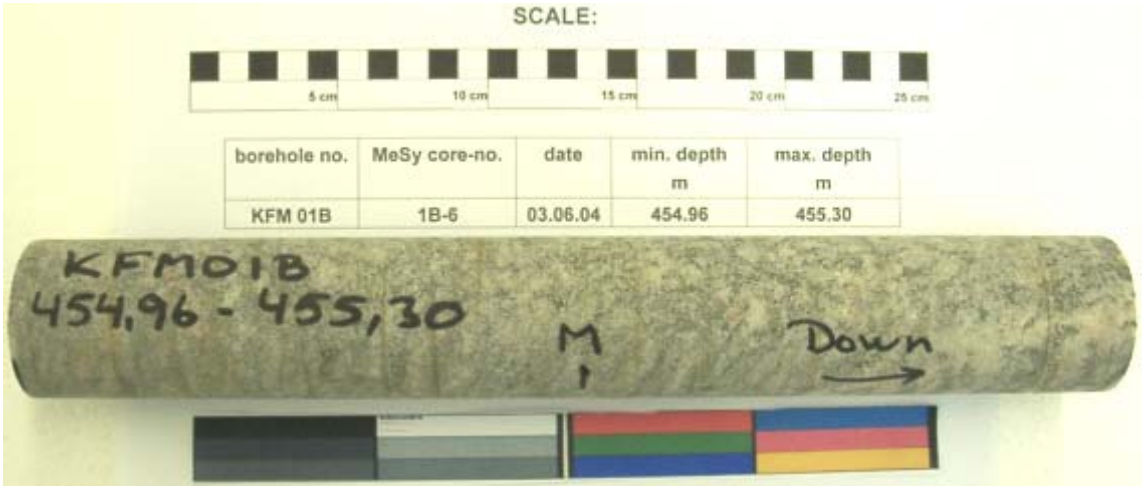

client:		SKB AB	
project:		SKB, Forsmark	
operator:		Seebald, Weber	
date:		04.06.04	
borehole:		KFM 01B	
core piece(s) number(s):		1B-7	
depth (min, max), m:		456.03-546.37	
core dimensions:			
length (min), mm:	340	diameter (min), mm:	50.8
length (max), mm:	341	diameter (max), mm:	50.8
core piece mass, g		1823.2	
remarks and observations:			

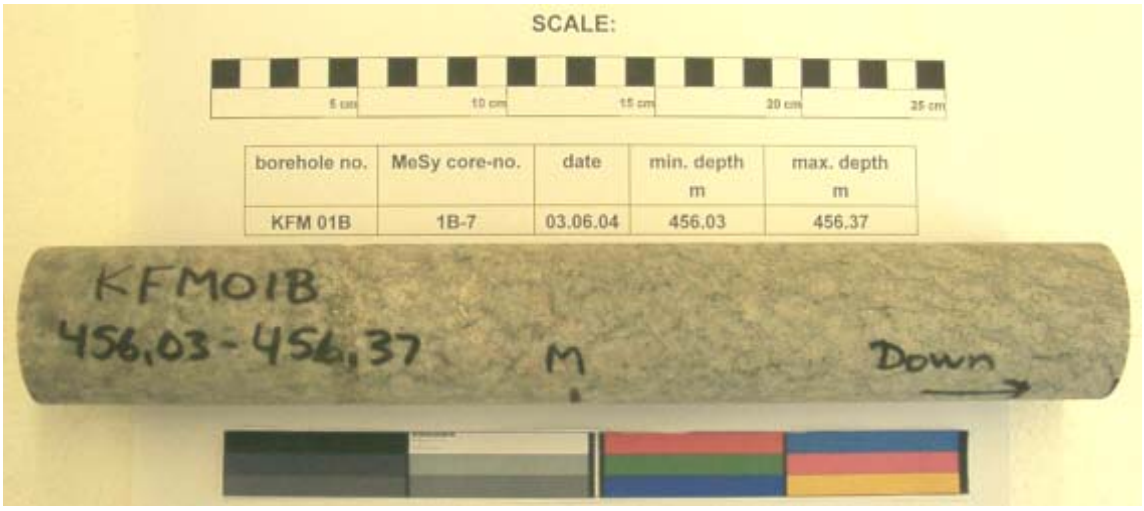

client:		SKB AB	
project:		SKB, Forsmark	
operator:		Seebald, Weber	
date:		04.06.04	
borehole:		KFM 02A	
core piece(s) number(s):		2A-1	
depth (min, max), m:		220.68-221.00	
core dimensions:			
length (min), mm:	320	diameter (min), mm:	50.9
length (max), mm:	321	diameter (max), mm:	51.0
core piece mass, g		1732.1	
remarks and observations:			

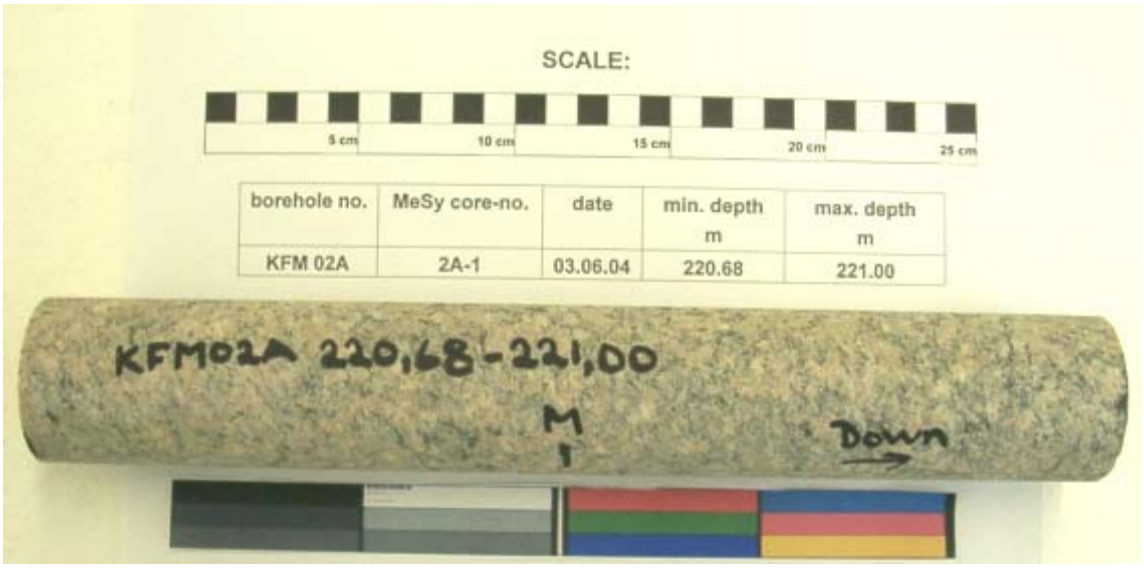

client:		SKB AB	
project:		SKB, Forsmark	
operator:		Seebald, Weber	
date:		04.06.04	
borehole:		KFM 02A	
core piece(s) number(s):		2A-2	
depth (min, max), m:		225.87-226.20	
core dimensions:			
length (min), mm:	328	diameter (min), mm:	51.0
length (max), mm:	328	diameter (max), mm:	51.0
core piece mass, g		1775.1	
remarks and observations:			

client:		SKB AB	
project:		SKB, Forsmark	
operator:		Seebald, Weber	
date:		04.06.04	
borehole:		KFM 02A	
core piece(s) number(s):		2A-3	
depth (min, max), m:		395.88 - 396.20	
core dimensions:			
length (min), mm:	320	diameter (min), mm:	50.8
length (max), mm:	321	diameter (max), mm:	50.8
core piece mass, g		1722.3	
remarks and observations:			

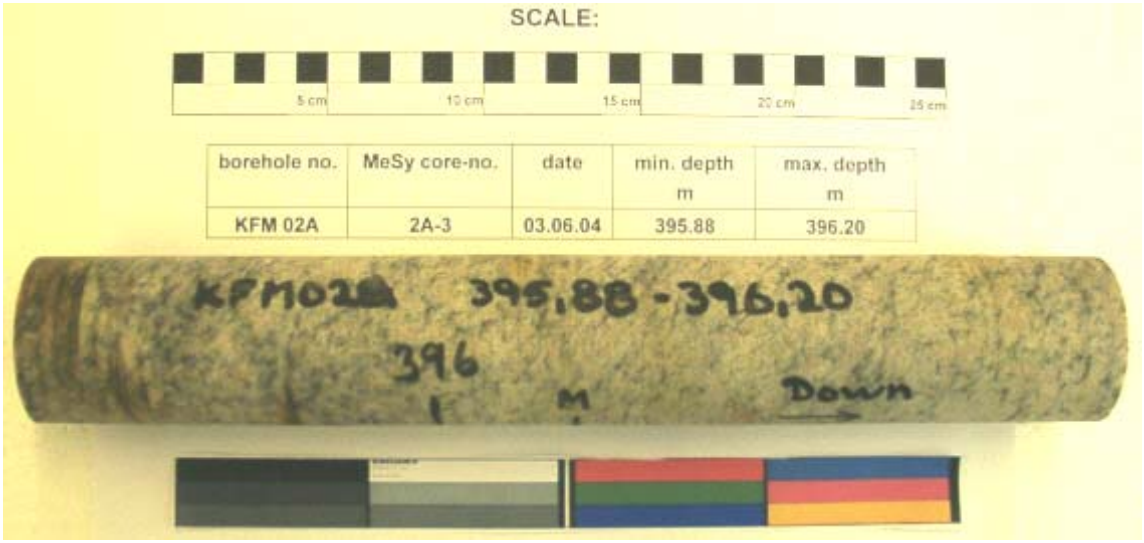

client:		SKB AB	
project:		SKB, Forsmark	
operator:		Seebald, Weber	
date:		04.06.04	
borehole:		KFM 02A	
core piece(s) number(s):		2A-4	
depth (min, max), m:		413.90-414.24	
core dimensions:			
length (min), mm:	339	diameter (min), mm:	50.9
length (max), mm:	339	diameter (max), mm:	50.9
core piece mass, g		1839.6	
remarks and observations:			

client:		SKB AB	
project:		SKB, Forsmark	
operator:		Seebald, Weber	
date:		04.06.04	
borehole:		KFM 02A	
core piece(s) number(s):		2A-5	
depth (min, max), m:		451.13-451.50	
core dimensions:			
length (min), mm:	372	diameter (min), mm:	50.8
length (max), mm:	377	diameter (max), mm:	50.7
core piece mass, g		2011.1	
remarks and observations:		lower end not sawed	

client:		SKB AB	
project:		SKB, Forsmark	
operator:		Seebald, Weber	
date:		04.06.04	
borehole:		KFM 02A	
core piece(s) number(s):		2A-6	
depth (min, max), m:		554.22 - 554.56	
core dimensions:			
length (min), mm:	343	diameter (min), mm:	50.7
length (max), mm:	347	diameter (max), mm:	50.8
core piece mass, g		1840.7	
remarks and observations:		upper end not sawed	

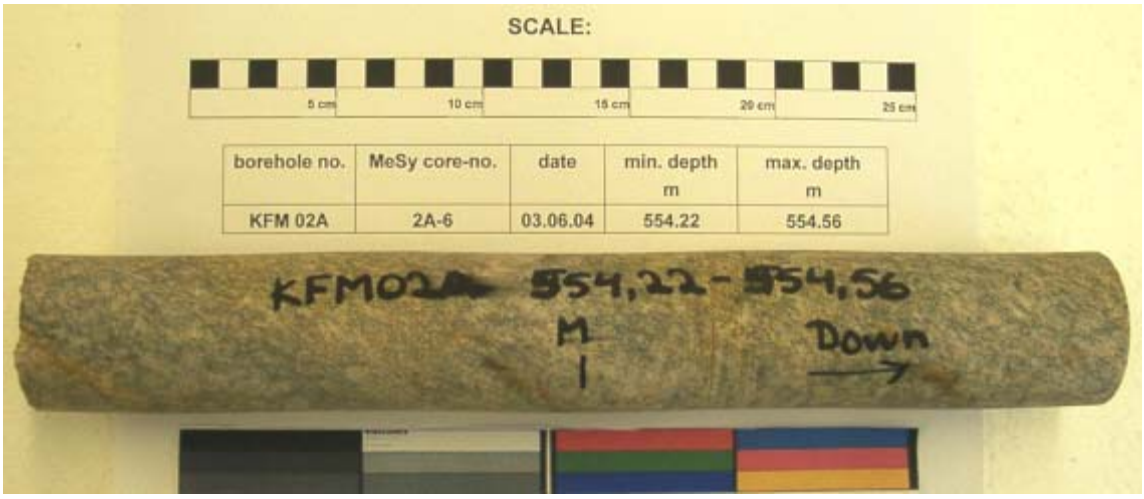

client:		SKB AB	
project:		SKB, Forsmark	
operator:		Seebald, Weber	
date:		04.06.04	
borehole:		KFM 02A	
core piece(s) number(s):		2A-7	
depth (min, max), m:		594.21 - 594.55	
core dimensions:			
length (min), mm:	338	diameter (min), mm:	51.0
length (max), mm:	339	diameter (max), mm:	51.0
core piece mass, g		1827.7	
remarks and observations:			

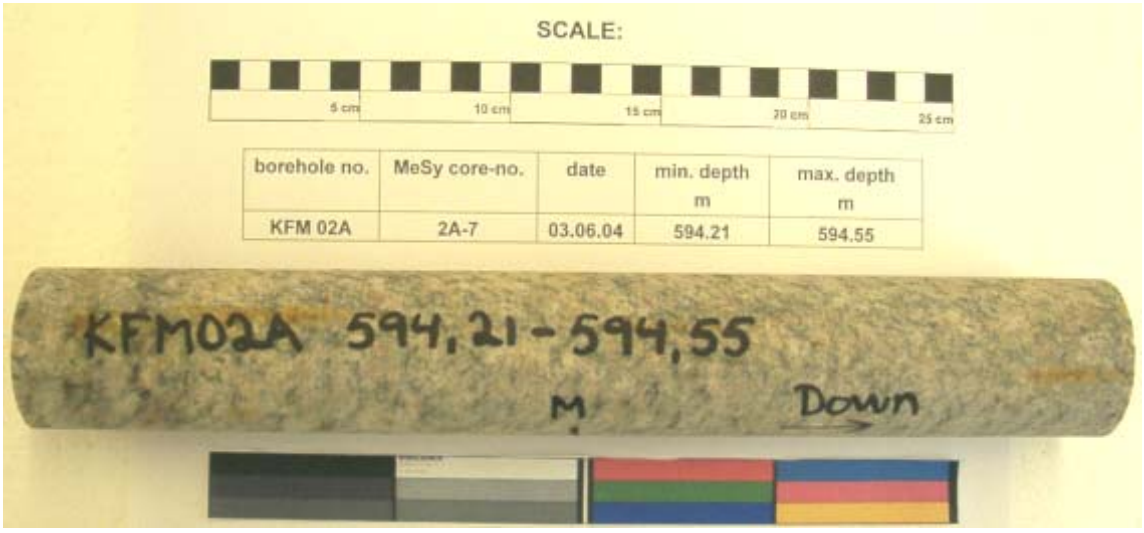

client:		SKB AB	
project:		SKB, Forsmark	
operator:		Seebald, Weber	
date:		04.06.04	
borehole:		KFM 02A	
core piece(s) number(s):		2A-8	
depth (min, max), m:		602.75-603.09	
core dimensions:			
length (min), mm:	341	diameter (min), mm:	51.0
length (max), mm:	342	diameter (max), mm:	51.0
core piece mass, g		1826.7	
remarks and observations:			

client:		SKB AB	
project:		SKB, Forsmark	
operator:		Seebald, Weber	
date:		04.06.04	
borehole:		KFM 02A	
core piece(s) number(s):		2A-9	
depth (min, max), m:		699.60 - 700.00	
core dimensions:			
length (min), mm:	341	diameter (min), mm:	50.8
length (max), mm:	341	diameter (max), mm:	50.8
core piece mass, g		1837.6	
remarks and observations:			

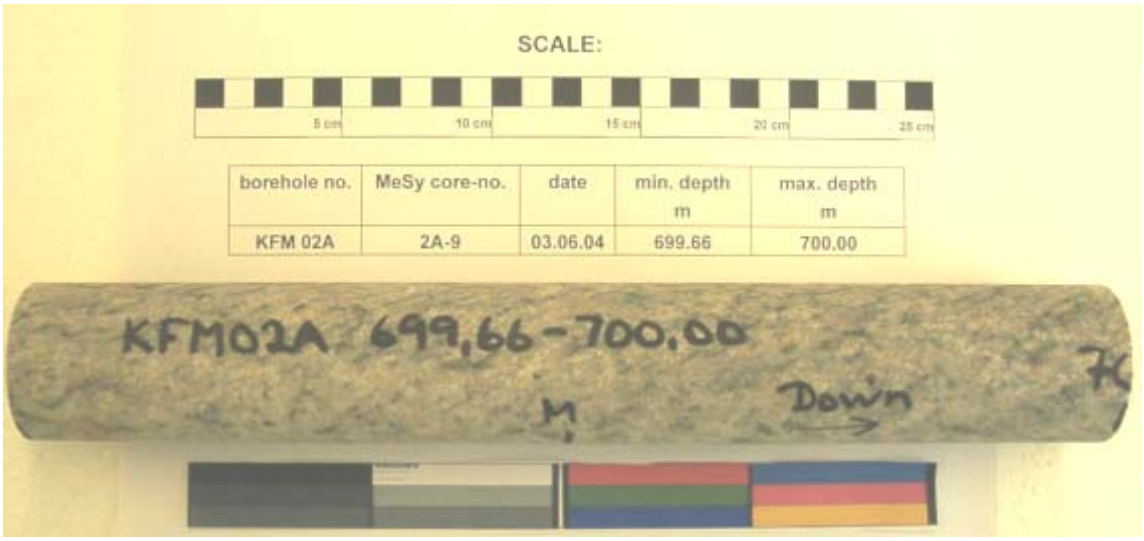

client:		SKB AB	
project:		SKB, Forsmark	
operator:		Seebald, Weber	
date:		04.06.04	
borehole:		KFM 02A	
core piece(s) number(s):		2A-10	
depth (min, max), m:		702.64-703.00	
core dimensions:			
length (min), mm:	359	diameter (min), mm:	50.8
length (max), mm:	360	diameter (max), mm:	50.8
core piece mass, g		1931.0	
remarks and observations:			

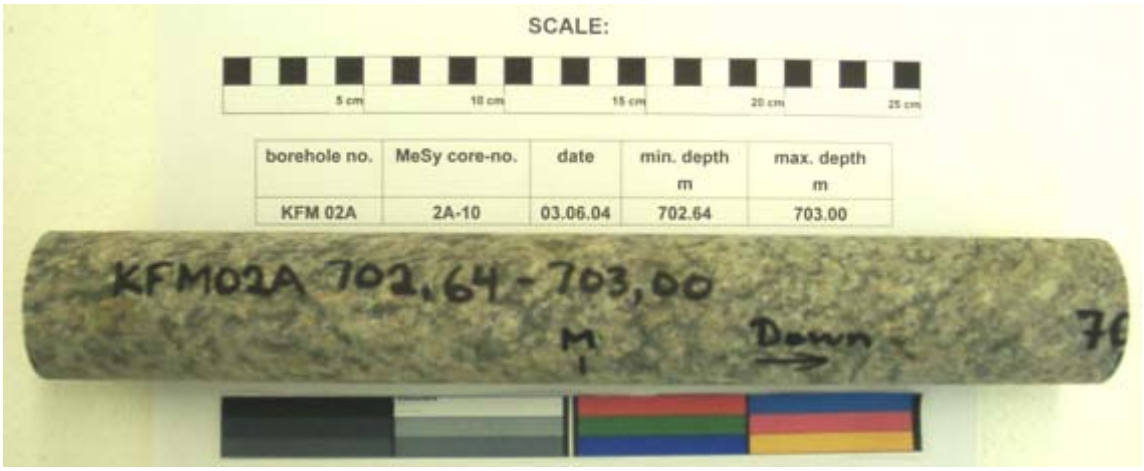

client:		SKB AB	
project:		SKB, Forsmark	
operator:		Seebald, Weber	
date:		04.06.04	
borehole:		KFM 04A	
core piece(s) number(s):		4A-1	
depth (min, max), m:		192.11 - 192.45	
core dimensions:			
length (min), mm:	336	diameter (min), mm:	50.8
length (max), mm:	336	diameter (max), mm:	50.8
core piece mass, g		1804.6	
remarks and observations:			

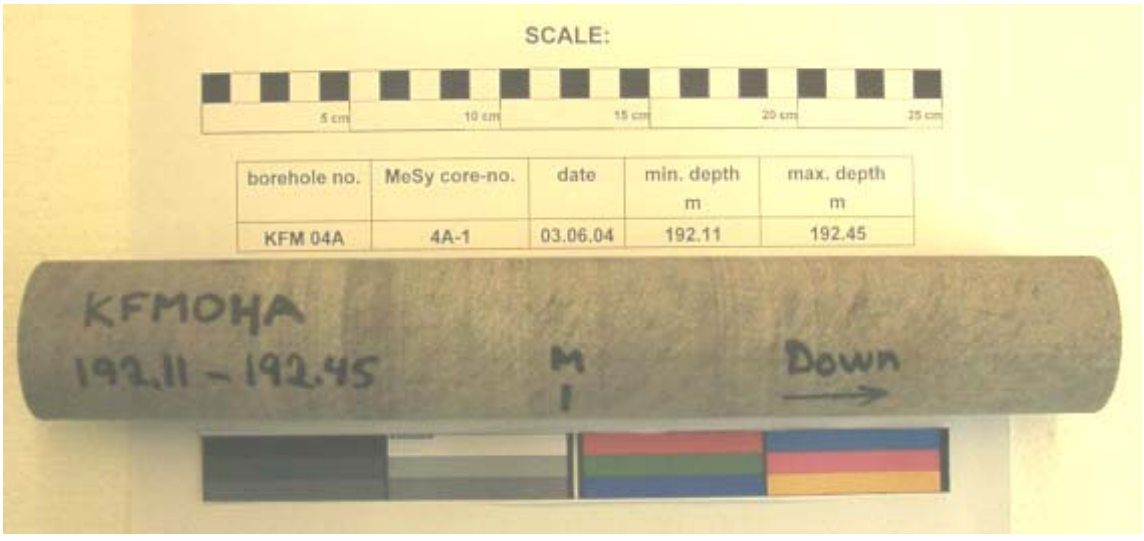

client:		SKB AB	
project:		SKB, Forsmark	
operator:		Seebald, Weber	
date:		04.06.04	
borehole:		KFM 04A	
core piece(s) number(s):		4A-2	
depth (min, max), m:		192.45 - 192.77	
core dimensions:			
length (min), mm:	318	diameter (min), mm:	50.8
length (max), mm:	318	diameter (max), mm:	50.8
core piece mass, g		1704.7	
remarks and observations:			

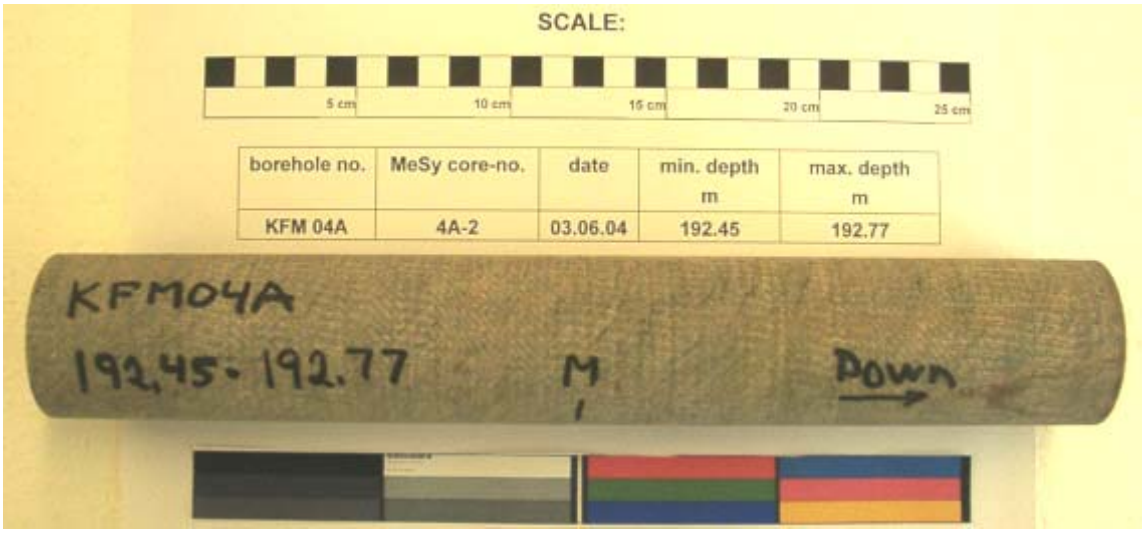

client:		SKB AB	
project:		SKB, Forsmark	
operator:		Seebald, Weber	
date:		04.06.04	
borehole:		KFM 04A	
core piece(s) number(s):		4A-3	
depth (min, max), m:		260.14 - 260.48	
core dimensions:			
length (min), mm:	339	diameter (min), mm:	50.7
length (max), mm:	340	diameter (max), mm:	50.8
core piece mass, g		1818.8	
remarks and observations:			

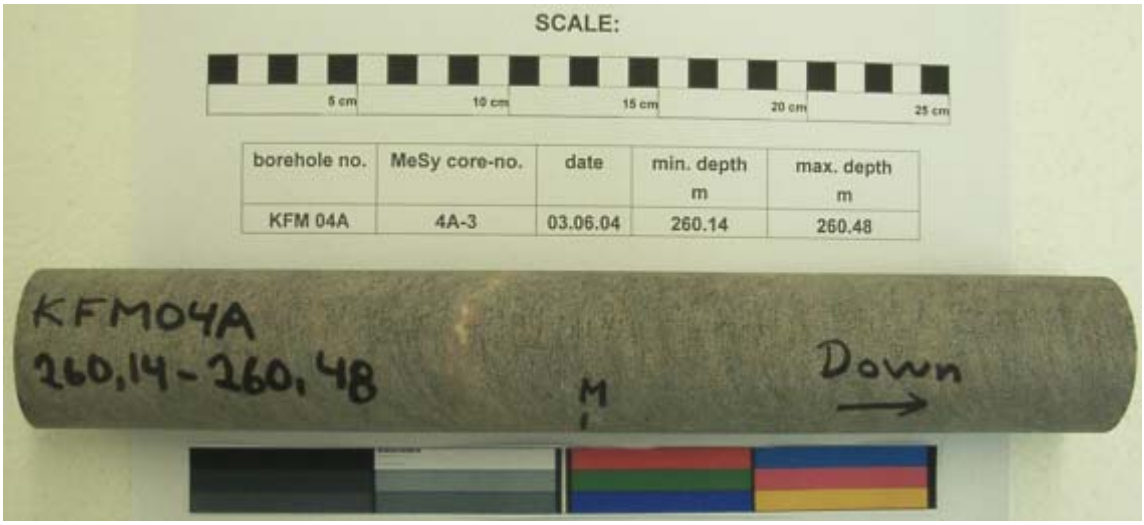

client:		SKB AB	
project:		SKB, Forsmark	
operator:		Seebald, Weber	
date:		04.06.04	
borehole:		KFM 04A	
core piece(s) number(s):		4A-4	
depth (min, max), m:		527.46 - 527.80	
core dimensions:			
length (min), mm:	335	diameter (min), mm:	50.7
length (max), mm:	339	diameter (max), mm:	50.7
core piece mass, g		1795.0	
remarks and observations:			

client:		SKB AB	
project:		SKB, Forsmark	
operator:		Seebald, Weber	
date:		04.06.04	
borehole:		KFM 04A	
core piece(s) number(s):		4A-5	
depth (min, max), m:		527.80 - 528.14	
core dimensions:			
length (min), mm:	342	diameter (min), mm:	50.7
length (max), mm:	342	diameter (max), mm:	50.7
core piece mass, g		1828.8	
remarks and observations:			

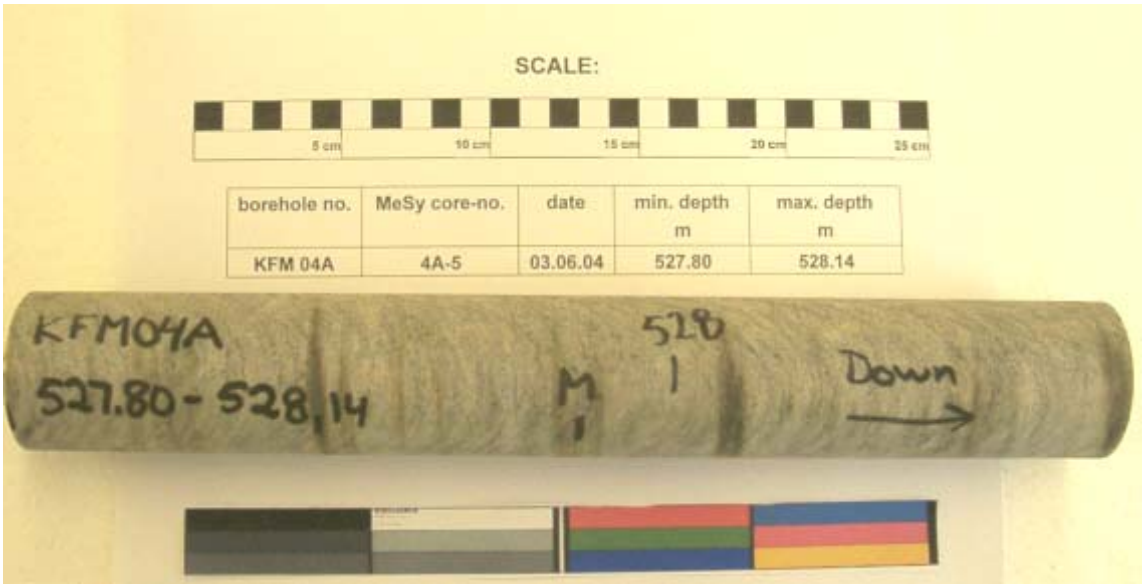

client:		SKB AB	
project:		SKB, Forsmark	
operator:		Seebald, Weber	
date:		04.06.04	
borehole:		KFM 04A	
core piece(s) number(s):		4A-6	
depth (min, max), m:		528.21-528.55	
core dimensions:			
length (min), mm:	340	diameter (min), mm:	50.7
length (max), mm:	340	diameter (max), mm:	50.7
core piece mass, g		1820.2	
remarks and observations:			

client:		SKB AB	
project:		SKB, Forsmark	
operator:		Seebald, Weber	
date:		04.06.04	
borehole:		KFM 04A	
core piece(s) number(s):		4A-7	
depth (min, max), m:		528.62-528.96	
core dimensions:			
length (min), mm:	338	diameter (min), mm:	50.7
length (max), mm:	338	diameter (max), mm:	50.7
core piece mass, g		1807.1	
remarks and observations:			

client:			SKB AB	
project:			SKB, Forsmark	
operator:			Seebald, Weber	
date:			04.06.04	
borehole:			KFM 04A	
core piece(s) number(s):			4A-8	
depth (min, max), m:			528.96-529.30	
core dimensions:				
length (min), mm:	338		diameter (min), mm:	50.7
length (max), mm:	338		diameter (max), mm:	50.7
core piece mass, g			1810.8	
remarks and observations:				

client:		SKB AB	
project:		SKB, Forsmark	
operator:		Seebald, Weber	
date:		04.06.04	
borehole:		KFM 04A	
core piece(s) number(s):		4A-9	
depth (min, max), m:		529.30-529.64	
core dimensions:			
length (min), mm:	336	diameter (min), mm:	50.8
length (max), mm:	338	diameter (max), mm:	50.8
core piece mass, g		1811.1	
remarks and observations:			

Appendix B

Seismograms of ultrasonic tests

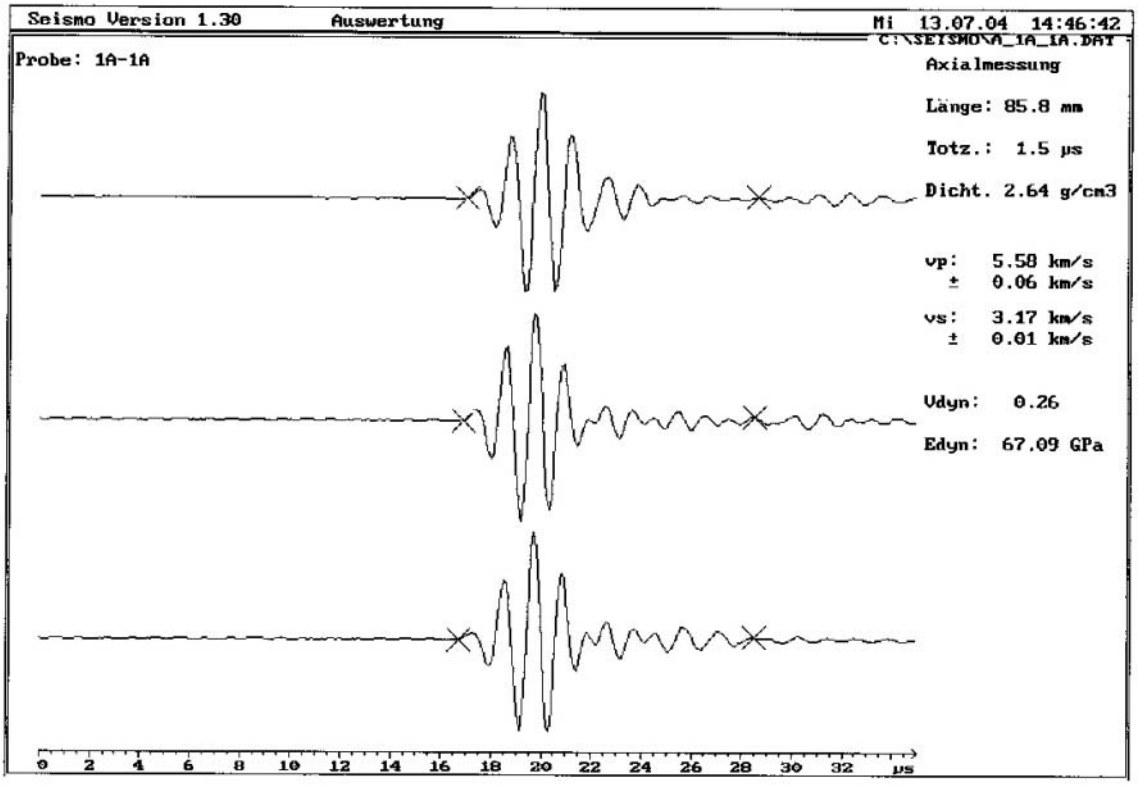

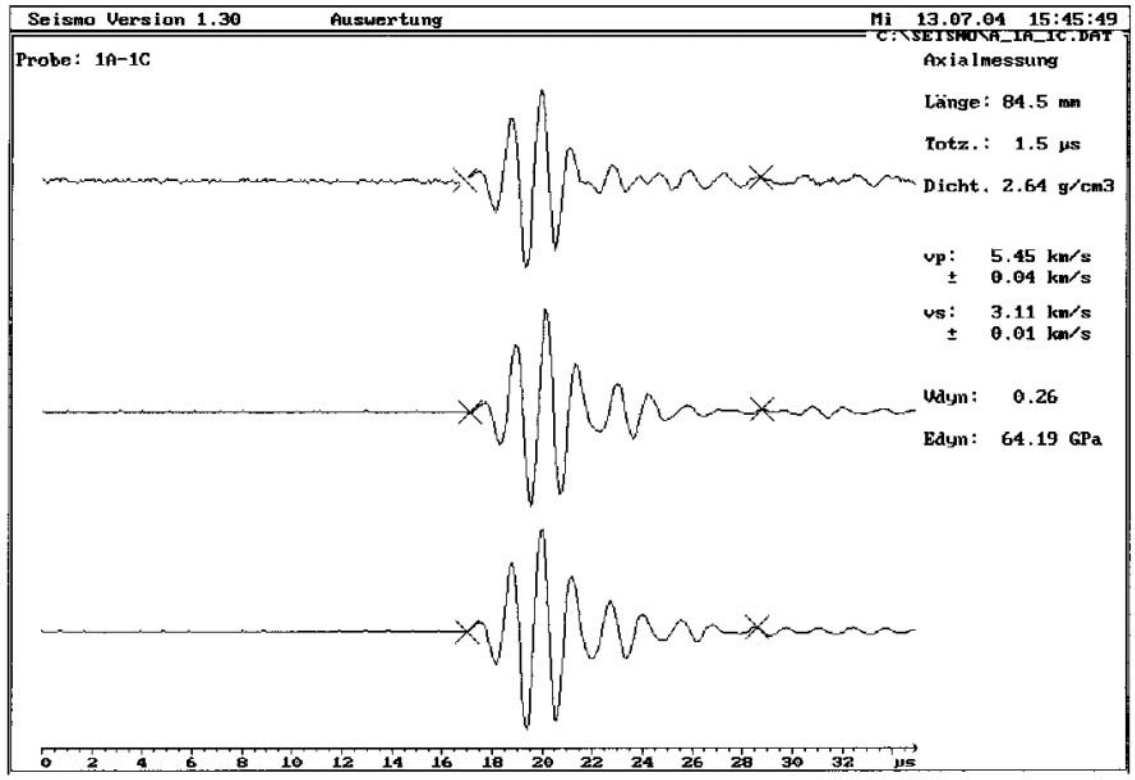

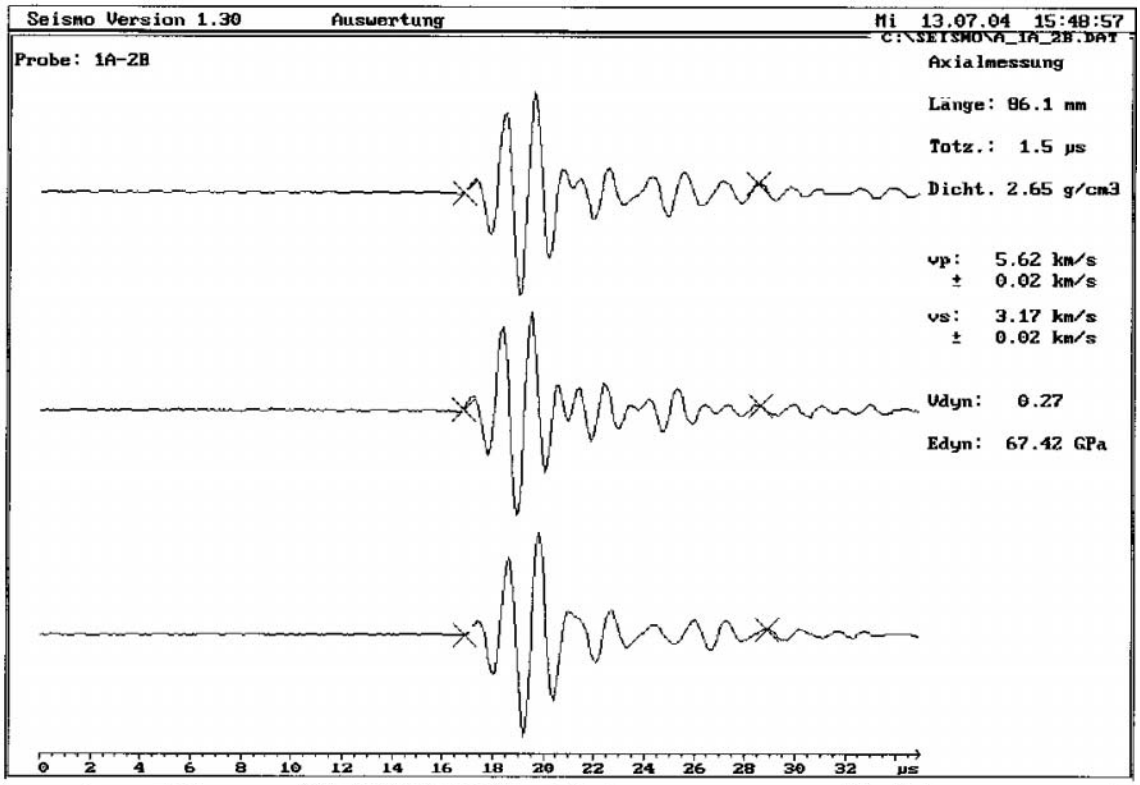
Seismo Version 1.30
Auswertung
Mi 13.07.04 15:48:57
C:\SEISMO\A_1A_2B.DAT
Probe: 1A-2B
Axialmessung
Länge: 86.1 mm
Totz.: 1.5 µs
Dicht. 2.65 g/cm3
vp: 5.62 km/s
± 0.02 km/s
vs: 3.17 km/s
± 0.02 km/s
Vdyn: 0.27
Edyn: 67.42 GPa
0 2 4 6 8 10 12 14 16 18 20 22 24 26 28 30 32 µs

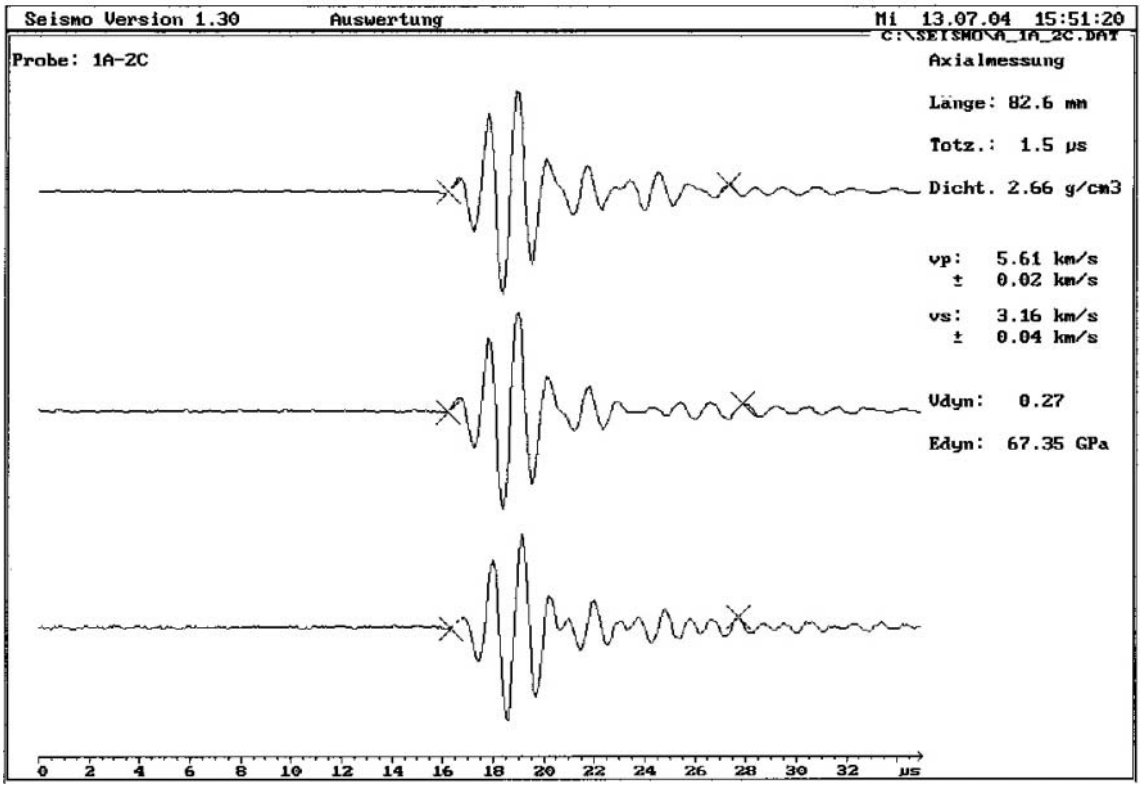
Seismo Version 1.30
Auswertung
Mi 13.07.04 15:51:20
C:\SEISMO\A_1A_2C.DAT
Probe: 1A-2C
Axialmessung
Länge: 82.6 mm
Totz.: 1.5 µs
Dicht. 2.66 g/cm3
vp: 5.61 km/s
± 0.02 km/s
vs: 3.16 km/s
± 0.04 km/s
Vdyn: 0.27
Edyn: 67.35 GPa
0 2 4 6 8 10 12 14 16 18 20 22 24 26 28 30 32 µs

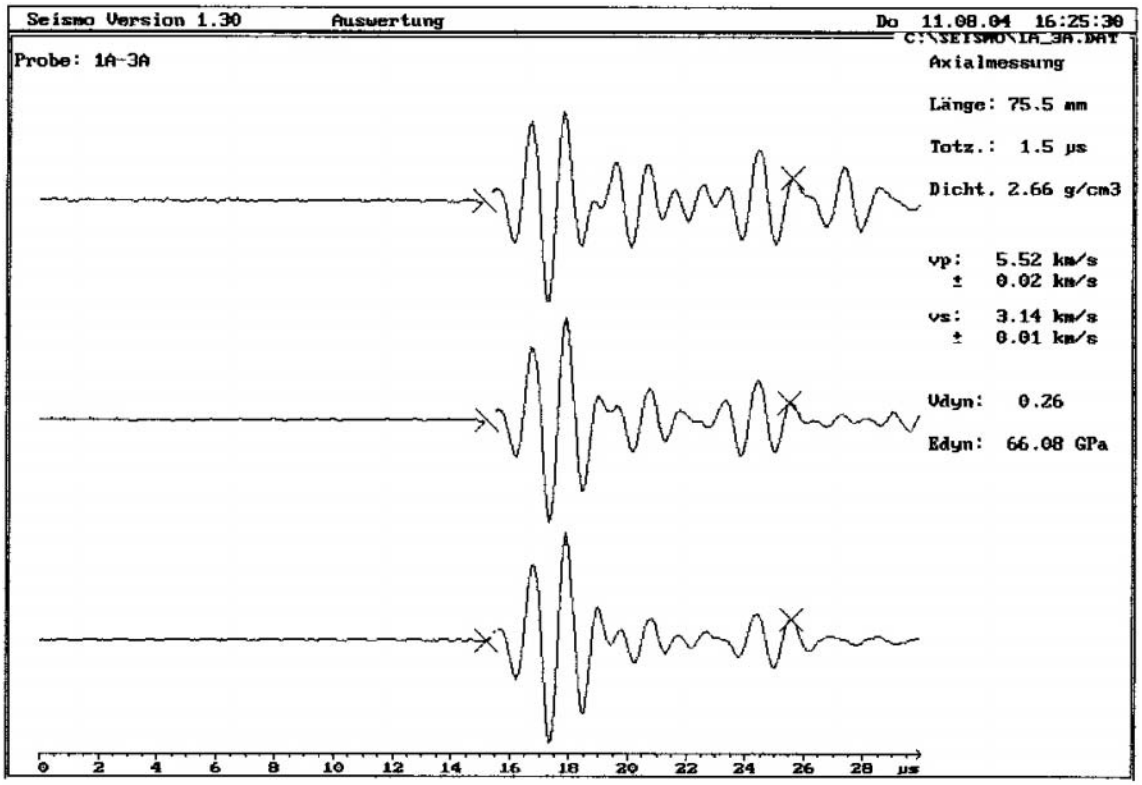
Seismo Version 1.30
Auswertung
Do 11.08.04 16:25:30
C:\SEISMO\1A_3A.DAT
Probe: 1A-3A
Axialmessung
Länge: 75.5 mm
Totz.: 1.5 µs
Dicht. 2.66 g/cm3
vp: 5.52 km/s
± 0.02 km/s
vs: 3.14 km/s
± 0.01 km/s
Udyn: 0.26
Edyn: 66.08 GPa
0 2 4 6 8 10 12 14 16 18 20 22 24 26 28 µs

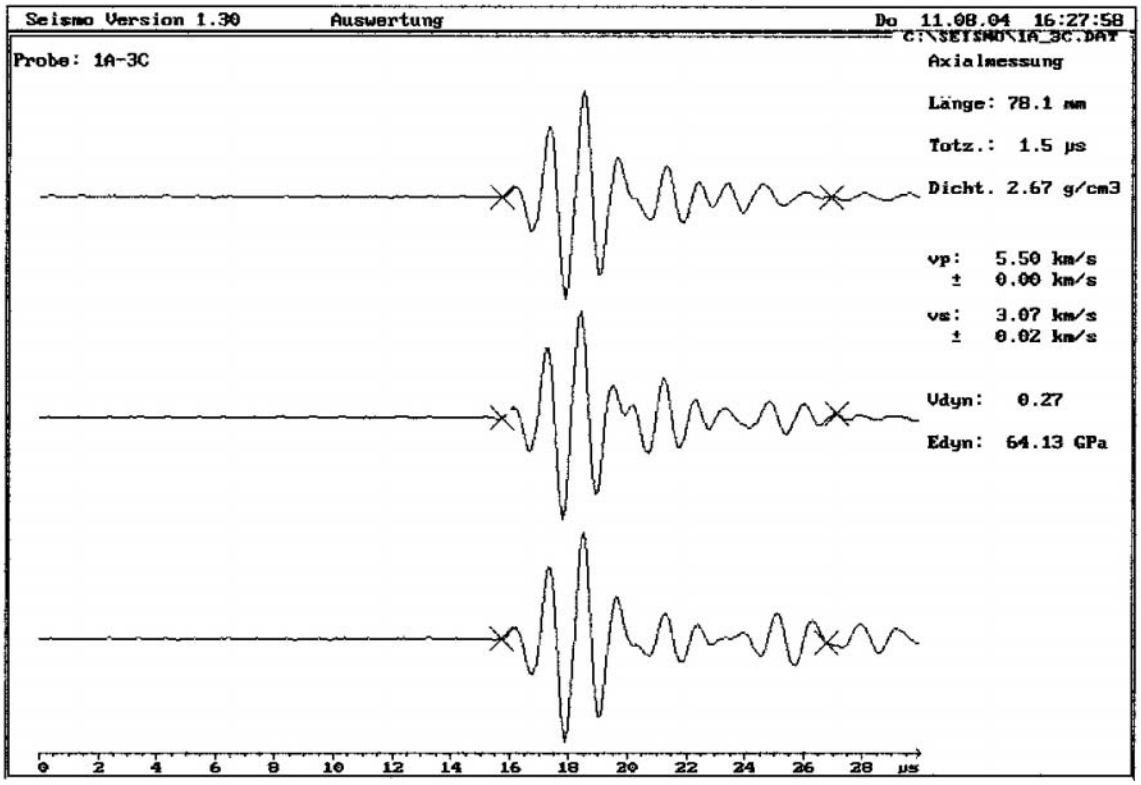
Seismo Version 1.30
Auswertung
Do 11.08.04 16:27:58
C:\SEISMO\1A_3C.DAT
Probe: 1A-3C
Axialmessung
Länge: 78.1 mm
Totz.: 1.5 µs
Dicht. 2.67 g/cm3
vp: 5.50 km/s
± 0.00 km/s
vs: 3.07 km/s
± 0.02 km/s
Udyn: 0.27
Edyn: 64.13 GPa
0 2 4 6 8 10 12 14 16 18 20 22 24 26 28 µs

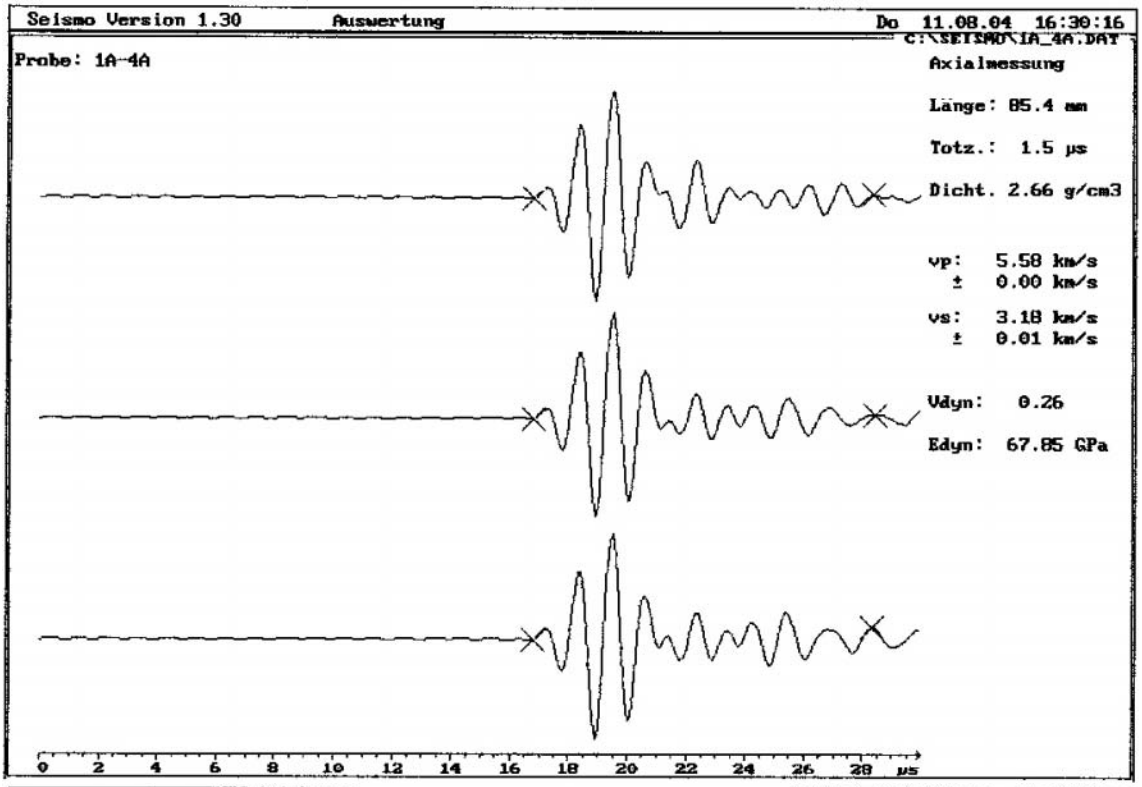
Seismo Version 1.30
Auswertung
Do 11.08.04 16:30:16
C:\SEISMO\1A_4A.DAT
Probe: 1A-4A
Axialmessung
Länge: 85.4 mm
Totz.: 1.5 µs
Dicht. 2.66 g/cm3
vp: 5.58 km/s
± 0.00 km/s
vs: 3.18 km/s
± 0.01 km/s
Vdyn: 0.26
Edyn: 67.85 GPa
0 2 4 6 8 10 12 14 16 18 20 22 24 26 28 µs

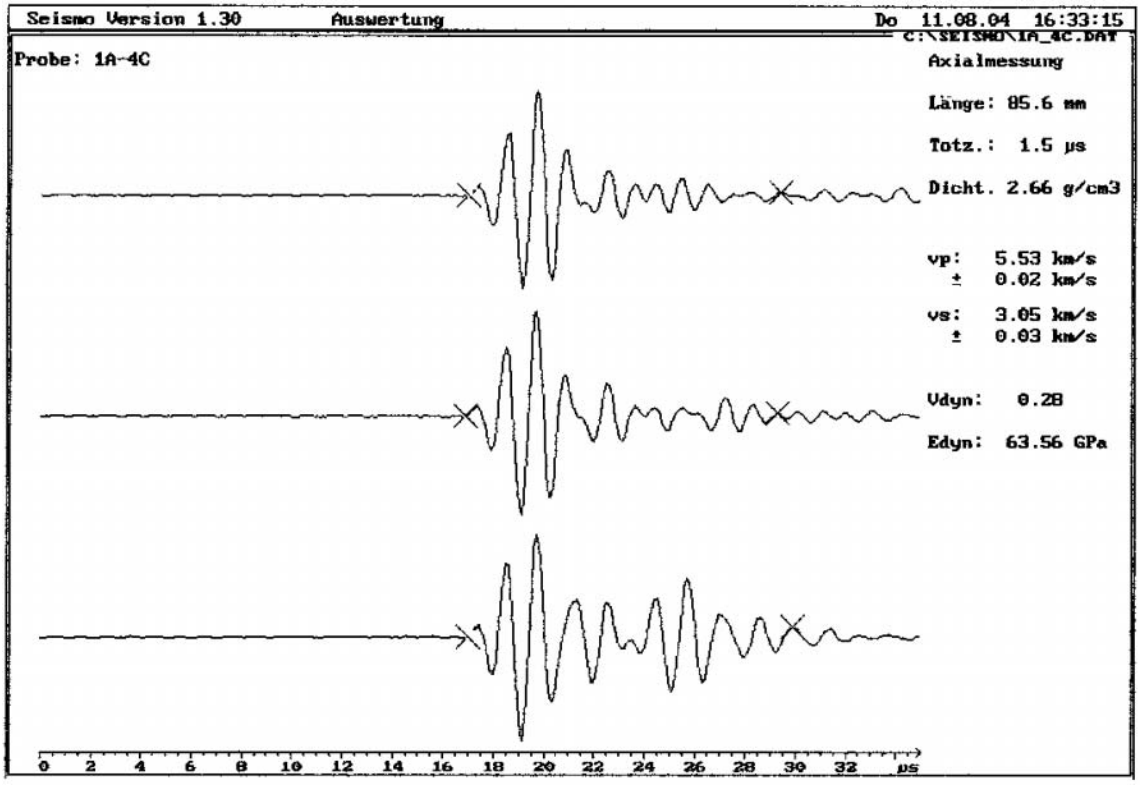
Seismo Version 1.30
Auswertung
Do 11.08.04 16:33:15
C:\SEISMO\1A_4C.DAT
Probe: 1A-4C
Axialmessung
Länge: 85.6 mm
Totz.: 1.5 µs
Dicht. 2.66 g/cm3
vp: 5.53 km/s
± 0.02 km/s
vs: 3.05 km/s
± 0.03 km/s
Vdyn: 0.28
Edyn: 63.56 GPa
0 2 4 6 8 10 12 14 16 18 20 22 24 26 28 30 32 µs

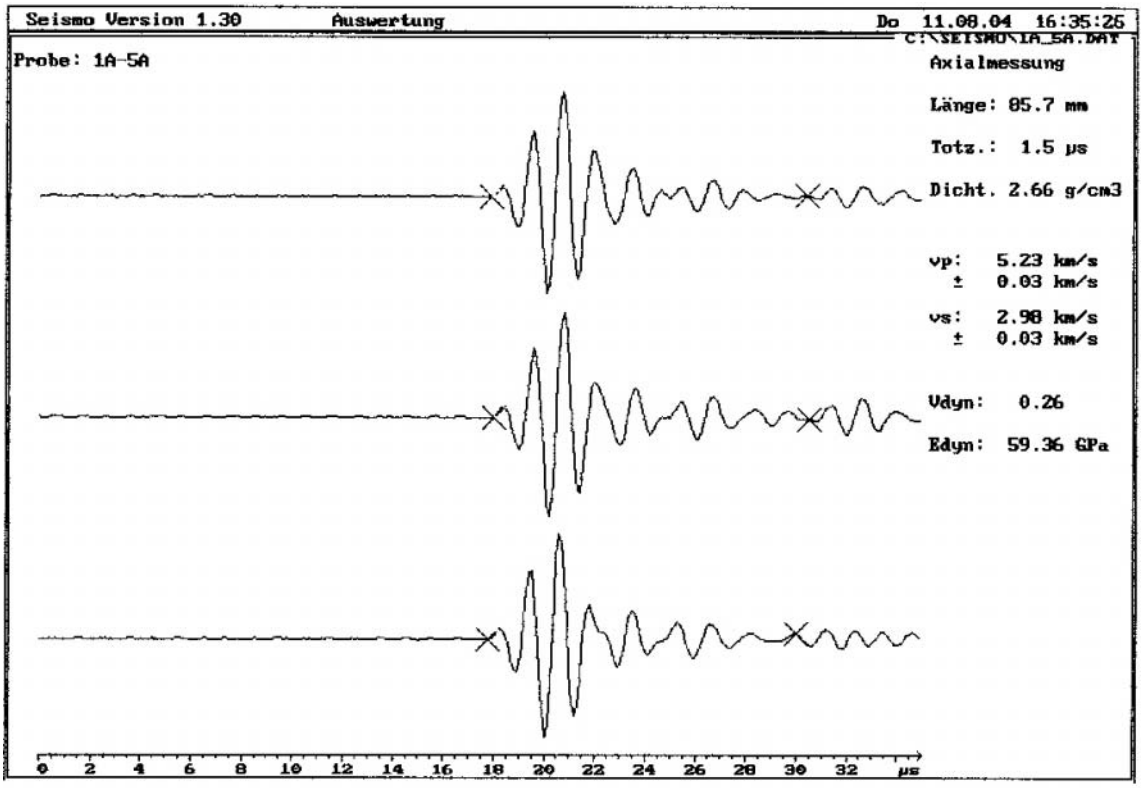
Seismo Version 1.30
Auswertung
Do 11.08.04 16:35:25
C:\SEISMO\1A_5A.DAT
Probe: 1A-5A
Axialmessung
Länge: 85.7 mm
Totz.: 1.5 µs
Dicht. 2.66 g/cm3
vp: 5.23 km/s
± 0.03 km/s
vs: 2.98 km/s
± 0.03 km/s
Vdyn: 0.26
Edyn: 59.36 GPa
0 2 4 6 8 10 12 14 16 18 20 22 24 26 28 30 32 µs

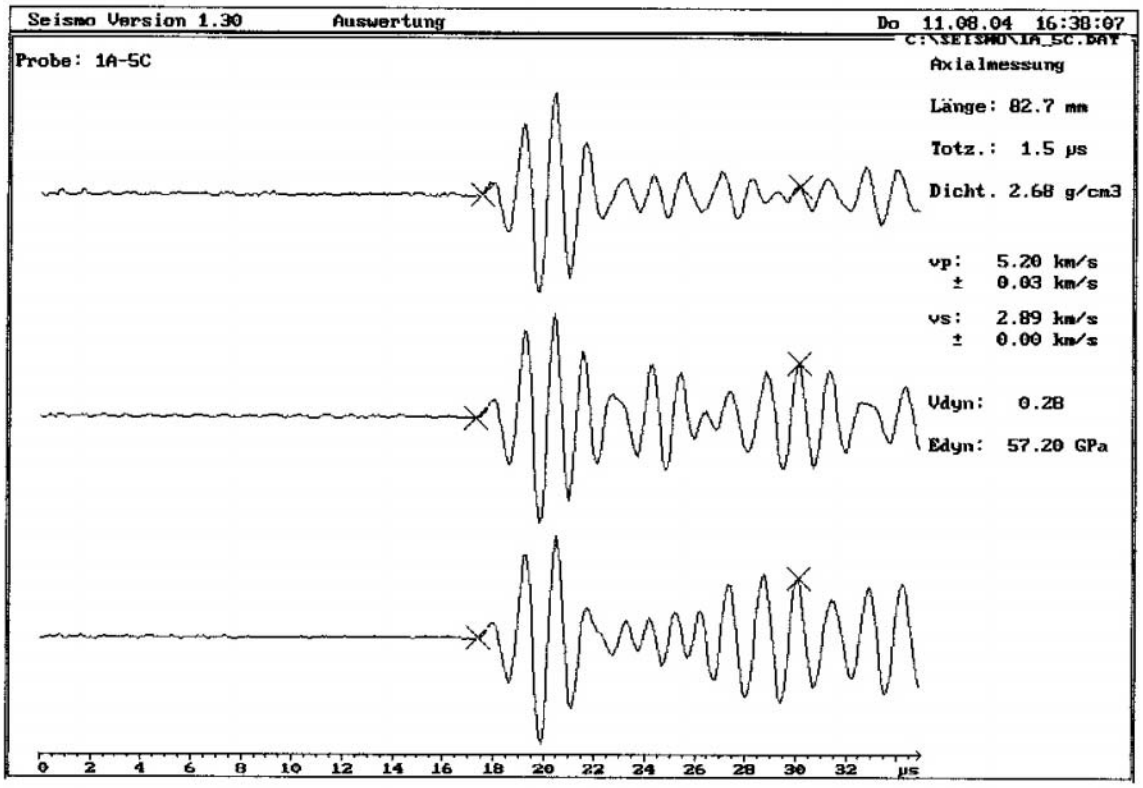
Seismo Version 1.30
Auswertung
Do 11.08.04 16:38:07
C:\SEISMO\1A_5C.DAT
Probe: 1A-5C
Axialmessung
Länge: 82.7 mm
Totz.: 1.5 µs
Dicht. 2.68 g/cm3
vp: 5.20 km/s
± 0.03 km/s
vs: 2.89 km/s
± 0.00 km/s
Vdyn: 0.28
Edyn: 57.20 GPa
0 2 4 6 8 10 12 14 16 18 20 22 24 26 28 30 32 µs

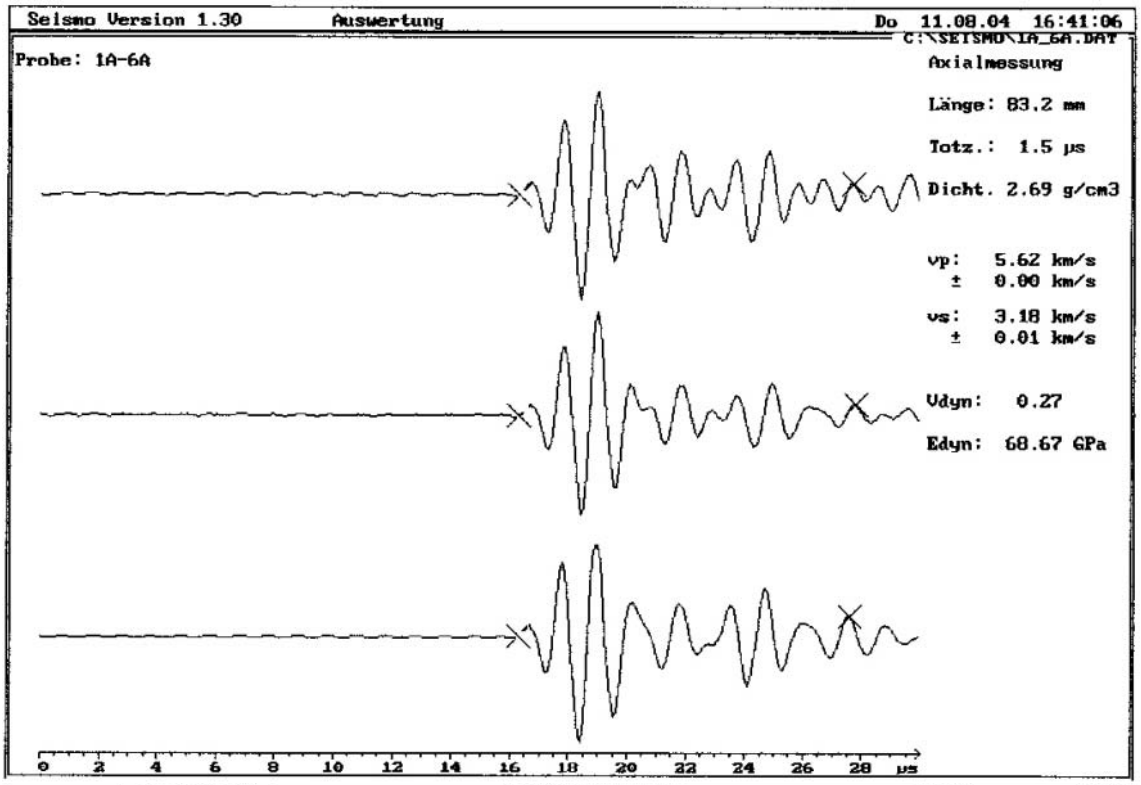
Seismo Version 1.30
Auswertung
Do 11.08.04 16:41:06
C:\SEISMO\1A_6A.DAT
Probe: 1A-6A
Axialmessung
Länge: 83.2 mm
Totz.: 1.5 µs
Dicht. 2.69 g/cm3
vp: 5.62 km/s
± 0.00 km/s
vs: 3.18 km/s
± 0.01 km/s
Vdyn: 0.27
Edyn: 68.67 GPa
0 2 4 6 8 10 12 14 16 18 20 22 24 26 28 µs

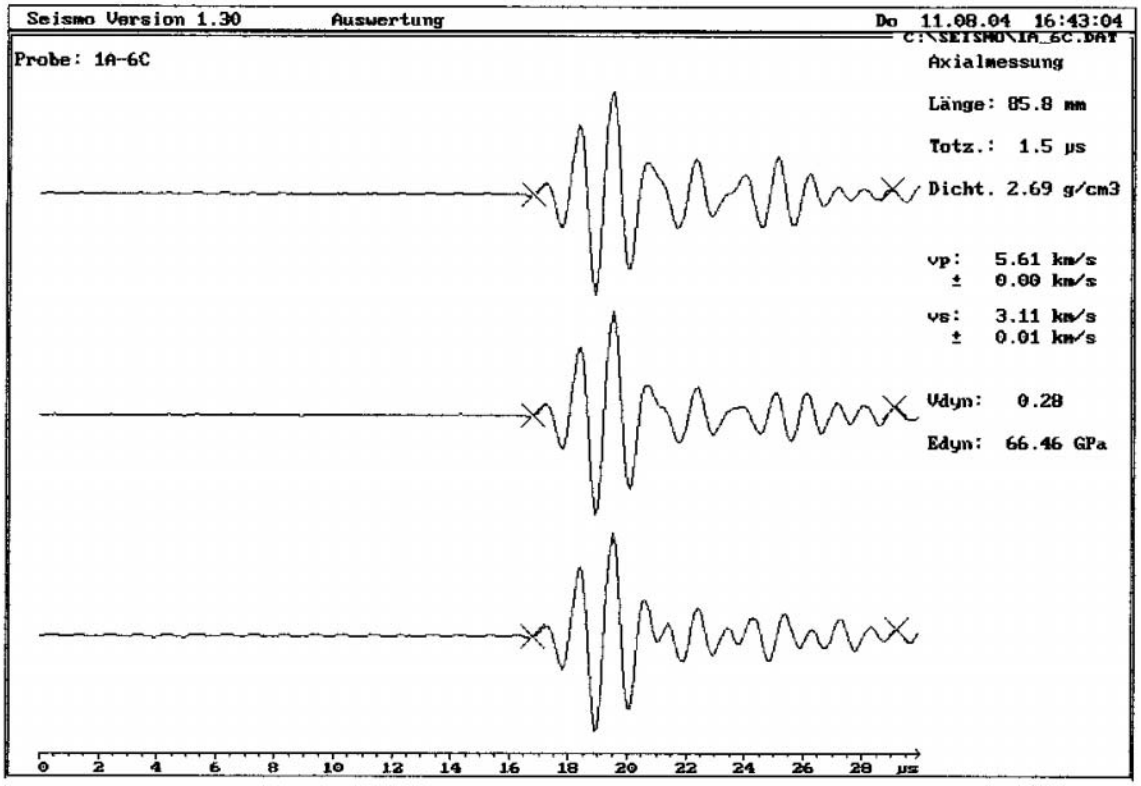
Seismo Version 1.30
Auswertung
Do 11.08.04 16:43:04
C:\SEISMO\1A_6C.DAT
Probe: 1A-6C
Axialmessung
Länge: 85.8 mm
Totz.: 1.5 µs
Dicht. 2.69 g/cm3
vp: 5.61 km/s
± 0.00 km/s
vs: 3.11 km/s
± 0.01 km/s
Vdyn: 0.28
Edyn: 66.46 GPa
0 2 4 6 8 10 12 14 16 18 20 22 24 26 28 µs

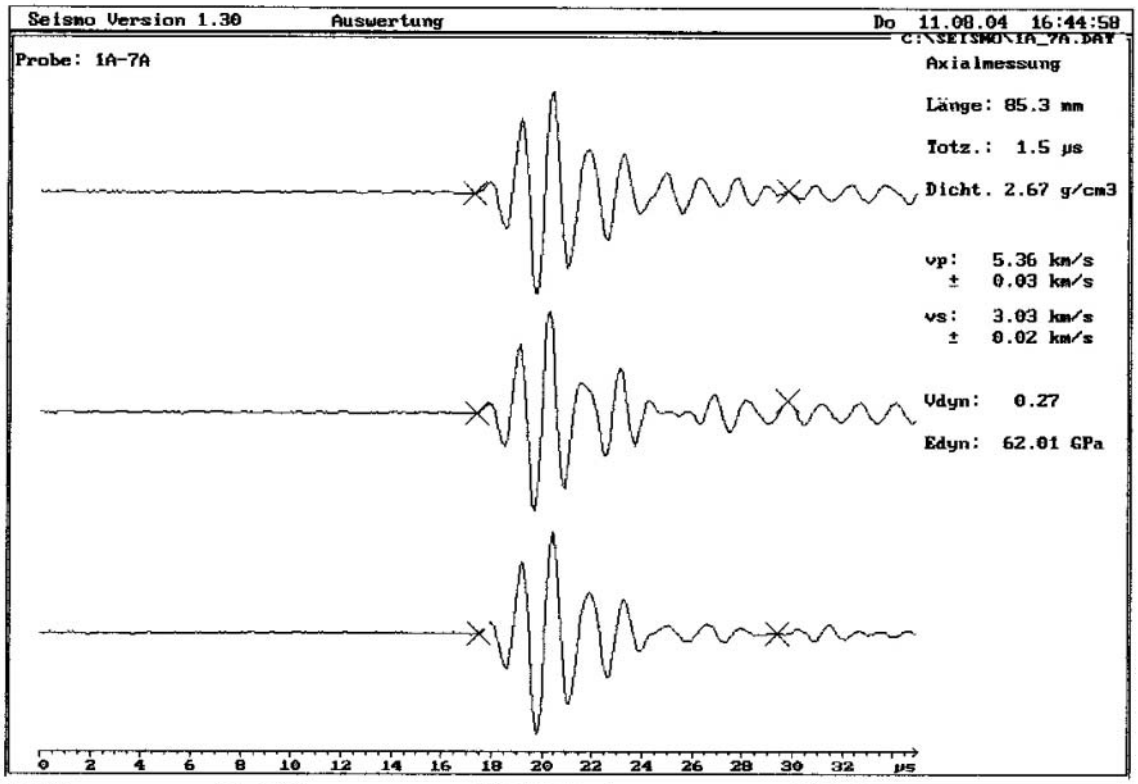
Seismo Version 1.30
Auswertung
Do 11.08.04 16:44:58
C:\SEISMO\1A_7A.DAT
Probe: 1A-7A
Axialmessung
Länge: 85.3 mm
Totz.: 1.5 µs
Dicht. 2.67 g/cm3
vp: 5.36 km/s
± 0.03 km/s
vs: 3.03 km/s
± 0.02 km/s
Vdyn: 0.27
Edyn: 62.01 GPa
0 2 4 6 8 10 12 14 16 18 20 22 24 26 28 30 32 µs

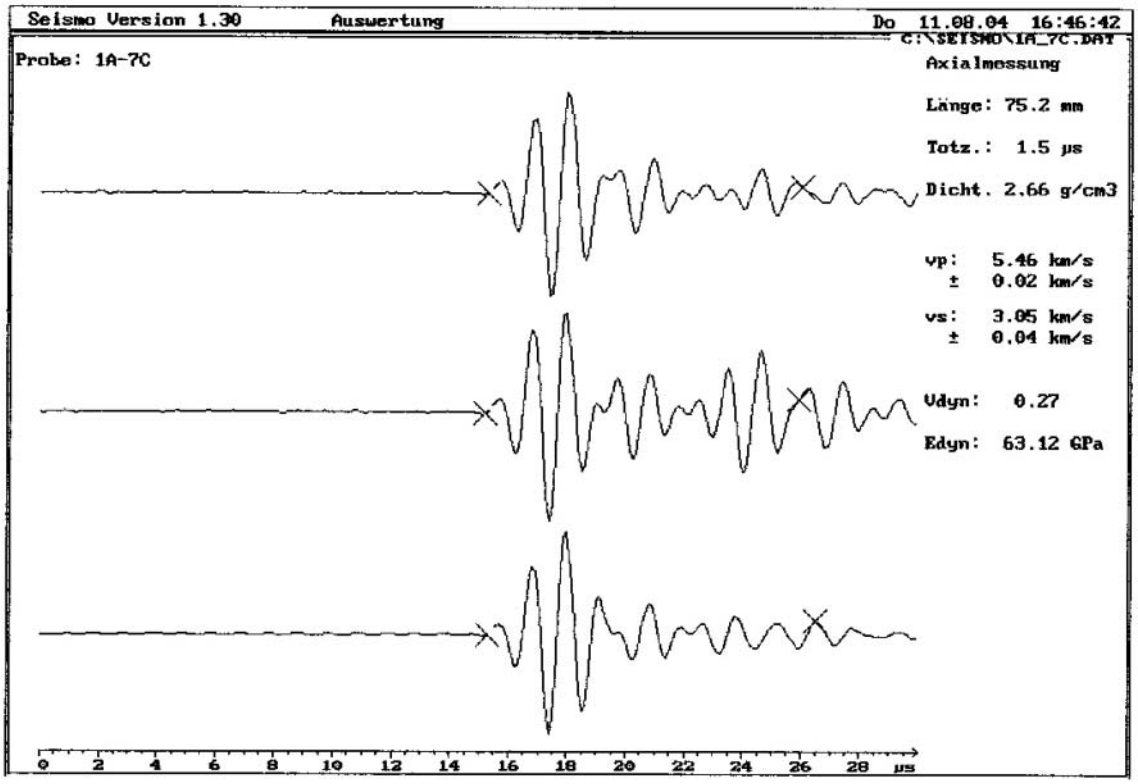
Seismo Version 1.30
Auswertung
Do 11.08.04 16:46:42
C:\SEISMO\1A_7C.DAT
Probe: 1A-7C
Axialmessung
Länge: 75.2 mm
Totz.: 1.5 µs
Dicht. 2.66 g/cm3
vp: 5.46 km/s
± 0.02 km/s
vs: 3.05 km/s
± 0.04 km/s
Vdyn: 0.27
Edyn: 63.12 GPa
0 2 4 6 8 10 12 14 16 18 20 22 24 26 28 µs

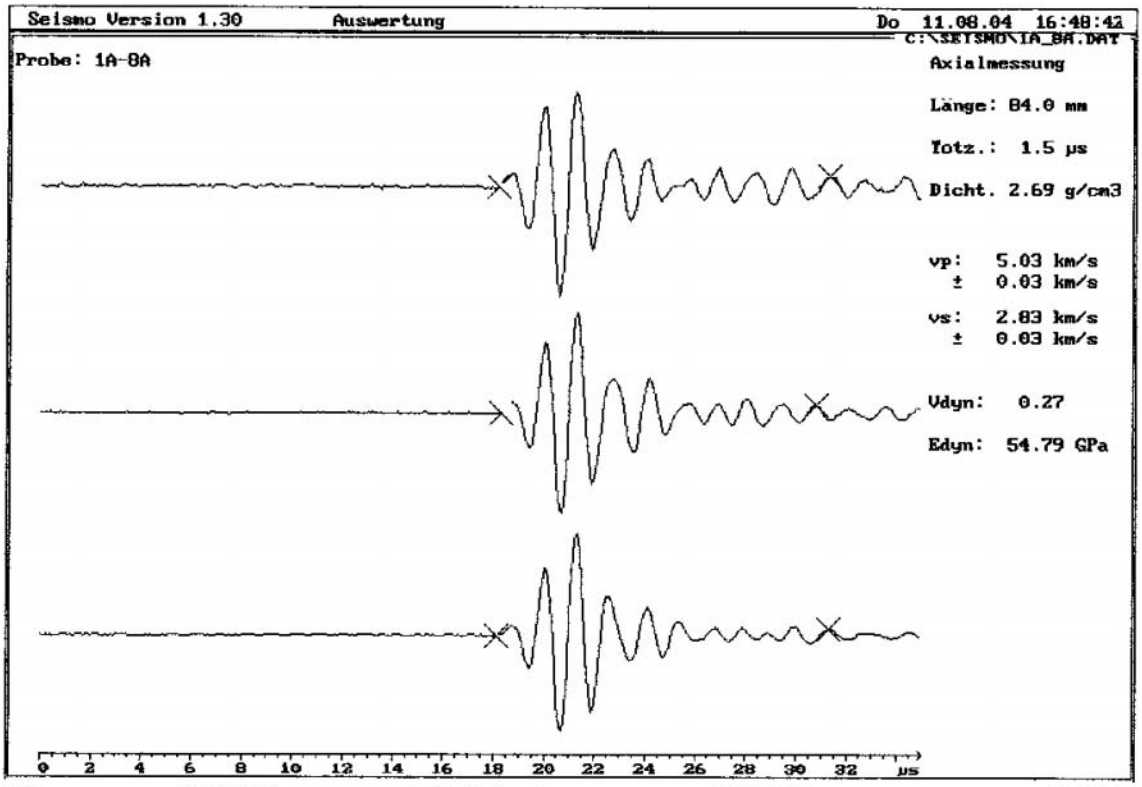
Seismo Version 1.30
Auswertung
Do 11.08.04 16:48:42
C:\SEISMO\1A_8A.DAT
Probe: 1A-8A
Axialmessung
Länge: 84.0 mm
Totz.: 1.5 µs
Dicht. 2.69 g/cm3
vp: 5.03 km/s
± 0.03 km/s
vs: 2.83 km/s
± 0.03 km/s
Vdyn: 0.27
Edyn: 54.79 GPa
0 2 4 6 8 10 12 14 16 18 20 22 24 26 28 30 32 µs

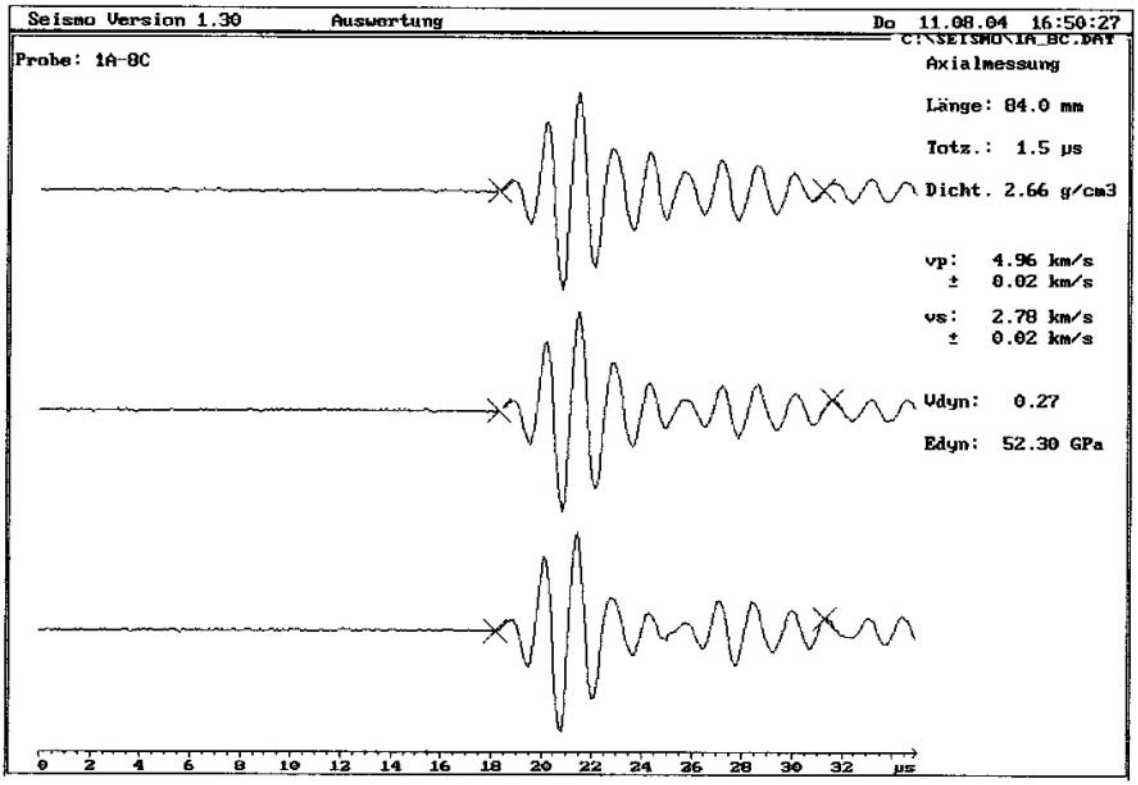
Seismo Version 1.30
Auswertung
Do 11.08.04 16:50:27
C:\SEISMO\1A_8C.DAT
Probe: 1A-8C
Axialmessung
Länge: 84.0 mm
Totz.: 1.5 µs
Dicht. 2.66 g/cm3
vp: 4.96 km/s
± 0.02 km/s
vs: 2.78 km/s
± 0.02 km/s
Vdyn: 0.27
Edyn: 52.30 GPa
0 2 4 6 8 10 12 14 16 18 20 22 24 26 28 30 32 µs

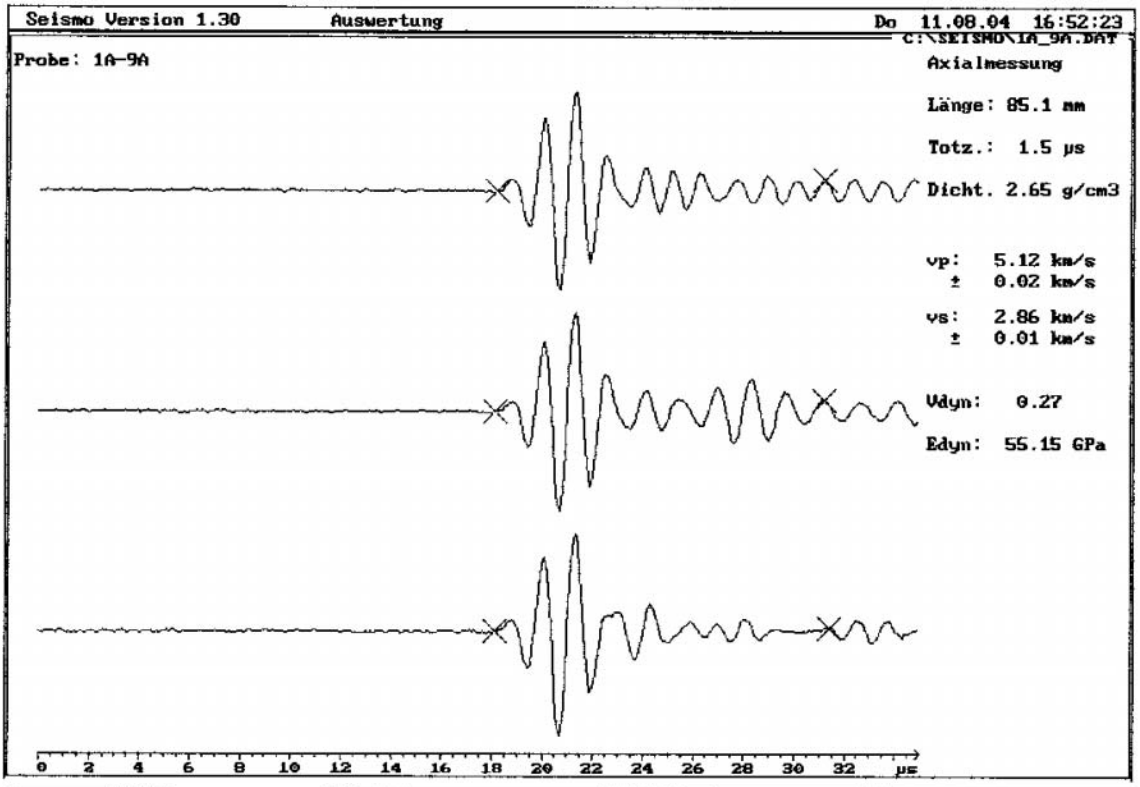
Seismo Version 1.30
Auswertung
Do 11.08.04 16:52:23
C:\SEISMO\1A_9A.DAT
Probe: 1A-9A
Axialmessung
Länge: 85.1 mm
Totz.: 1.5 µs
Dicht. 2.65 g/cm3
vp: 5.12 km/s
± 0.02 km/s
vs: 2.86 km/s
± 0.01 km/s
Vdyn: 0.27
Edyn: 55.15 GPa
0 2 4 6 8 10 12 14 16 18 20 22 24 26 28 30 32 µs

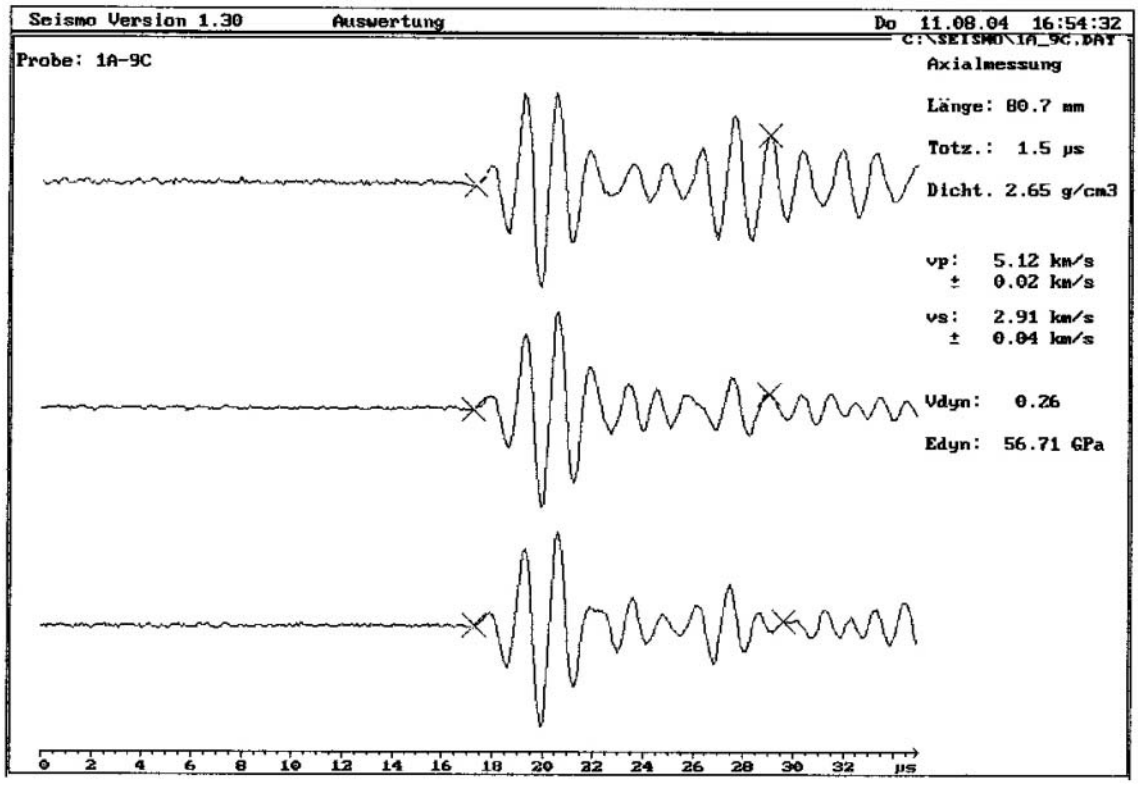
Seismo Version 1.30
Auswertung
Do 11.08.04 16:54:32
C:\SEISMO\1A_9C.DAT
Probe: 1A-9C
Axialmessung
Länge: 80.7 mm
Totz.: 1.5 µs
Dicht. 2.65 g/cm3
vp: 5.12 km/s
± 0.02 km/s
vs: 2.91 km/s
± 0.04 km/s
Vdyn: 0.26
Edyn: 56.71 GPa
0 2 4 6 8 10 12 14 16 18 20 22 24 26 28 30 32 µs

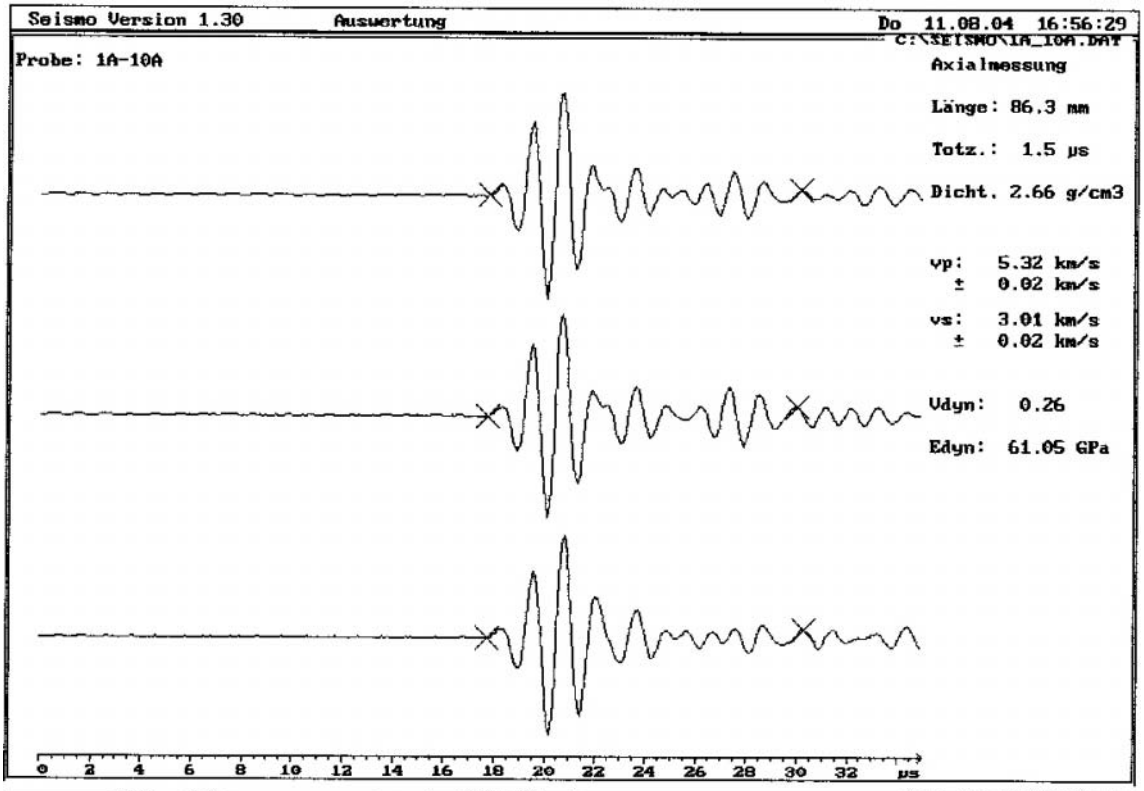
Seismo Version 1.30
Auswertung
Do 11.08.04 16:56:29
C:\SEISMO\1A_10A.DAT
Probe: 1A-10A
Axialmessung
Länge: 86.3 mm
Totz.: 1.5 µs
Dicht. 2.66 g/cm3
vp: 5.32 km/s
± 0.02 km/s
vs: 3.01 km/s
± 0.02 km/s
Vdyn: 0.26
Edyn: 61.05 GPa
0 2 4 6 8 10 12 14 16 18 20 22 24 26 28 30 32 µs

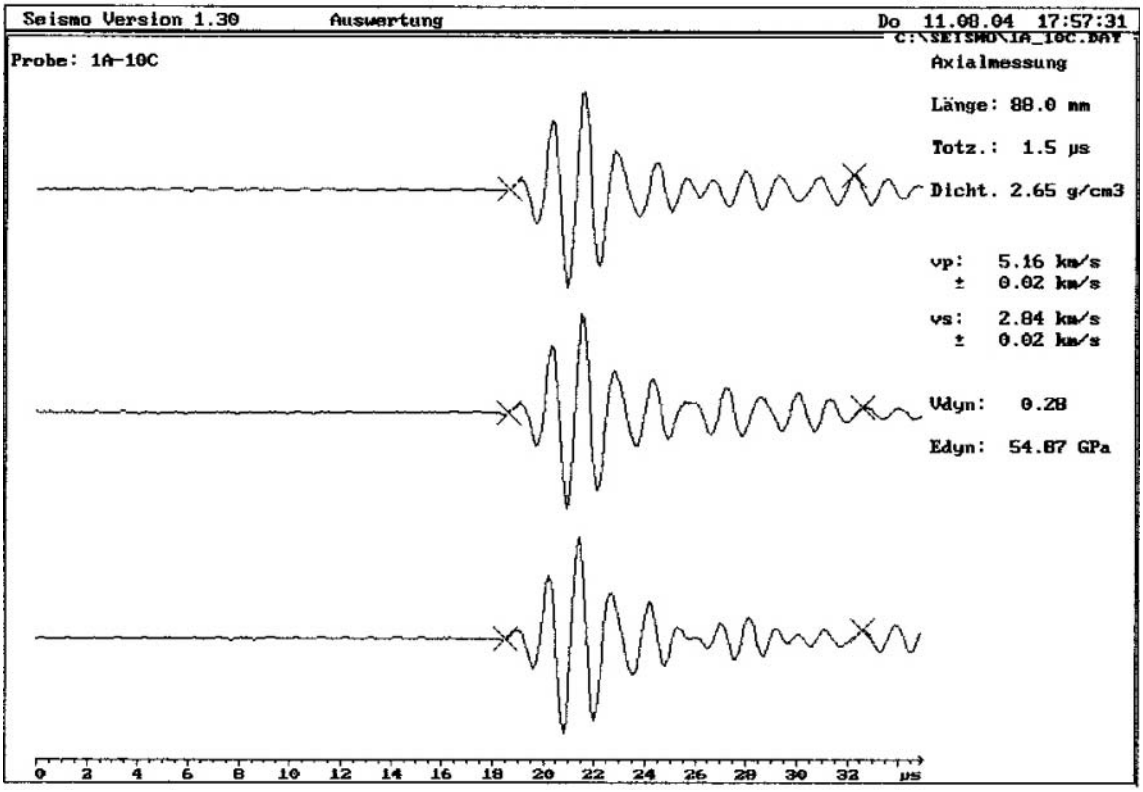
Seismo Version 1.30
Auswertung
Do 11.08.04 17:57:31
C:\SEISMO\1A_10C.DAT
Probe: 1A-10C
Axialmessung
Länge: 88.0 mm
Totz.: 1.5 µs
Dicht. 2.65 g/cm3
vp: 5.16 km/s
± 0.02 km/s
vs: 2.84 km/s
± 0.02 km/s
Vdyn: 0.28
Edyn: 54.87 GPa
0 2 4 6 8 10 12 14 16 18 20 22 24 26 28 30 32 µs

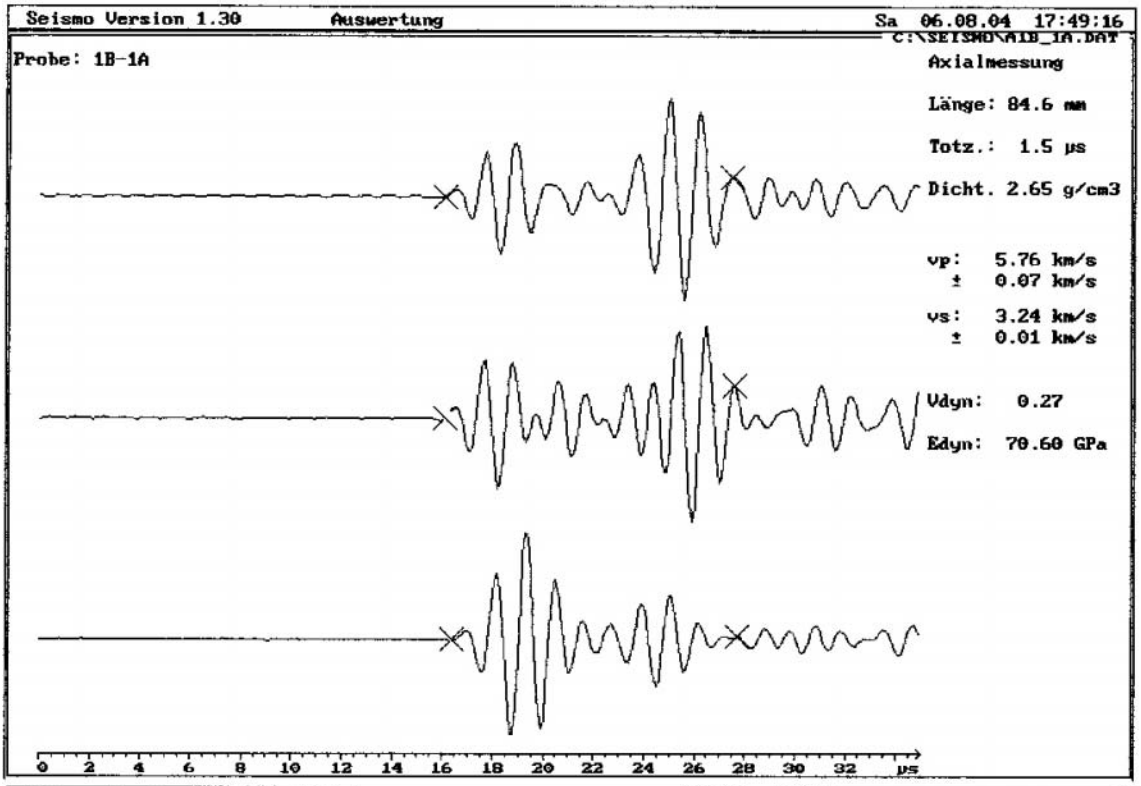
Seismo Version 1.30
Auswertung
Sa 06.08.04 17:49:16
C:\SEISMO\A1B_1A.DAT
Probe: 1B-1A
Axialmessung
Länge: 84.6 mm
Totz.: 1.5 µs
Dicht. 2.65 g/cm3
vp: 5.76 km/s
± 0.07 km/s
vs: 3.24 km/s
± 0.01 km/s
Vdyn: 0.27
Edyn: 70.60 GPa
0 2 4 6 8 10 12 14 16 18 20 22 24 26 28 30 32 µs

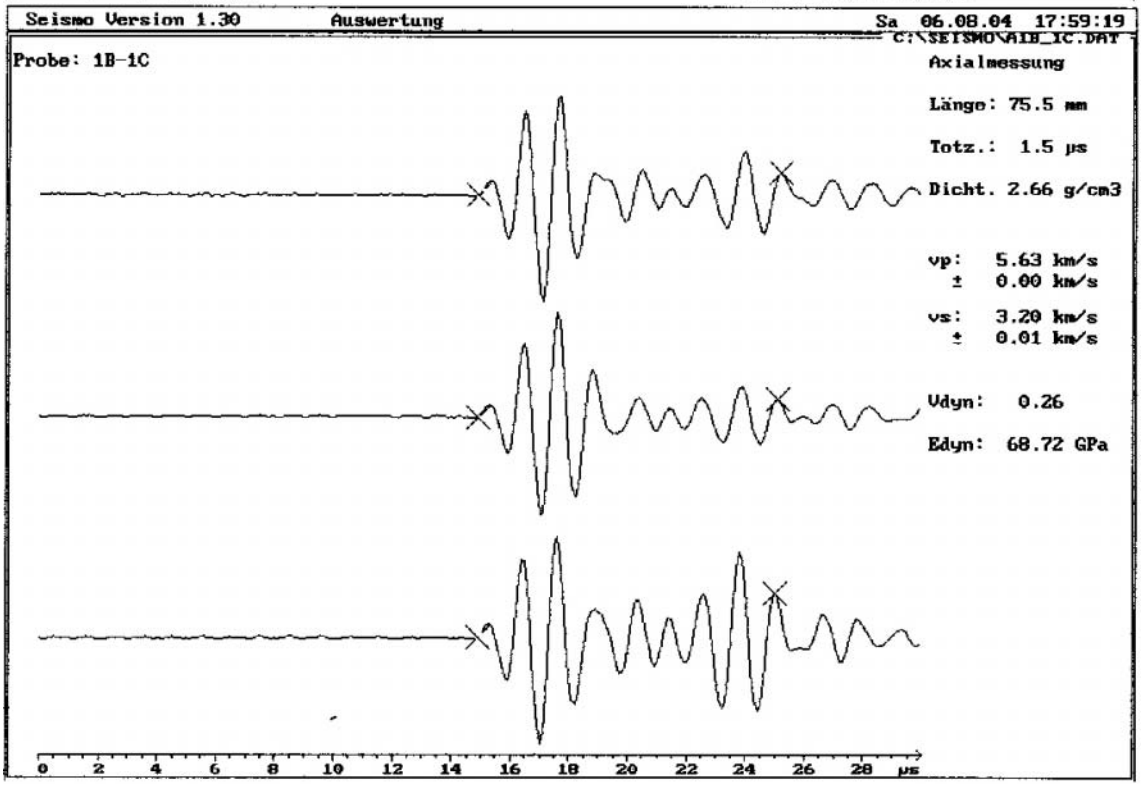
Seismo Version 1.30
Auswertung
Sa 06.08.04 17:59:19
C:\SEISMO\A1B_1C.DAT
Probe: 1B-1C
Axialmessung
Länge: 75.5 mm
Totz.: 1.5 µs
Dicht. 2.66 g/cm3
vp: 5.63 km/s
± 0.00 km/s
vs: 3.20 km/s
± 0.01 km/s
Vdyn: 0.26
Edyn: 68.72 GPa
0 2 4 6 8 10 12 14 16 18 20 22 24 26 28 µs

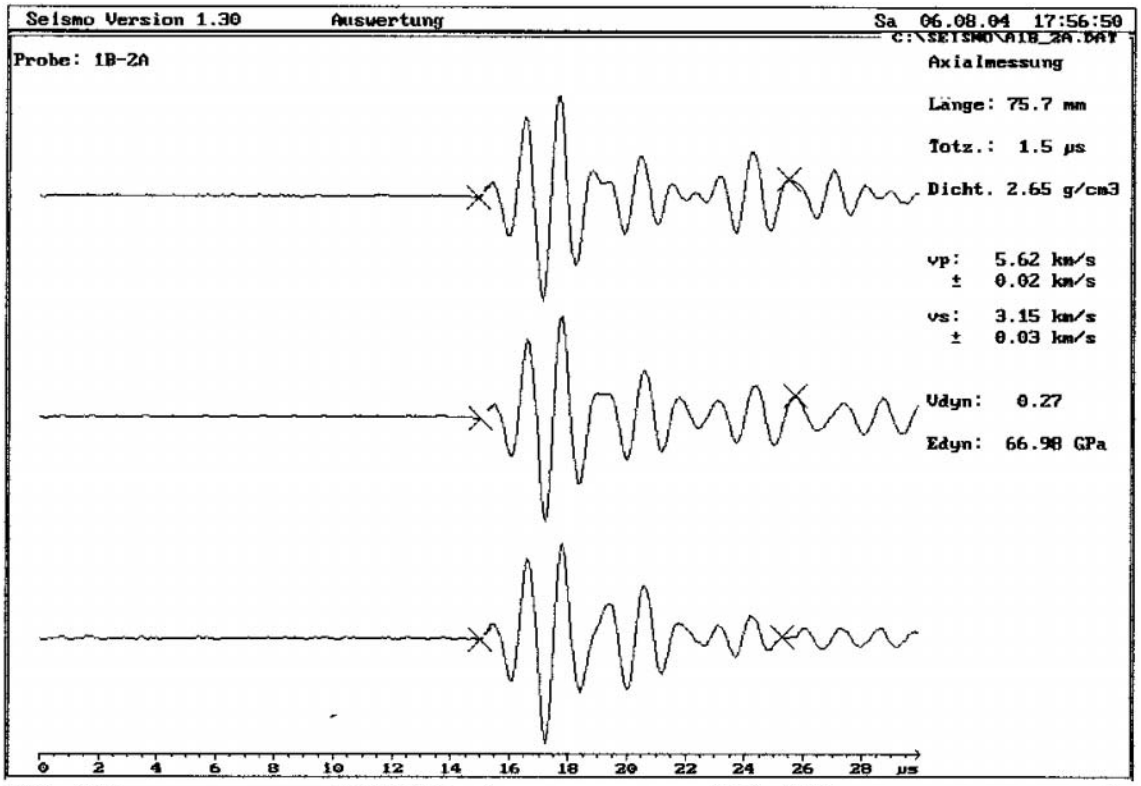
Seismo Version 1.30
Auswertung
Sa 06.08.04 17:56:50
C:\SEISMO\A1B_2A.DAT
Probe: 1B-2A
Axialmessung
Länge: 75.7 mm
Totz.: 1.5 µs
Dicht. 2.65 g/cm3
vp: 5.62 km/s
± 0.02 km/s
vs: 3.15 km/s
± 0.03 km/s
Udyn: 0.27
Edyn: 66.98 GPa
0 2 4 6 8 10 12 14 16 18 20 22 24 26 28 µs

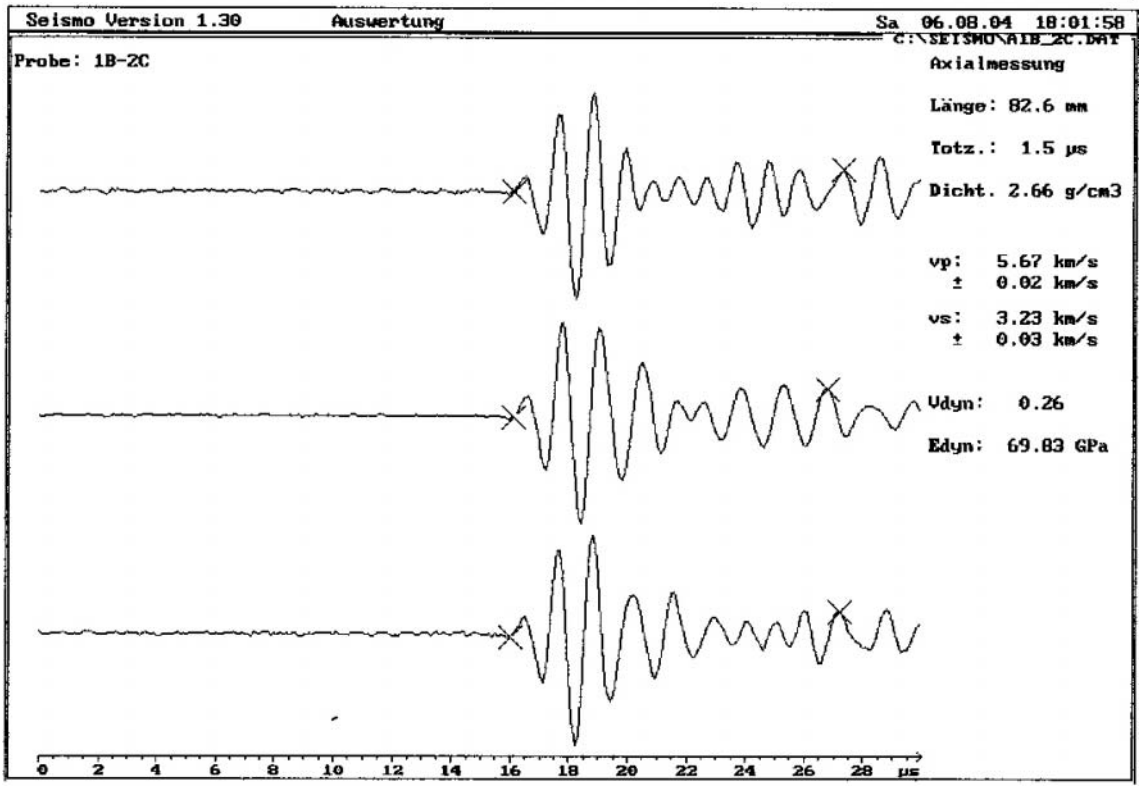
Seismo Version 1.30
Auswertung
Sa 06.08.04 18:01:58
C:\SEISMO\A1B_2C.DAT
Probe: 1B-2C
Axialmessung
Länge: 82.6 mm
Totz.: 1.5 µs
Dicht. 2.66 g/cm3
vp: 5.67 km/s
± 0.02 km/s
vs: 3.23 km/s
± 0.03 km/s
Udyn: 0.26
Edyn: 69.83 GPa
0 2 4 6 8 10 12 14 16 18 20 22 24 26 28 µs

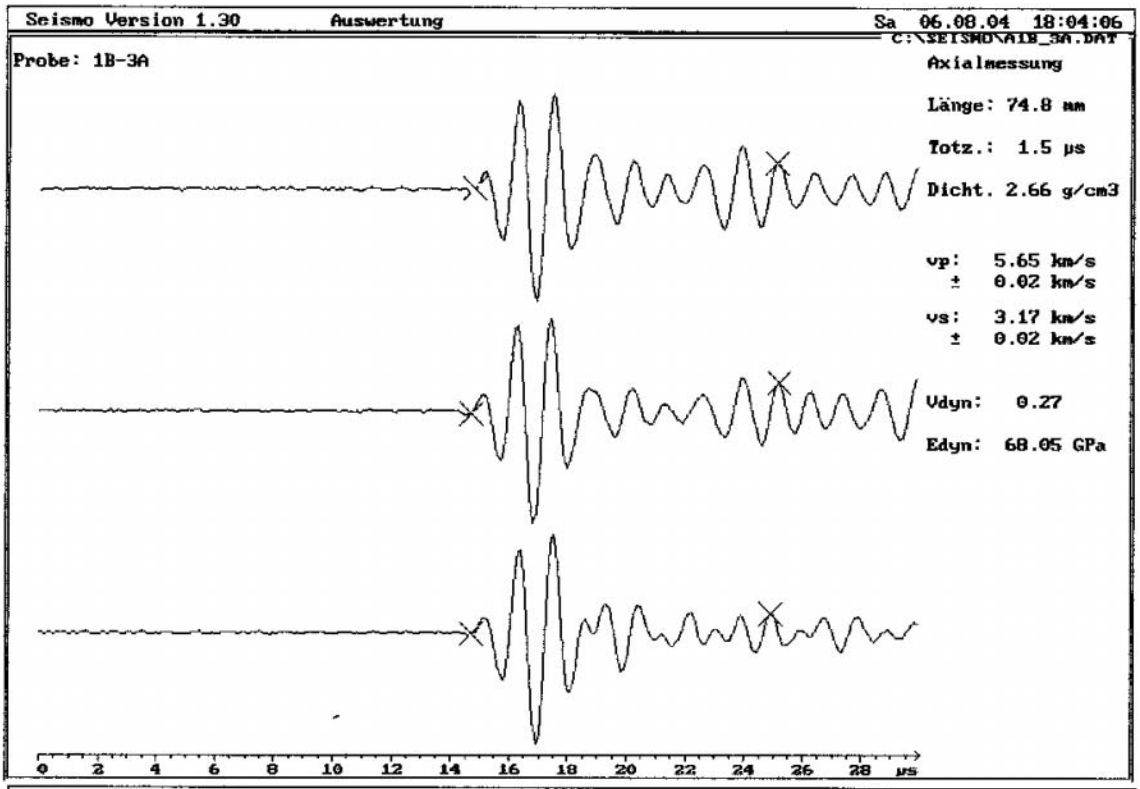
Seismo Version 1.30
Auswertung
Sa 06.08.04 18:04:06
C:\SEISMO\A1B_3A.DAT
Probe: 1B-3A
Axialmessung
Länge: 74.8 mm
Totz.: 1.5 µs
Dicht. 2.66 g/cm3
vp: 5.65 km/s
± 0.02 km/s
vs: 3.17 km/s
± 0.02 km/s
Vdyn: 0.27
Edyn: 68.05 GPa
0 2 4 6 8 10 12 14 16 18 20 22 24 26 28 µs

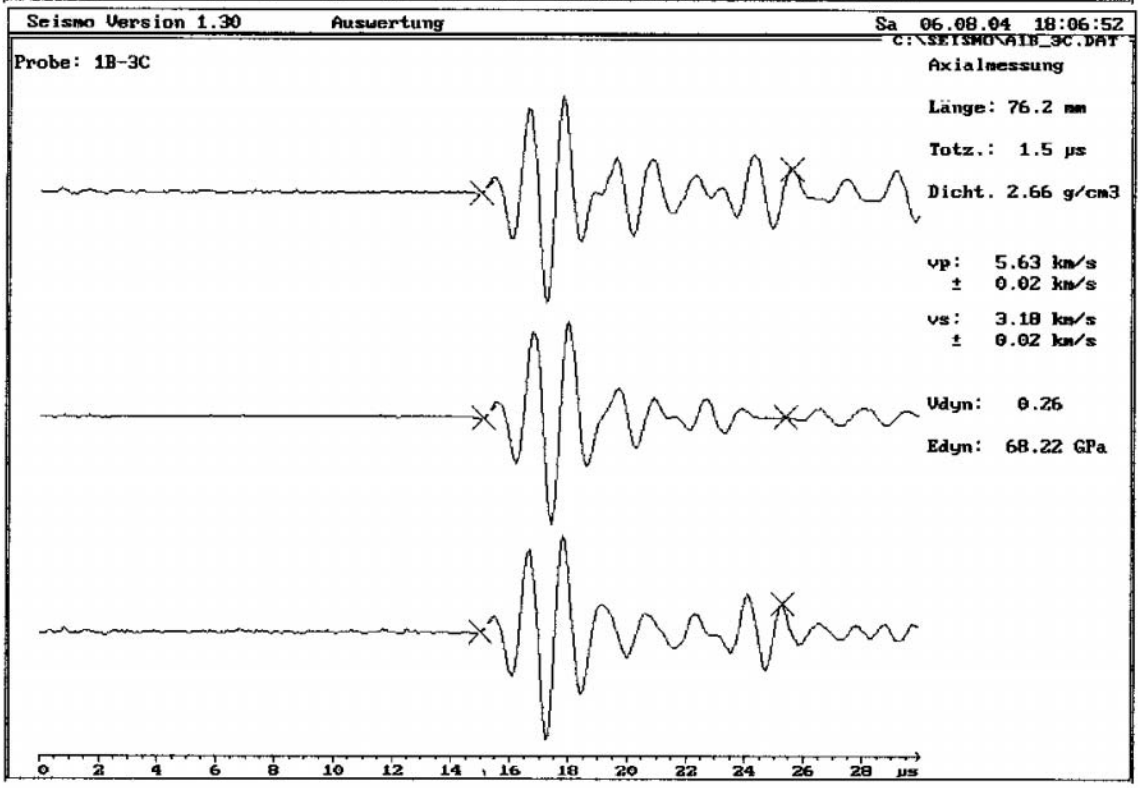
Seismo Version 1.30
Auswertung
Sa 06.08.04 18:06:52
C:\SEISMO\A1B_3C.DAT
Probe: 1B-3C
Axialmessung
Länge: 76.2 mm
Totz.: 1.5 µs
Dicht. 2.66 g/cm3
vp: 5.63 km/s
± 0.02 km/s
vs: 3.18 km/s
± 0.02 km/s
Vdyn: 0.26
Edyn: 68.22 GPa
0 2 4 6 8 10 12 14 16 18 20 22 24 26 28 µs

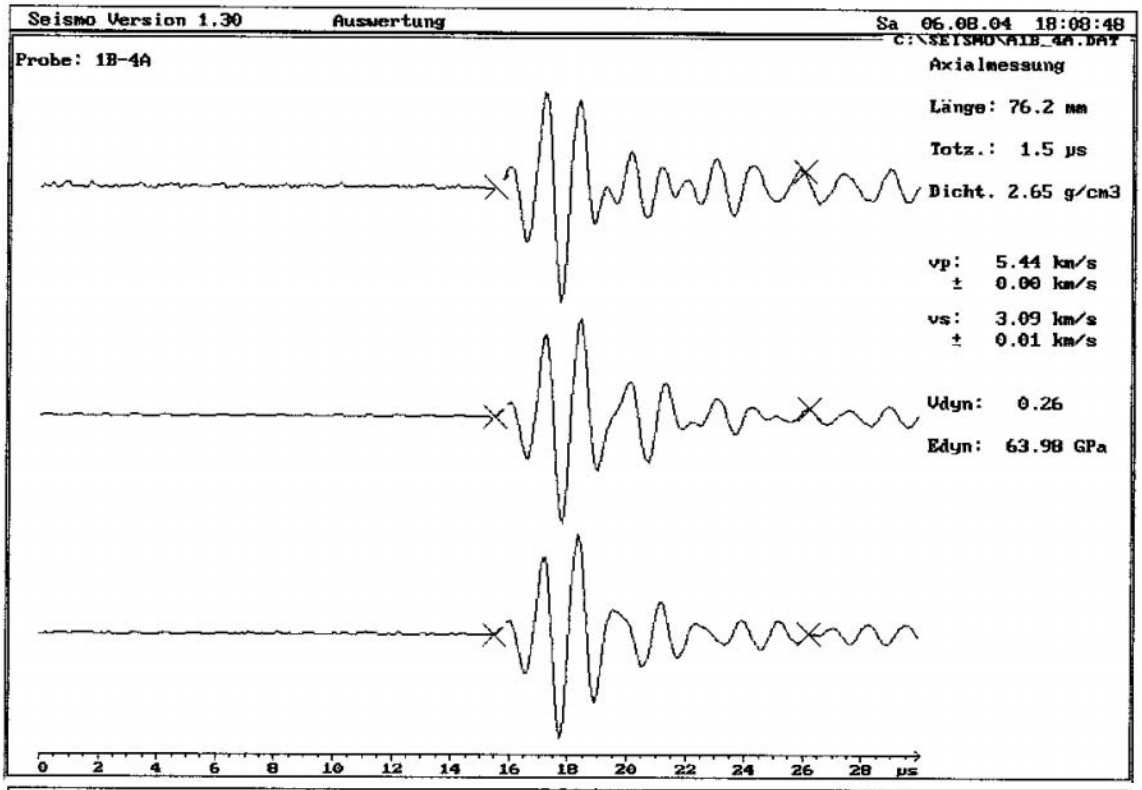
Seismo Version 1.30
Auswertung
Sa 06.08.04 18:08:48
C:\SEISMO\A1B_4A.DAT
Probe: 1B-4A
Axialmessung
Länge: 76.2 mm
Totz.: 1.5 µs
Dicht. 2.65 g/cm3
vp: 5.44 km/s
± 0.00 km/s
vs: 3.09 km/s
± 0.01 km/s
Udyn: 0.26
Edyn: 63.98 GPa
0 2 4 6 8 10 12 14 16 18 20 22 24 26 28 µs

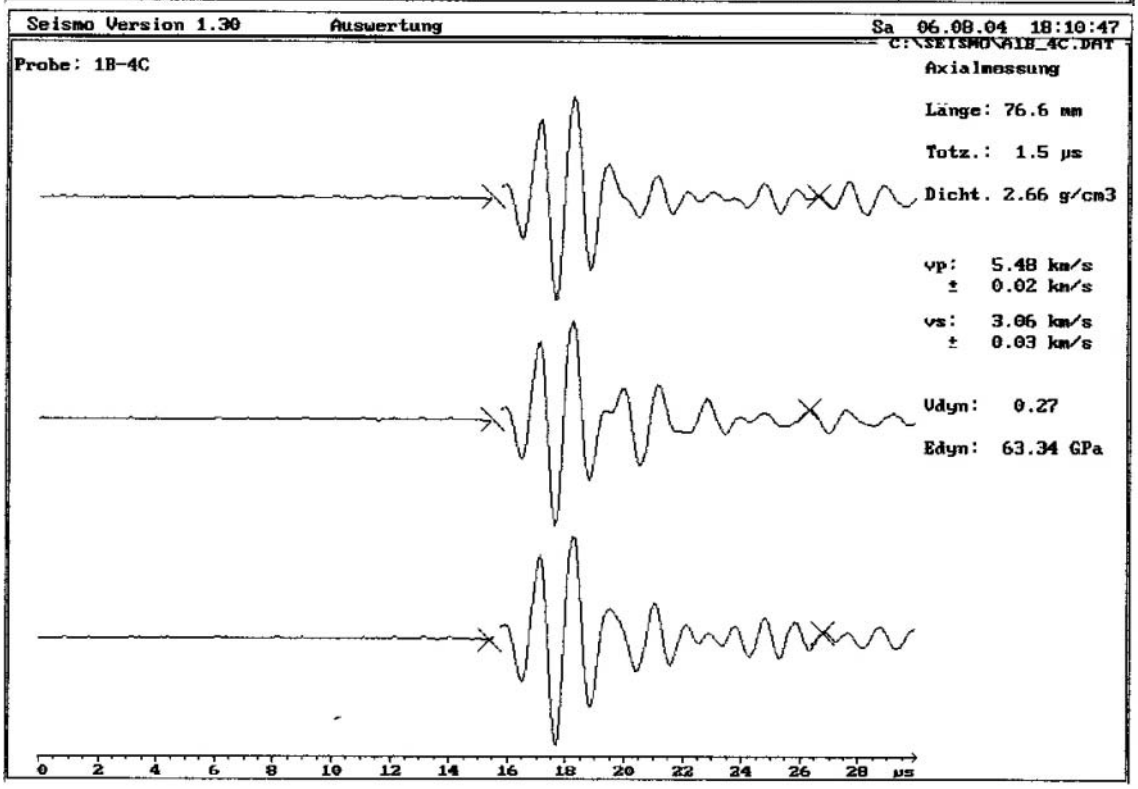
Seismo Version 1.30
Auswertung
Sa 06.08.04 18:10:47
C:\SEISMO\A1B_4C.DAT
Probe: 1B-4C
Axialmessung
Länge: 76.6 mm
Totz.: 1.5 µs
Dicht. 2.66 g/cm3
vp: 5.48 km/s
± 0.02 km/s
vs: 3.06 km/s
± 0.03 km/s
Udyn: 0.27
Edyn: 63.34 GPa
0 2 4 6 8 10 12 14 16 18 20 22 24 26 28 µs

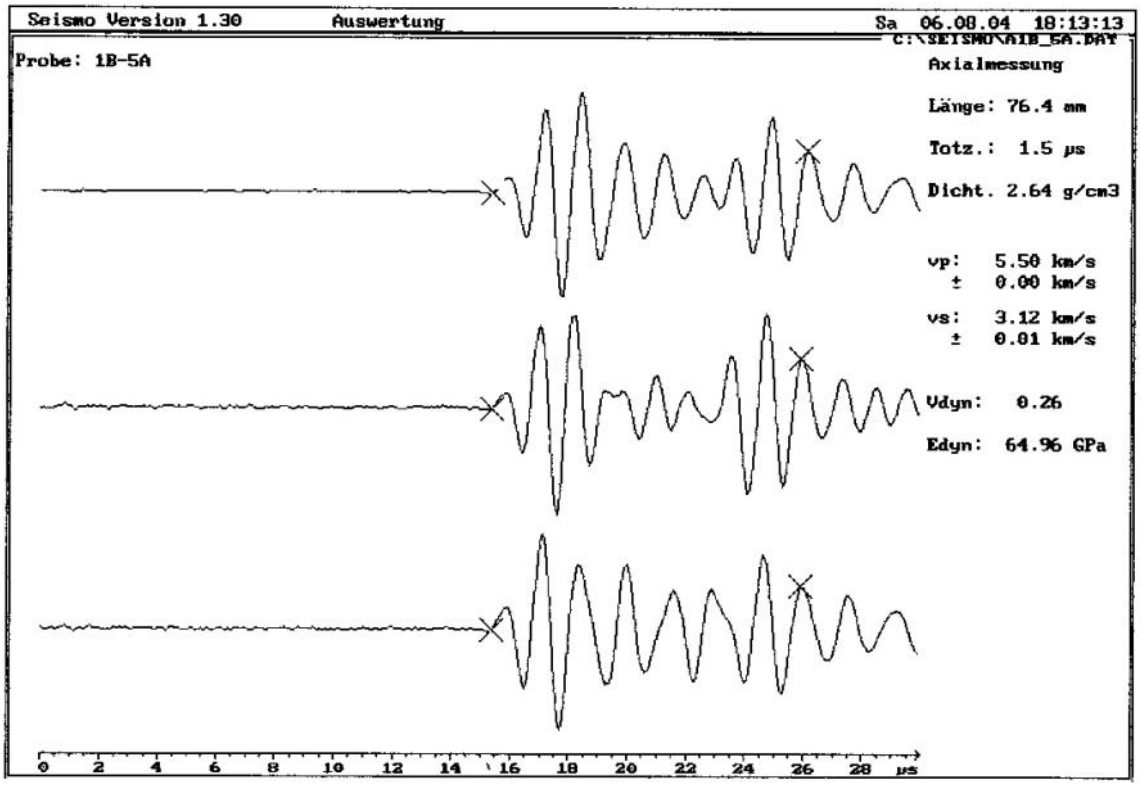
Seismo Version 1.30
Auswertung
Sa 06.08.04 18:13:13
C:\SEISMO\A1B_5A.DAT
Probe: 1B-5A
Axialmessung
Länge: 76.4 mm
Totz.: 1.5 µs
Dicht. 2.64 g/cm3
vp: 5.50 km/s
± 0.00 km/s
vs: 3.12 km/s
± 0.01 km/s
Vdyn: 0.26
Edyn: 64.96 GPa
0 2 4 6 8 10 12 14 16 18 20 22 24 26 28 µs

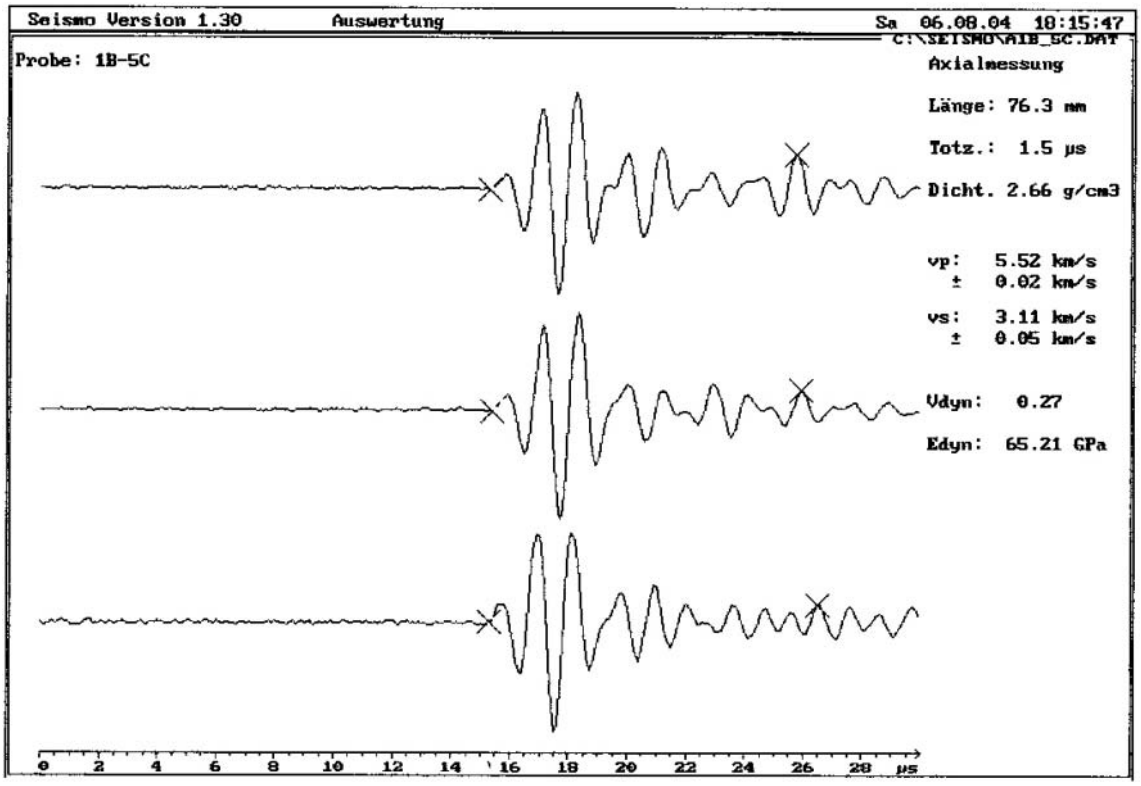
Seismo Version 1.30
Auswertung
Sa 06.08.04 18:15:47
C:\SEISMO\A1B_5C.DAT
Probe: 1B-5C
Axialmessung
Länge: 76.3 mm
Totz.: 1.5 µs
Dicht. 2.66 g/cm3
vp: 5.52 km/s
± 0.02 km/s
vs: 3.11 km/s
± 0.05 km/s
Vdyn: 0.27
Edyn: 65.21 GPa
0 2 4 6 8 10 12 14 16 18 20 22 24 26 28 µs

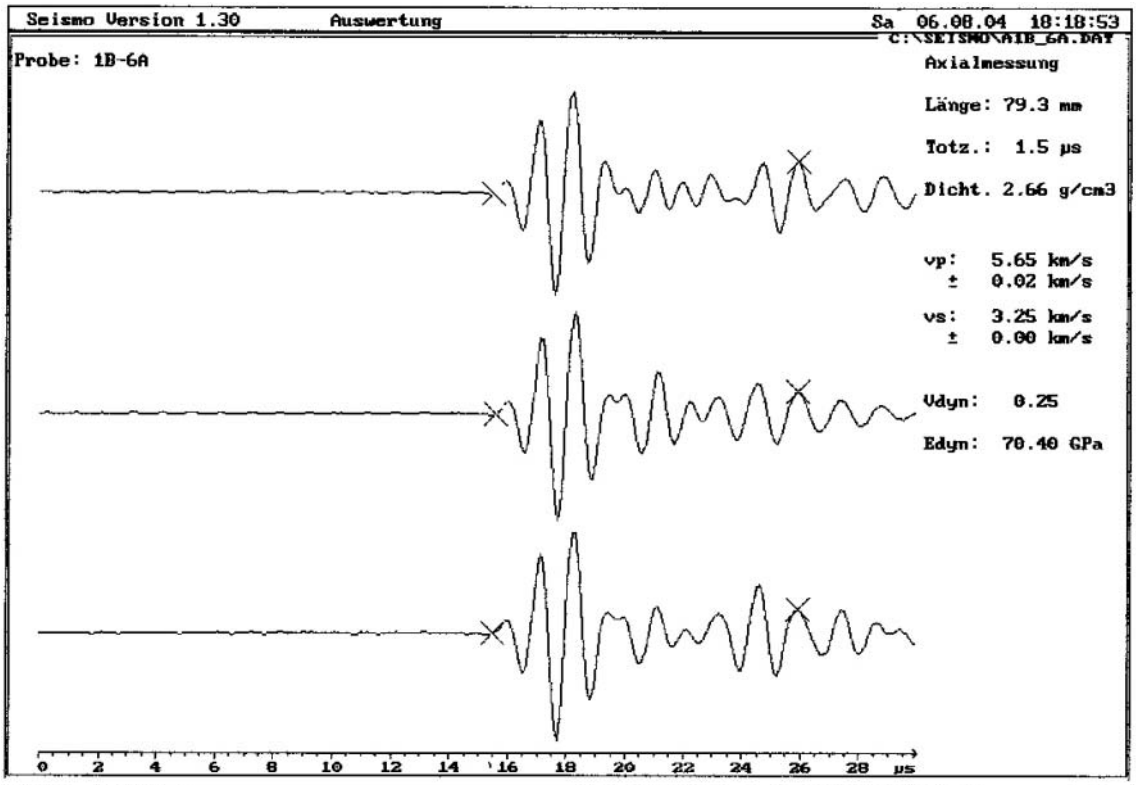
Seismo Version 1.30
Auswertung
Sa 06.08.04 18:18:53
C:\SEISMO\A1B_6A.DAT
Probe: 1B-6A
Axialmessung
Länge: 79.3 mm
Totz.: 1.5 µs
Dicht. 2.66 g/cm3
vp: 5.65 km/s
± 0.02 km/s
vs: 3.25 km/s
± 0.00 km/s
Vdyn: 0.25
Edyn: 70.40 GPa
0 2 4 6 8 10 12 14 16 18 20 22 24 26 28 µs

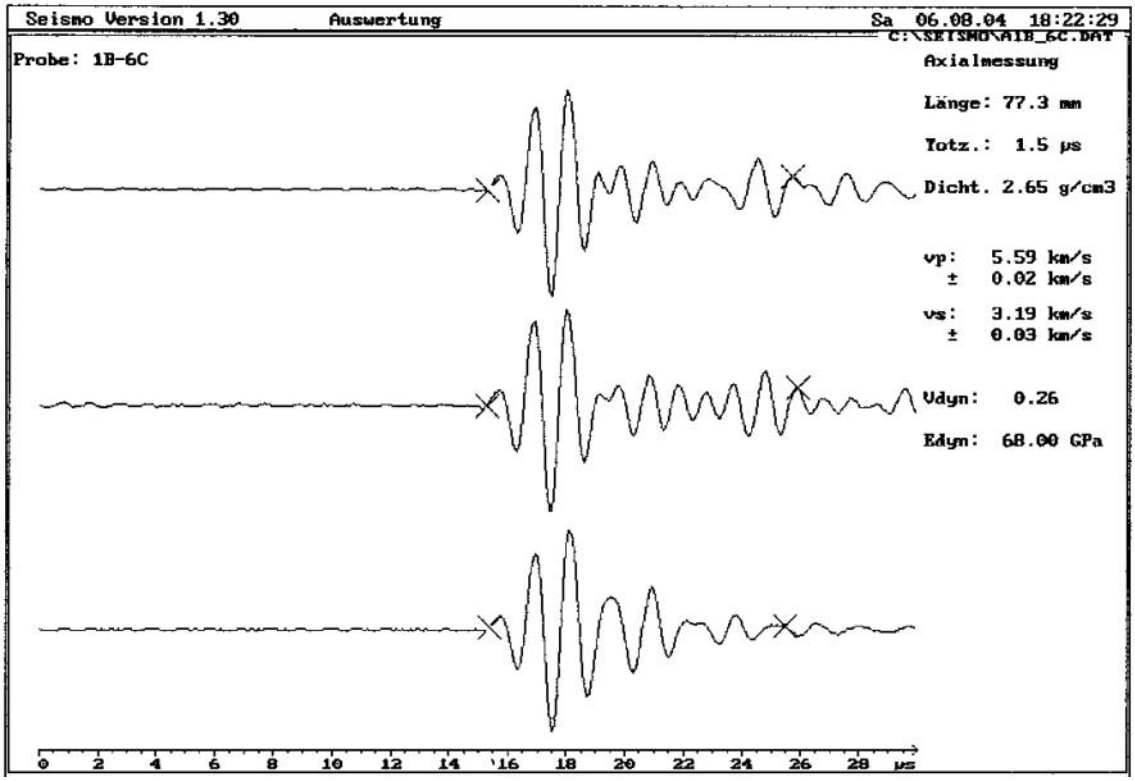
Seismo Version 1.30
Auswertung
Sa 06.08.04 18:22:29
C:\SEISMO\A1B_6C.DAT
Probe: 1B-6C
Axialmessung
Länge: 77.3 mm
Totz.: 1.5 µs
Dicht. 2.65 g/cm3
vp: 5.59 km/s
± 0.02 km/s
vs: 3.19 km/s
± 0.03 km/s
Vdyn: 0.26
Edyn: 68.00 GPa
0 2 4 6 8 10 12 14 16 18 20 22 24 26 28 µs

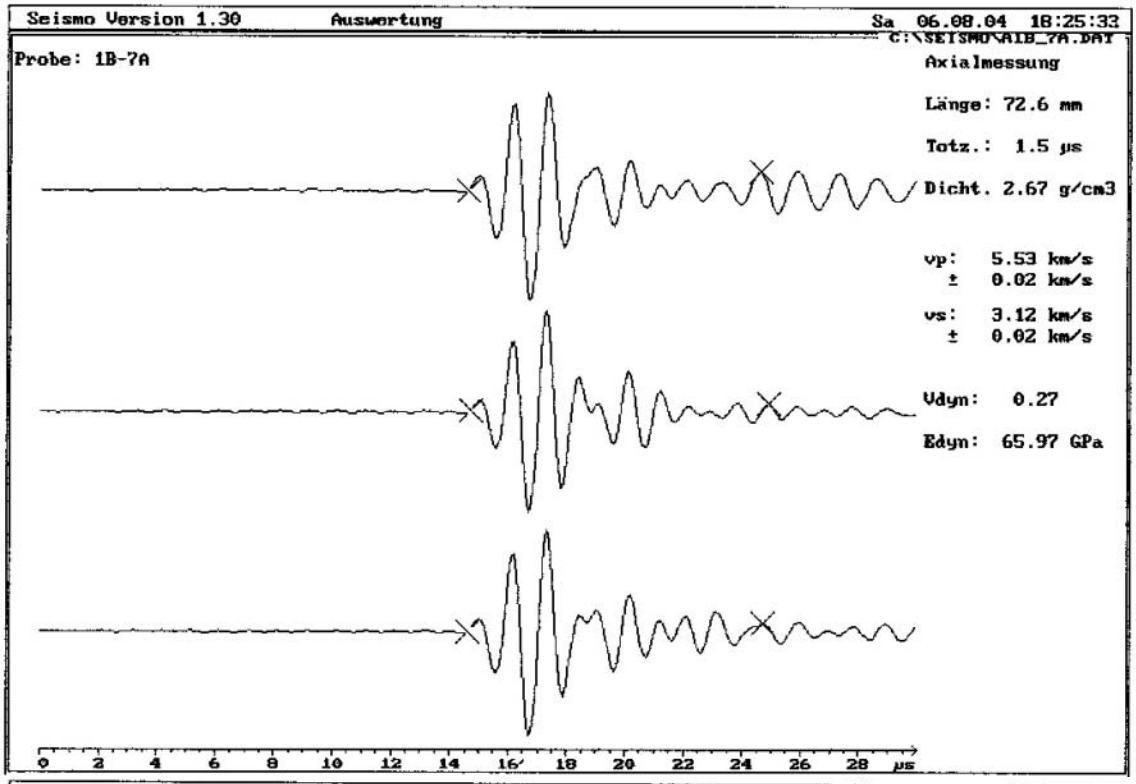
Seismo Version 1.30
Auswertung
Sa 06.08.04 18:25:33
C:\SEISMO\A1B_7A.DAT
Probe: 1B-7A
Axialmessung
Länge: 72.6 mm
Totz.: 1.5 µs
Dicht. 2.67 g/cm3
vp: 5.53 km/s
± 0.02 km/s
vs: 3.12 km/s
± 0.02 km/s
Vdyn: 0.27
Edyn: 65.97 GPa
0 2 4 6 8 10 12 14 16 18 20 22 24 26 28 µs

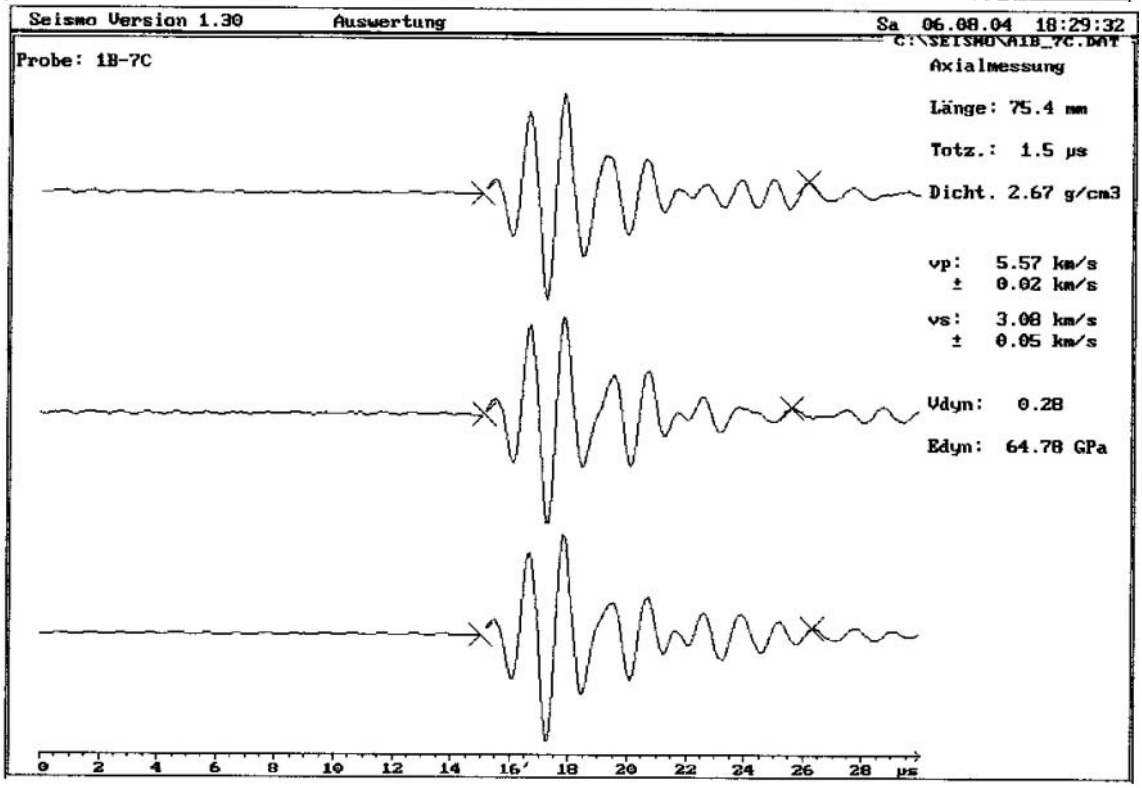
Seismo Version 1.30
Auswertung
Sa 06.08.04 18:29:32
C:\SEISMO\A1B_7C.DAT
Probe: 1B-7C
Axialmessung
Länge: 75.4 mm
Totz.: 1.5 µs
Dicht. 2.67 g/cm3
vp: 5.57 km/s
± 0.02 km/s
vs: 3.08 km/s
± 0.05 km/s
Vdyn: 0.28
Edyn: 64.78 GPa
0 2 4 6 8 10 12 14 16 18 20 22 24 26 28 µs

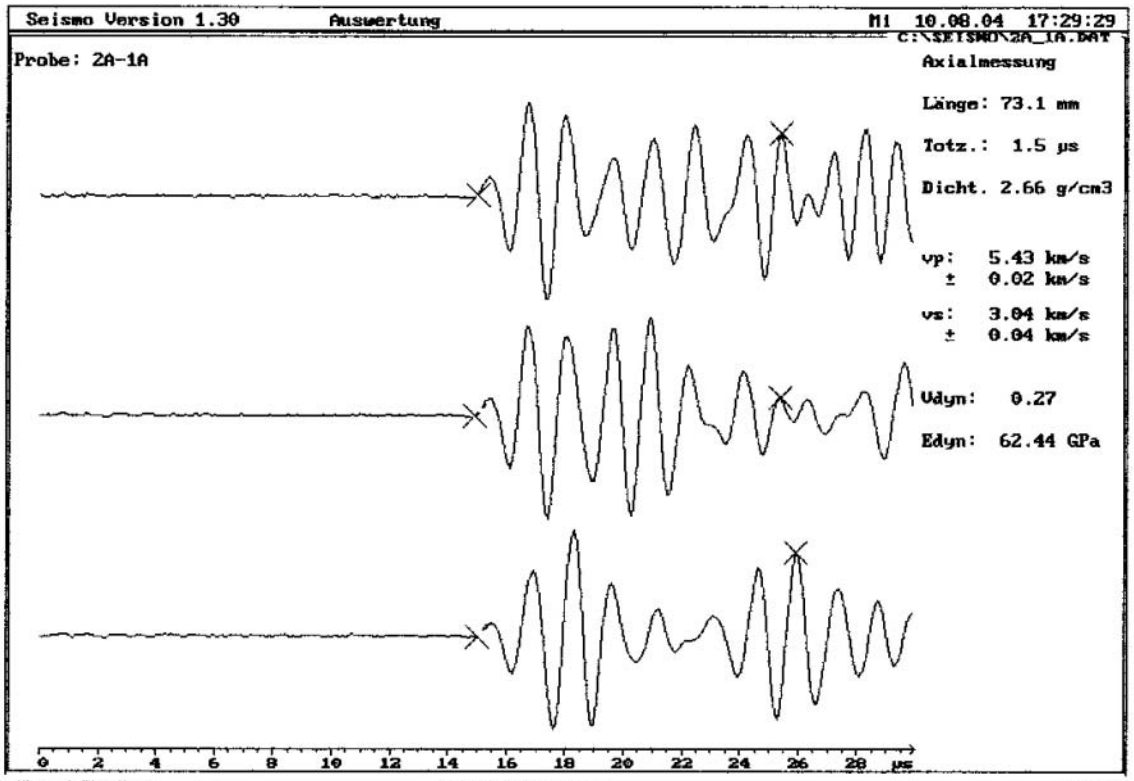
Seismo Version 1.30
Auswertung
Mi 10.08.04 17:29:29
C:\SEISMO\2A_1A.DAT
Probe: 2A-1A
Axialmessung
Länge: 73.1 mm
Totz.: 1.5 µs
Dicht. 2.66 g/cm3
vp: 5.43 km/s
± 0.02 km/s
vs: 3.04 km/s
± 0.04 km/s
Udyn: 0.27
Edyn: 62.44 GPa
0 2 4 6 8 10 12 14 16 18 20 22 24 26 28 µs

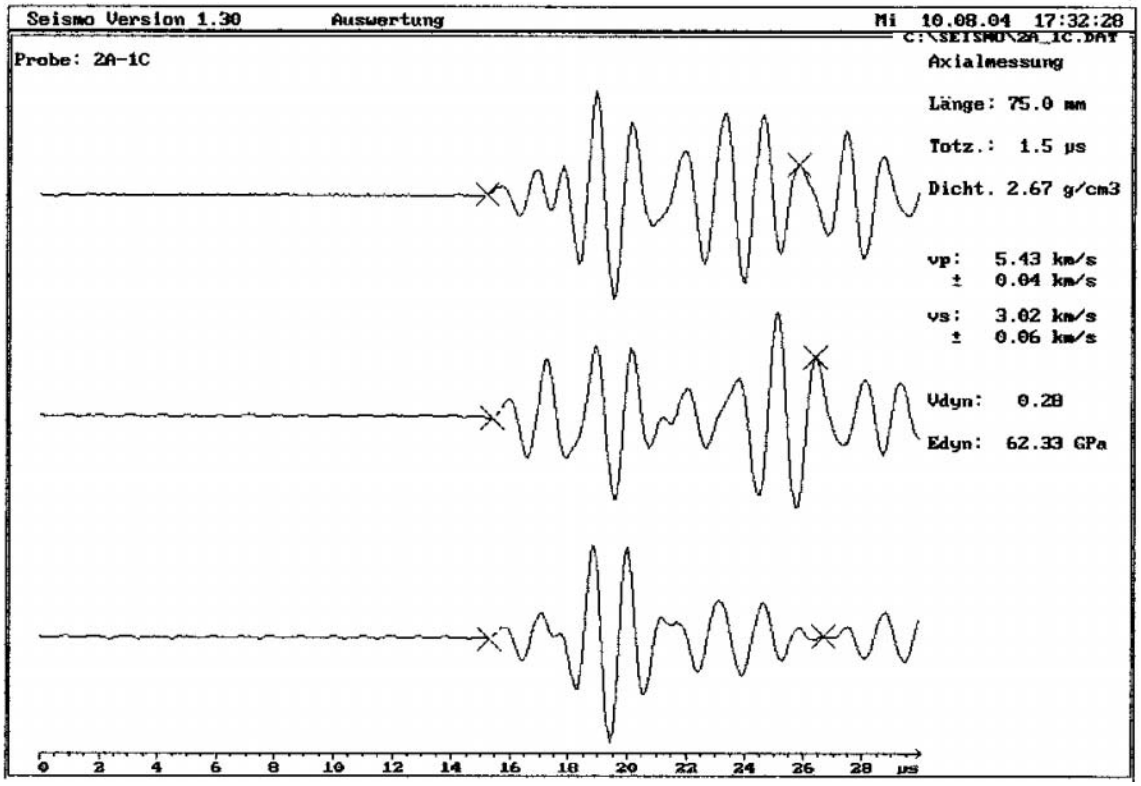
Seismo Version 1.30
Auswertung
Mi 10.08.04 17:32:28
C:\SEISMO\2A_1C.DAT
Probe: 2A-1C
Axialmessung
Länge: 75.0 mm
Totz.: 1.5 µs
Dicht. 2.67 g/cm3
vp: 5.43 km/s
± 0.04 km/s
vs: 3.02 km/s
± 0.06 km/s
Udyn: 0.28
Edyn: 62.33 GPa
0 2 4 6 8 10 12 14 16 18 20 22 24 26 28 µs

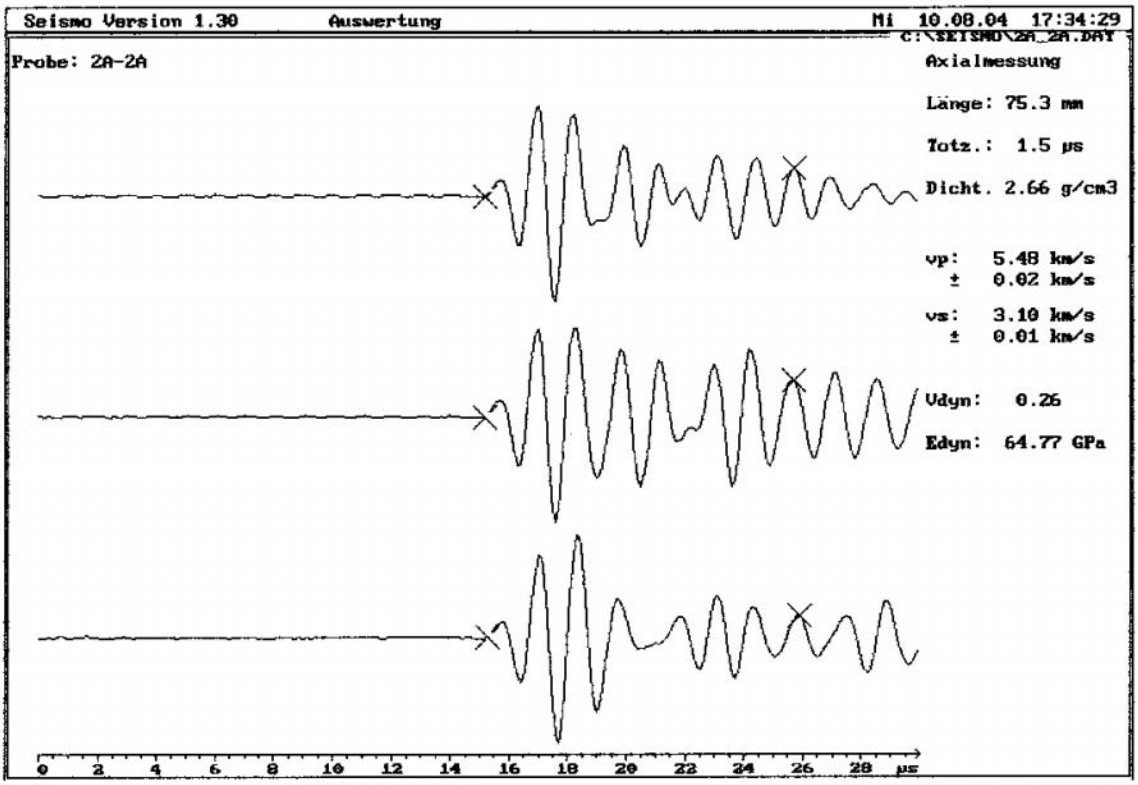
Seismo Version 1.30
Auswertung
Mi 10.08.04 17:34:29
C:\SEISMO\2A_2A.DAT
Probe: 2A-2A
Axialmessung
Länge: 75.3 mm
Totz.: 1.5 µs
Dicht. 2.66 g/cm3
vp: 5.48 km/s
± 0.02 km/s
vs: 3.10 km/s
± 0.01 km/s
Vdyn: 0.26
Edyn: 64.77 GPa
0 2 4 6 8 10 12 14 16 18 20 22 24 26 28 µs

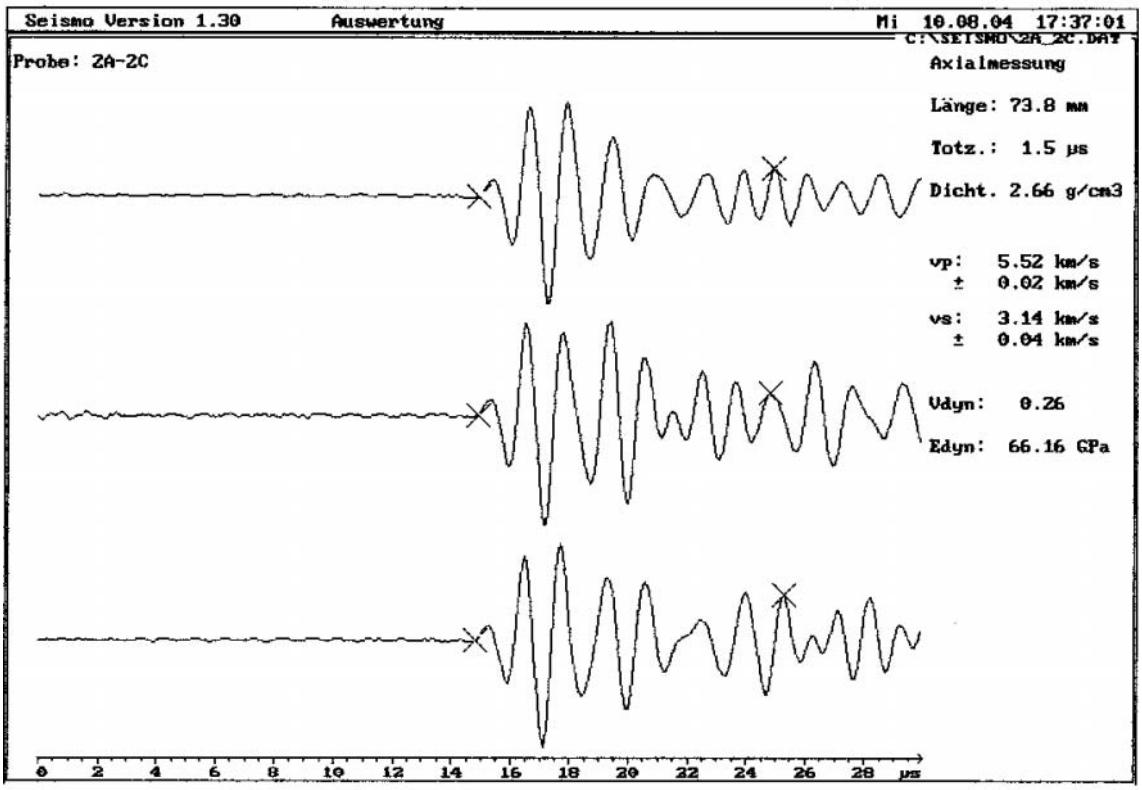
Seismo Version 1.30
Auswertung
Mi 10.08.04 17:37:01
C:\SEISMO\2A_2C.DAT
Probe: 2A-2C
Axialmessung
Länge: 73.8 mm
Totz.: 1.5 µs
Dicht. 2.66 g/cm3
vp: 5.52 km/s
± 0.02 km/s
vs: 3.14 km/s
± 0.04 km/s
Vdyn: 0.26
Edyn: 66.16 GPa
0 2 4 6 8 10 12 14 16 18 20 22 24 26 28 µs

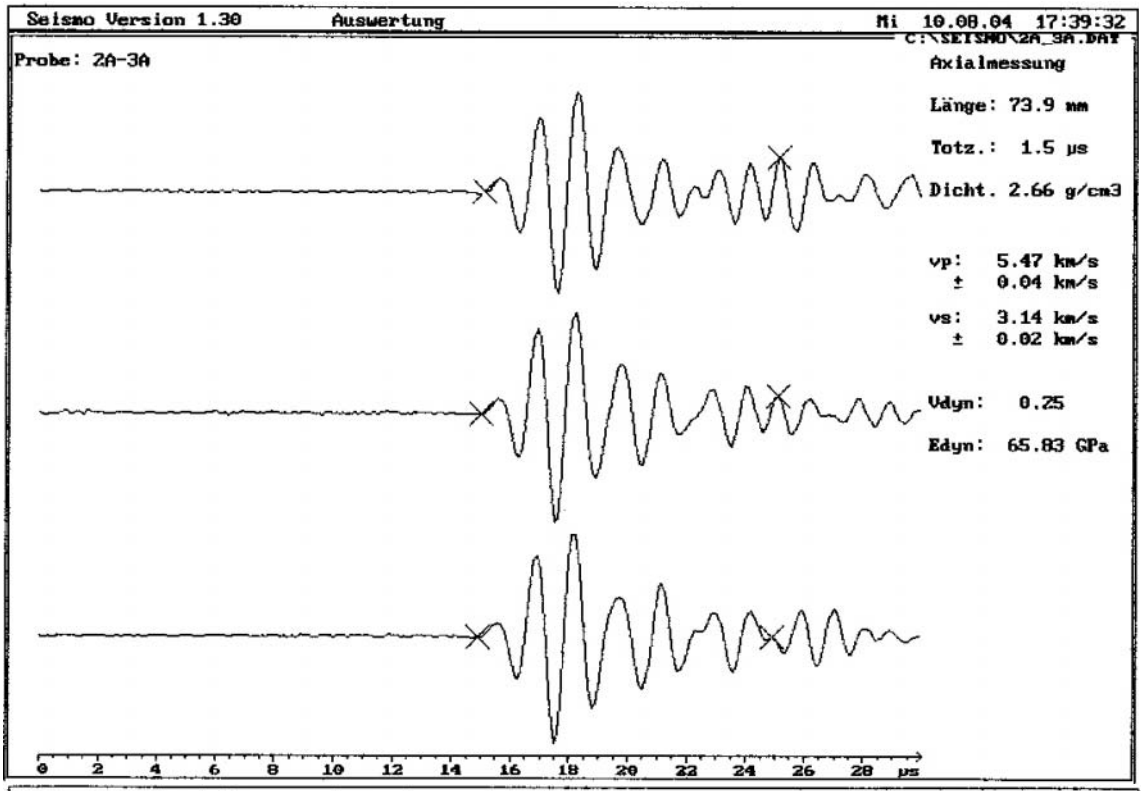
Seismo Version 1.30
Auswertung
Mi 10.08.04 17:39:32
C:\SEISMO\2A_3A.DAT
Probe: 2A-3A
Axialmessung
Länge: 73.9 mm
Totz.: 1.5 µs
Dicht. 2.66 g/cm3
vp: 5.47 km/s
± 0.04 km/s
vs: 3.14 km/s
± 0.02 km/s
Vdyn: 0.25
Edyn: 65.83 GPa
0 2 4 6 8 10 12 14 16 18 20 22 24 26 28 µs

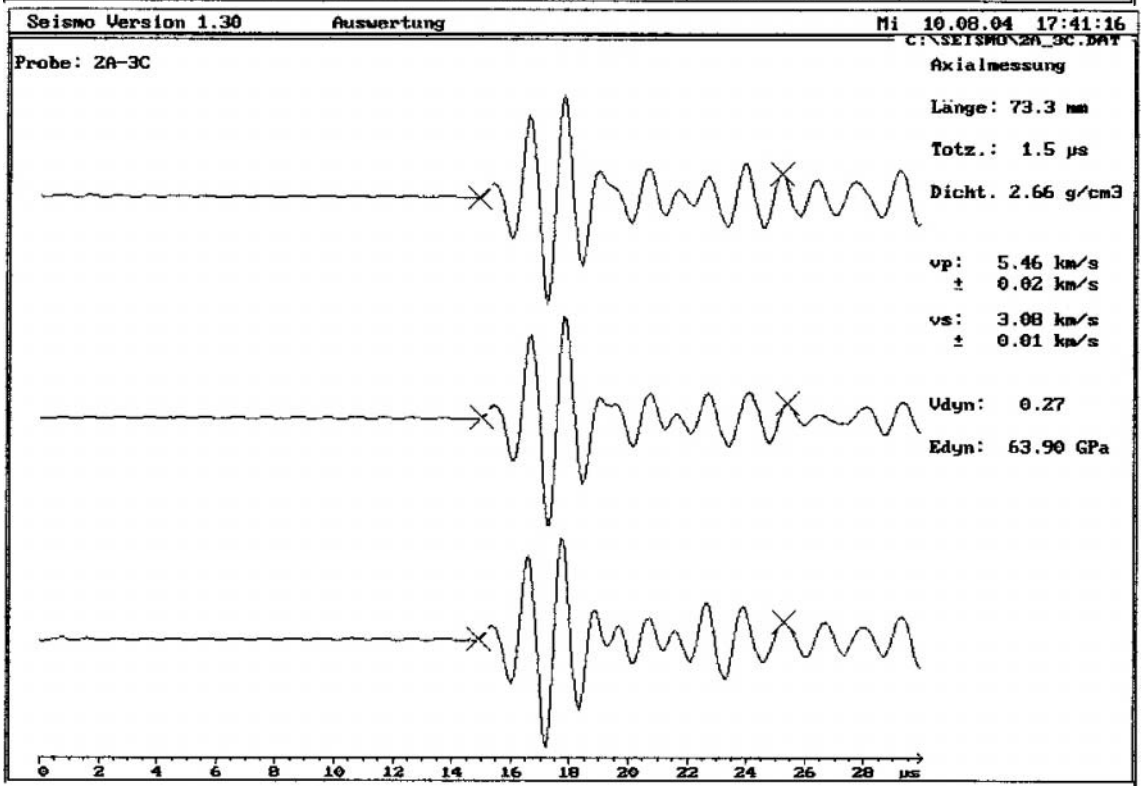
Seismo Version 1.30
Auswertung
Mi 10.08.04 17:41:16
C:\SEISMO\2A_3C.DAT
Probe: 2A-3C
Axialmessung
Länge: 73.3 mm
Totz.: 1.5 µs
Dicht. 2.66 g/cm3
vp: 5.46 km/s
± 0.02 km/s
vs: 3.08 km/s
± 0.01 km/s
Vdyn: 0.27
Edyn: 63.90 GPa
0 2 4 6 8 10 12 14 16 18 20 22 24 26 28 µs

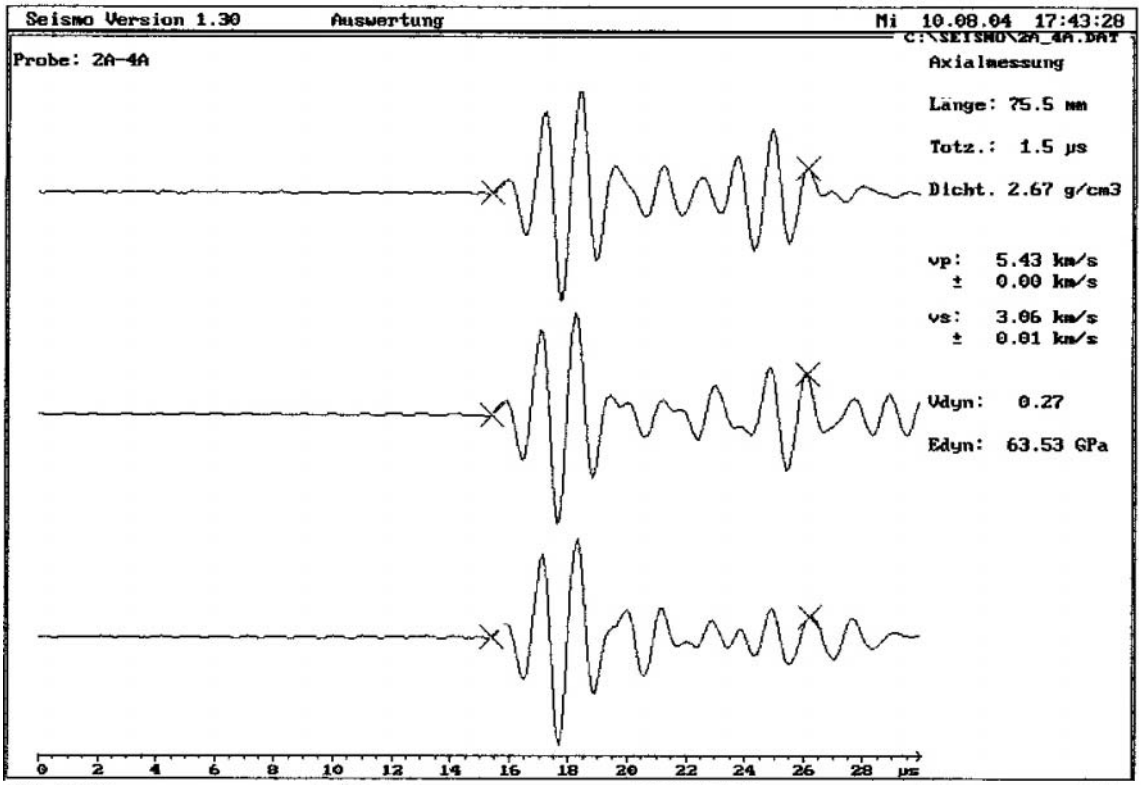
Seismo Version 1.30
Auswertung
Mi 10.08.04 17:43:28
C:\SEISMO\2A_4A.DAT
Probe: 2A-4A
Axialmessung
Länge: 75.5 mm
Totz.: 1.5 µs
Dicht. 2.67 g/cm3
vp: 5.43 km/s
± 0.00 km/s
vs: 3.06 km/s
± 0.01 km/s
Vdyn: 0.27
Edyn: 63.53 GPa
0 2 4 6 8 10 12 14 16 18 20 22 24 26 28 µs

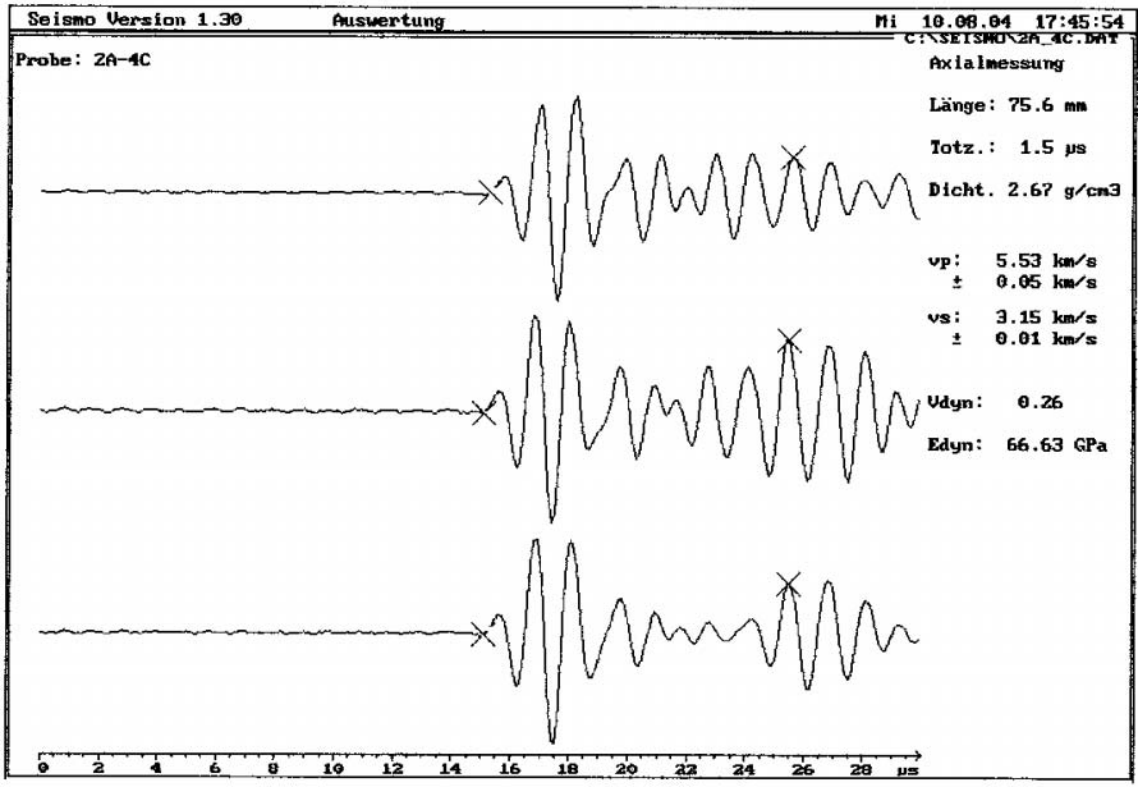
Seismo Version 1.30
Auswertung
Mi 10.08.04 17:45:54
C:\SEISMO\2A_4C.DAT
Probe: 2A-4C
Axialmessung
Länge: 75.6 mm
Totz.: 1.5 µs
Dicht. 2.67 g/cm3
vp: 5.53 km/s
± 0.05 km/s
vs: 3.15 km/s
± 0.01 km/s
Vdyn: 0.26
Edyn: 66.63 GPa
0 2 4 6 8 10 12 14 16 18 20 22 24 26 28 µs

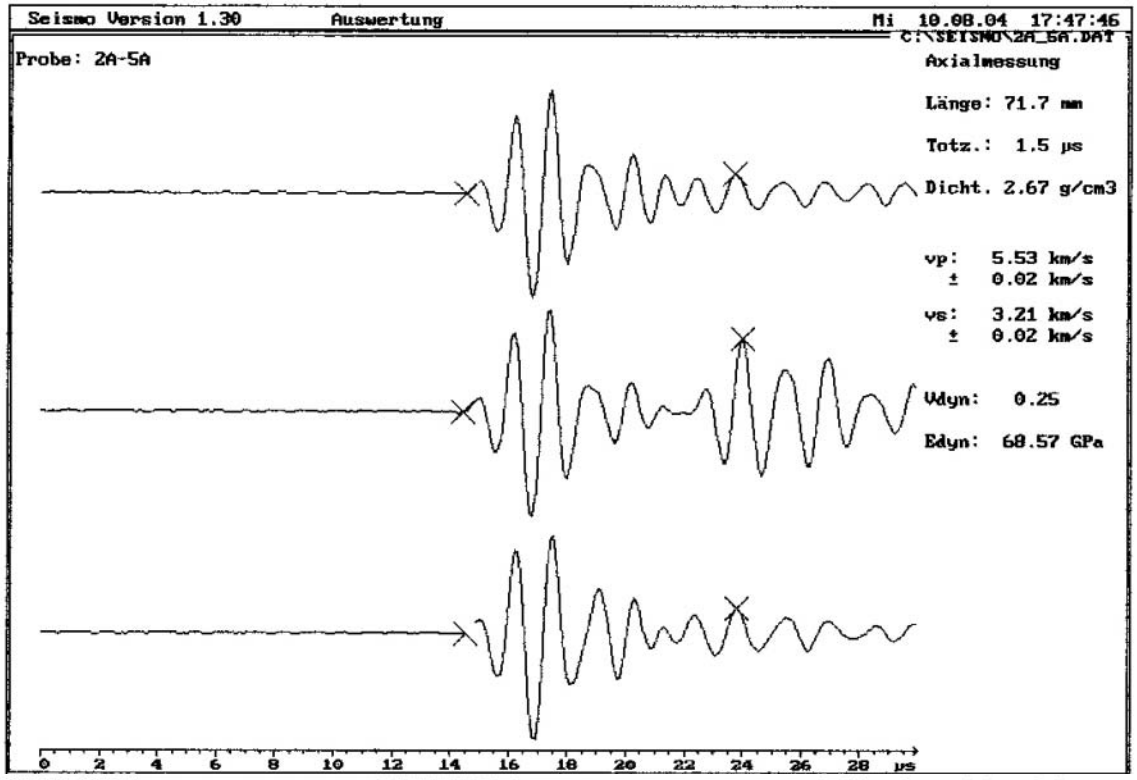
Seismo Version 1.30
Auswertung
Mi 10.08.04 17:47:46
C:\SEISMO\2A_5A.DAT
Probe: 2A-5A
Axialmessung
Länge: 71.7 mm
Totz.: 1.5 µs
Dicht. 2.67 g/cm3
vp: 5.53 km/s
± 0.02 km/s
vs: 3.21 km/s
± 0.02 km/s
Vdyn: 0.25
Edyn: 68.57 GPa
0 2 4 6 8 10 12 14 16 18 20 22 24 26 28 µs

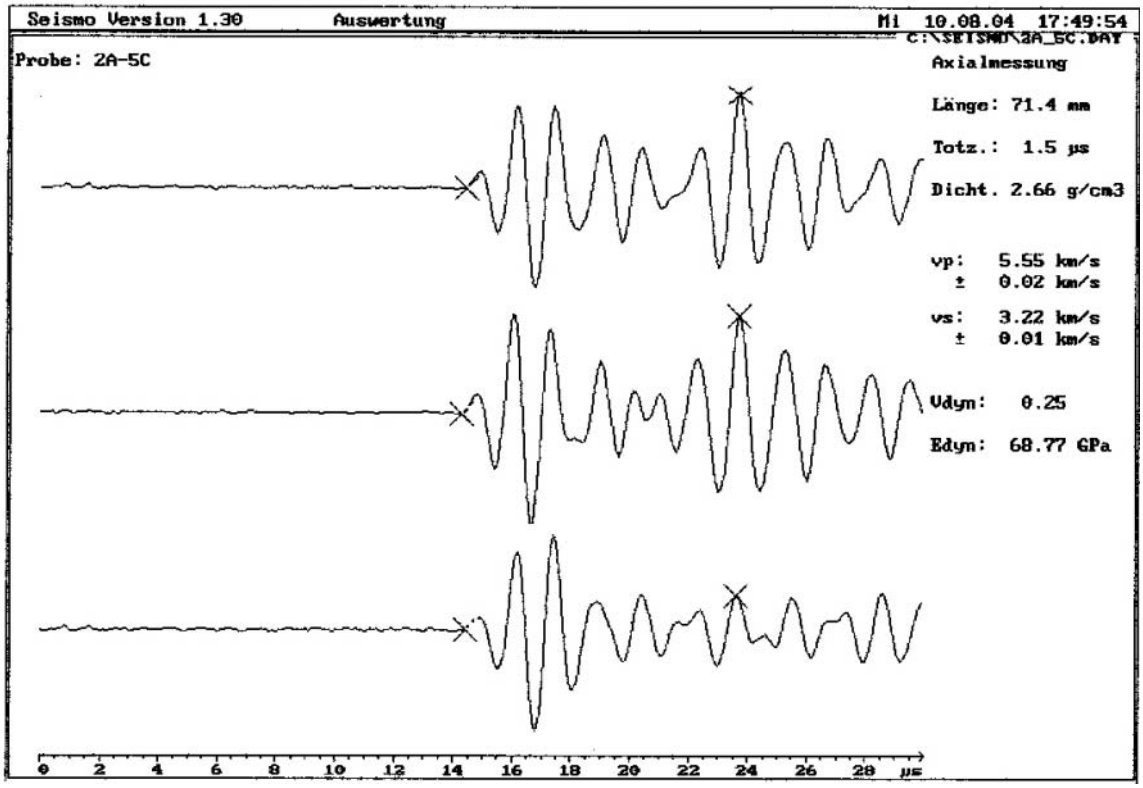
Seismo Version 1.30
Auswertung
Mi 10.08.04 17:49:54
C:\SEISMO\2A_5C.DAT
Probe: 2A-5C
Axialmessung
Länge: 71.4 mm
Totz.: 1.5 µs
Dicht. 2.66 g/cm3
vp: 5.55 km/s
± 0.02 km/s
vs: 3.22 km/s
± 0.01 km/s
Vdyn: 0.25
Edyn: 68.77 GPa
0 2 4 6 8 10 12 14 16 18 20 22 24 26 28 µs

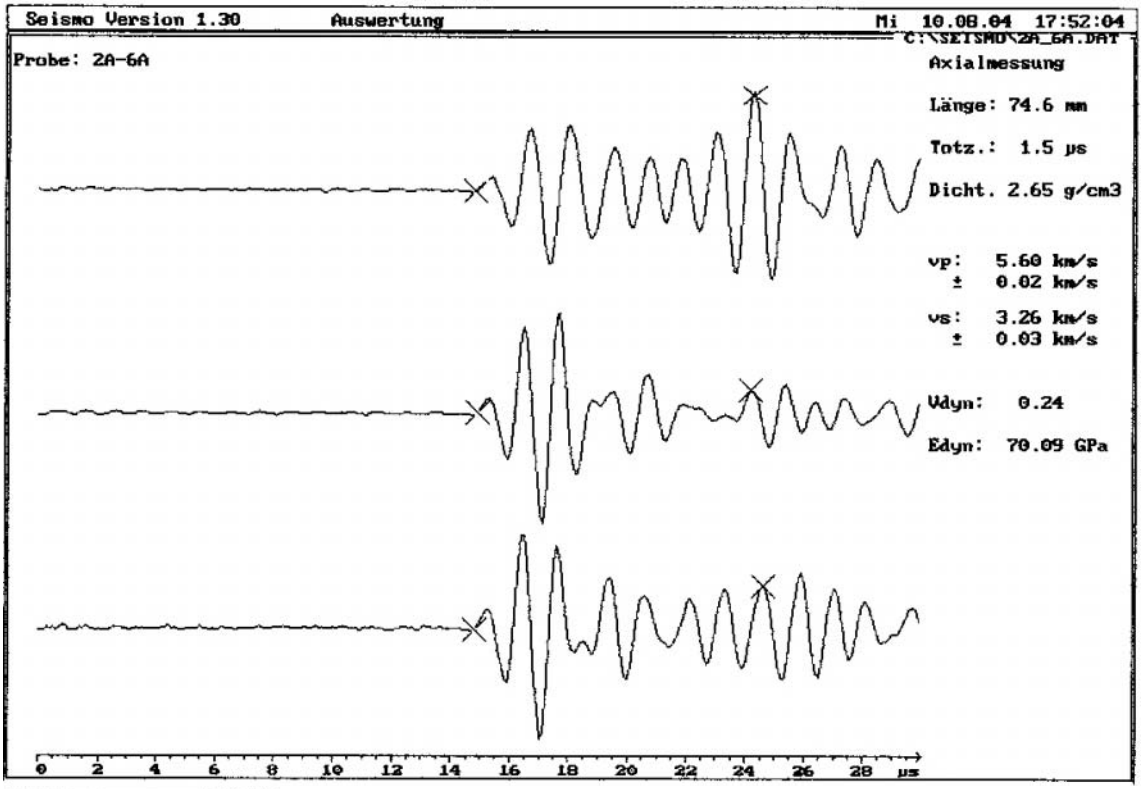
Seismo Version 1.30
Auswertung
Mi 10.08.04 17:52:04
C:\SEISMO\2A_6A.DAT
Probe: 2A-6A
Axialmessung
Länge: 74.6 mm
Totz.: 1.5 µs
Dicht. 2.65 g/cm3
vp: 5.60 km/s
± 0.02 km/s
vs: 3.26 km/s
± 0.03 km/s
Vdyn: 0.24
Edyn: 70.09 GPa
0 2 4 6 8 10 12 14 16 18 20 22 24 26 28 µs

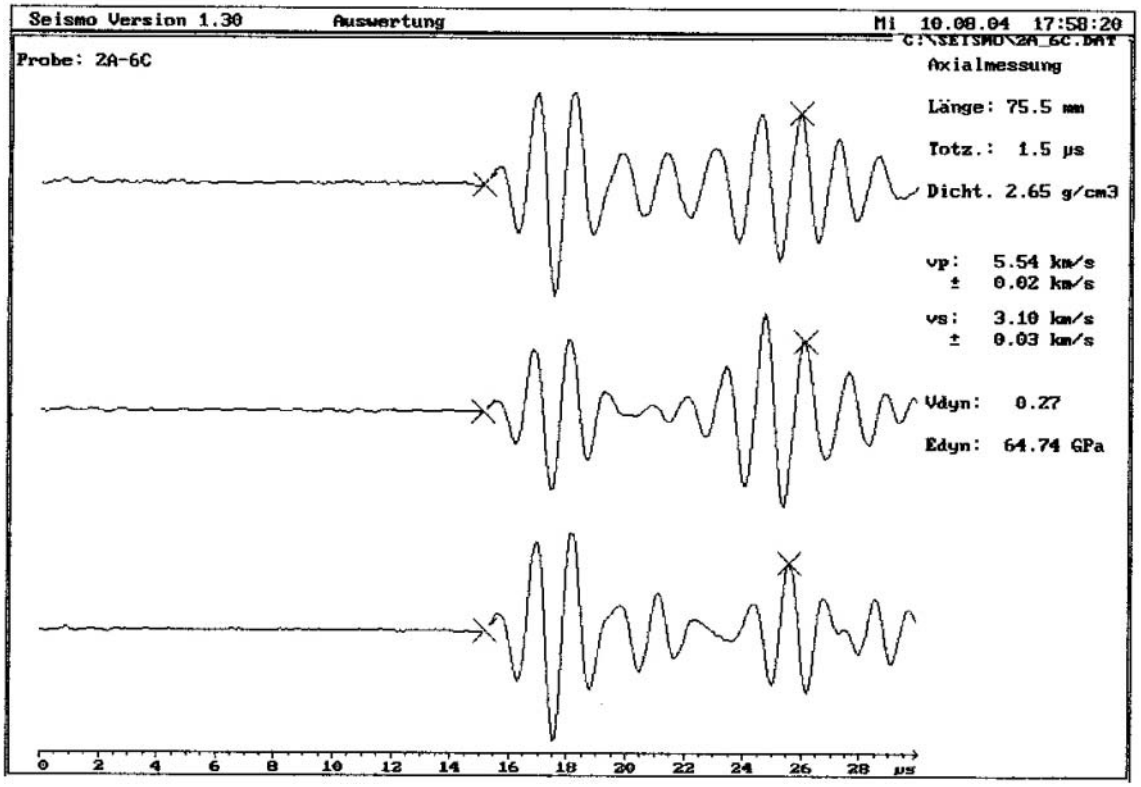
Seismo Version 1.30
Auswertung
Mi 10.08.04 17:58:20
C:\SEISMO\2A_6C.DAT
Probe: 2A-6C
Axialmessung
Länge: 75.5 mm
Totz.: 1.5 µs
Dicht. 2.65 g/cm3
vp: 5.54 km/s
± 0.02 km/s
vs: 3.10 km/s
± 0.03 km/s
Vdyn: 0.27
Edyn: 64.74 GPa
0 2 4 6 8 10 12 14 16 18 20 22 24 26 28 µs

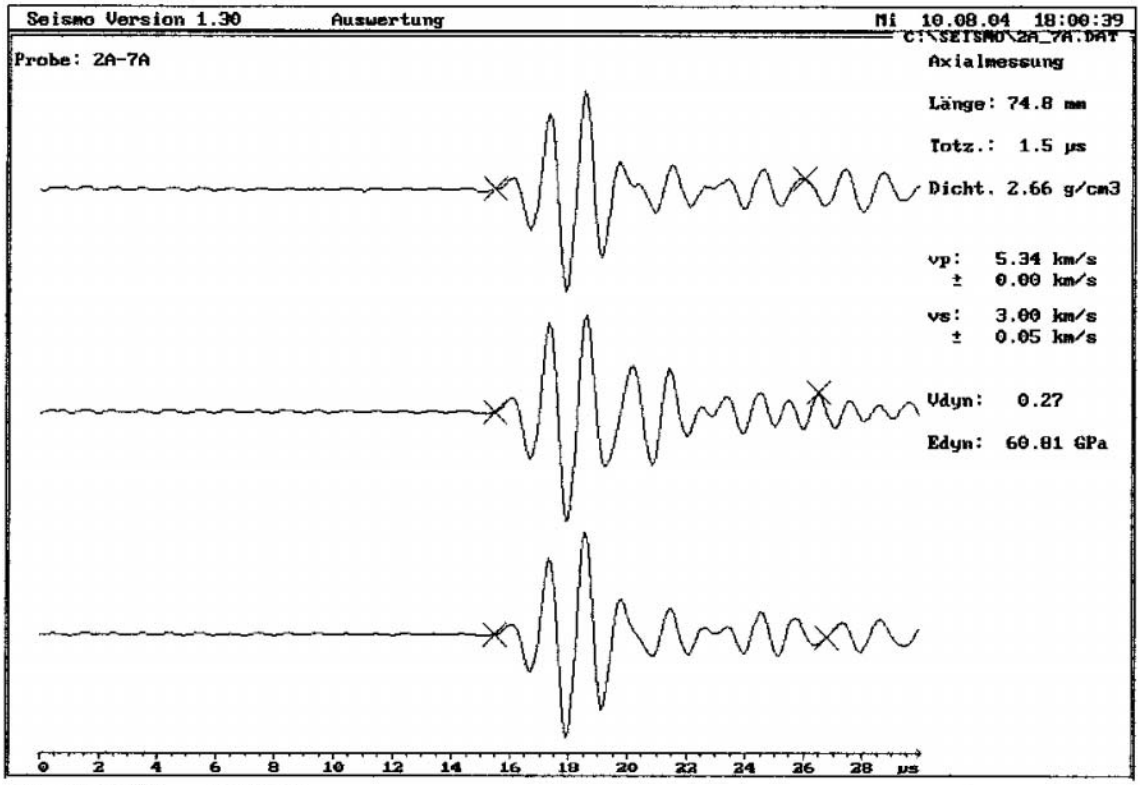
Seismo Version 1.30
Auswertung
Mi 10.08.04 18:00:39
C:\SEISMO\2A_7A.DAT
Probe: 2A-7A
Axialmessung
Länge: 74.8 mm
Totz.: 1.5 µs
Dicht. 2.66 g/cm3
vp: 5.34 km/s
± 0.00 km/s
vs: 3.00 km/s
± 0.05 km/s
Vdyn: 0.27
Edyn: 60.81 GPa
0 2 4 6 8 10 12 14 16 18 20 22 24 26 28 µs

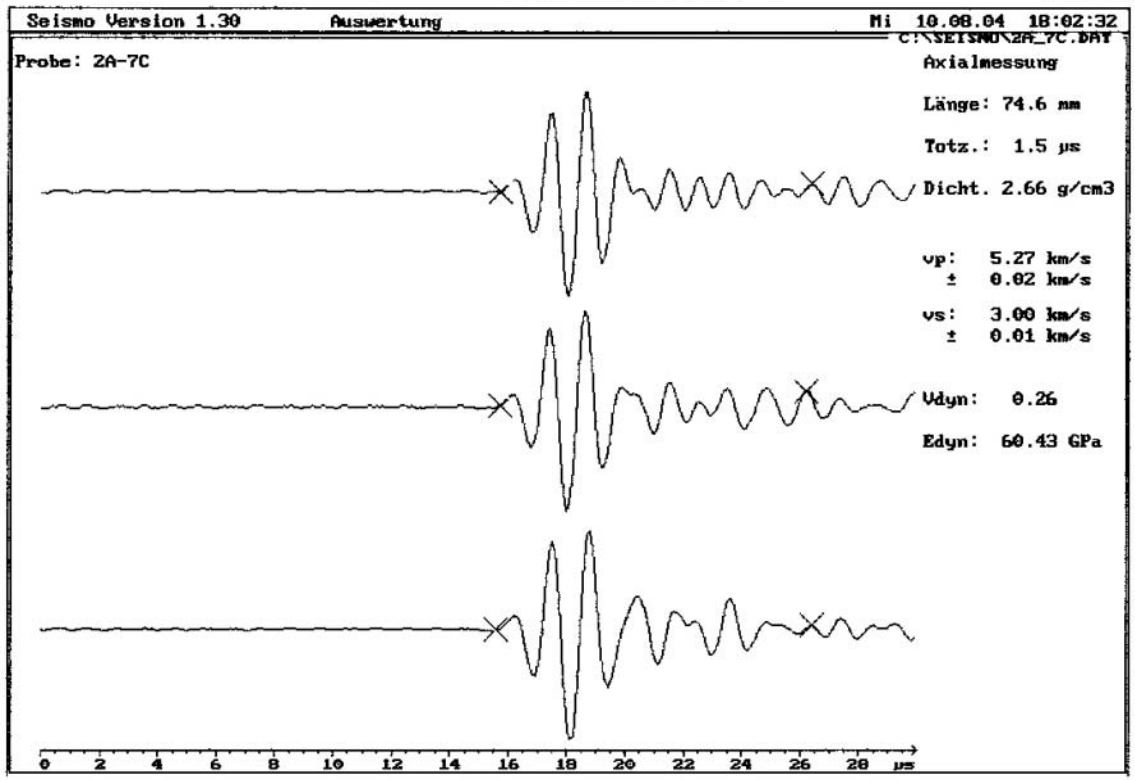
Seismo Version 1.30
Auswertung
Mi 10.08.04 18:02:32
C:\SEISMO\2A_7C.DAT
Probe: 2A-7C
Axialmessung
Länge: 74.6 mm
Totz.: 1.5 µs
Dicht. 2.66 g/cm3
vp: 5.27 km/s
± 0.02 km/s
vs: 3.00 km/s
± 0.01 km/s
Vdyn: 0.26
Edyn: 60.43 GPa
0 2 4 6 8 10 12 14 16 18 20 22 24 26 28 µs

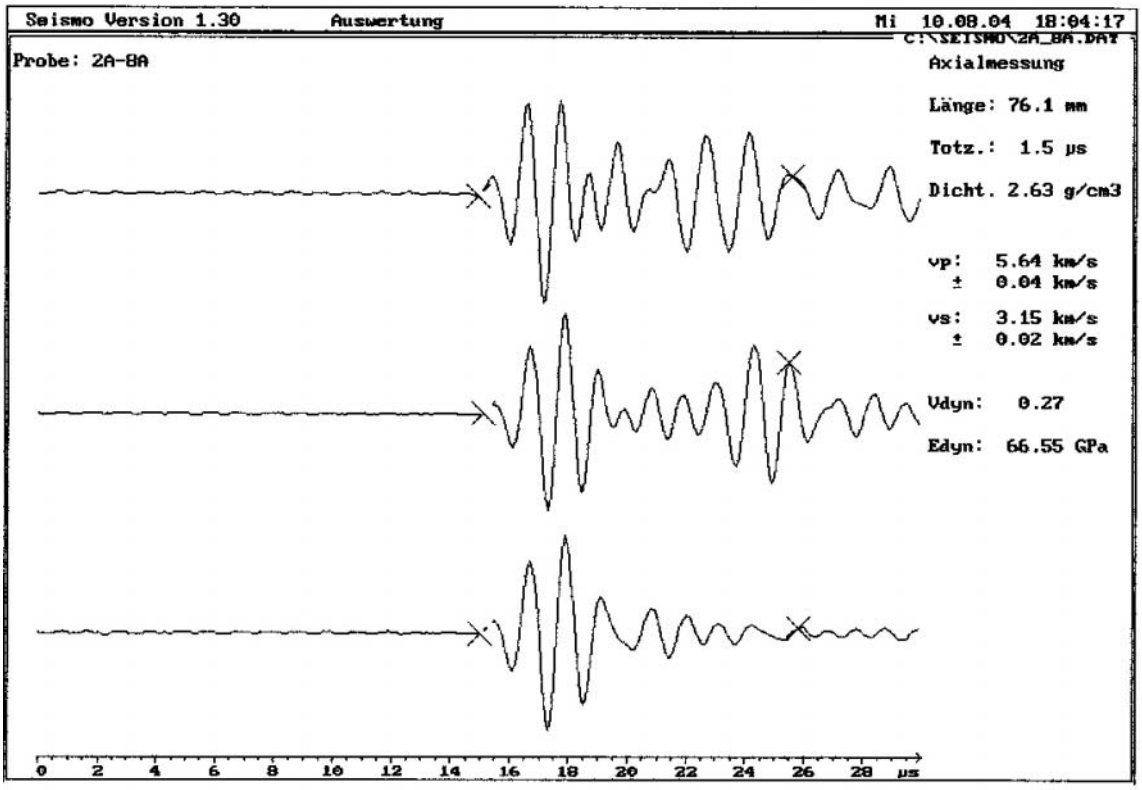
Seismo Version 1.30
Auswertung
Mi 10.08.04 18:04:17
C:\SEISMO\2A_8A.DAT
Probe: 2A-8A
Axialmessung
Länge: 76.1 mm
Totz.: 1.5 µs
Dicht. 2.63 g/cm3
vp: 5.64 km/s
± 0.04 km/s
vs: 3.15 km/s
± 0.02 km/s
Vdyn: 0.27
Edyn: 66.55 GPa
0 2 4 6 8 10 12 14 16 18 20 22 24 26 28 µs

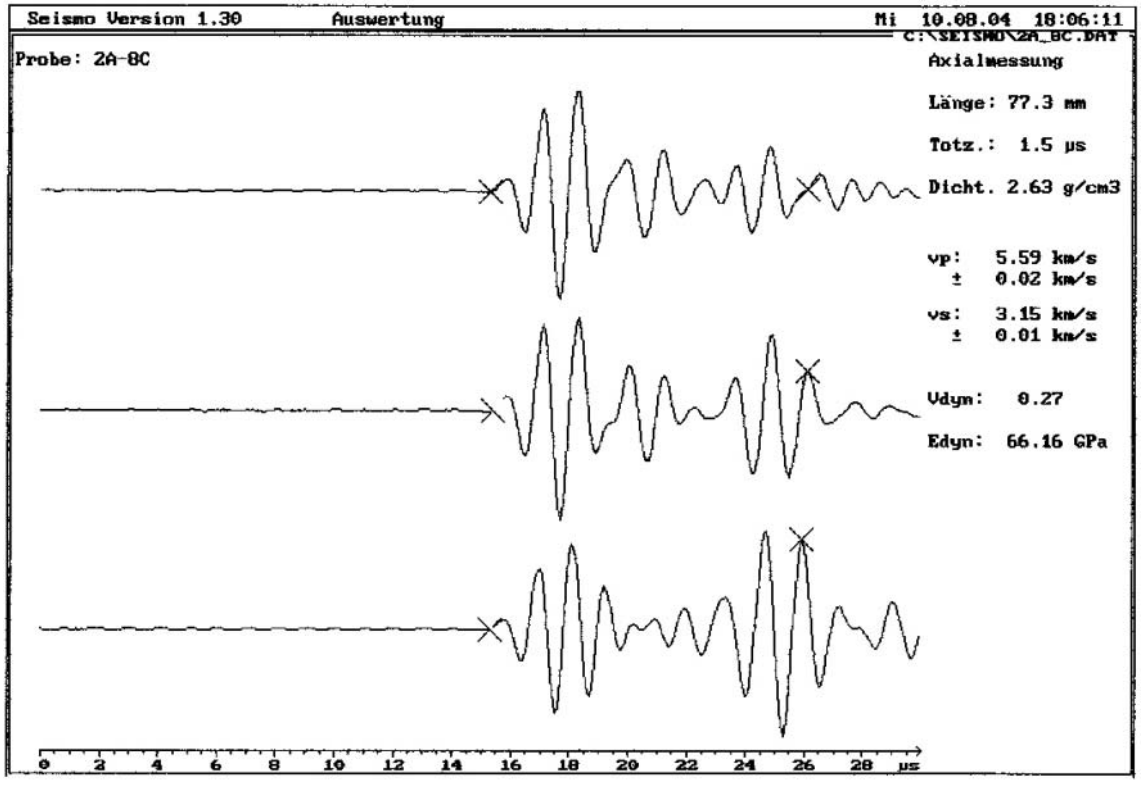
Seismo Version 1.30
Auswertung
Mi 10.08.04 18:06:11
C:\SEISMO\2A_8C.DAT
Probe: 2A-8C
Axialmessung
Länge: 77.3 mm
Totz.: 1.5 µs
Dicht. 2.63 g/cm3
vp: 5.59 km/s
± 0.02 km/s
vs: 3.15 km/s
± 0.01 km/s
Vdyn: 0.27
Edyn: 66.16 GPa
0 2 4 6 8 10 12 14 16 18 20 22 24 26 28 µs

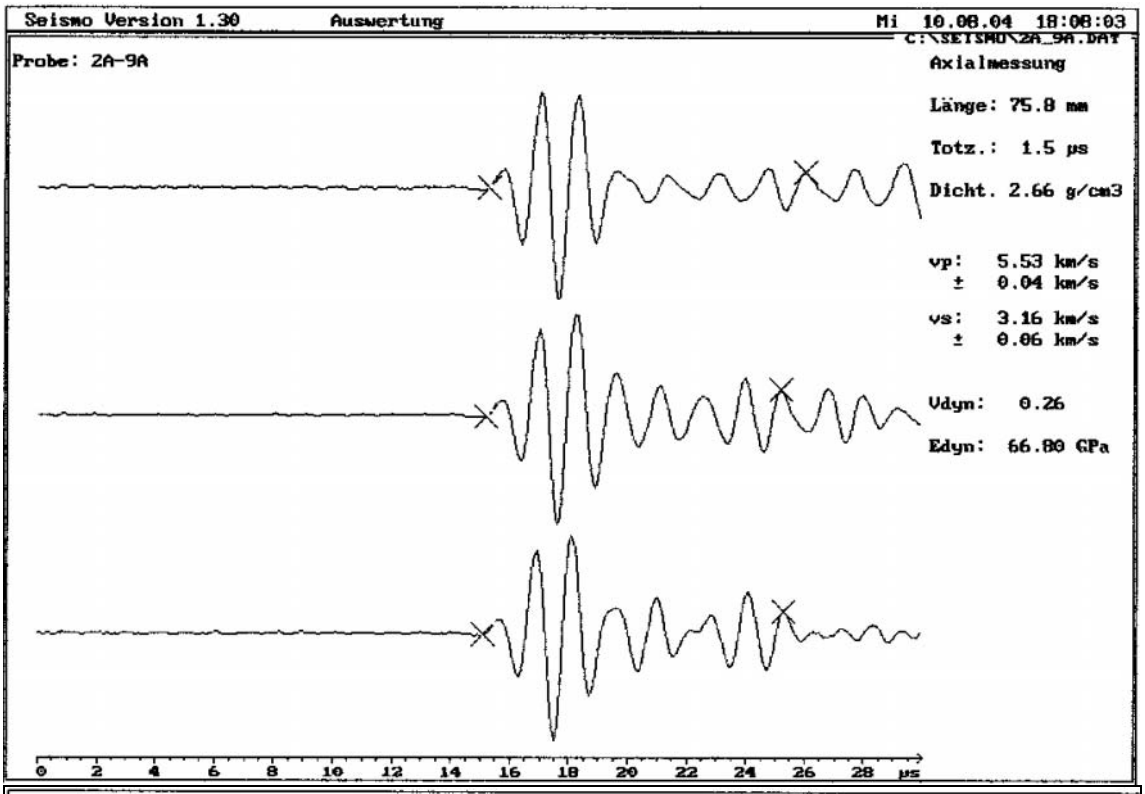
Seismo Version 1.30
Auswertung
Mi 10.08.04 18:08:03
C:\SEISMO\2A_9A.DAT
Probe: 2A-9A
Axialmessung
Länge: 75.8 mm
Totz.: 1.5 µs
Dicht. 2.66 g/cm3
vp: 5.53 km/s
± 0.04 km/s
vs: 3.16 km/s
± 0.06 km/s
Vdyn: 0.26
Edyn: 66.80 GPa
0 2 4 6 8 10 12 14 16 18 20 22 24 26 28 µs

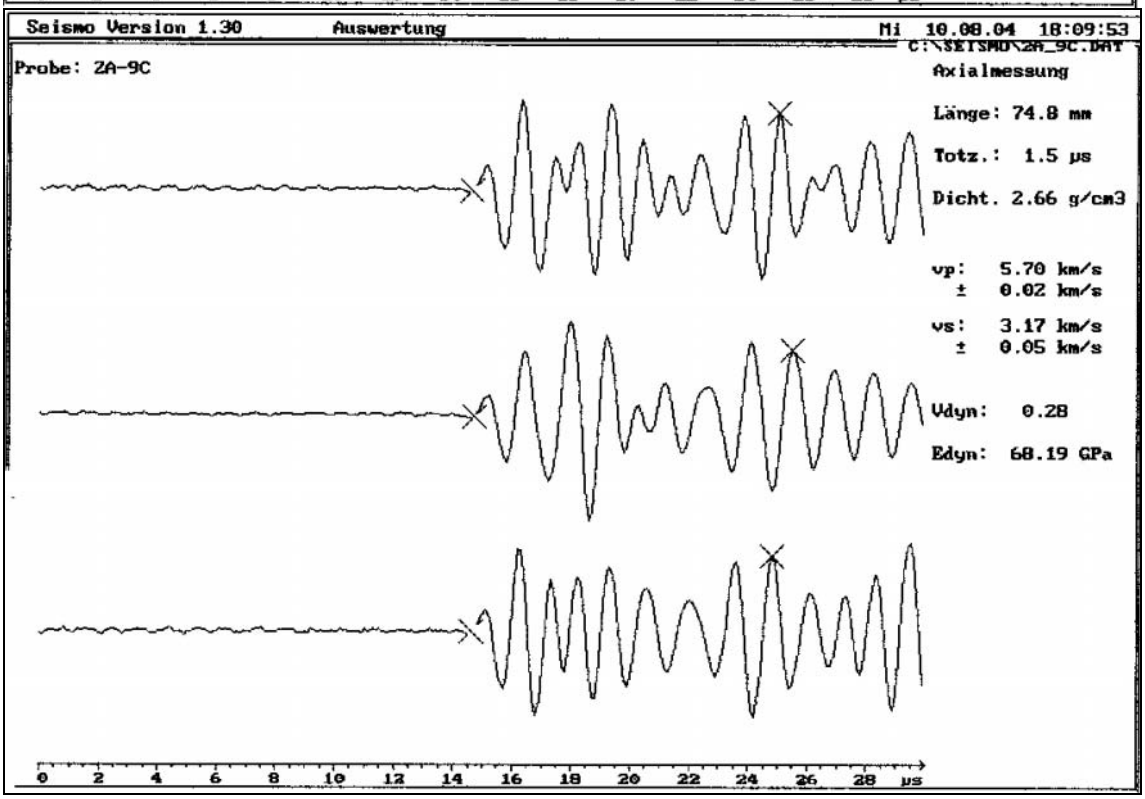
Seismo Version 1.30
Auswertung
Mi 10.08.04 18:09:53
C:\SEISMO\2A_9C.DAT
Probe: 2A-9C
Axialmessung
Länge: 74.8 mm
Totz.: 1.5 µs
Dicht. 2.66 g/cm3
vp: 5.70 km/s
± 0.02 km/s
vs: 3.17 km/s
± 0.05 km/s
Vdyn: 0.28
Edyn: 68.19 GPa
0 2 4 6 8 10 12 14 16 18 20 22 24 26 28 µs

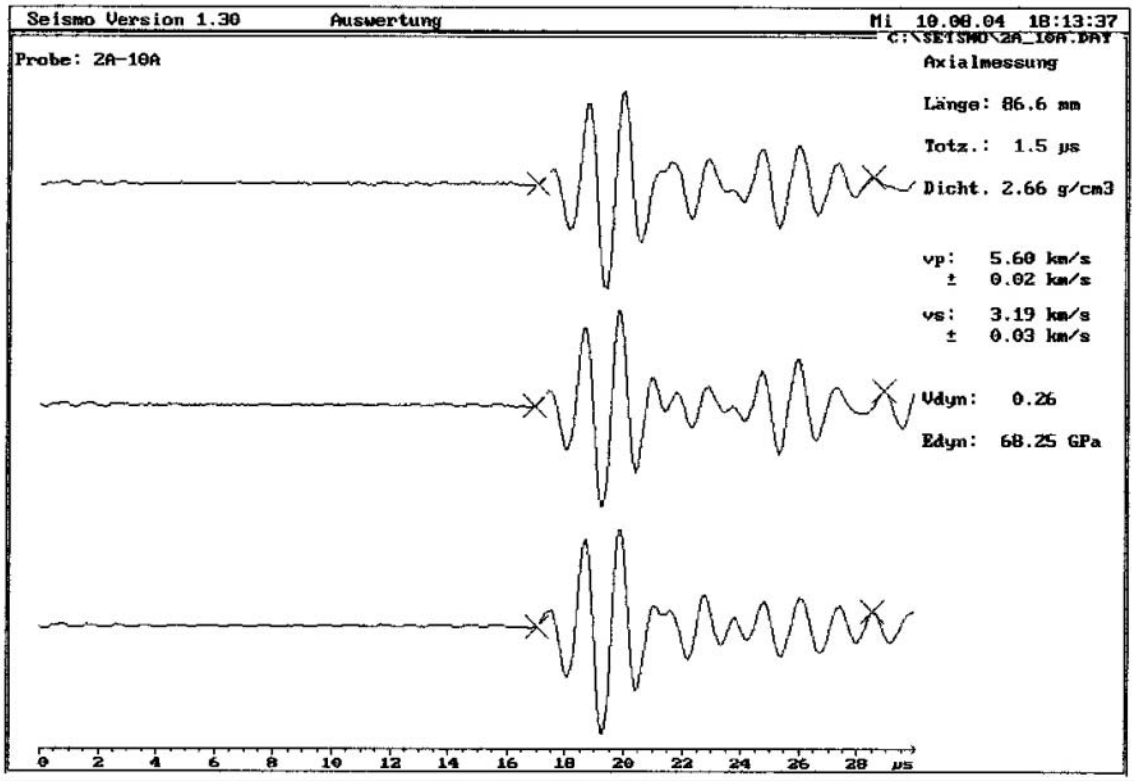
Seismo Version 1.30
Auswertung
Mi 10.08.04 18:13:37
C:\SEISMO\2A_10A.DAT
Probe: 2A-10A
Axialmessung
Länge: 86.6 mm
Totz.: 1.5 µs
Dicht. 2.66 g/cm3
vp: 5.60 km/s
± 0.02 km/s
vs: 3.19 km/s
± 0.03 km/s
Vdyn: 0.26
Edyn: 68.25 GPa
0 2 4 6 8 10 12 14 16 18 20 22 24 26 28 µs

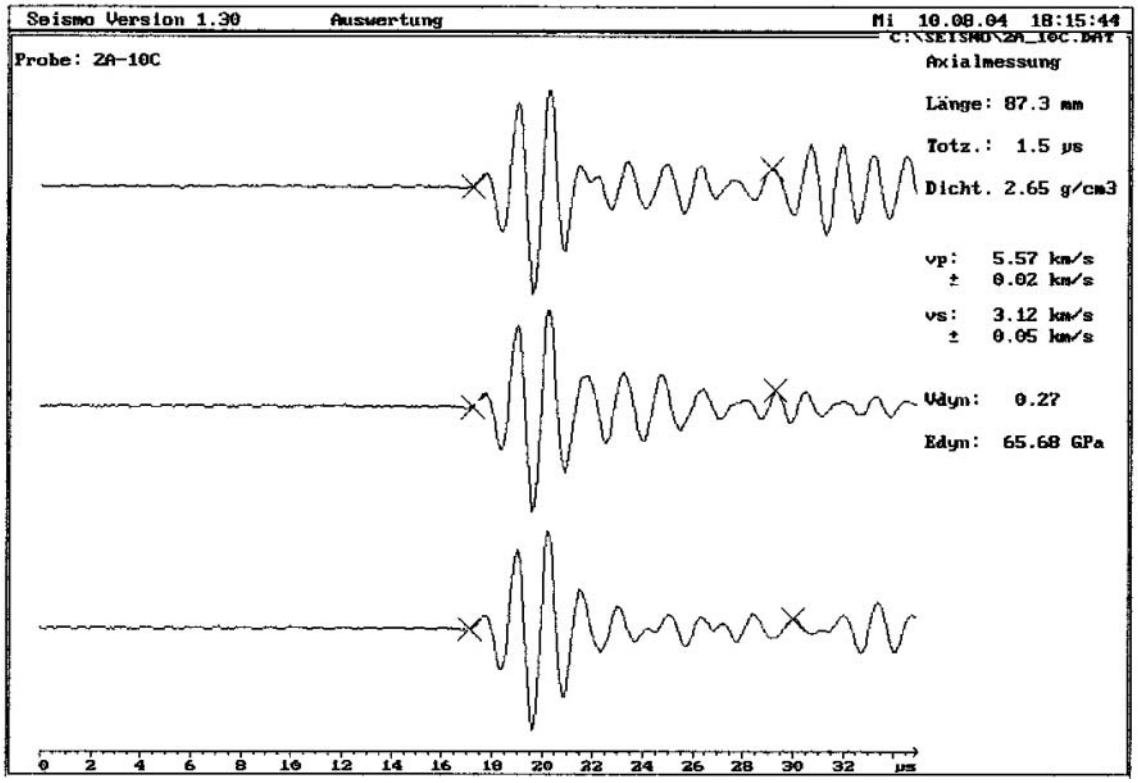
Seismo Version 1.30
Auswertung
Mi 10.08.04 18:15:44
C:\SEISMO\2A_10C.DAT
Probe: 2A-10C
Axialmessung
Länge: 87.3 mm
Totz.: 1.5 µs
Dicht. 2.65 g/cm3
vp: 5.57 km/s
± 0.02 km/s
vs: 3.12 km/s
± 0.05 km/s
Vdyn: 0.27
Edyn: 65.68 GPa
0 2 4 6 8 10 12 14 16 18 20 22 24 26 28 30 32 µs

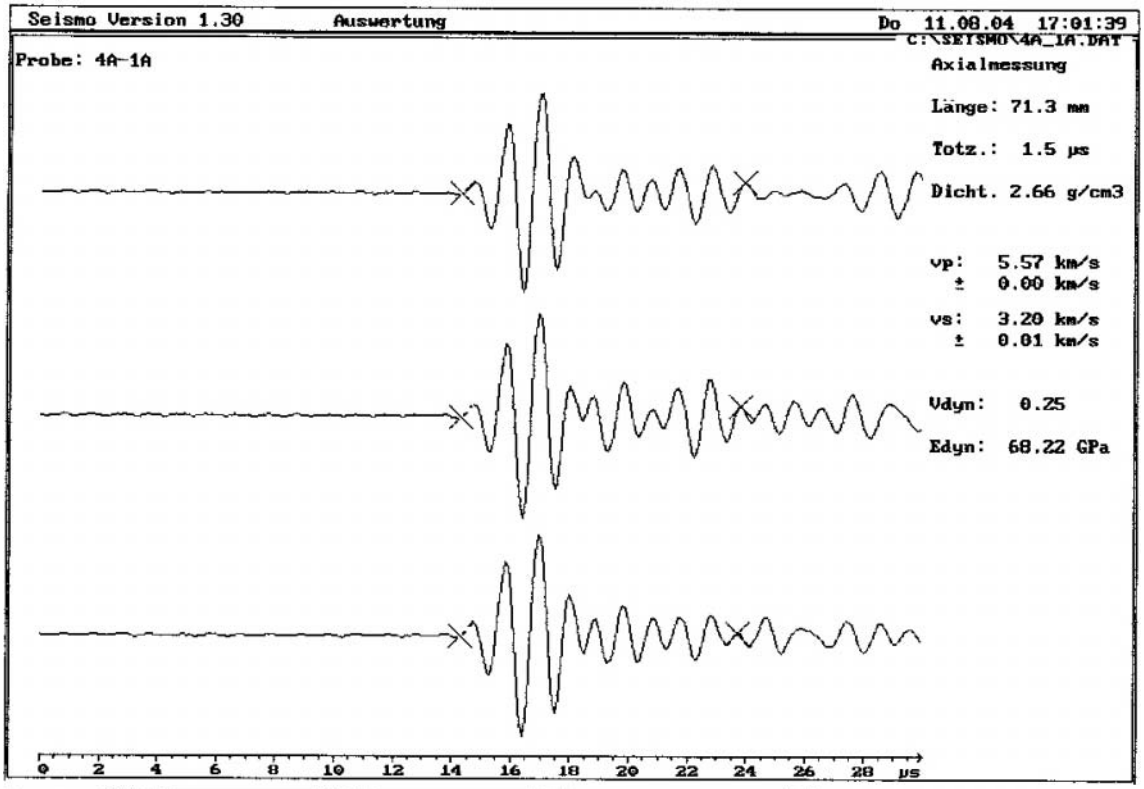
Seismo Version 1.30
Auswertung
Do 11.08.04 17:01:39
C:\SEISMO\4A_1A.DAT
Probe: 4A-1A
Axialmessung
Länge: 71.3 mm
Totz.: 1.5 µs
Dicht. 2.66 g/cm3
vp: 5.57 km/s
± 0.00 km/s
vs: 3.20 km/s
± 0.01 km/s
Vdyn: 0.25
Edyn: 68.22 GPa
0 2 4 6 8 10 12 14 16 18 20 22 24 26 28 µs

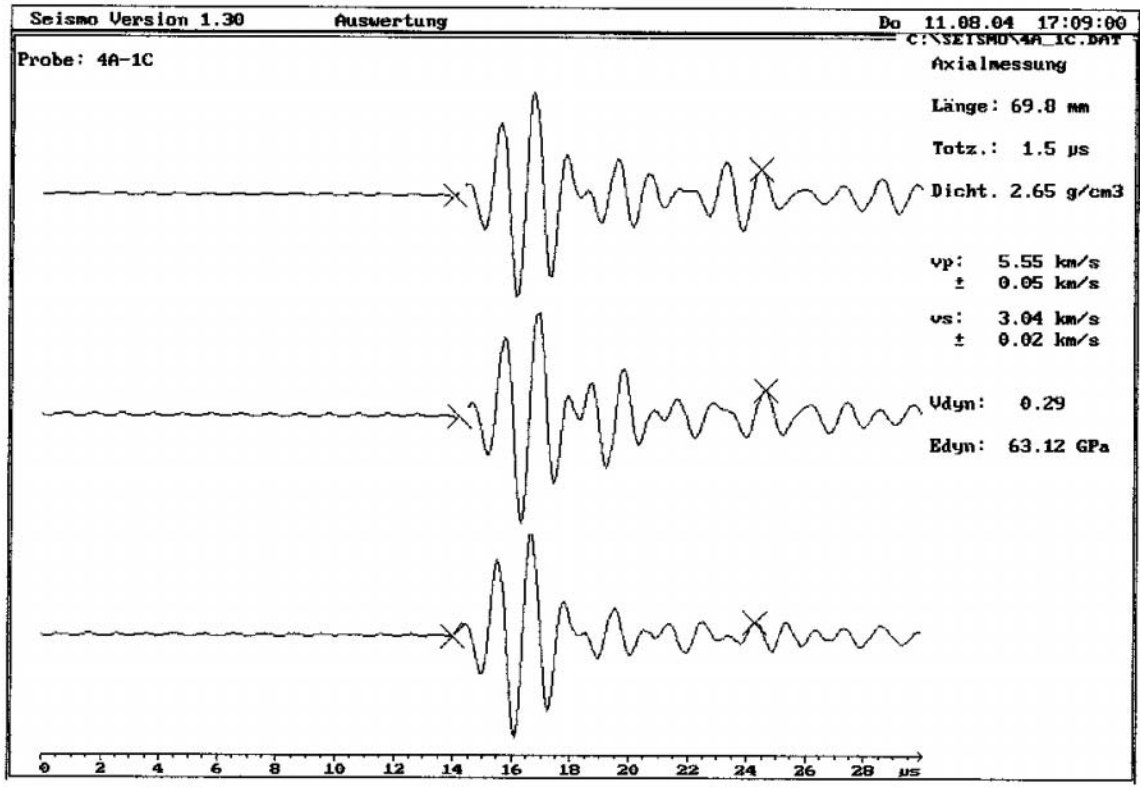
Seismo Version 1.30
Auswertung
Do 11.08.04 17:09:00
C:\SEISMO\4A_1C.DAT
Probe: 4A-1C
Axialmessung
Länge: 69.8 mm
Totz.: 1.5 µs
Dicht. 2.65 g/cm3
vp: 5.55 km/s
± 0.05 km/s
vs: 3.04 km/s
± 0.02 km/s
Vdyn: 0.29
Edyn: 63.12 GPa
0 2 4 6 8 10 12 14 16 18 20 22 24 26 28 µs

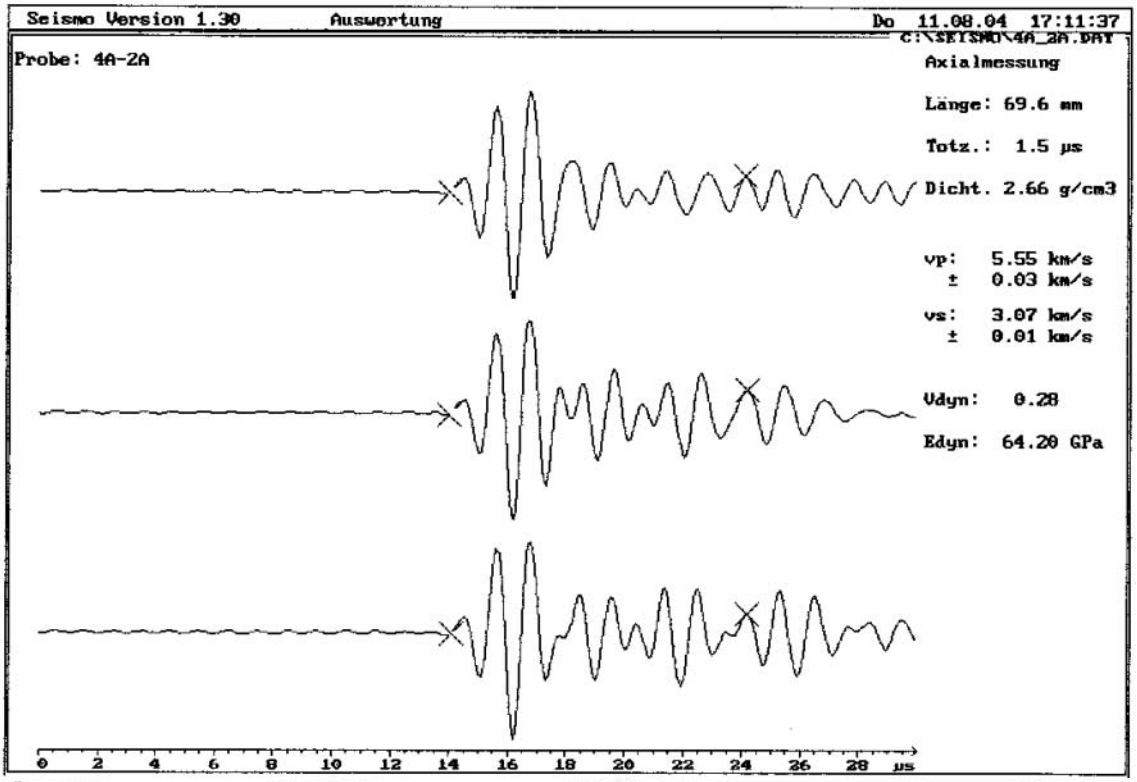
Seismo Version 1.30
Auswertung
Do 11.08.04 17:11:37
C:\SEISMO\4A_2A.DAT
Probe: 4A-2A
Axialmessung
Länge: 69.6 mm
Totz.: 1.5 µs
Dicht. 2.66 g/cm3
vp: 5.55 km/s
± 0.03 km/s
vs: 3.07 km/s
± 0.01 km/s
Vdyn: 0.28
Edyn: 64.20 GPa
0 2 4 6 8 10 12 14 16 18 20 22 24 26 28 µs

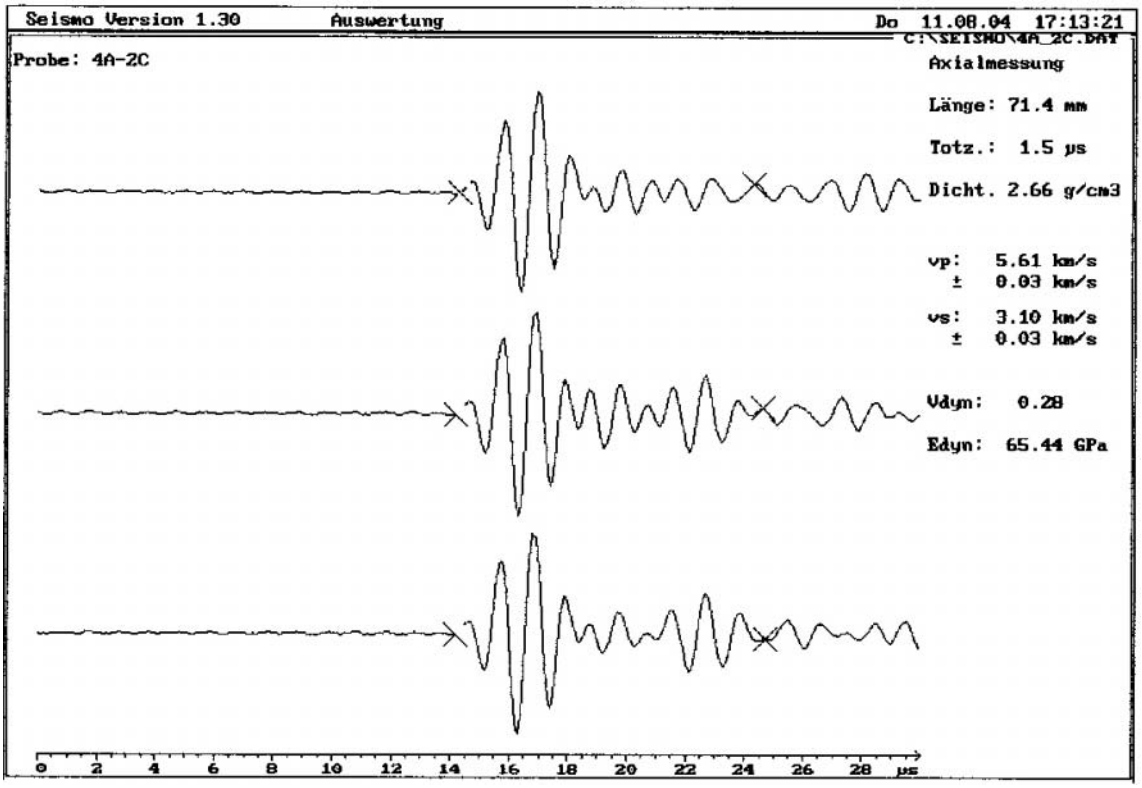
Seismo Version 1.30
Auswertung
Do 11.08.04 17:13:21
C:\SEISMO\4A_2C.DAT
Probe: 4A-2C
Axialmessung
Länge: 71.4 mm
Totz.: 1.5 µs
Dicht. 2.66 g/cm3
vp: 5.61 km/s
± 0.03 km/s
vs: 3.10 km/s
± 0.03 km/s
Vdyn: 0.28
Edyn: 65.44 GPa
0 2 4 6 8 10 12 14 16 18 20 22 24 26 28 µs

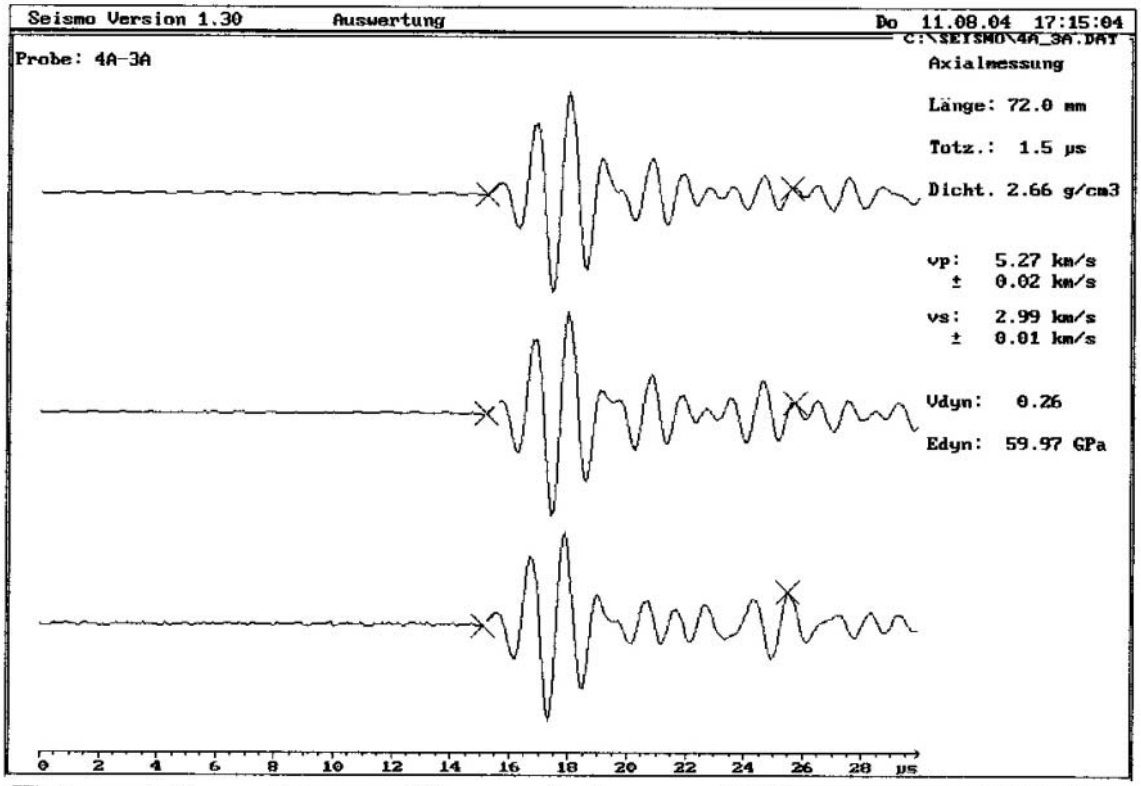
Seismo Version 1.30
Auswertung
Do 11.08.04 17:15:04
C:\SEISMO\4A_3A.DAT
Probe: 4A-3A
Axialmessung
Länge: 72.0 mm
Totz.: 1.5 µs
Dicht. 2.66 g/cm3
vp: 5.27 km/s
± 0.02 km/s
vs: 2.99 km/s
± 0.01 km/s
Vdyn: 0.26
Edyn: 59.97 GPa
0 2 4 6 8 10 12 14 16 18 20 22 24 26 28 µs

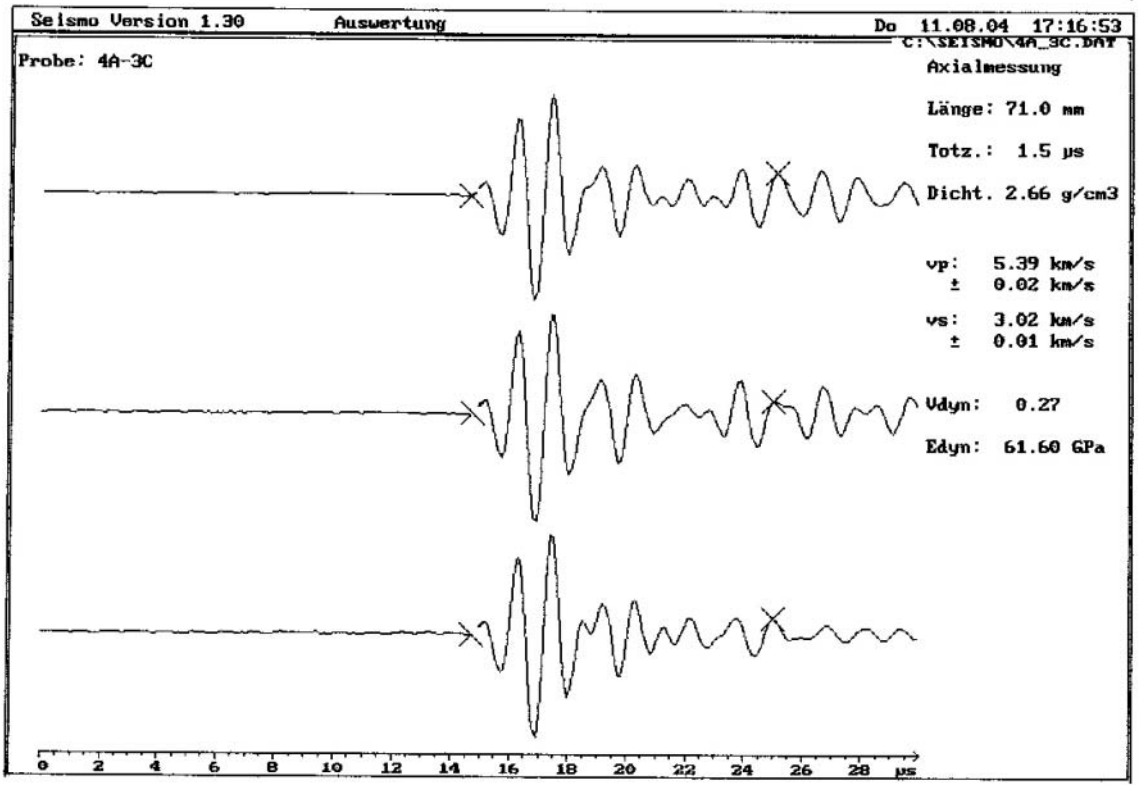
Seismo Version 1.30
Auswertung
Do 11.08.04 17:16:53
C:\SEISMO\4A_3C.DAT
Probe: 4A-3C
Axialmessung
Länge: 71.0 mm
Totz.: 1.5 µs
Dicht. 2.66 g/cm3
vp: 5.39 km/s
± 0.02 km/s
vs: 3.02 km/s
± 0.01 km/s
Vdyn: 0.27
Edyn: 61.60 GPa
0 2 4 6 8 10 12 14 16 18 20 22 24 26 28 µs

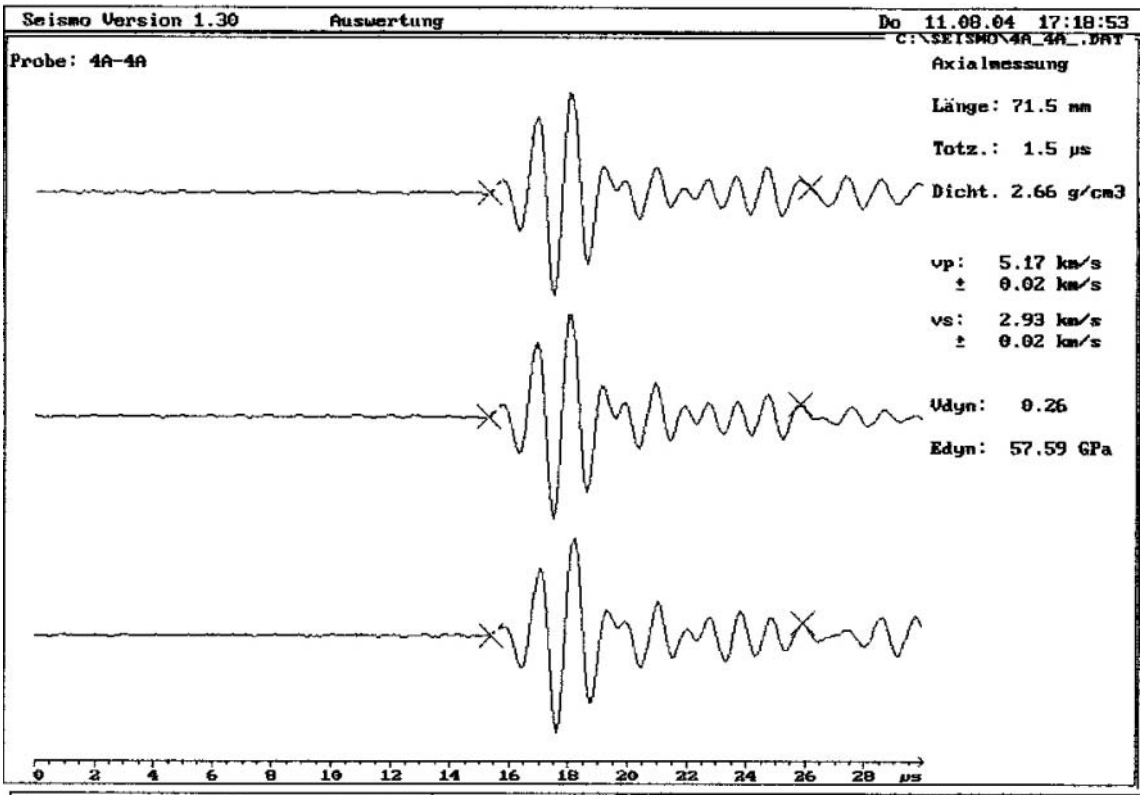
Seismo Version 1.30
Auswertung
Do 11.08.04 17:18:53
C:\SEISMO\4A_4A_.DAT
Probe: 4A-4A
Axialmessung
Länge: 71.5 mm
Totz.: 1.5 µs
Dicht. 2.66 g/cm3
vp: 5.17 km/s
± 0.02 km/s
vs: 2.93 km/s
± 0.02 km/s
Vdyn: 0.26
Edyn: 57.59 GPa
0 2 4 6 8 10 12 14 16 18 20 22 24 26 28 µs

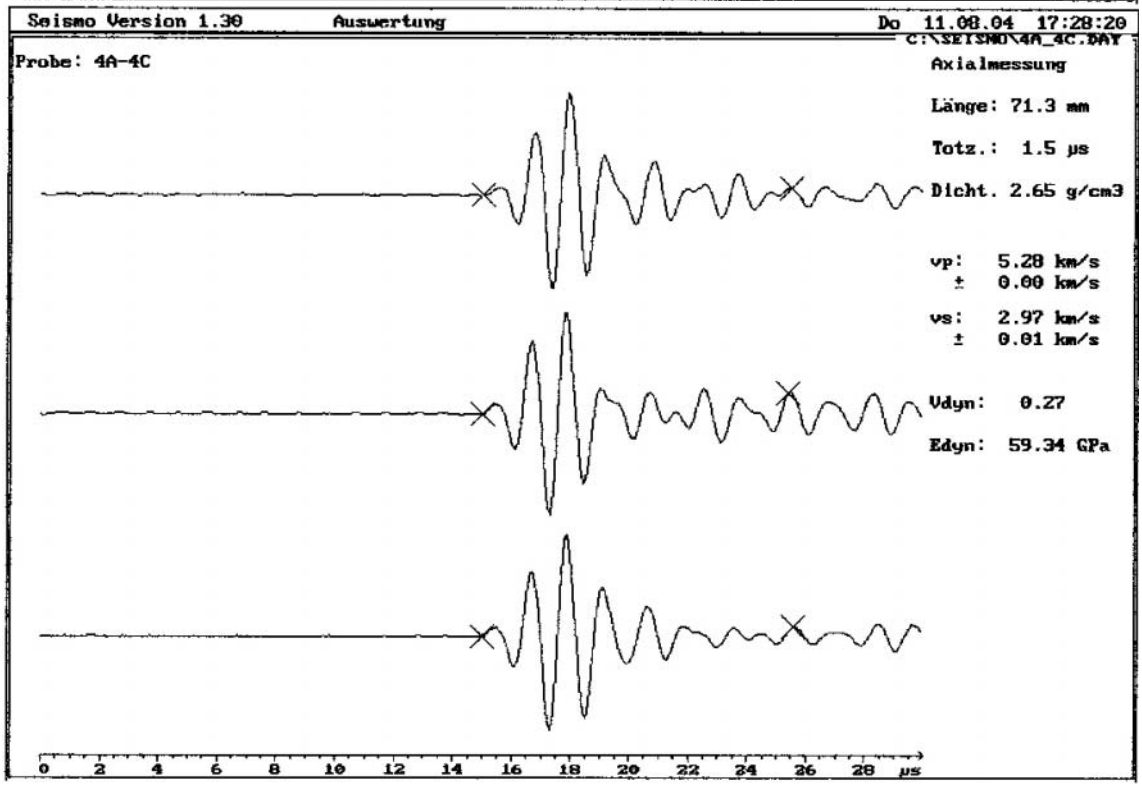
Seismo Version 1.30
Auswertung
Do 11.08.04 17:28:20
C:\SEISMO\4A_4C.DAT
Probe: 4A-4C
Axialmessung
Länge: 71.3 mm
Totz.: 1.5 µs
Dicht. 2.65 g/cm3
vp: 5.28 km/s
± 0.00 km/s
vs: 2.97 km/s
± 0.01 km/s
Vdyn: 0.27
Edyn: 59.34 GPa
0 2 4 6 8 10 12 14 16 18 20 22 24 26 28 µs

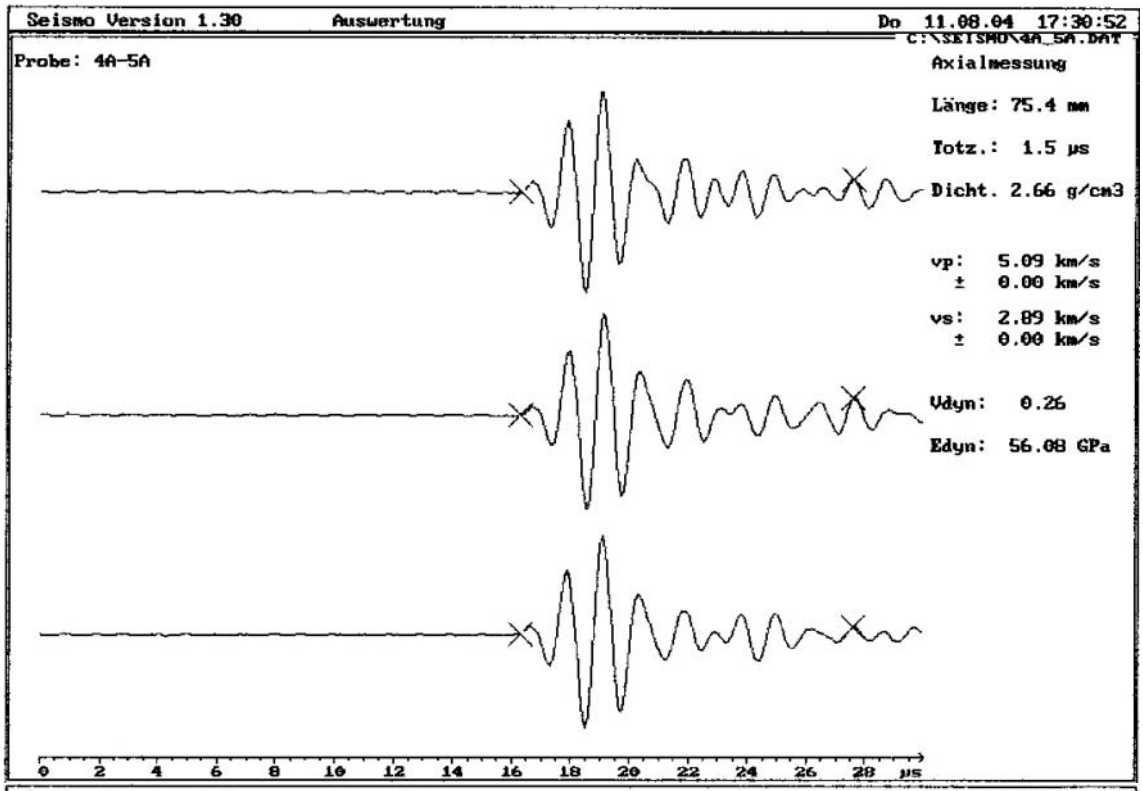
Seismo Version 1.30
Auswertung
Do 11.08.04 17:30:52
C:\SEISMO\4A_5A.DAT
Probe: 4A-5A
Axialmessung
Länge: 75.4 mm
Totz.: 1.5 µs
Dicht. 2.66 g/cm3
vp: 5.09 km/s
± 0.00 km/s
vs: 2.89 km/s
± 0.00 km/s
Vdyn: 0.26
Edyn: 56.08 GPa
0 2 4 6 8 10 12 14 16 18 20 22 24 26 28 µs

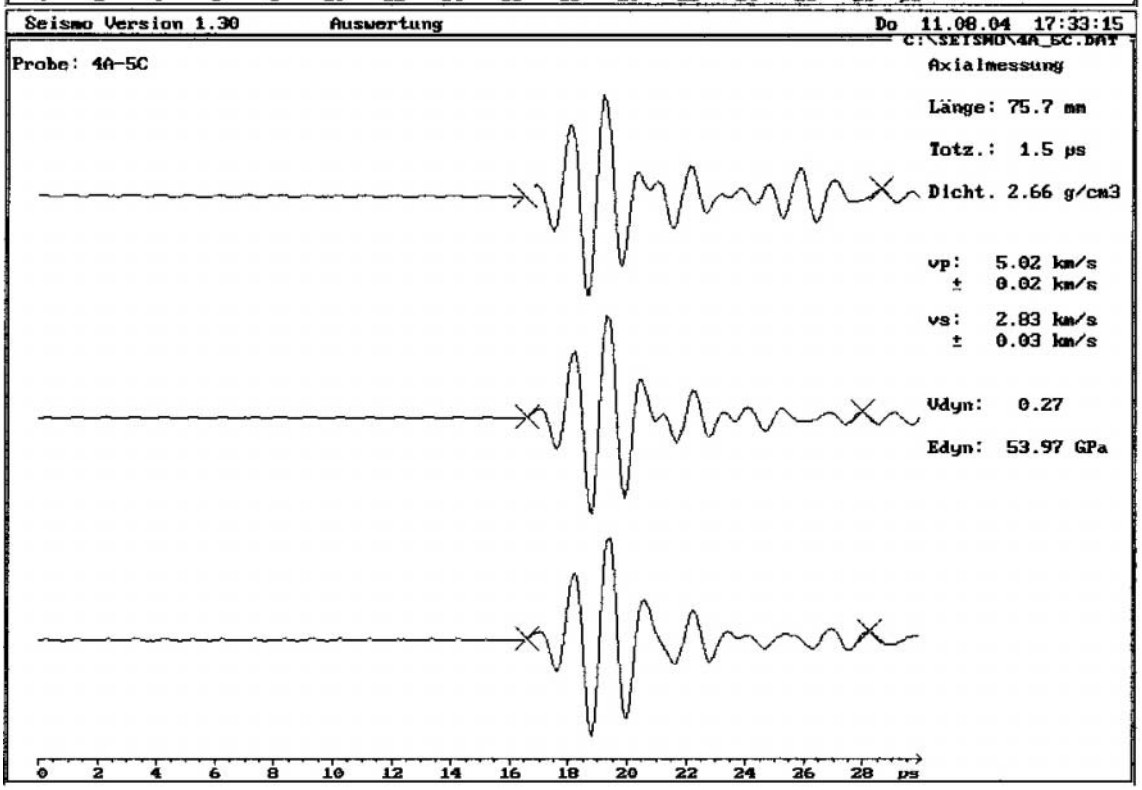
Seismo Version 1.30
Auswertung
Do 11.08.04 17:33:15
C:\SEISMO\4A_5C.DAT
Probe: 4A-5C
Axialmessung
Länge: 75.7 mm
Totz.: 1.5 µs
Dicht. 2.66 g/cm3
vp: 5.02 km/s
± 0.02 km/s
vs: 2.83 km/s
± 0.03 km/s
Vdyn: 0.27
Edyn: 53.97 GPa
0 2 4 6 8 10 12 14 16 18 20 22 24 26 28 µs

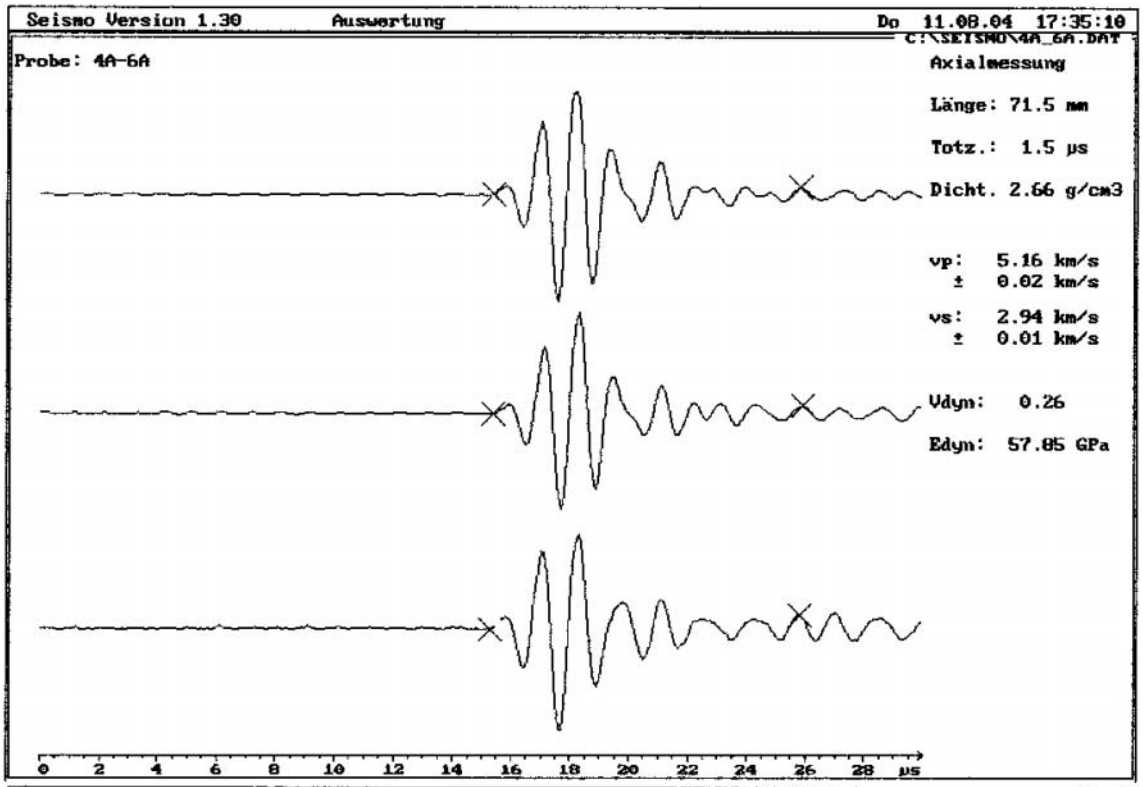
Seismo Version 1.30
Auswertung
Do 11.08.04 17:35:10
C:\SEISMO\4A_6A.DAT
Probe: 4A-6A
Axialmessung
Länge: 71.5 mm
Totz.: 1.5 µs
Dicht. 2.66 g/cm3
vp: 5.16 km/s
± 0.02 km/s
vs: 2.94 km/s
± 0.01 km/s
Vdyn: 0.26
Edyn: 57.85 GPa
0 2 4 6 8 10 12 14 16 18 20 22 24 26 28 µs

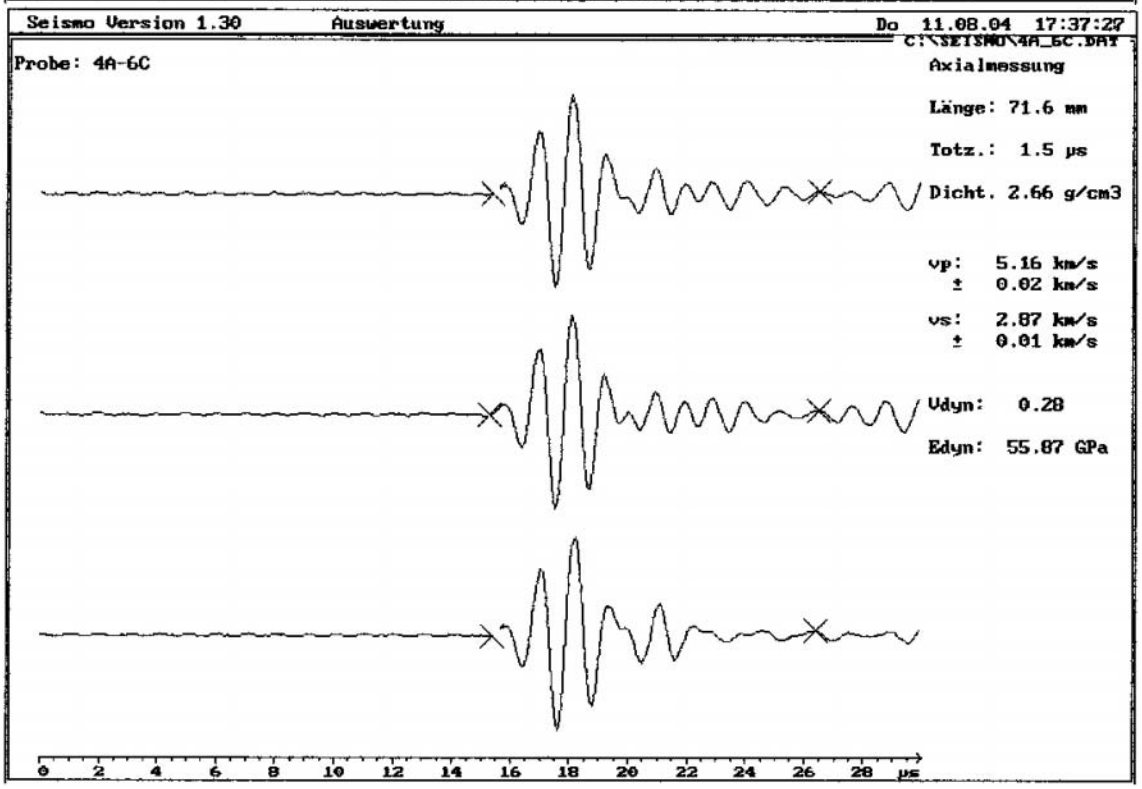
Seismo Version 1.30
Auswertung
Do 11.08.04 17:37:27
C:\SEISMO\4A_6C.DAT
Probe: 4A-6C
Axialmessung
Länge: 71.6 mm
Totz.: 1.5 µs
Dicht. 2.66 g/cm3
vp: 5.16 km/s
± 0.02 km/s
vs: 2.87 km/s
± 0.01 km/s
Vdyn: 0.28
Edyn: 55.87 GPa
0 2 4 6 8 10 12 14 16 18 20 22 24 26 28 µs

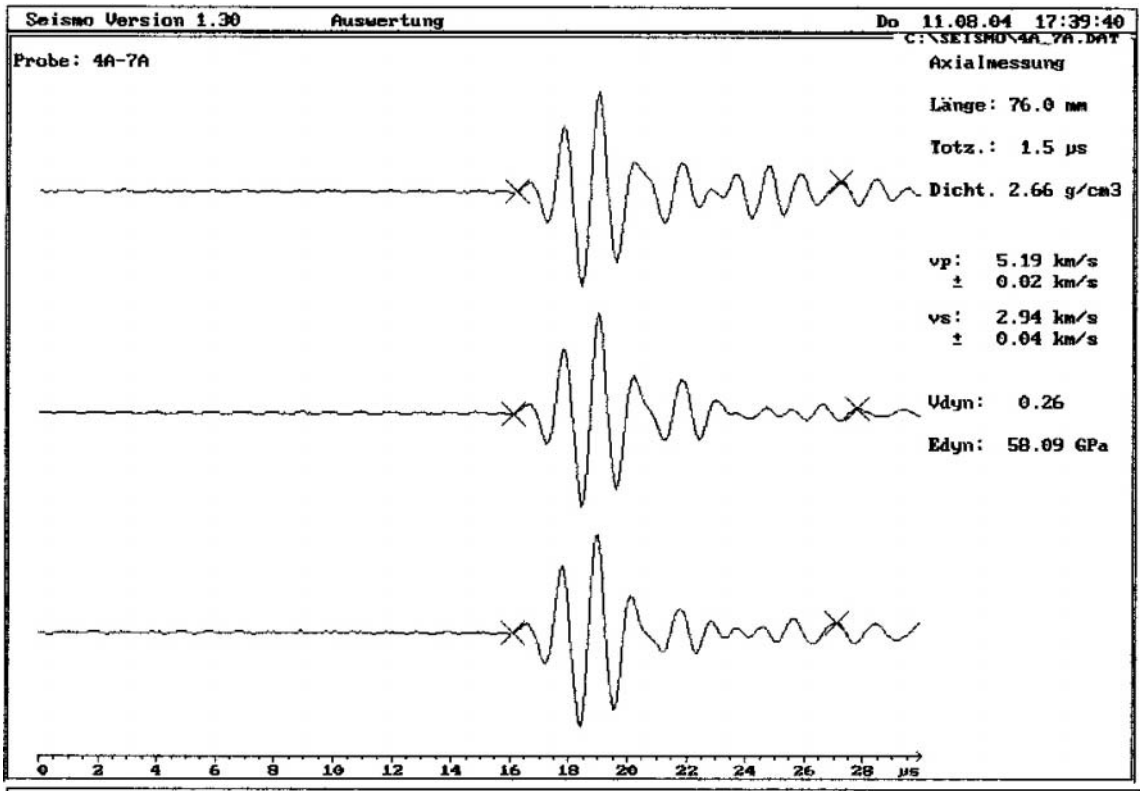
Seismo Version 1.30
Auswertung
Do 11.08.04 17:39:40
C:\SEISMO\4A_7A.DAT
Probe: 4A-7A
Axialmessung
Länge: 76.0 mm
Totz.: 1.5 µs
Dicht. 2.66 g/cm3
vp: 5.19 km/s
± 0.02 km/s
vs: 2.94 km/s
± 0.04 km/s
Vdyn: 0.26
Edyn: 58.09 GPa
0 2 4 6 8 10 12 14 16 18 20 22 24 26 28 µs

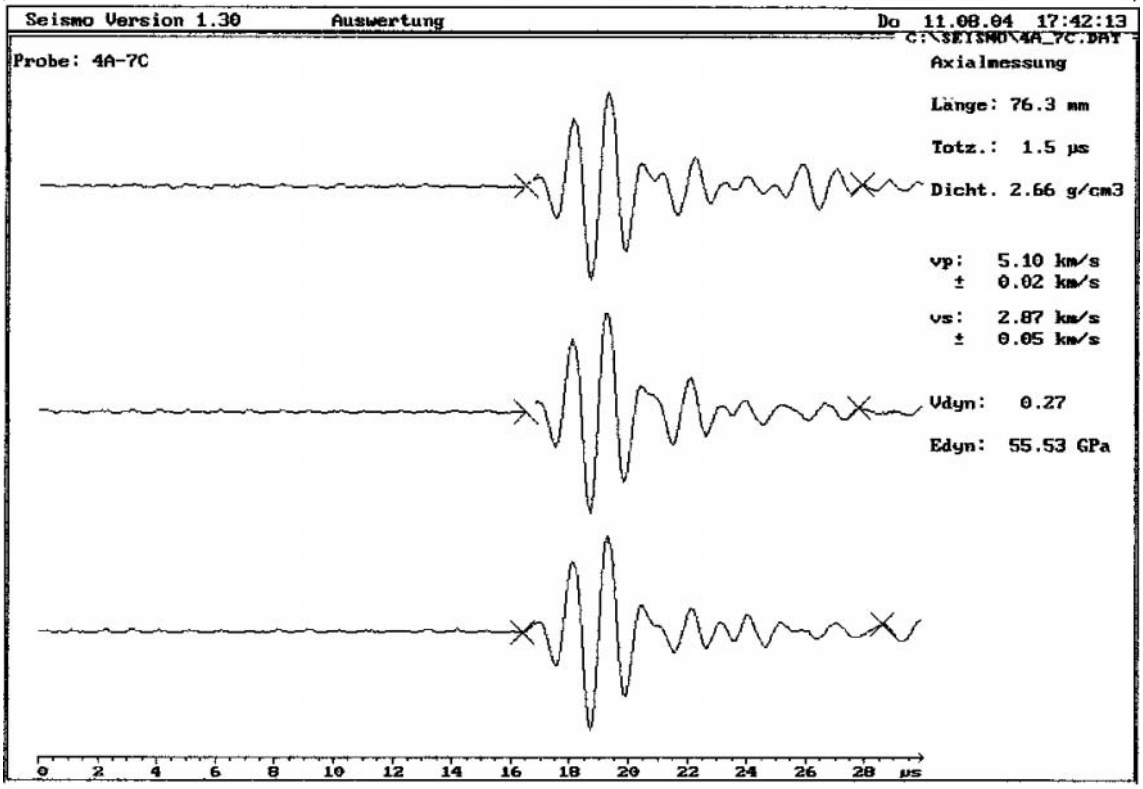
Seismo Version 1.30
Auswertung
Do 11.08.04 17:42:13
C:\SEISMO\4A_7C.DAT
Probe: 4A-7C
Axialmessung
Länge: 76.3 mm
Totz.: 1.5 µs
Dicht. 2.66 g/cm3
vp: 5.10 km/s
± 0.02 km/s
vs: 2.87 km/s
± 0.05 km/s
Vdyn: 0.27
Edyn: 55.53 GPa
0 2 4 6 8 10 12 14 16 18 20 22 24 26 28 µs

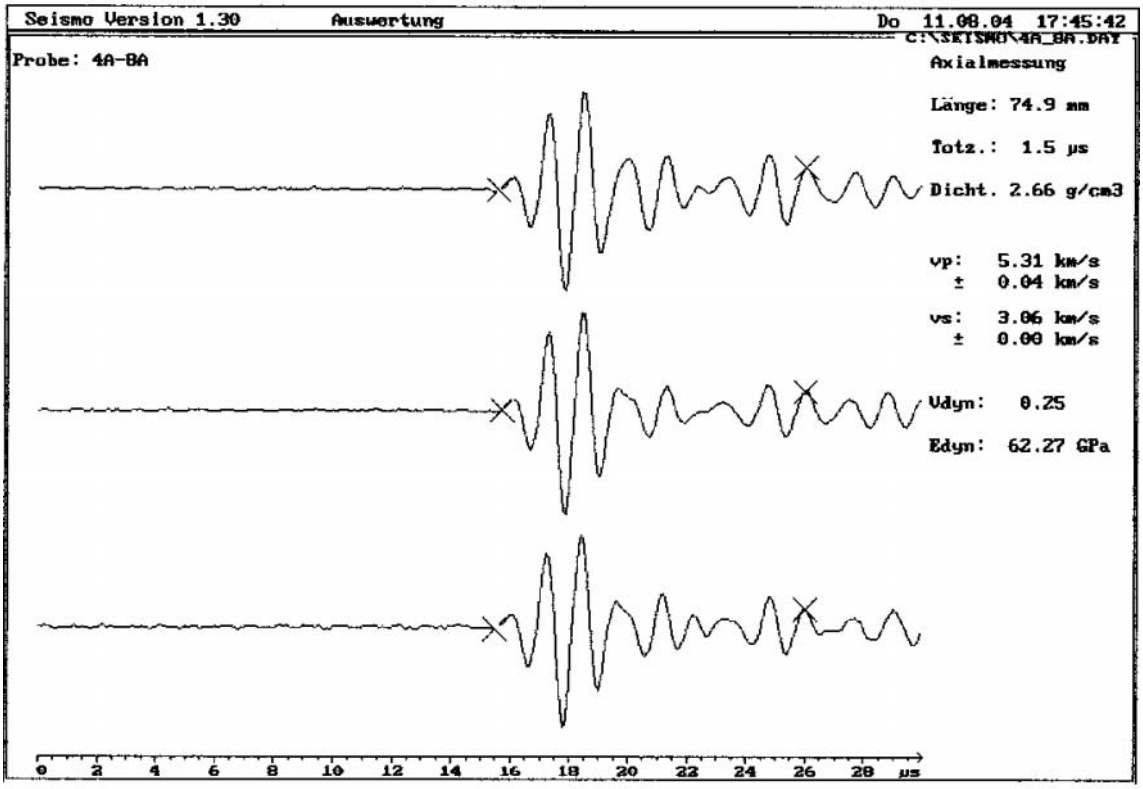
Seismo Version 1.30
Auswertung
Do 11.08.04 17:45:42
C:\SEISMO\4A_8A.DAT
Probe: 4A-8A
Axialmessung
Länge: 74.9 mm
Totz.: 1.5 µs
Dicht. 2.66 g/cm3
vp: 5.31 km/s
± 0.04 km/s
vs: 3.06 km/s
± 0.00 km/s
Vdyn: 0.25
Edyn: 62.27 GPa
0 2 4 6 8 10 12 14 16 18 20 22 24 26 28 µs

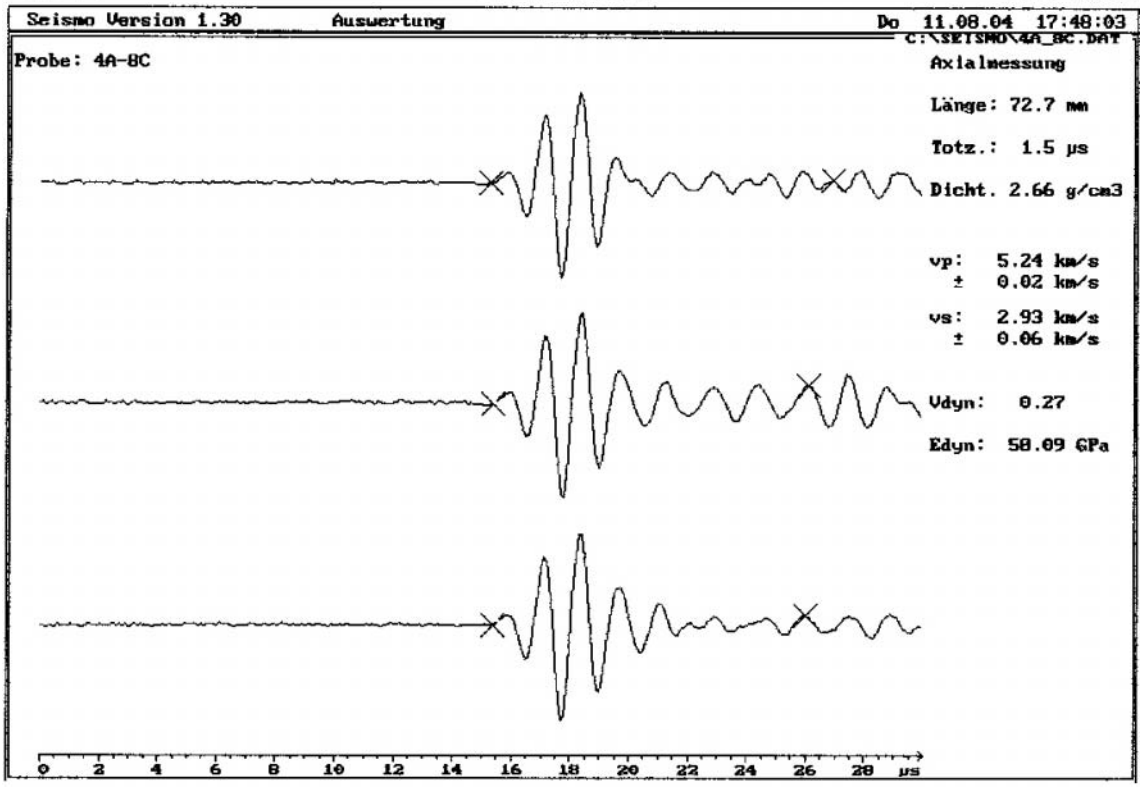
Seismo Version 1.30
Auswertung
Do 11.08.04 17:48:03
C:\SEISMO\4A_8C.DAT
Probe: 4A-8C
Axialmessung
Länge: 72.7 mm
Totz.: 1.5 µs
Dicht. 2.66 g/cm3
vp: 5.24 km/s
± 0.02 km/s
vs: 2.93 km/s
± 0.06 km/s
Vdyn: 0.27
Edyn: 58.09 GPa
0 2 4 6 8 10 12 14 16 18 20 22 24 26 28 µs

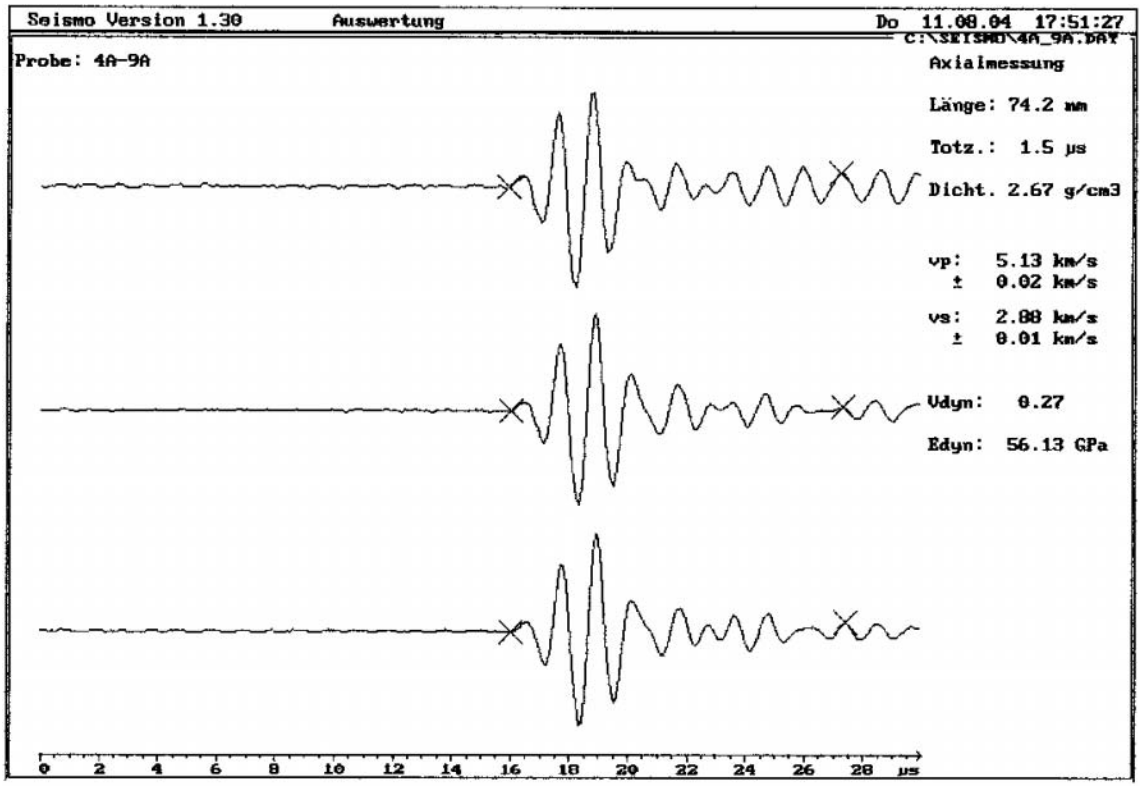
Seismo Version 1.30
Auswertung
Do 11.08.04 17:51:27
C:\SEISMO\4A_9A.DAT
Probe: 4A-9A
Axialmessung
Länge: 74.2 mm
Totz.: 1.5 µs
Dicht. 2.67 g/cm3
vp: 5.13 km/s
± 0.02 km/s
vs: 2.88 km/s
± 0.01 km/s
Vdyn: 0.27
Edyn: 56.13 GPa
0 2 4 6 8 10 12 14 16 18 20 22 24 26 28 µs

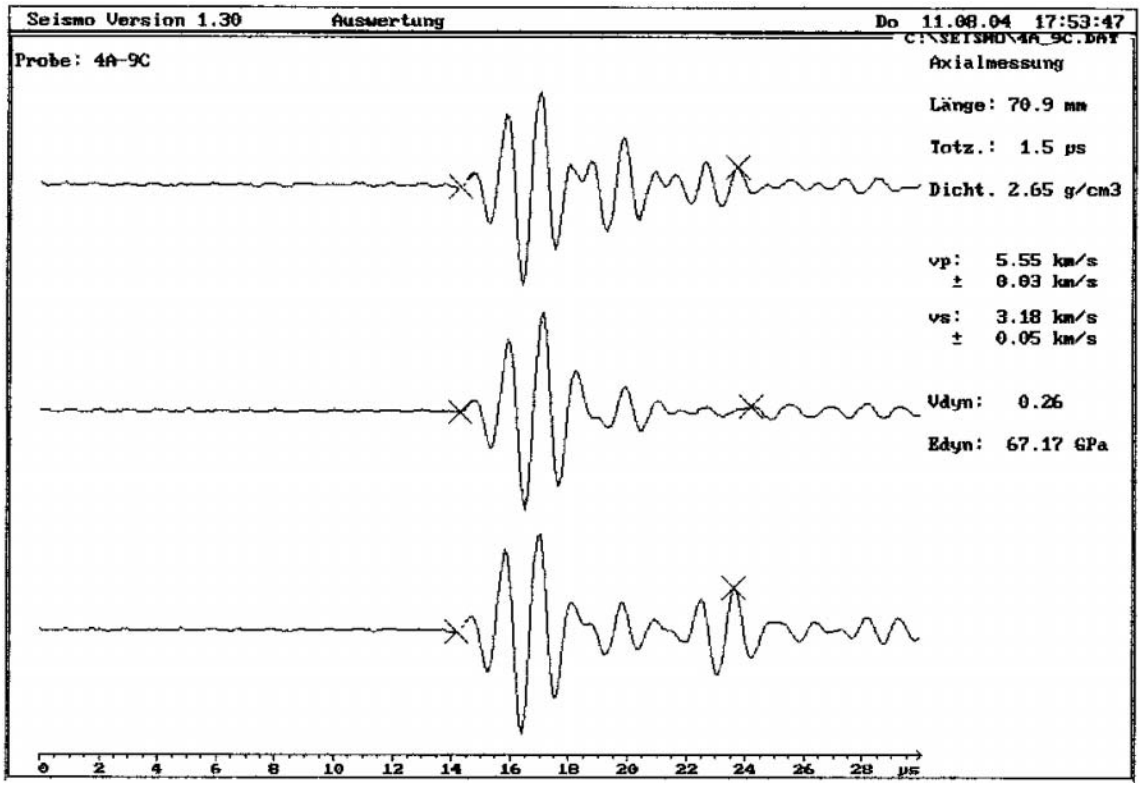
Seismo Version 1.30
Auswertung
Do 11.08.04 17:53:47
C:\SEISMO\4A_9C.DAT
Probe: 4A-9C
Axialmessung
Länge: 70.9 mm
Totz.: 1.5 µs
Dicht. 2.65 g/cm3
vp: 5.55 km/s
± 0.03 km/s
vs: 3.18 km/s
± 0.05 km/s
Vdyn: 0.26
Edyn: 67.17 GPa
0 2 4 6 8 10 12 14 16 18 20 22 24 26 28 µs

Appendix C

Records of fracture toughness tests

ISRM standard 1988

borehole:	KFM01A
sample - no.:	01A-1AB
mean depth, m:	423.17
diameter, mm:	50.6
initial crack length, mm:	7.6
max. Force, kN:	2.40
KIC, MN/m3/2:	2.20
date of testing:	11.06.04
operated by	F. Seebald, U. Weber
checked by	U. Weber

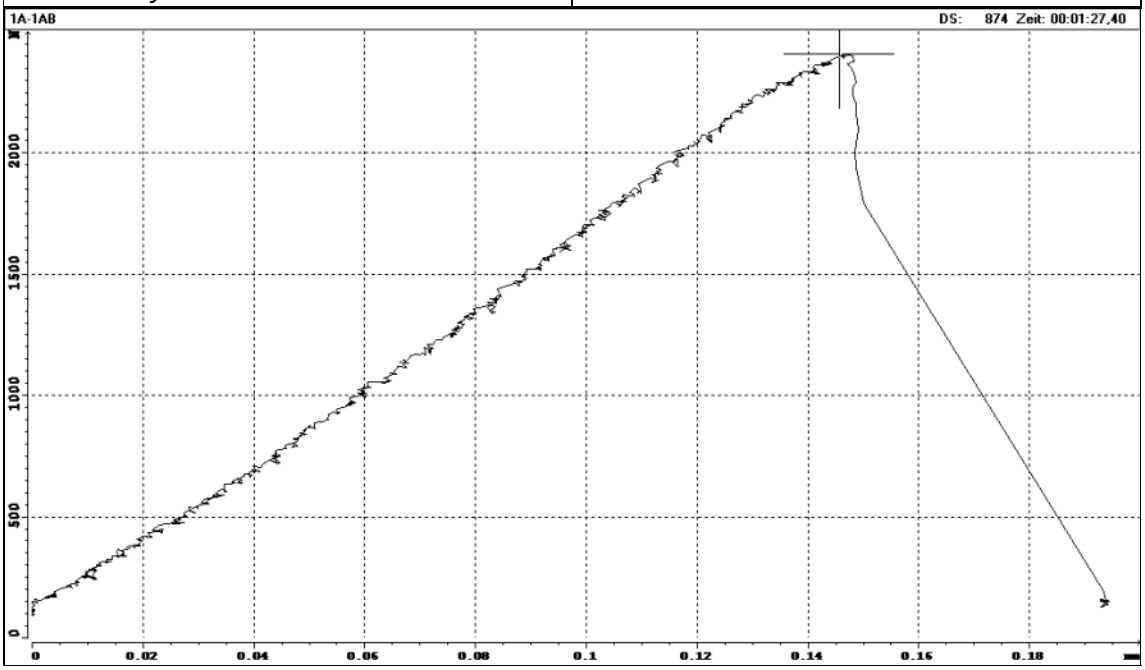

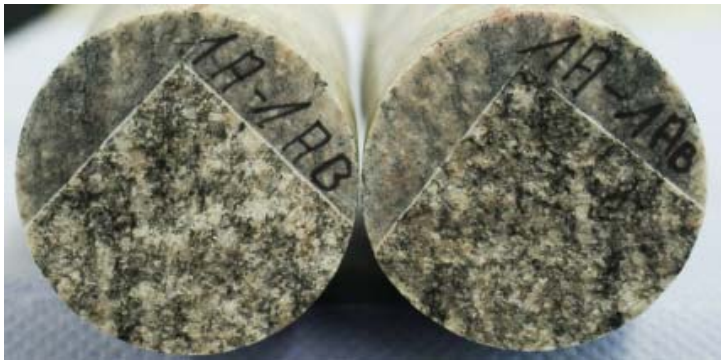

borehole:	KFM01A
sample - no.:	1A-1BC
mean depth, m:	423.17
diameter, mm:	50.6
initial crack length, mm:	6.7
max. Force, kN:	2.66
KIC, MN/m3/2:	2.30
date of testing:	11.06.04
operated by	F. Seebald, U. Weber
checked by	U. Weber

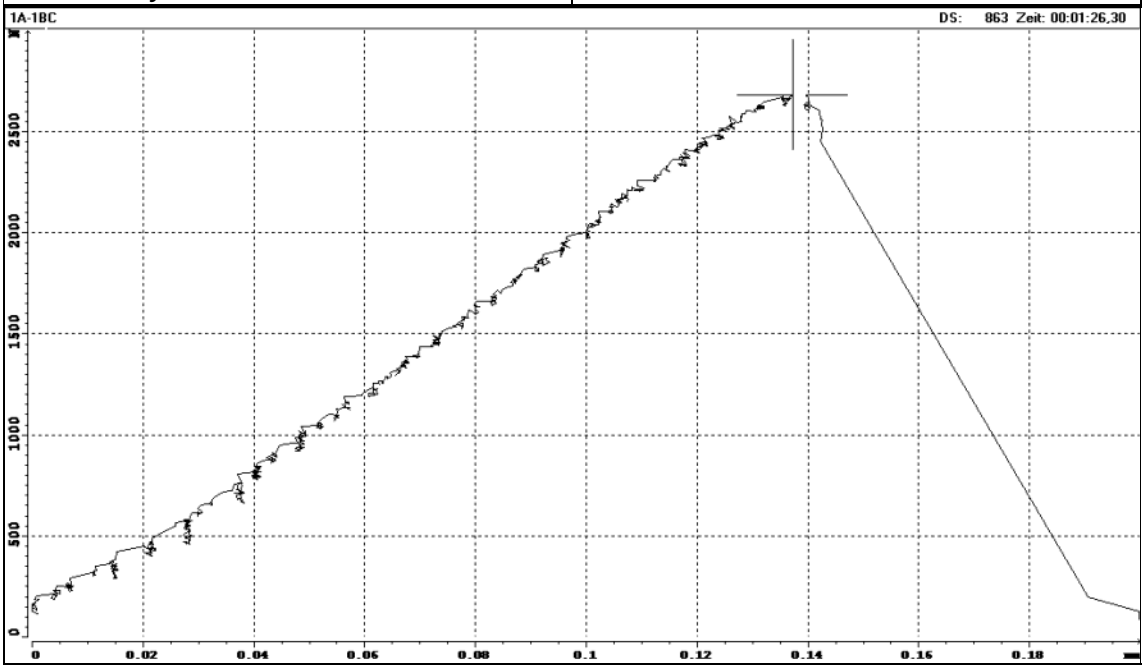

borehole:	KFM01A
sample - no.:	1A-2AB
mean depth, m:	424.83
diameter, mm:	50.5
initial crack length, mm:	7.2
max. Force, kN:	2.23
KIC, MN/m3/2:	2.00
date of testing:	11.06.04
operated by	F. Seebald, U. Weber
checked by	U. Weber

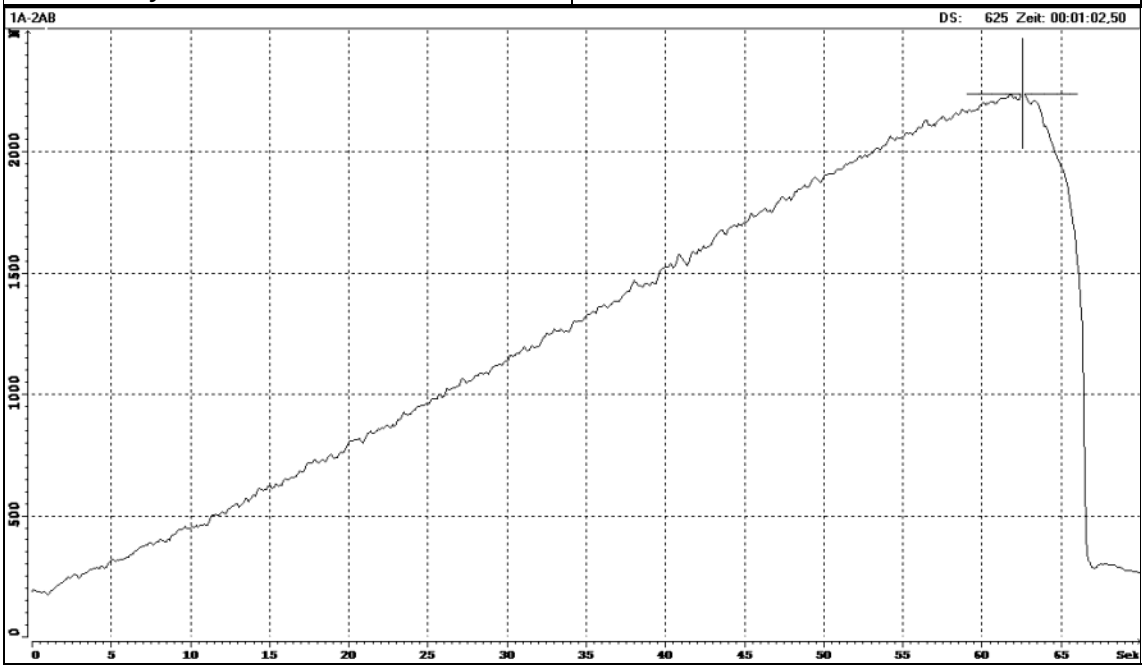

borehole:	KFM01A
sample - no.:	1A-2BC
mean depth, m:	424.83
diameter, mm:	50.6
initial crack length, mm:	7.0
max. Force, kN:	2.55
KIC, MN/m3/2:	2.25
date of testing:	11.06.04
operated by	F. Seebald, U. Weber
checked by	U. Weber

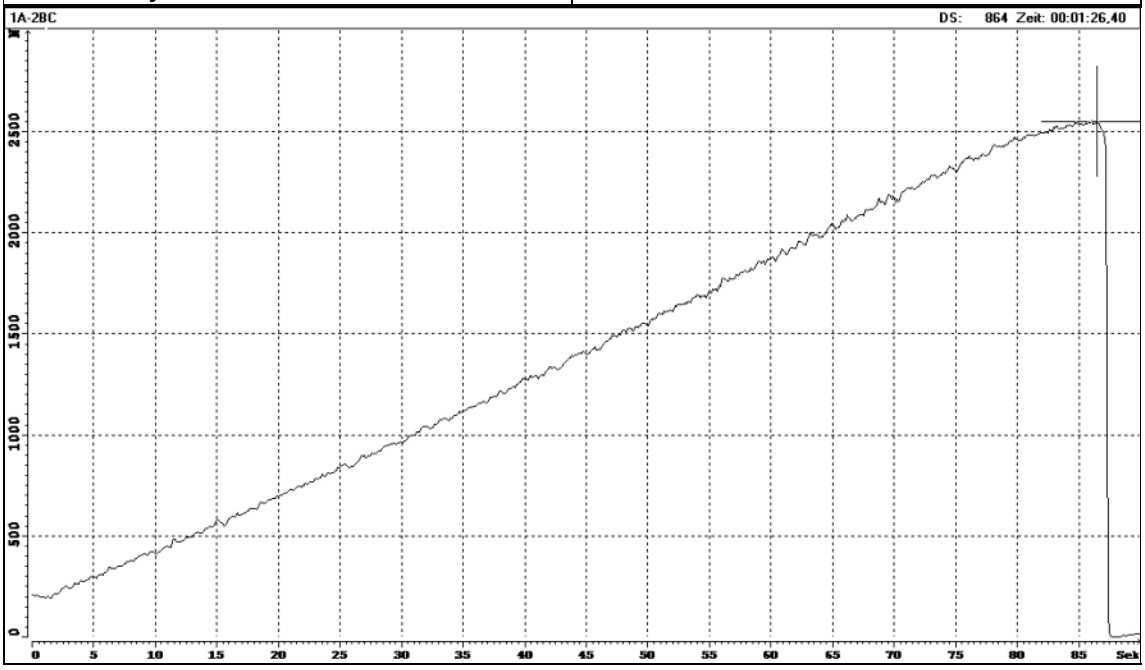

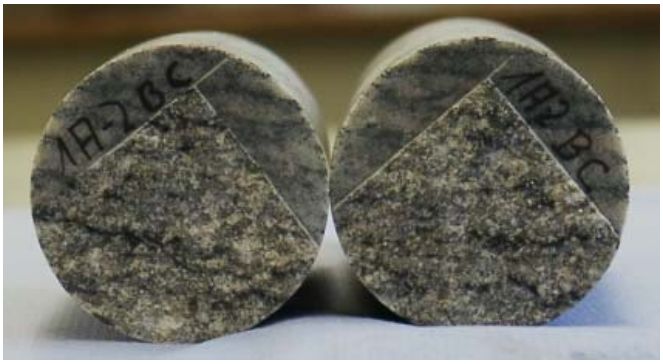

borehole:	KFM01A
sample - no.:	1A-3AB
mean depth, m:	428.17
diameter, mm:	50.7
initial crack length, mm:	7.1
max. Force, kN:	2.53
KIC, MN/m3/2:	2.24
date of testing:	11.06.04
operated by	F. Seebald, U. Weber
checked by	U. Weber

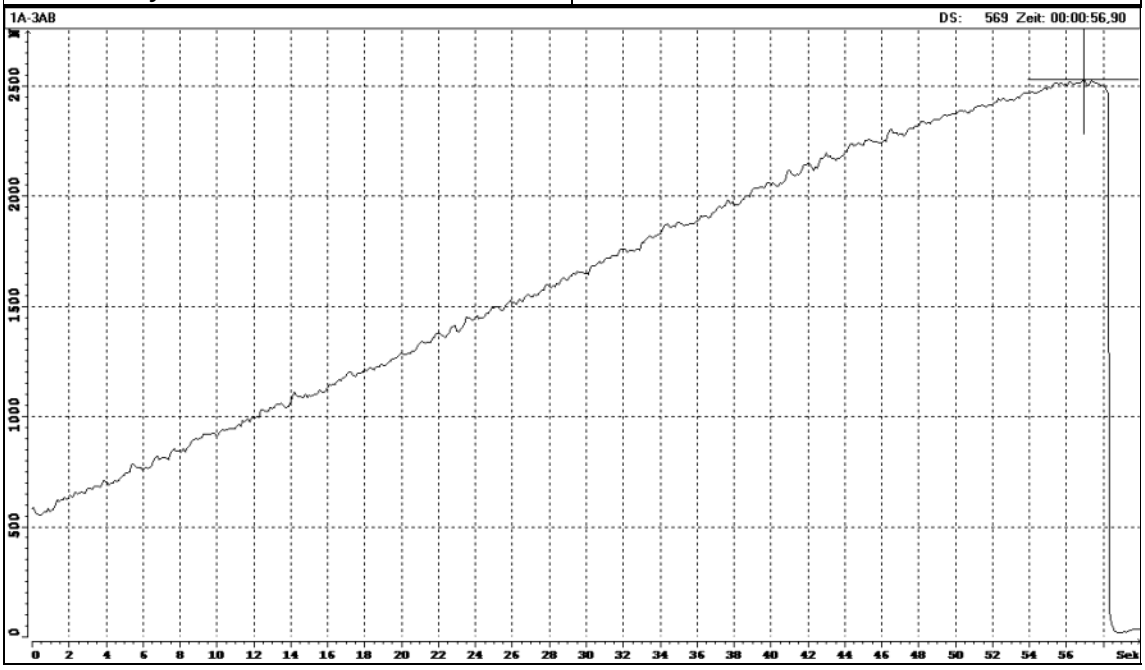

borehole:	KFM01A
sample - no.:	1A-3BC
mean depth, m:	428.17
diameter, mm:	50.7
initial crack length, mm:	6.7
max. Force, kN:	2.26
KIC, MN/m3/2:	1.95
date of testing:	11.06.04
operated by	F. Seebald, U. Weber
checked by	U. Weber

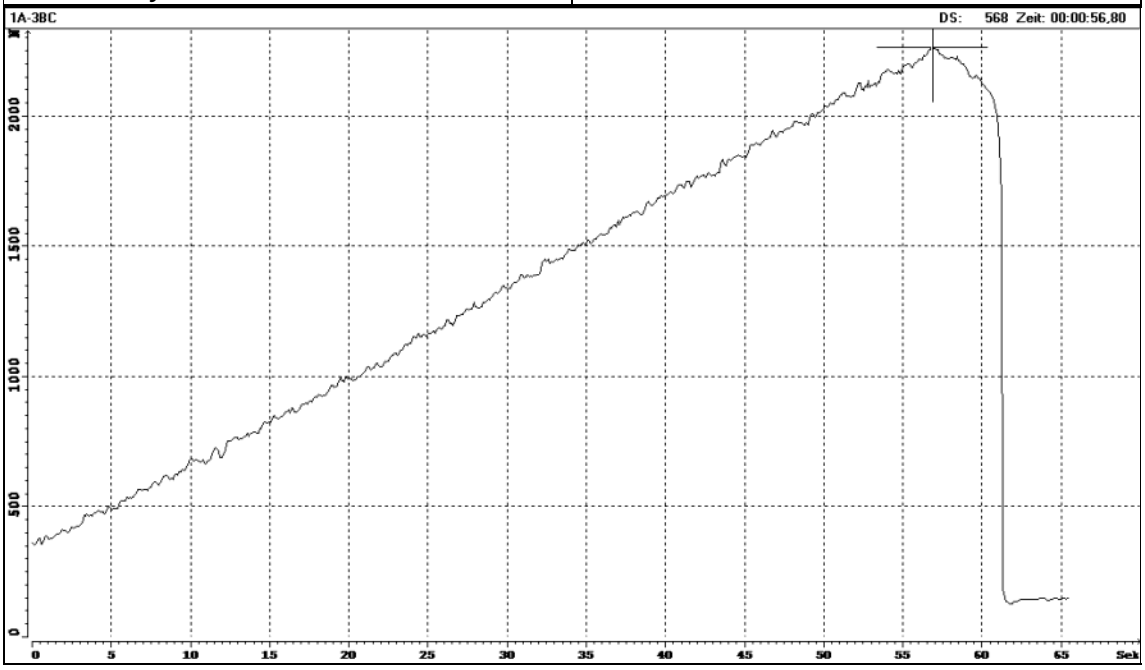

borehole:	KFM01A
sample - no.:	1A-4AB
mean depth, m:	484.59
diameter, mm:	50.6
initial crack length, mm:	6.9
max. Force, kN:	2.20
KIC, MN/m3/2:	1.93
date of testing:	11.06.04
operated by	F. Seebald, U. Weber
checked by	U. Weber

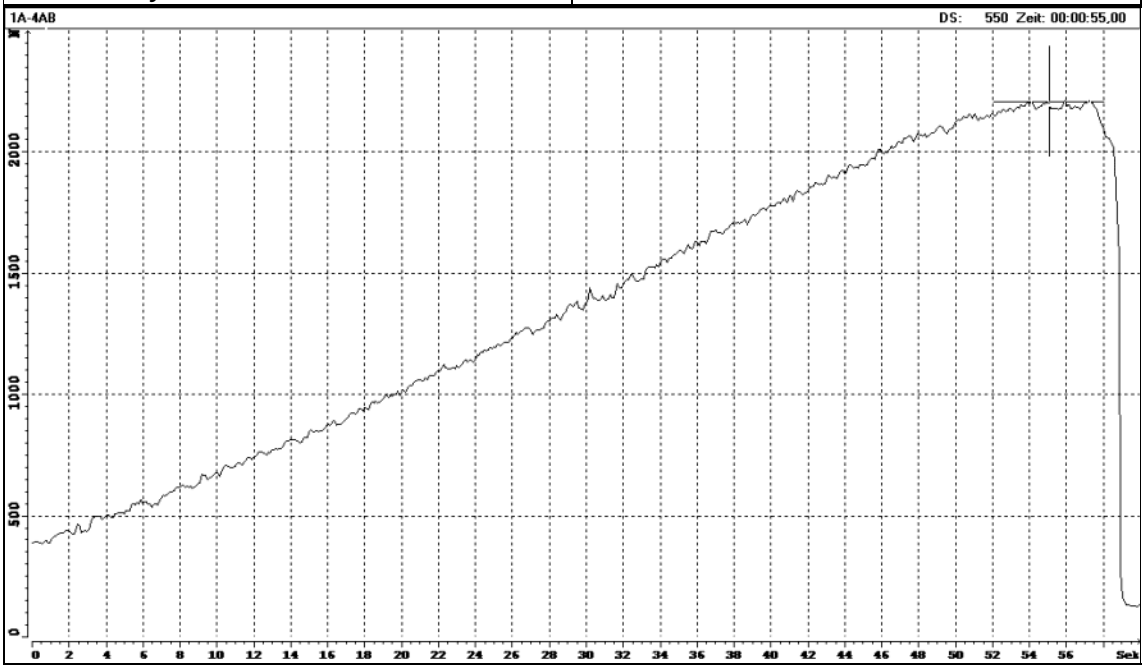

borehole:	KFM01A
sample - no.:	1A-4BC
mean depth, m:	484.59
diameter, mm:	50.6
initial crack length, mm:	7.1
max. Force, kN:	2.21
KIC, MN/m3/2:	1.96
date of testing:	11.06.04
operated by	F. Seebald, U. Weber
checked by	U. Weber

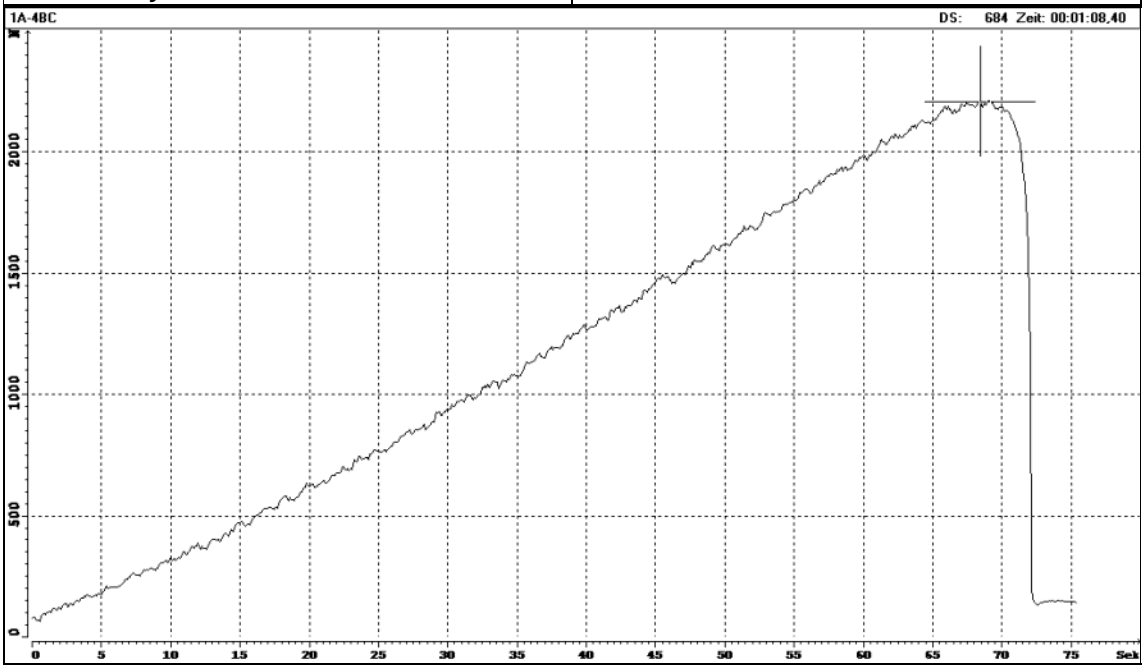

borehole:	KFM01A
sample - no.:	1A-5AB
mean depth, m:	489.95
diameter, mm:	50.8
initial crack length, mm:	7.1
max. Force, kN:	2.23
KIC, MN/m3/2:	1.96
date of testing:	11.06.04
operated by	F. Seebald, U. Weber
checked by	U. Weber

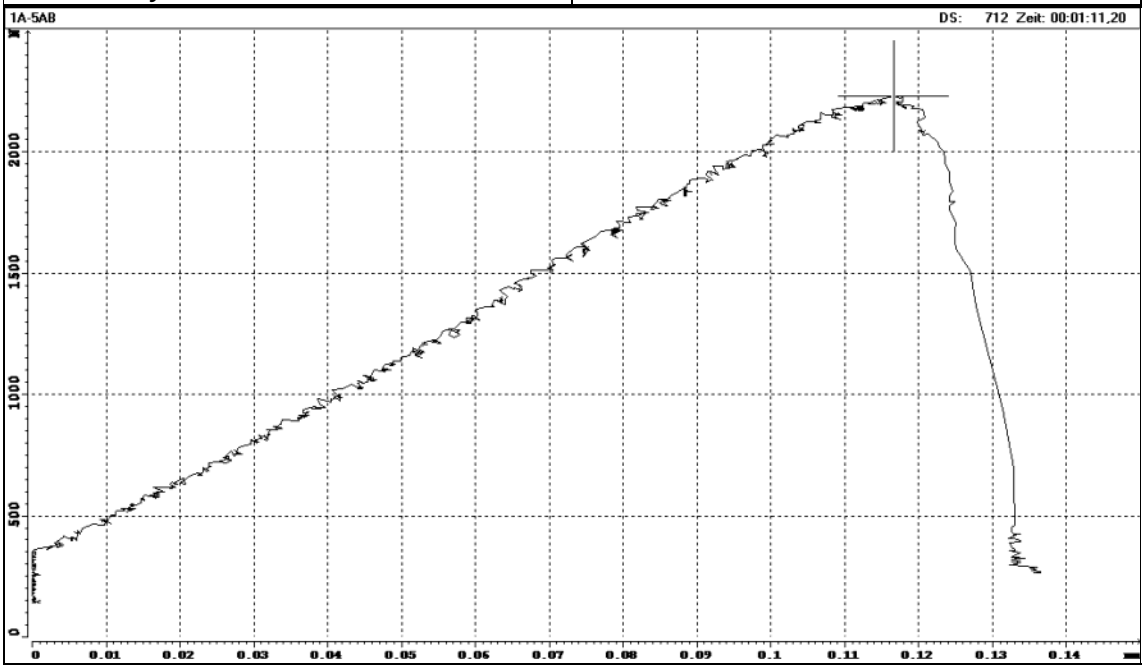

borehole:	KFM01A
sample - no.:	1A-5BC
mean depth, m:	489.95
diameter, mm:	50.9
initial crack length, mm:	7.3
max. Force, kN:	0.80
KIC, MN/m3/2:	0.71
date of testing:	11.06.04
operated by	F. Seebald, U. Weber
checked by	U. Weber

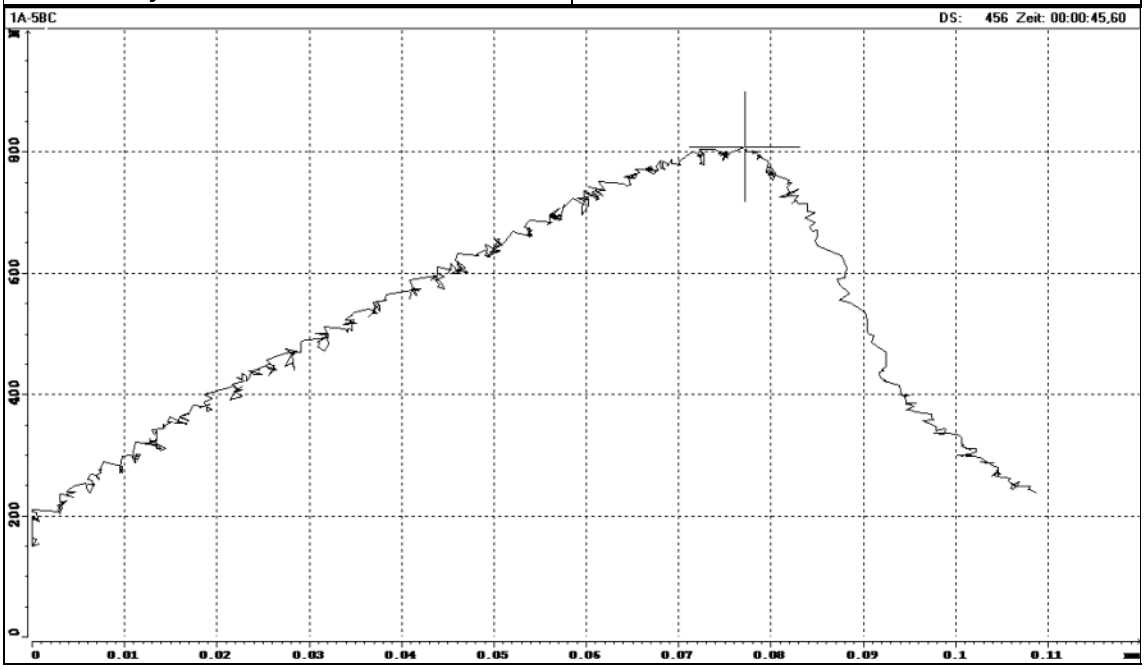

borehole:	KFM01A
sample - no.:	1A-6AB
mean depth, m:	504.69
diameter, mm:	50.8
initial crack length, mm:	7.1
max. Force, kN:	2.35
KIC, MN/m3/2:	2.07
date of testing:	11.06.04
operated by	F. Seebald, U. Weber
checked by	U. Weber

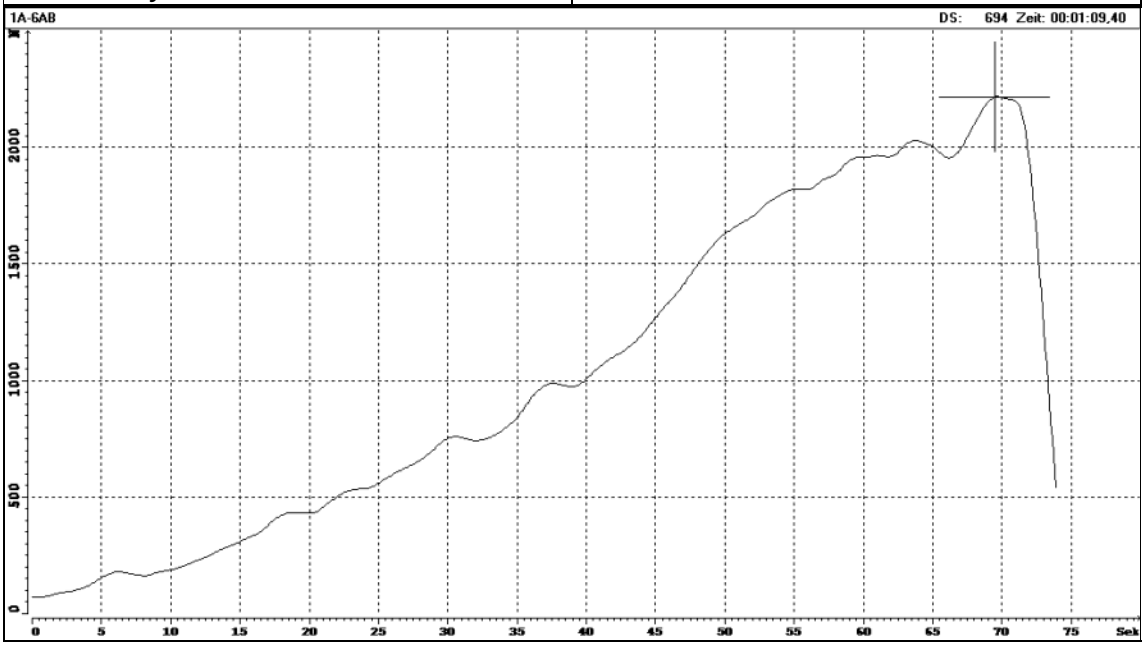

borehole:	KFM01A
sample - no.:	1A-6BC
mean depth, m:	504.69
diameter, mm:	50.7
initial crack length, mm:	7.2
max. Force, kN:	2.42
KIC, MN/m3/2:	2.15
date of testing:	11.06.04
operated by	F. Seebald, U. Weber
checked by	U. Weber

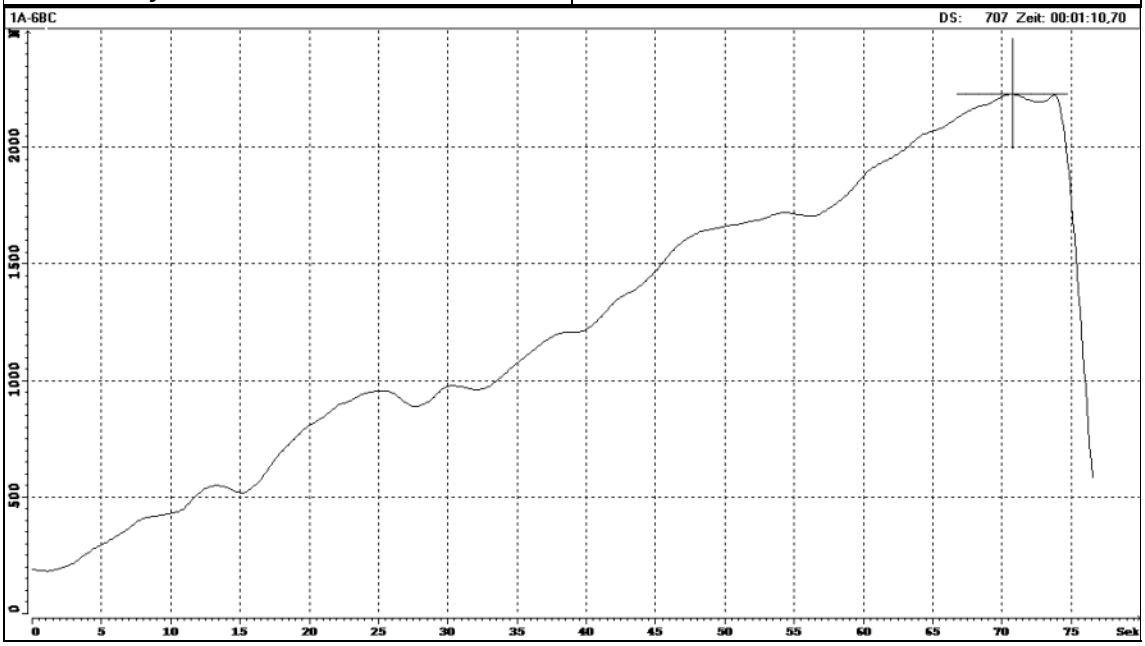

borehole:	KFM01A
sample - no.:	1A-7AB
mean depth, m:	688.13
diameter, mm:	51.0
initial crack length, mm:	7.3
max. Force, kN:	1.94
KIC, MN/m3/2:	1.72
date of testing:	11.06.04
operated by	F. Seebald, U. Weber
checked by	U. Weber

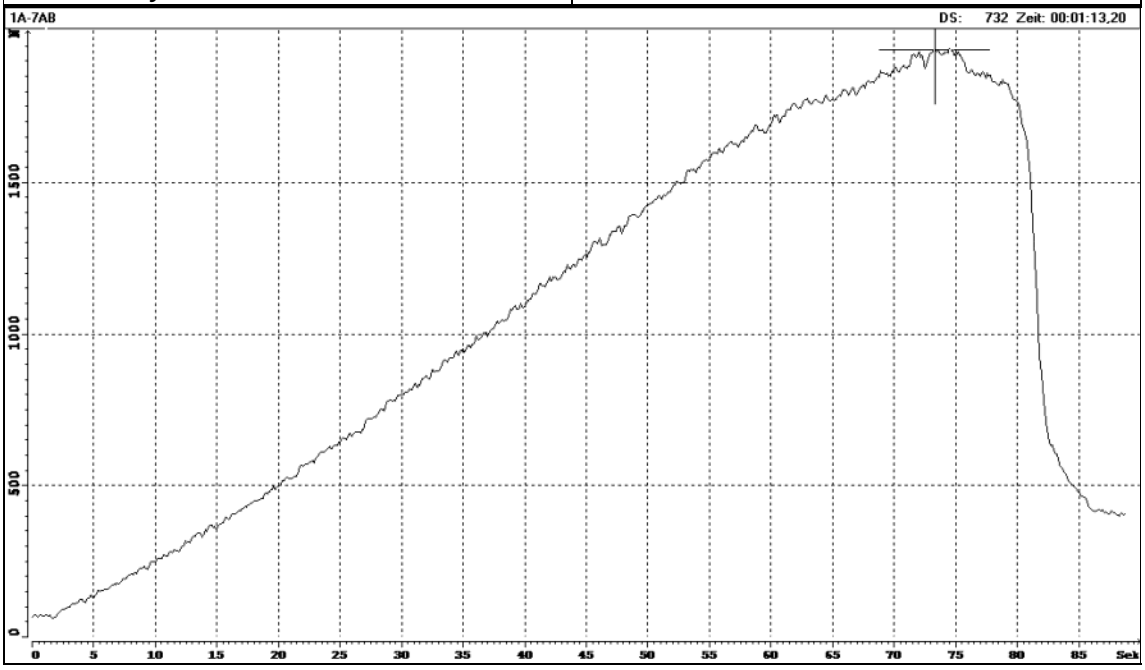

borehole:	KFM01A
sample - no.:	1A-7BC
mean depth, m:	688.13
diameter, mm:	51.0
initial crack length, mm:	7.3
max. Force, kN:	2.35
KIC, MN/m3/2:	2.08
date of testing:	11.06.04
operated by	F. Seebald, U. Weber
checked by	U. Weber

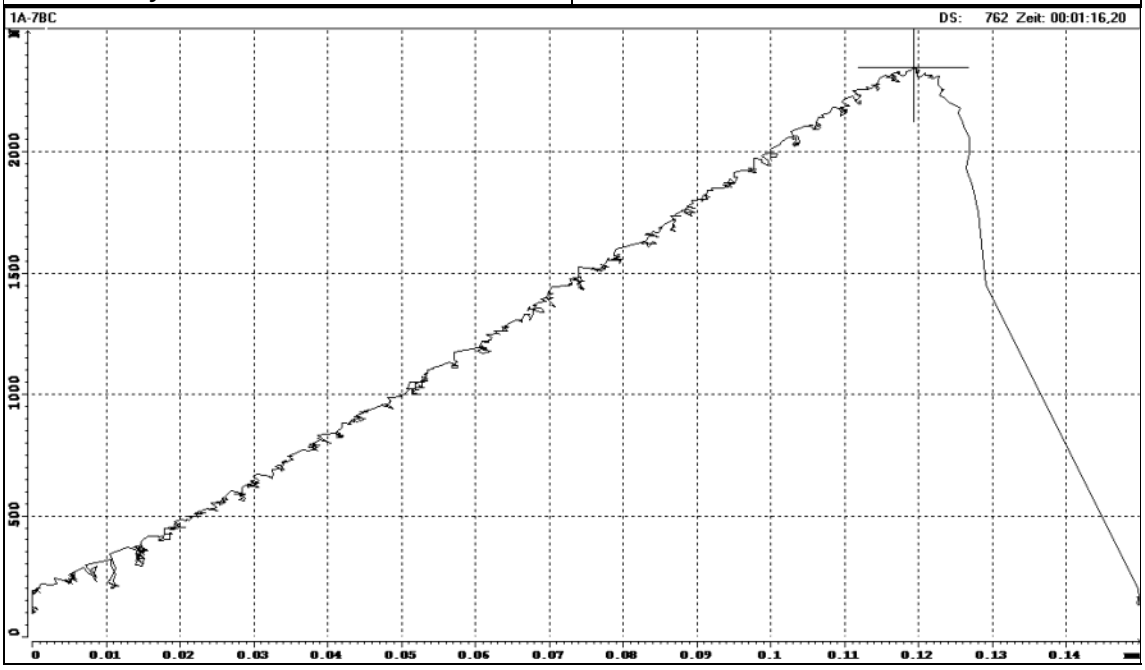

borehole:	KFM01A
sample - no.:	1A-8AB
mean depth, m:	950.00
diameter, mm:	50.8
initial crack length, mm:	7.2
max. Force, kN:	1.95
KIC, MN/m3/2:	1.73
date of testing:	11.06.04
operated by	F. Seebald, U. Weber
checked by	U. Weber

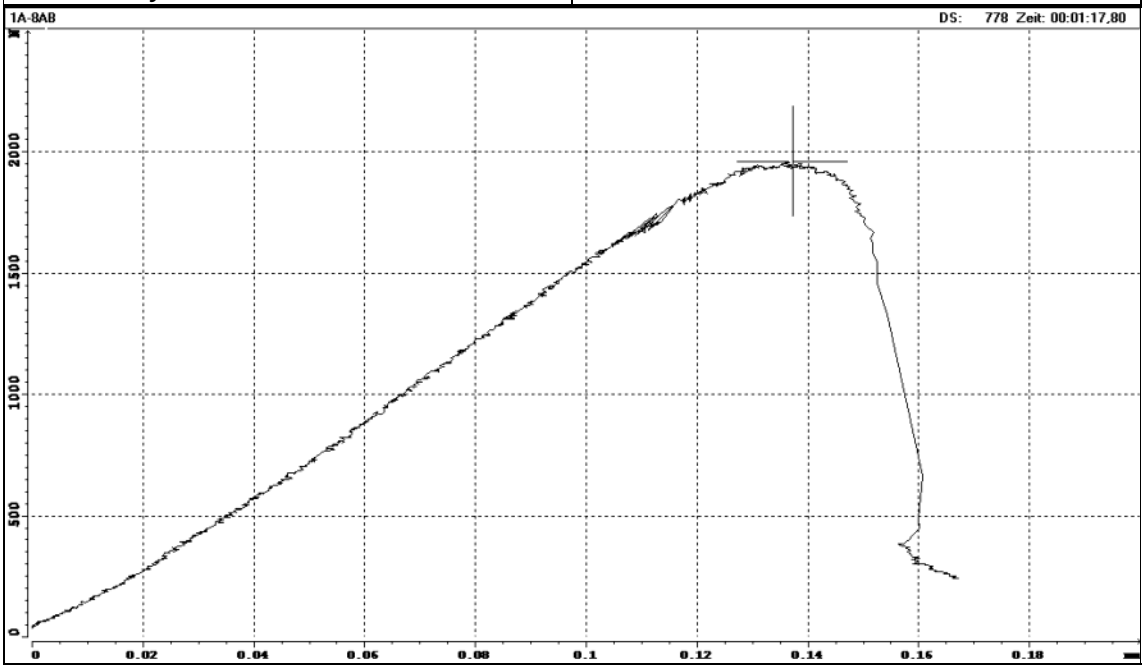

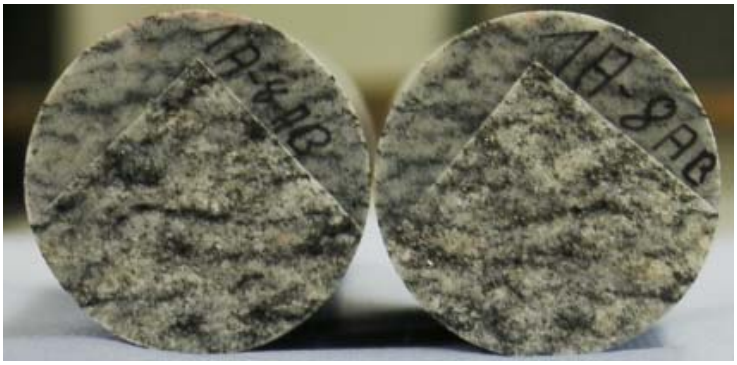

borehole:	KFM01A
sample - no.:	1A-8BC
mean depth, m:	950.00
diameter, mm:	50.9
initial crack length, mm:	7.3
max. Force, kN:	1.94
KIC, MN/m3/2:	1.72
date of testing:	11.06.04
operated by	F. Seebald, U. Weber
checked by	U. Weber

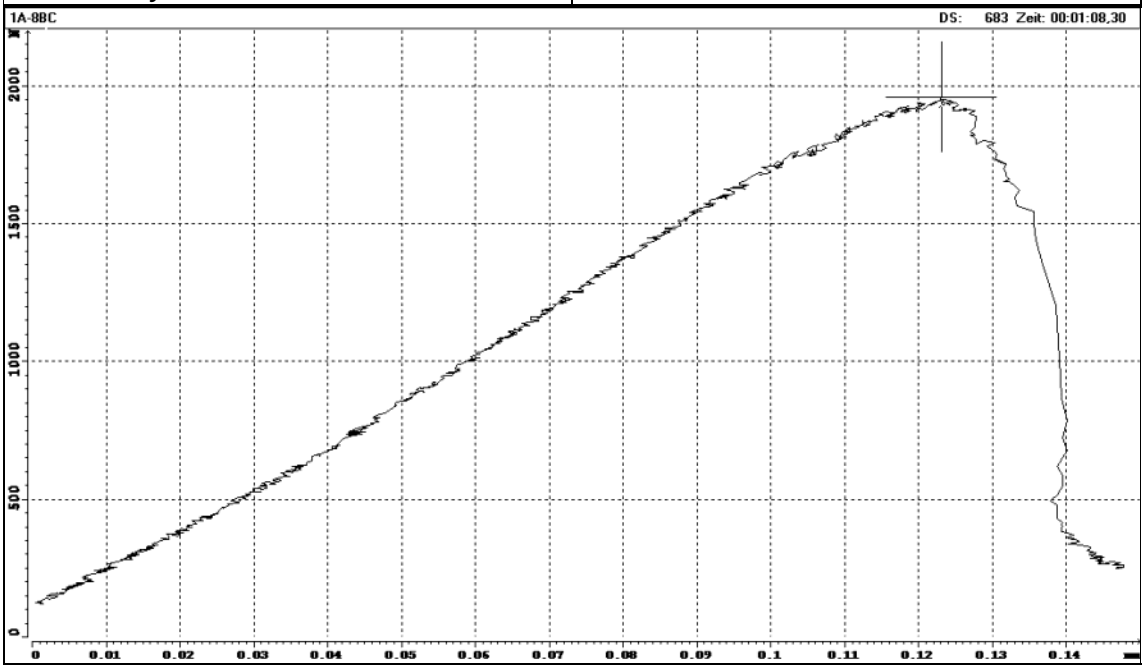

borehole:	KFM01A
sample - no.:	1A-9AB
mean depth, m:	971.57
diameter, mm:	50.8
initial crack length, mm:	6.7
max. Force, kN:	2.15
KIC, MN/m3/2:	1.84
date of testing:	11.06.04
operated by	F. Seebald, U. Weber
checked by	U. Weber

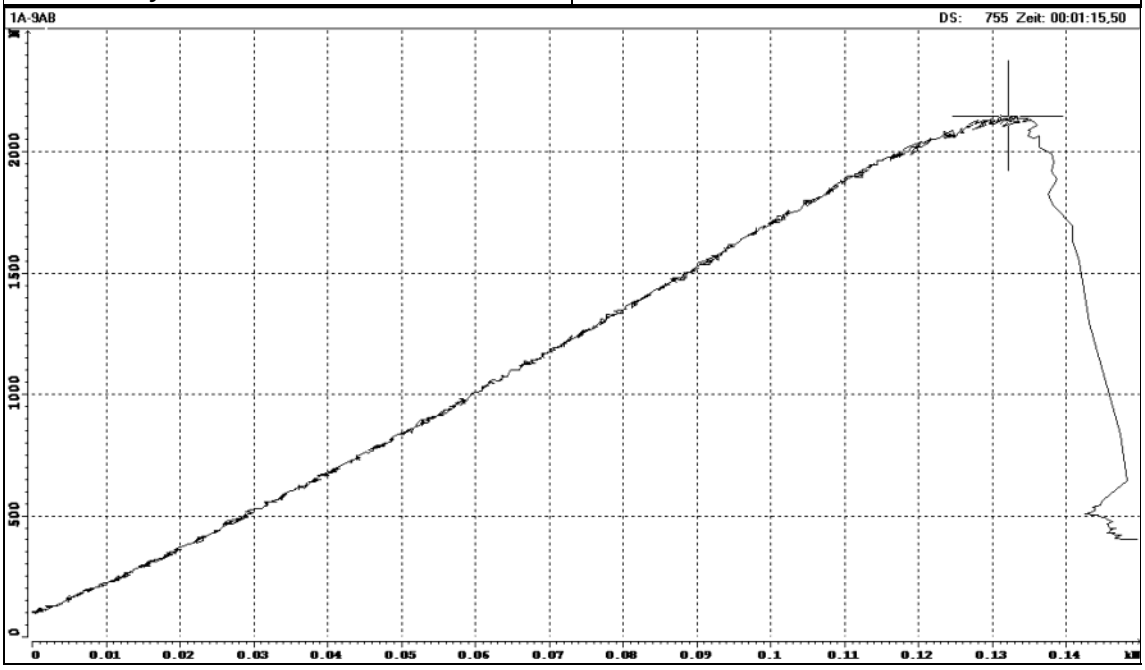

borehole:	KFM01A
sample - no.:	1A-9BC
mean depth, m:	971.57
diameter, mm:	50.8
initial crack length, mm:	7.0
max. Force, kN:	2.07
KIC, MN/m3/2:	1.81
date of testing:	11.06.04
operated by	F. Seebald, U. Weber
checked by	U. Weber

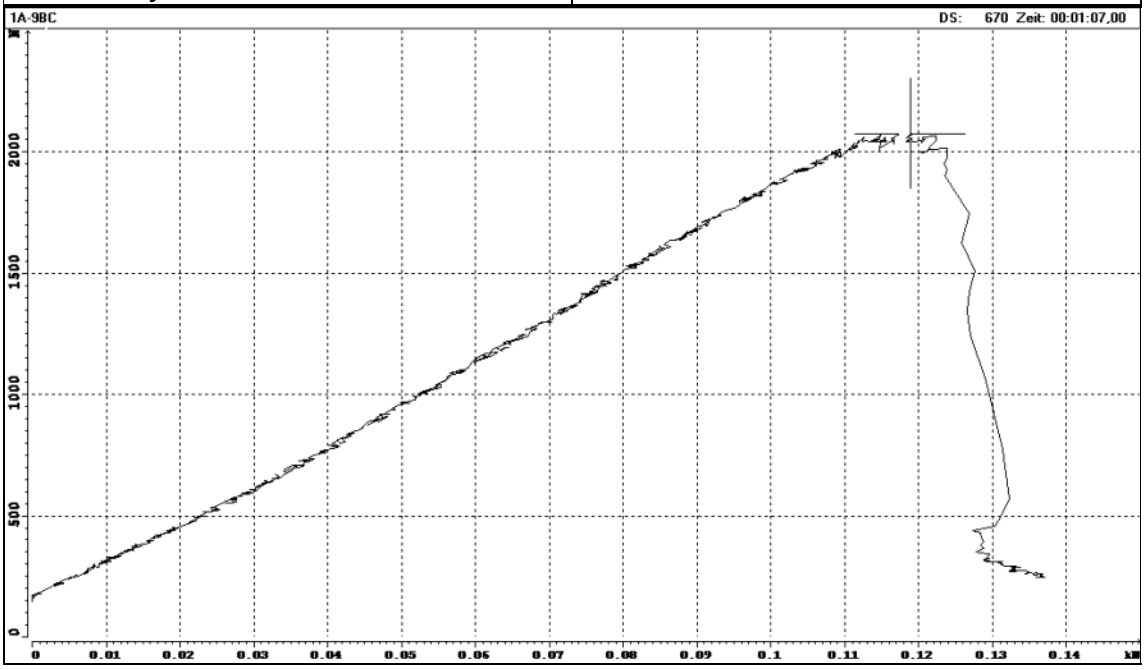

borehole:	KFM01A
sample - no.:	1A-10AB
mean depth, m:	978.53
diameter, mm:	50.7
initial crack length, mm:	6.9
max. Force, kN:	2.12
KIC, MN/m3/2:	1.85
date of testing:	11.06.04
operated by	F. Seebald, U. Weber
checked by	U. Weber

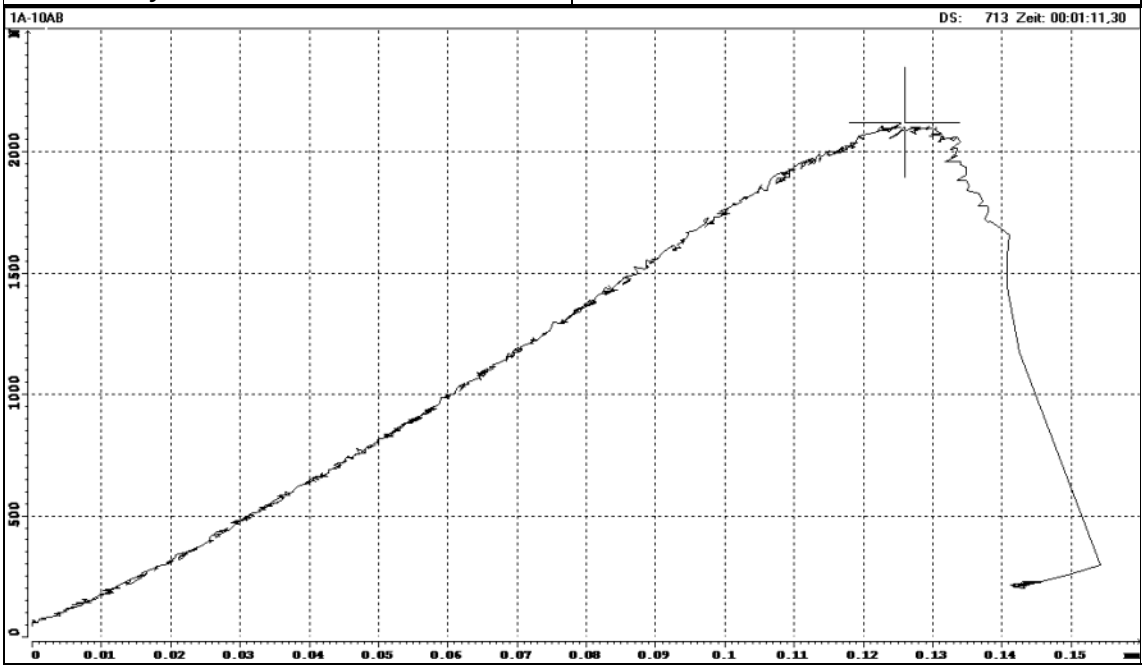

borehole:	KFM01A
sample - no.:	1A-10BC
mean depth, m:	978.53
diameter, mm:	50.8
initial crack length, mm:	7.4
max. Force, kN:	2.15
KIC, MN/m3/2:	1.93
date of testing:	11.06.04
operated by	F. Seebald, U. Weber
checked by	U. Weber

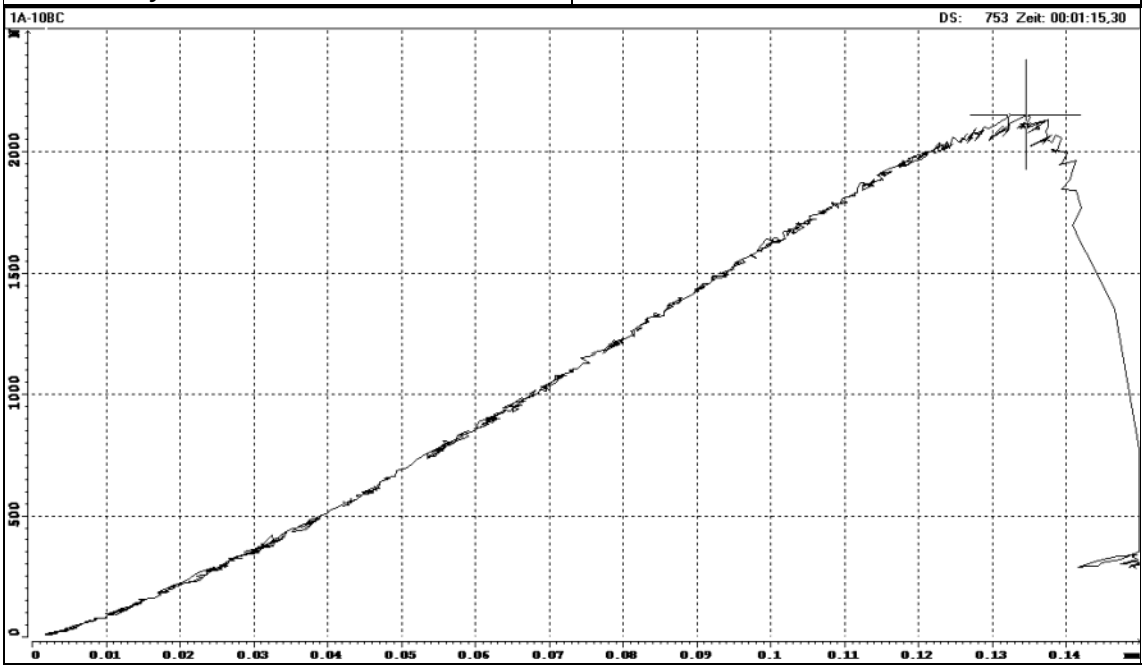

borehole:	KFM01B
sample - no.:	1B-1AB
mean depth, m:	421.03
diameter, mm:	50.7
initial crack length, mm:	7.0
max. Force, kN:	2.46
KIC, MN/m3/2:	2.16
date of testing:	23.07.04
operated by	F. Seebald, U. Weber
checked by	U. Weber

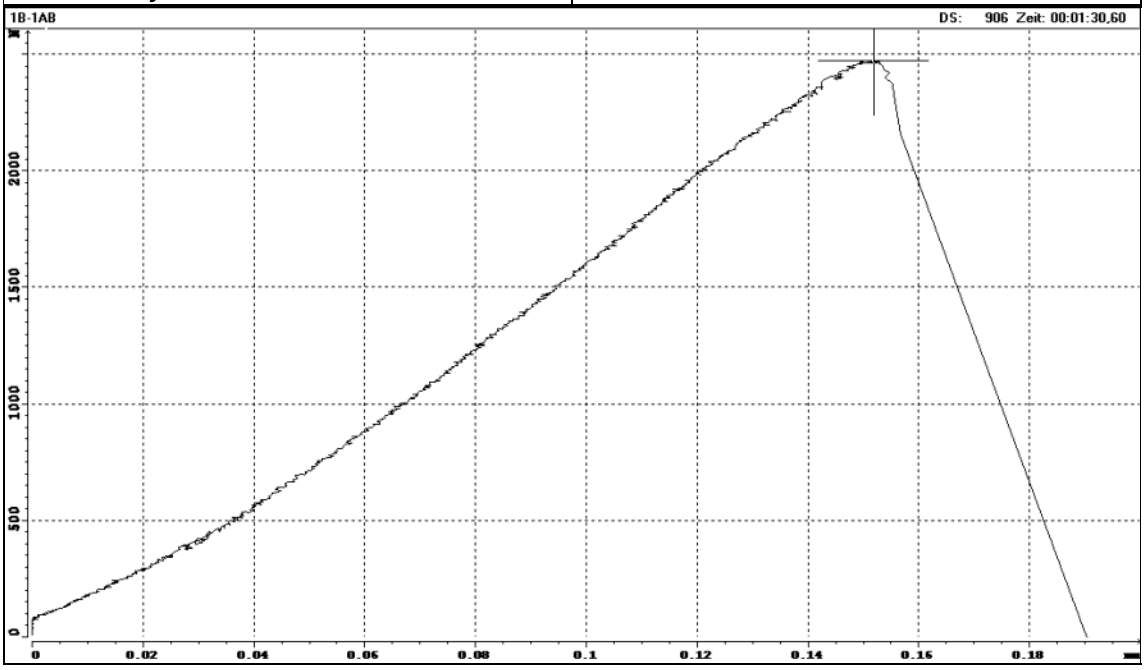

borehole:	KFM01B
sample - no.:	1B-1BC
mean depth, m:	421.03
diameter, mm:	50.7
initial crack length, mm:	7.4
max. Force, kN:	2.49
KIC, MN/m3/2:	2.24
date of testing:	23.07.04
operated by	F. Seebald, U. Weber
checked by	U. Weber

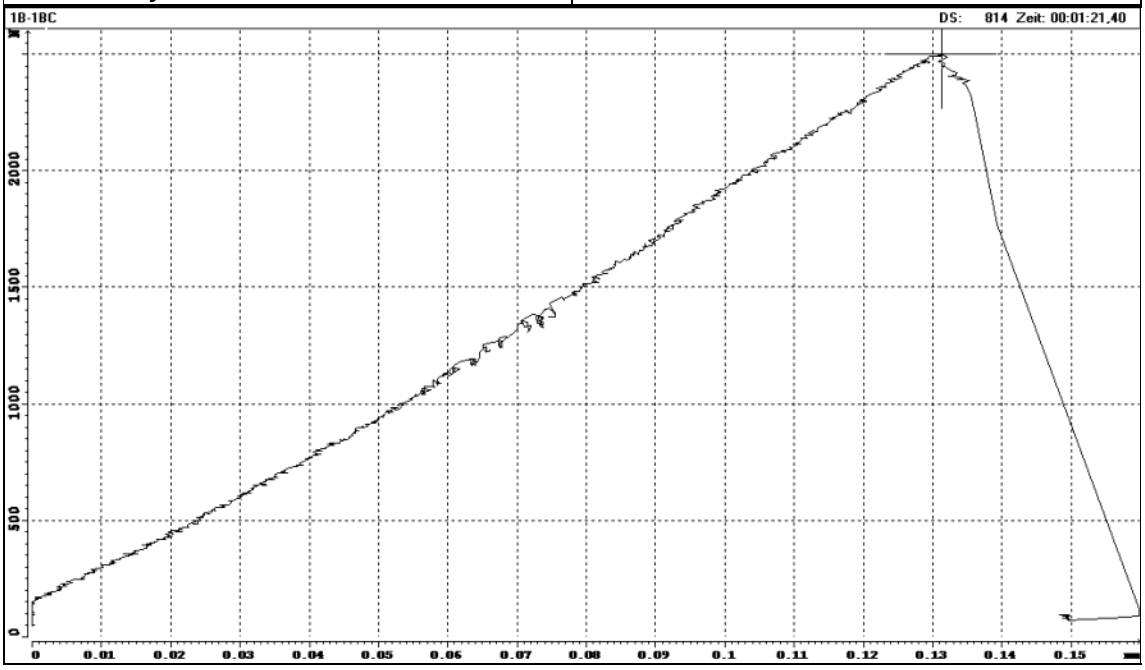

borehole:	KFM01B
sample - no.:	1B-2AB
mean depth, m:	421.60
diameter, mm:	50.7
initial crack length, mm:	7.4
max. Force, kN:	2.54
KIC, MN/m3/2:	2.29
date of testing:	23.07.04
operated by	F. Seebald, U. Weber
checked by	U. Weber

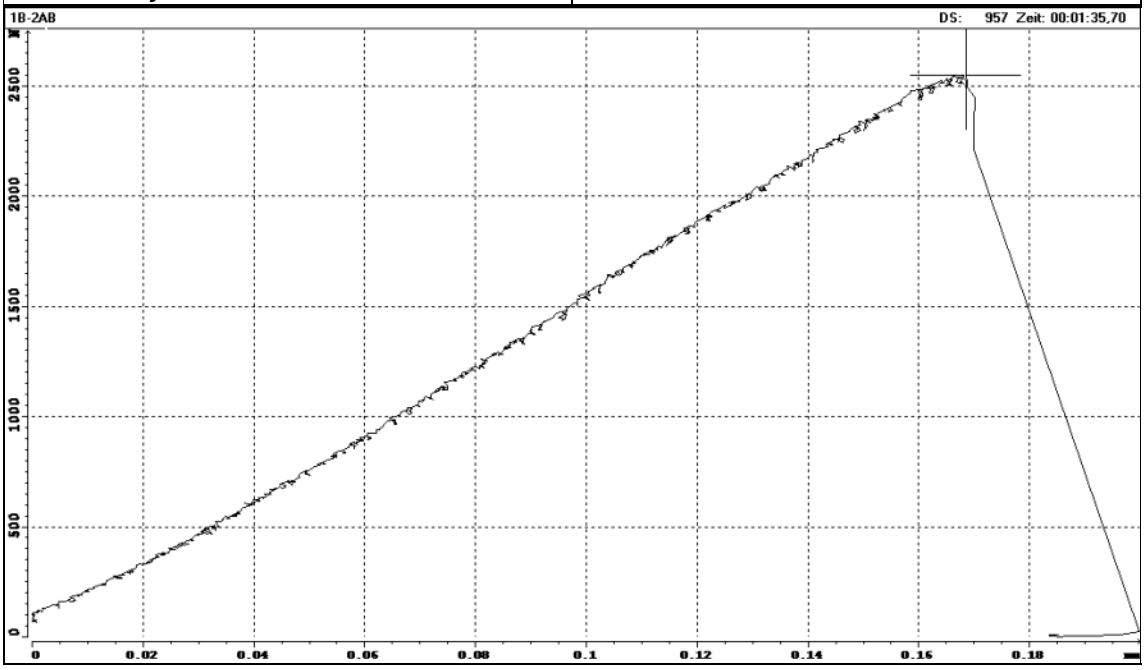

borehole:	KFM01B
sample - no.:	1B-2BC
mean depth, m:	421.60
diameter, mm:	50.7
initial crack length, mm:	7.4
max. Force, kN:	2.23
KIC, MN/m3/2:	2.01
date of testing:	23.07.04
operated by	F. Seebald, U. Weber
checked by	U. Weber

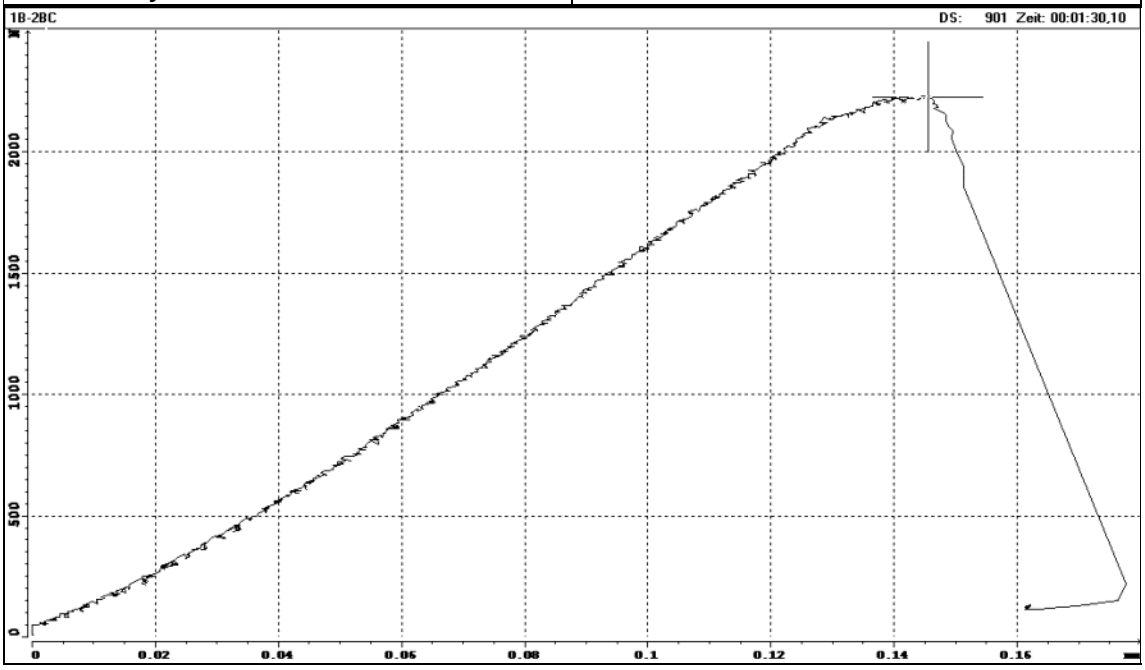

borehole:	KFM01B
sample - no.:	1B-3AB
mean depth, m:	428.09
diameter, mm:	50.8
initial crack length, mm:	7.3
max. Force, kN:	2.64
KIC, MN/m3/2:	2.35
date of testing:	23.07.04
operated by	F. Seebald, U. Weber
checked by	U. Weber

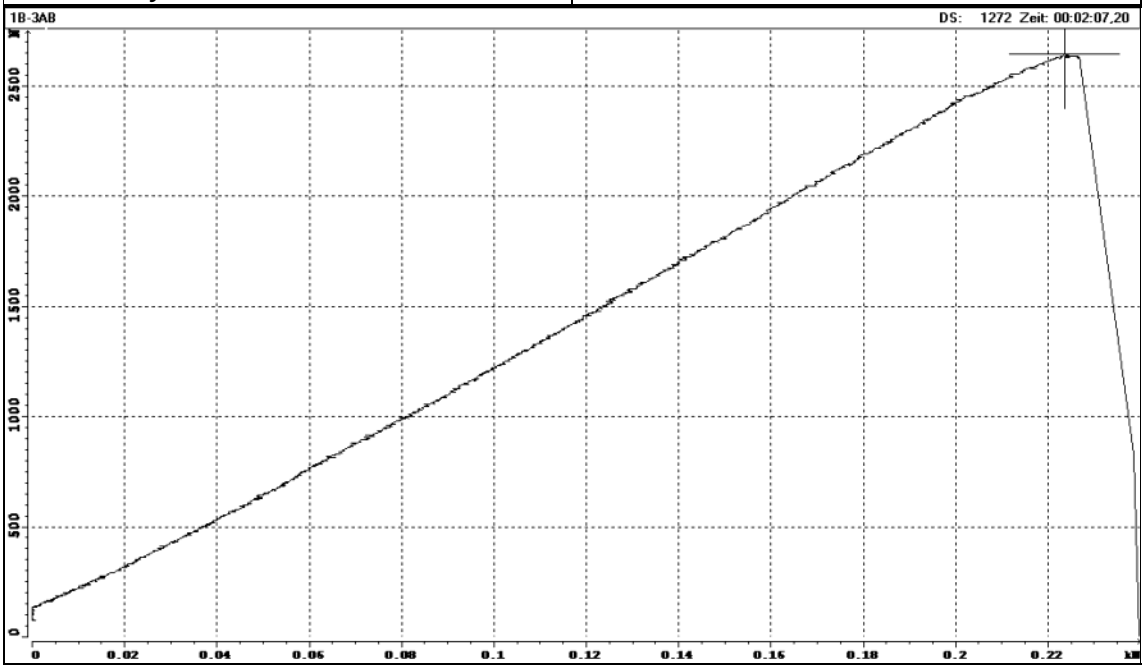

borehole:	KFM01B
sample - no.:	1B-3BC
mean depth, m:	428.09
diameter, mm:	50.8
initial crack length, mm:	7.0
max. Force, kN:	2.24
KIC, MN/m3/2:	1.96
date of testing:	23.07.04
operated by	F. Seebald, U. Weber
checked by	U. Weber

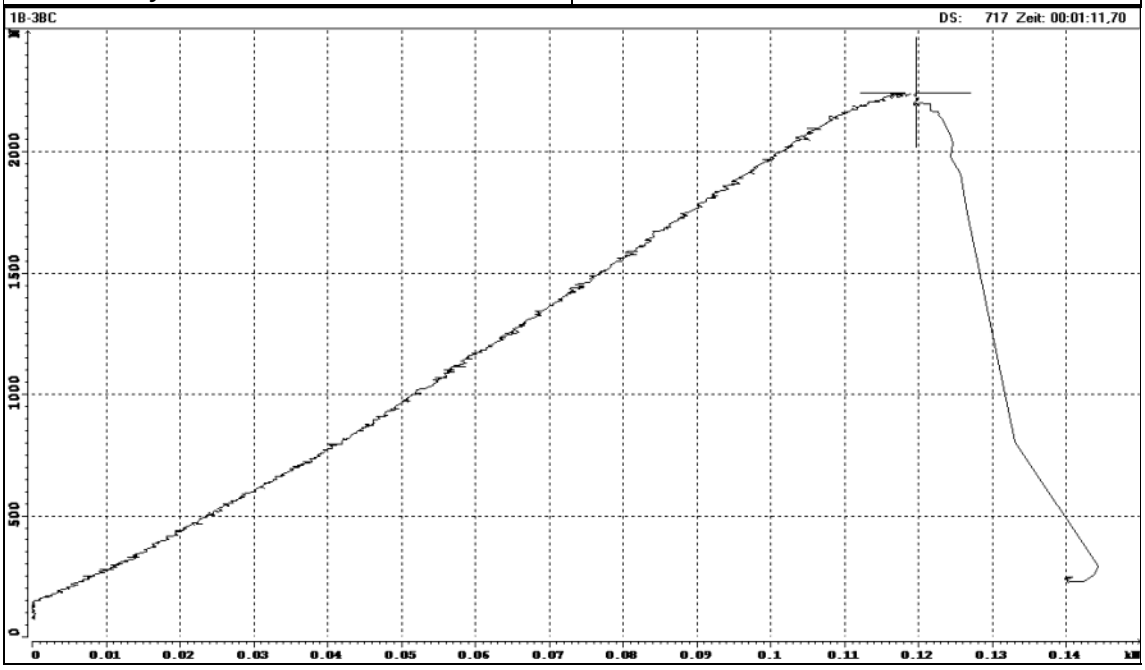

borehole:	KFM01B
sample - no.:	1B-4AB
mean depth, m:	429.97
diameter, mm:	50.8
initial crack length, mm:	6.8
max. Force, kN:	2.12
KIC, MN/m3/2:	1.83
date of testing:	23.07.04
operated by	F. Seebald, U. Weber
checked by	U. Weber

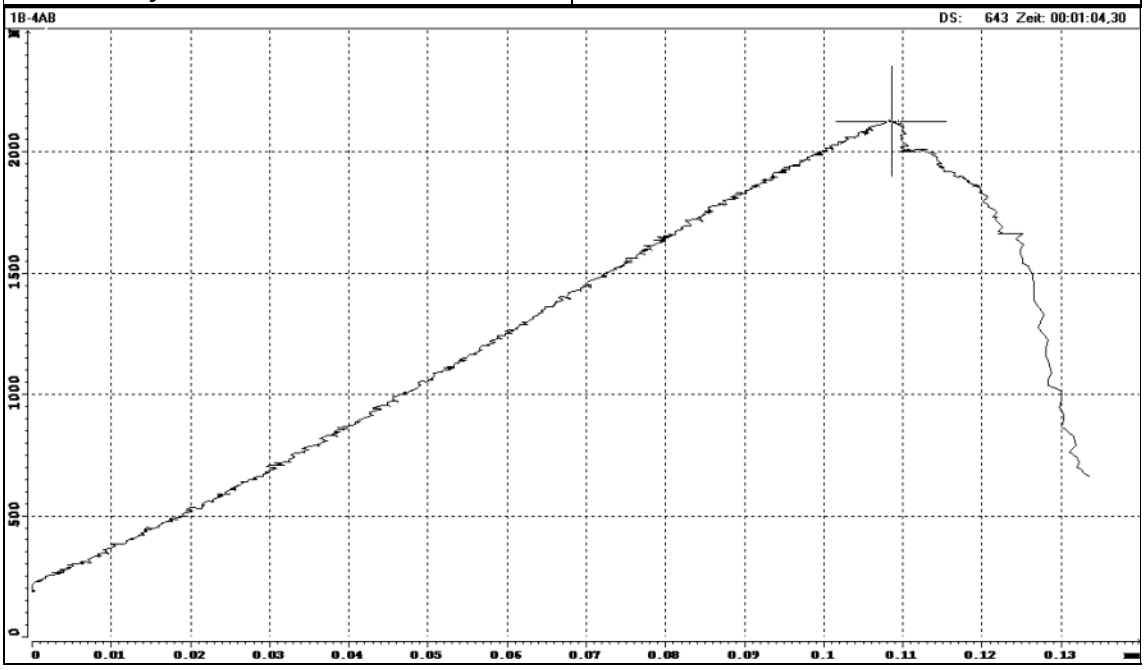

borehole:	KFM01B
sample - no.:	1B-4BC
mean depth, m:	429.97
diameter, mm:	50.8
initial crack length, mm:	6.8
max. Force, kN:	2.22
KIC, MN/m3/2:	1.92
date of testing:	23.07.04
operated by	F. Seebald, U. Weber
checked by	U. Weber

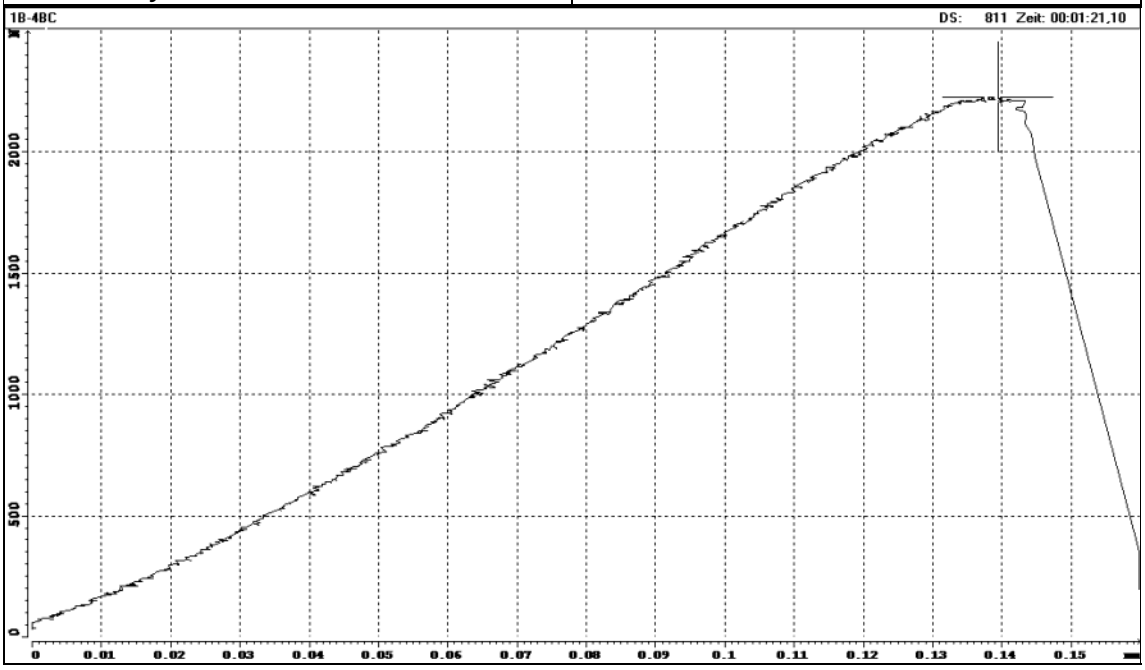

borehole:	KFM01B
sample - no.:	1B-5AB
mean depth, m:	430.43
diameter, mm:	50.8
initial crack length, mm:	7.5
max. Force, kN:	3.06
KIC, MN/m3/2:	2.76
date of testing:	23.07.04
operated by	F. Seebald, U. Weber
checked by	U. Weber

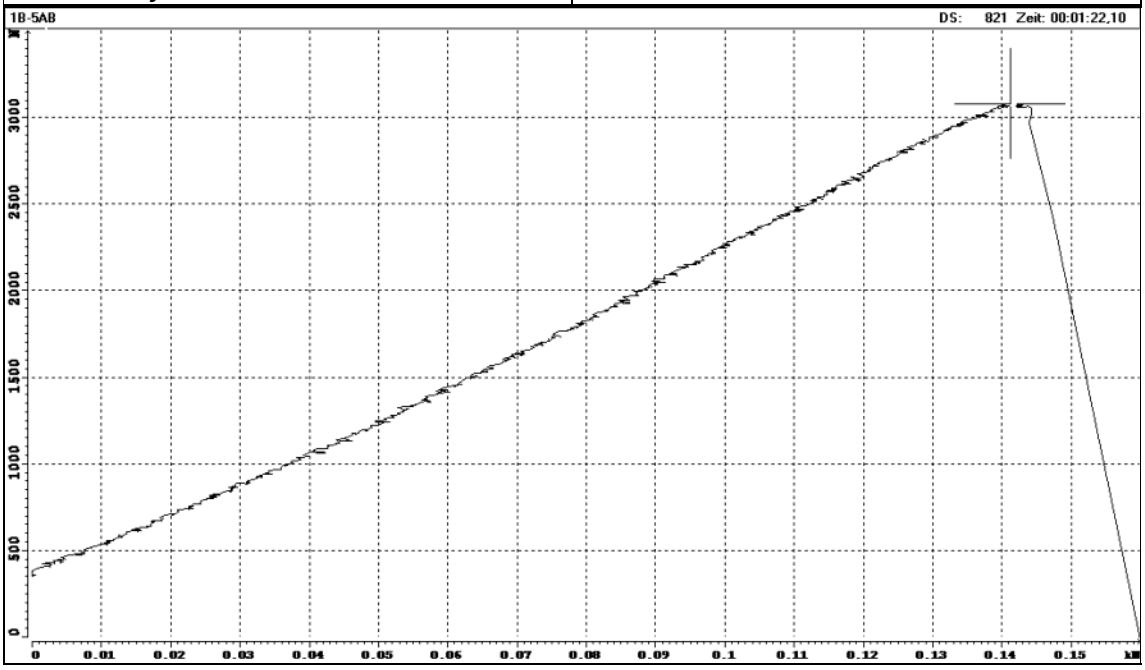

borehole:	KFM01B
sample - no.:	1B-5BC
mean depth, m:	430.43
diameter, mm:	50.8
initial crack length, mm:	6.9
max. Force, kN:	2.21
KIC, MN/m3/2:	1.92
date of testing:	23.07.04
operated by	F. Seebald, U. Weber
checked by	U. Weber

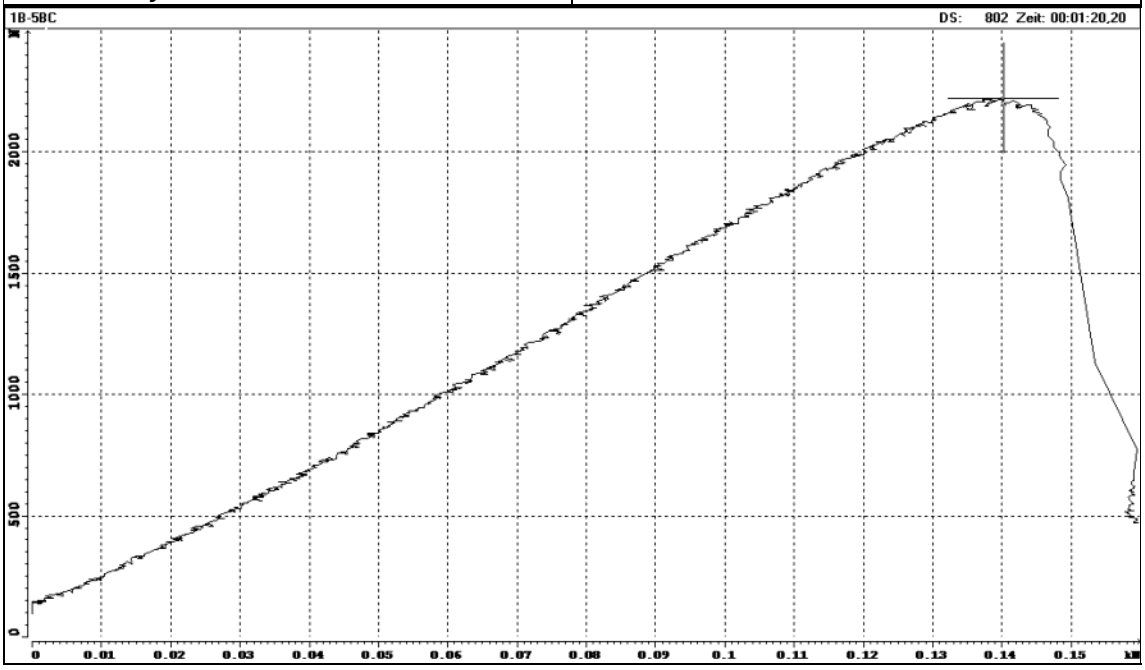

borehole:	KFM01B
sample - no.:	1B-6AB
mean depth, m:	455.13
diameter, mm:	50.8
initial crack length, mm:	6.5
max. Force, kN:	2.48
KIC, MN/m3/2:	2.10
date of testing:	23.07.04
operated by	F. Seebald, U. Weber
checked by	U. Weber

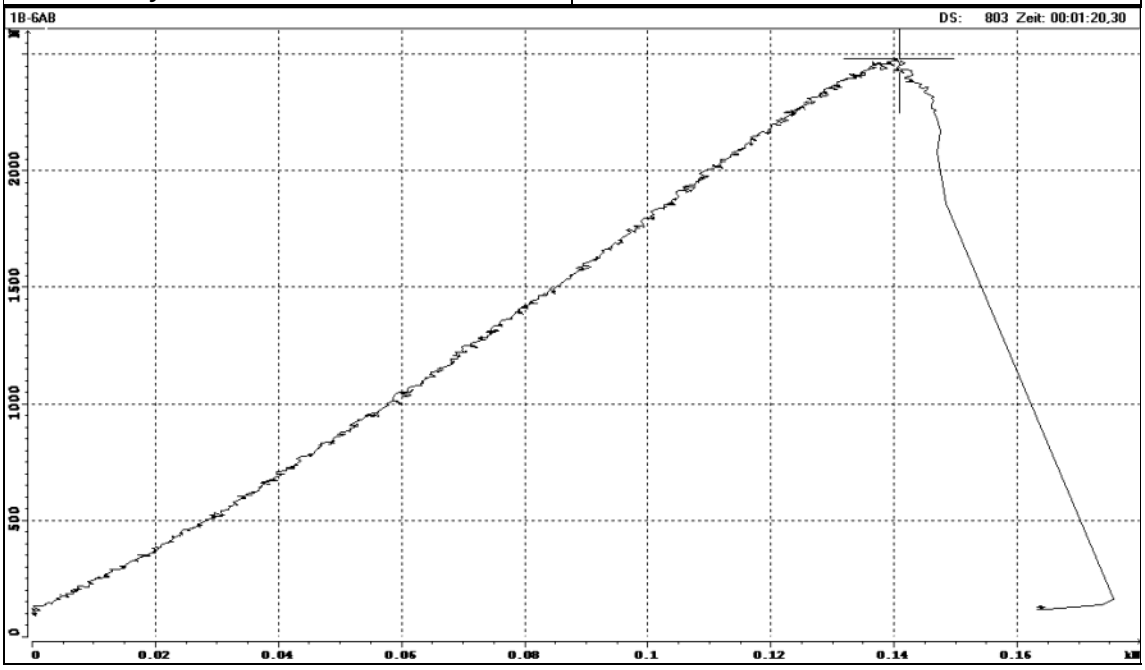

borehole:	KFM01B
sample - no.:	1B-6BC
mean depth, m:	455.13
diameter, mm:	50.8
initial crack length, mm:	7.0
max. Force, kN:	2.30
KIC, MN/m3/2:	2.01
date of testing:	23.07.04
operated by	F. Seebald, U. Weber
checked by	U. Weber

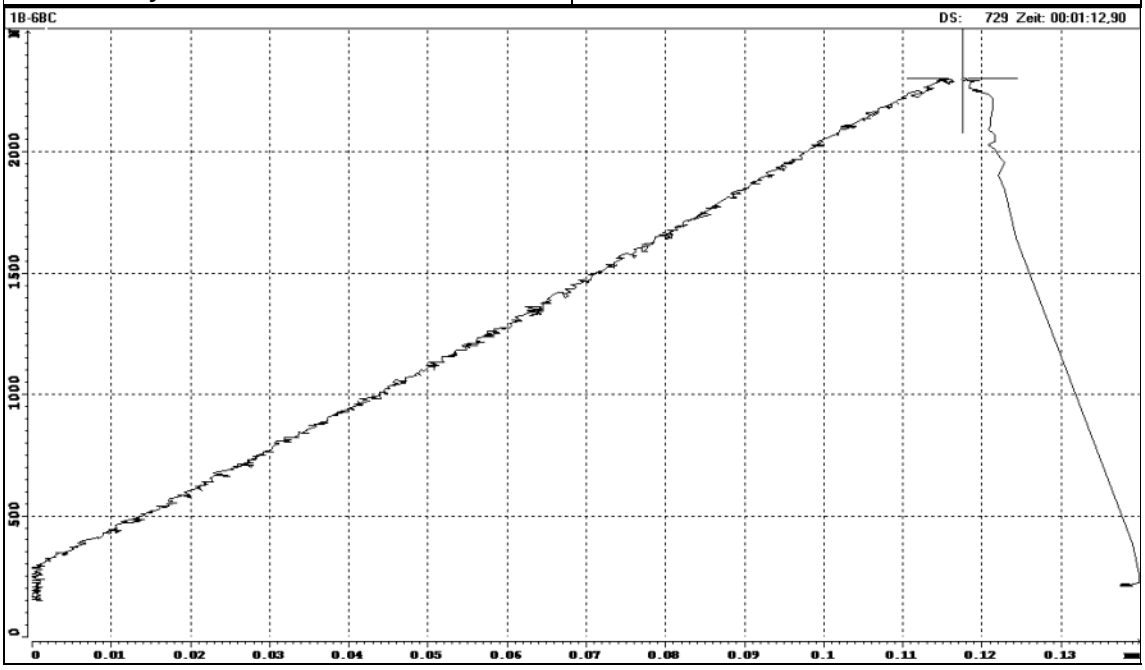

borehole:	KFM01B
sample - no.:	1B-7AB
mean depth, m:	456.20
diameter, mm:	50.7
initial crack length, mm:	7.3
max. Force, kN:	2.24
KIC, MN/m3/2:	2.01
date of testing:	23.07.04
operated by	F. Seebald, U. Weber
checked by	U. Weber

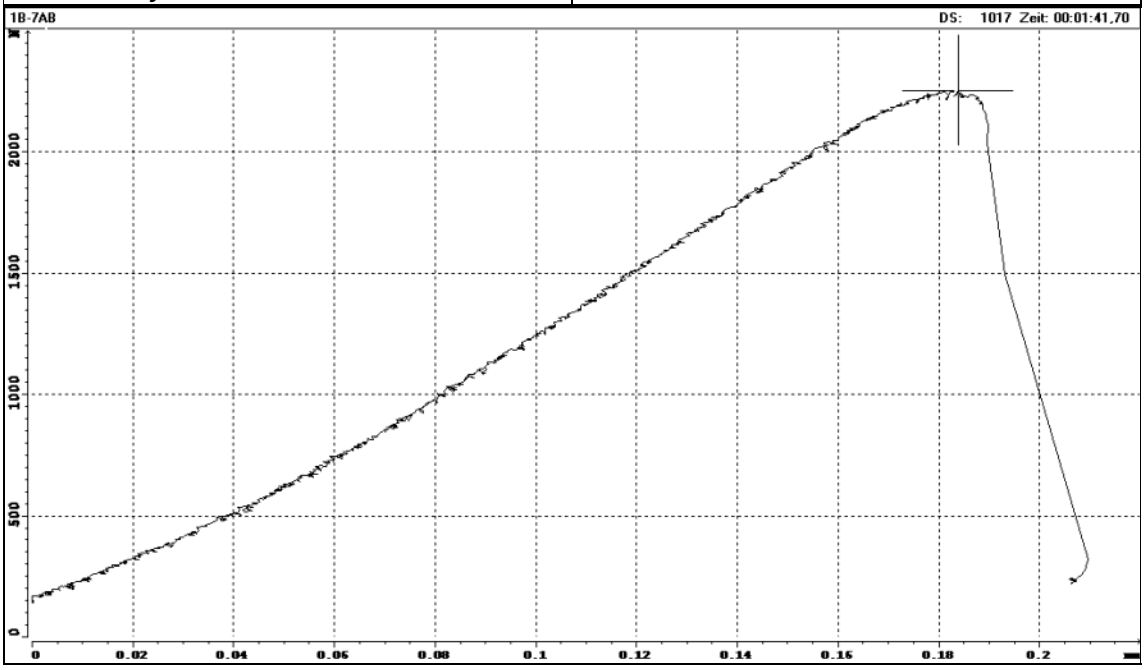

borehole:	KFM01B
sample - no.:	1B-7BC
mean depth, m:	456.20
diameter, mm:	50.7
initial crack length, mm:	7.4
max. Force, kN:	2.37
KIC, MN/m3/2:	2.14
date of testing:	23.07.04
operated by	F. Seebald, U. Weber
checked by	U. Weber

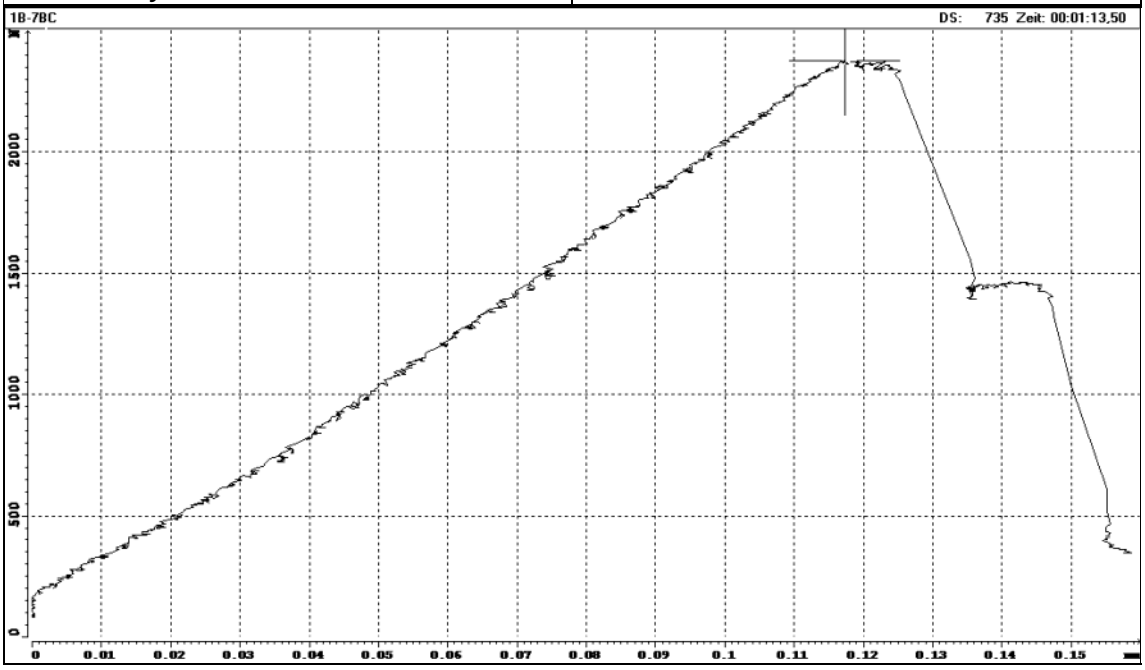

borehole:	KFM02A
sample - no.:	2A-1AB
mean depth, m:	220.84
diameter, mm:	50.9
initial crack length, mm:	7.3
max. Force, kN:	2.39
KIC, MN/m3/2:	2.12
date of testing:	23.07.04
operated by	F. Seebald, U. Weber
checked by	U. Weber

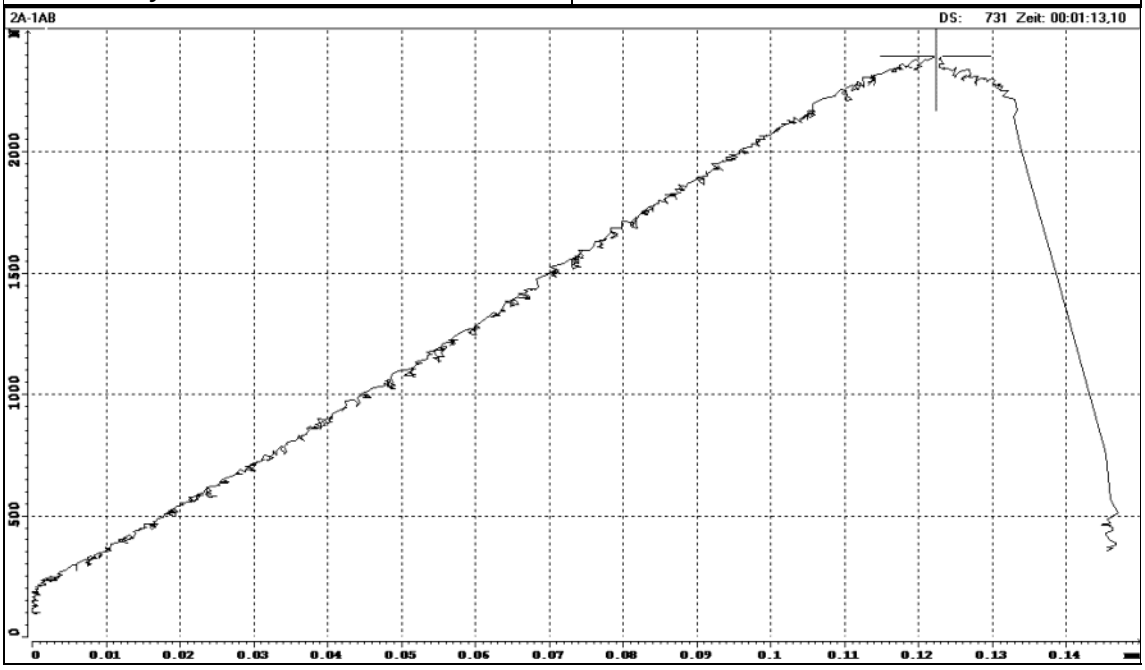

borehole:	KFM02A
sample - no.:	2A-1BC
mean depth, m:	220.84
diameter, mm:	50.9
initial crack length, mm:	7.5
max. Force, kN:	2.60
KIC, MN/m3/2:	2.34
date of testing:	23.07.04
operated by	F. Seebald, U. Weber
checked by	U. Weber

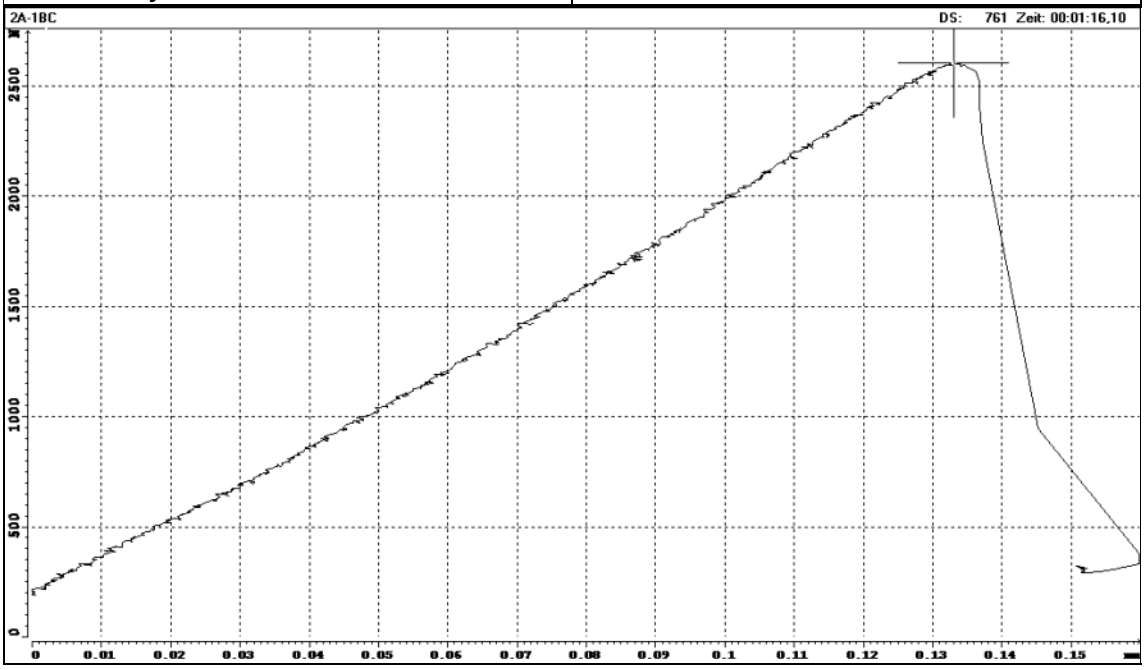

borehole:	KFM02A
sample - no.:	2A-2AB
mean depth, m:	226.04
diameter, mm:	50.9
initial crack length, mm:	7.2
max. Force, kN:	2.70
KIC, MN/m3/2:	2.38
date of testing:	23.07.04
operated by	F. Seebald, U. Weber
checked by	U. Weber

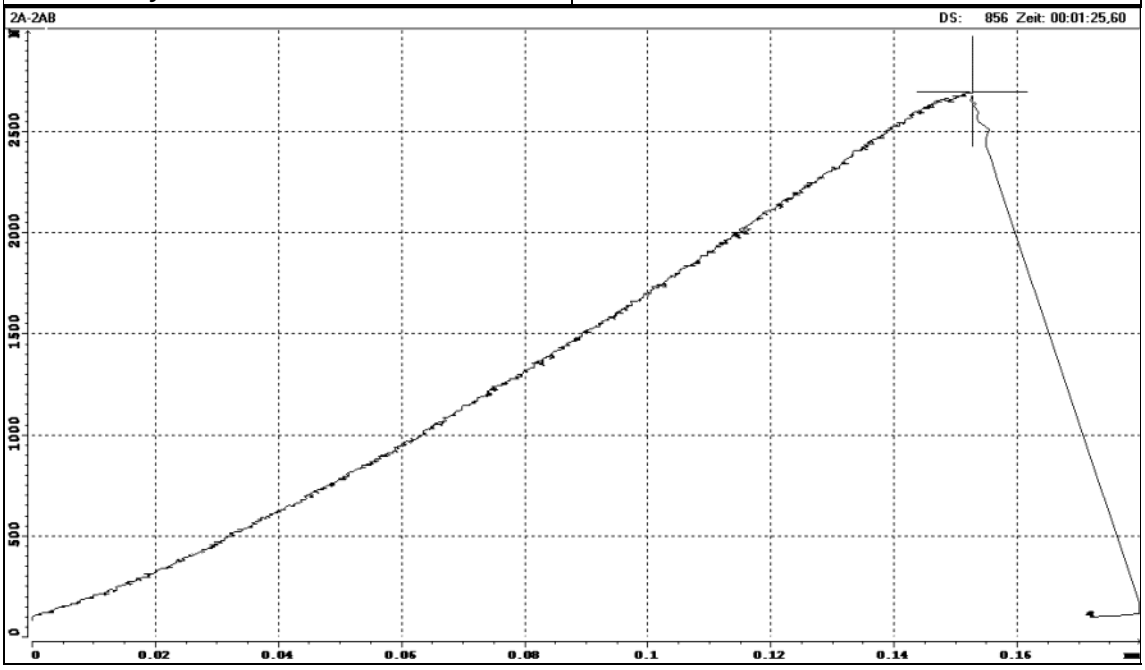

borehole:	KFM02A
sample - no.:	2A-2BC
mean depth, m:	226.04
diameter, mm:	50.9
initial crack length, mm:	7.6
max. Force, kN:	2.53
KIC, MN/m3/2:	2.29
date of testing:	23.07.04
operated by	F. Seebald, U. Weber
checked by	U. Weber

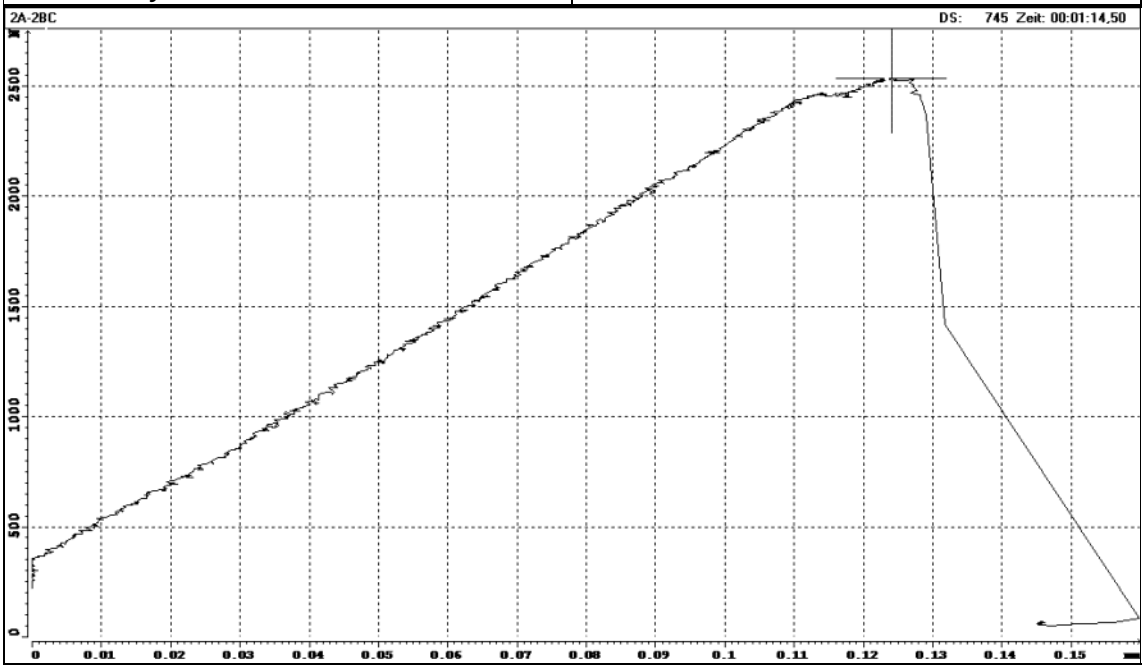

borehole:	KFM02A
sample - no.:	2A-3AB
mean depth, m:	396.04
diameter, mm:	50.8
initial crack length, mm:	6.8
max. Force, kN:	2.48
KIC, MN/m3/2:	2.14
date of testing:	23.07.04
operated by	F. Seebald, U. Weber
checked by	U. Weber

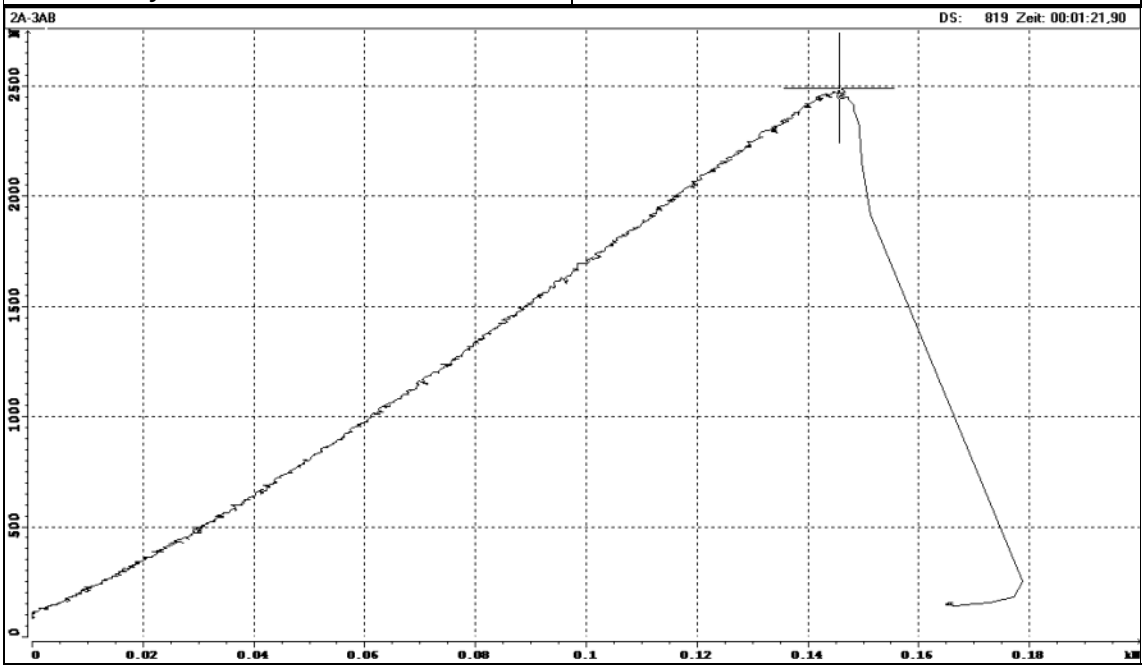

borehole:	KFM02A
sample - no.:	2A-3BC
mean depth, m:	396.04
diameter, mm:	50.7
initial crack length, mm:	7.3
max. Force, kN:	2.43
KIC, MN/m3/2:	2.18
date of testing:	23.07.04
operated by	F. Seebald, U. Weber
checked by	U. Weber

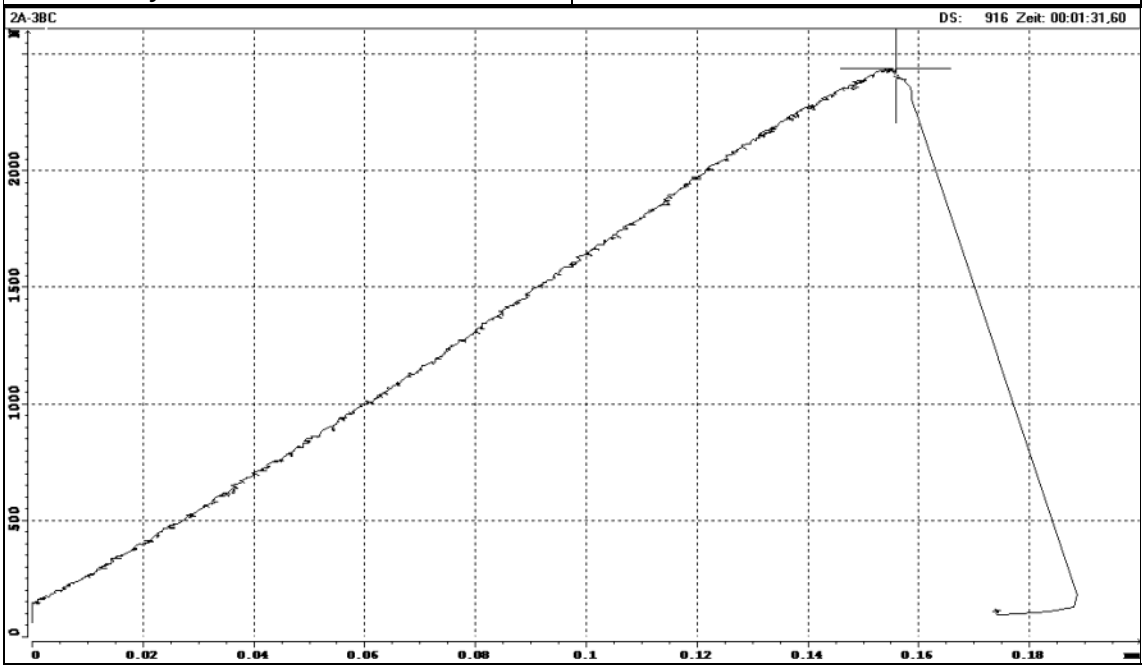

borehole:	KFM02A
sample - no.:	2A-4AB
mean depth, m:	414.07
diameter, mm:	50.8
initial crack length, mm:	7.2
max. Force, kN:	2.55
KIC, MN/m3/2:	2.26
date of testing:	23.07.04
operated by	F. Seebald, U. Weber
checked by	U. Weber

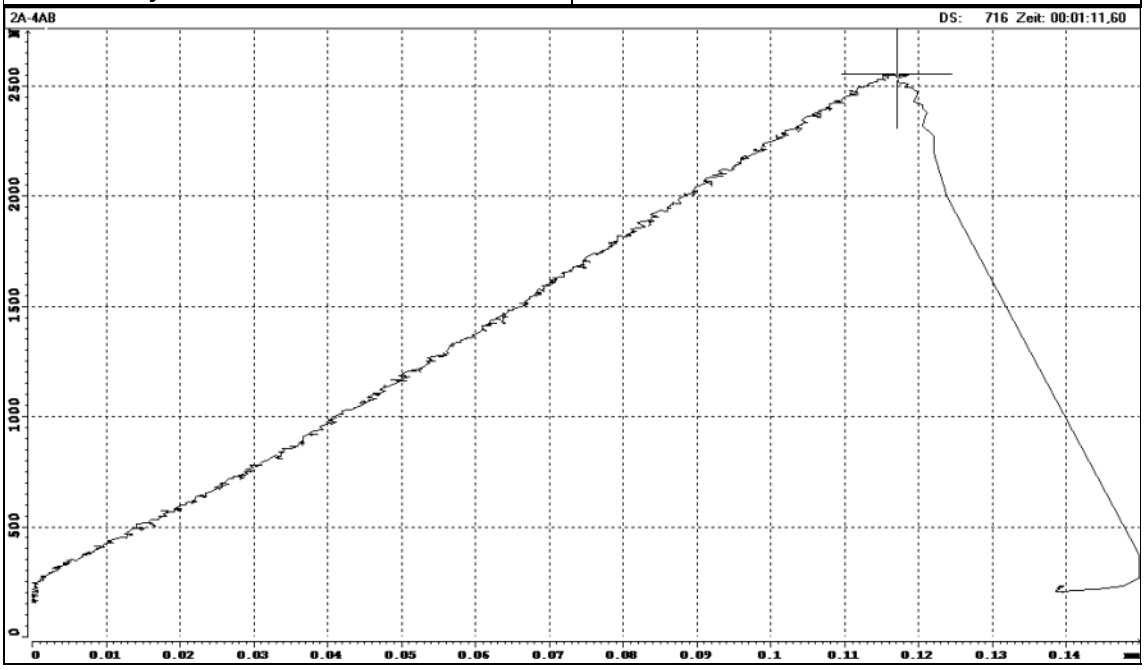

borehole:	KFM02A
sample - no.:	2A-4BC
mean depth, m:	414.07
diameter, mm:	50.8
initial crack length, mm:	7.1
max. Force, kN:	2.19
KIC, MN/m3/2:	1.93
date of testing:	23.07.04
operated by	F. Seebald, U. Weber
checked by	U. Weber

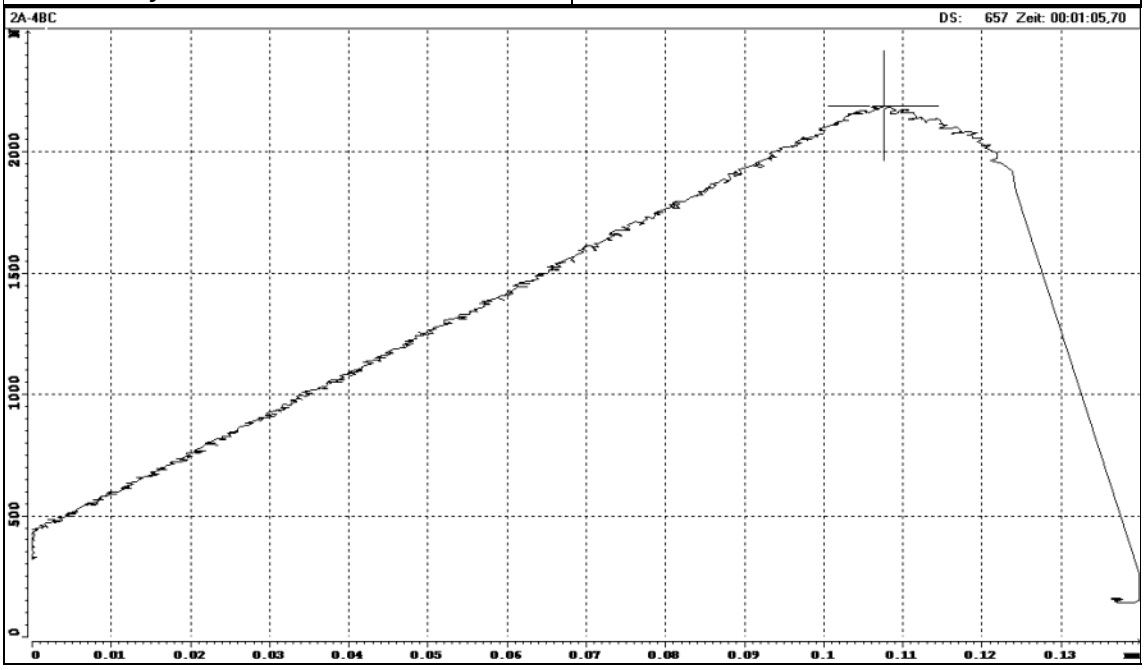

borehole:	KFM02A
sample - no.:	2A-5AB
mean depth, m:	451.32
diameter, mm:	50.7
initial crack length, mm:	7.2
max. Force, kN:	2.60
KIC, MN/m3/2:	2.31
date of testing:	23.07.04
operated by	F. Seebald, U. Weber
checked by	U. Weber

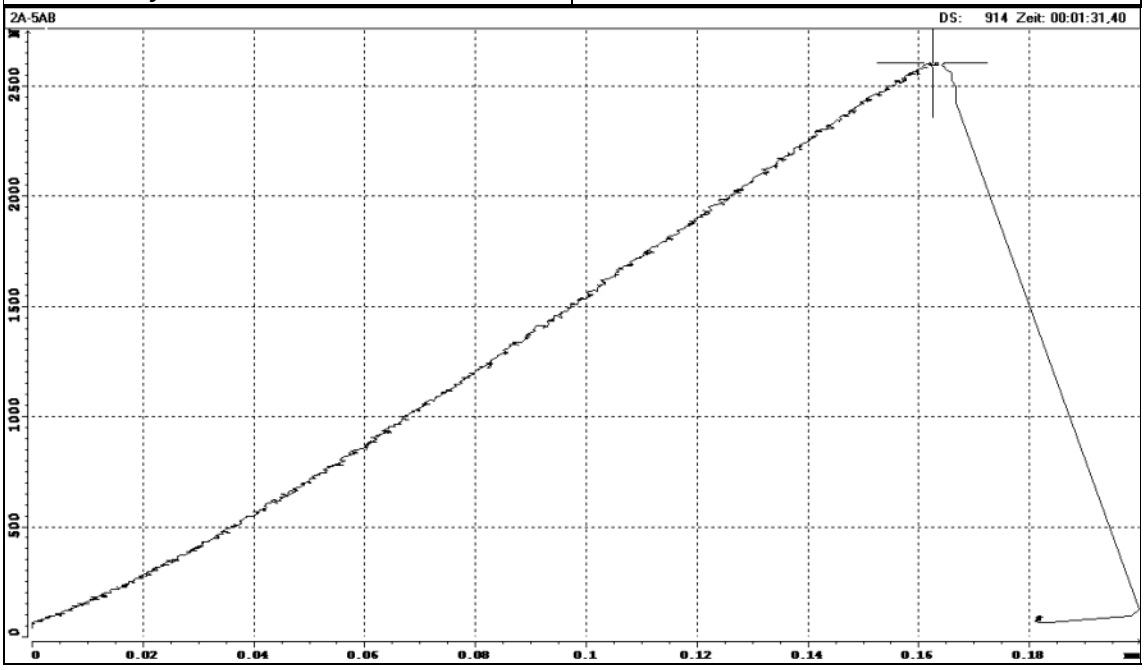

borehole:	KFM02A
sample - no.:	2A-5BC
mean depth, m:	451.32
diameter, mm:	50.7
initial crack length, mm:	7.0
max. Force, kN:	2.34
KIC, MN/m3/2:	2.05
date of testing:	23.07.04
operated by	F. Seebald, U. Weber
checked by	U. Weber

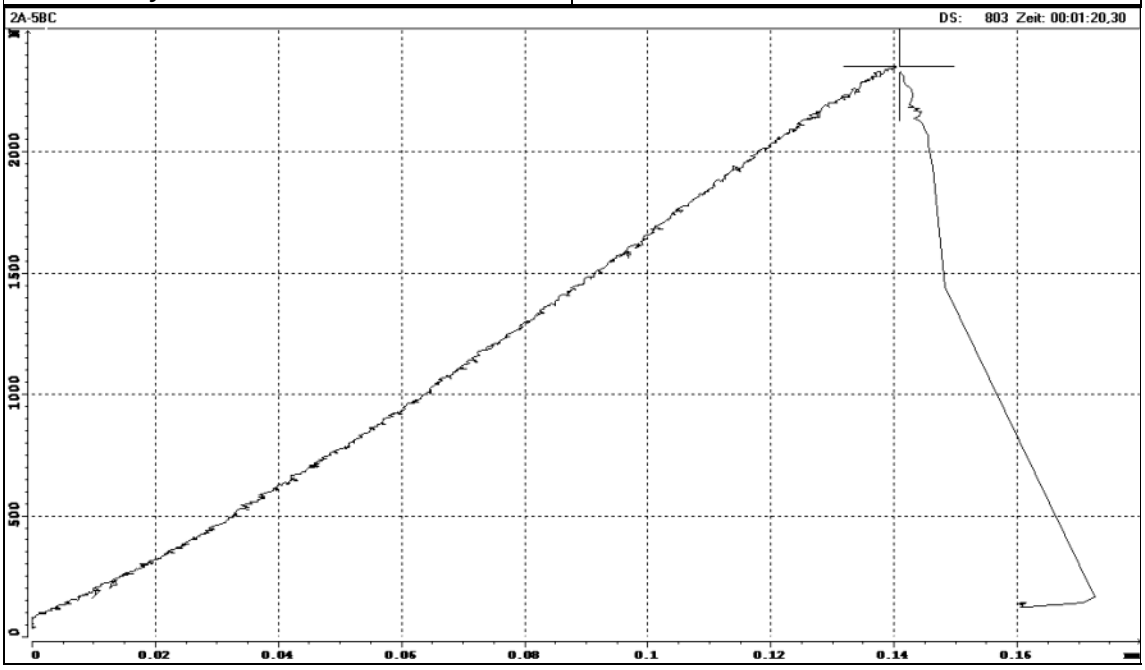

borehole:	KFM02A
sample - no.:	2A-6AB
mean depth, m:	554.39
diameter, mm:	50.6
initial crack length, mm:	7.4
max. Force, kN:	2.59
KIC, MN/m3/2:	2.34
date of testing:	23.07.04
operated by	F. Seebald, U. Weber
checked by	U. Weber

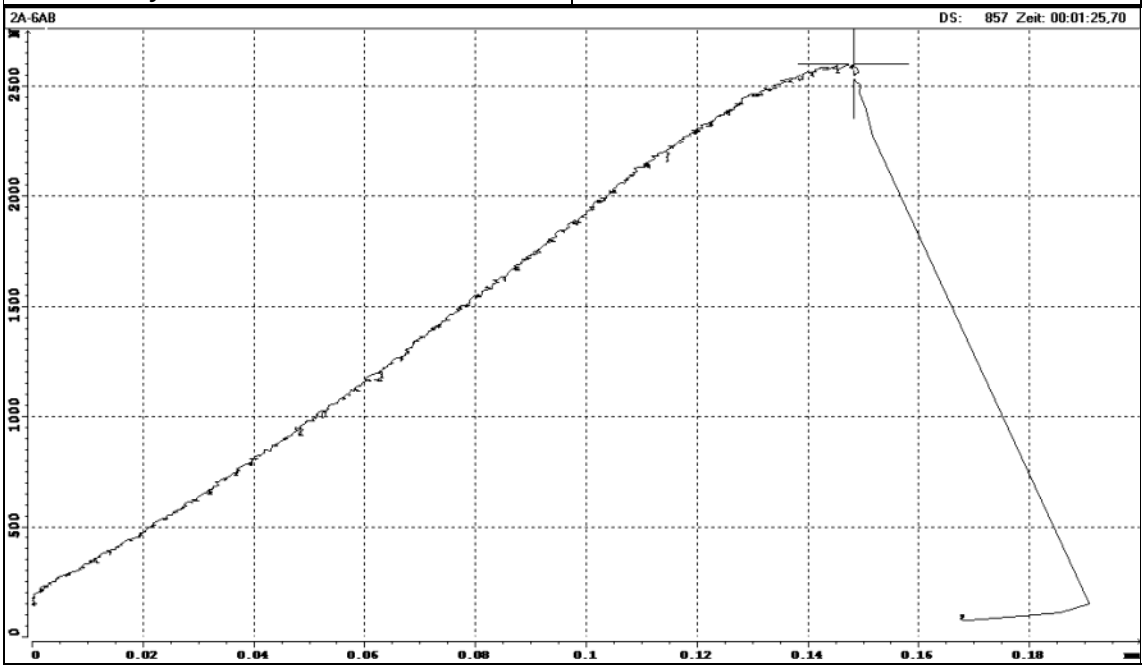

borehole:	KFM02A
sample - no.:	2A-6BC
mean depth, m:	554.39
diameter, mm:	50.8
initial crack length, mm:	6.5
max. Force, kN:	-
KIC, MN/m3/2:	-
date of testing:	23.07.04
operated by	F. Seebald, U. Weber
checked by	U. Weber

sample broken during set-up, no test record

borehole:	KFM02A
sample - no.:	2A-7AB
mean depth, m:	594.38
diameter, mm:	50.9
initial crack length, mm:	7.0
max. Force, kN:	2.50
KIC, MN/m3/2:	2.18
date of testing:	23.07.04
operated by	F. Seebald, U. Weber
checked by	U. Weber

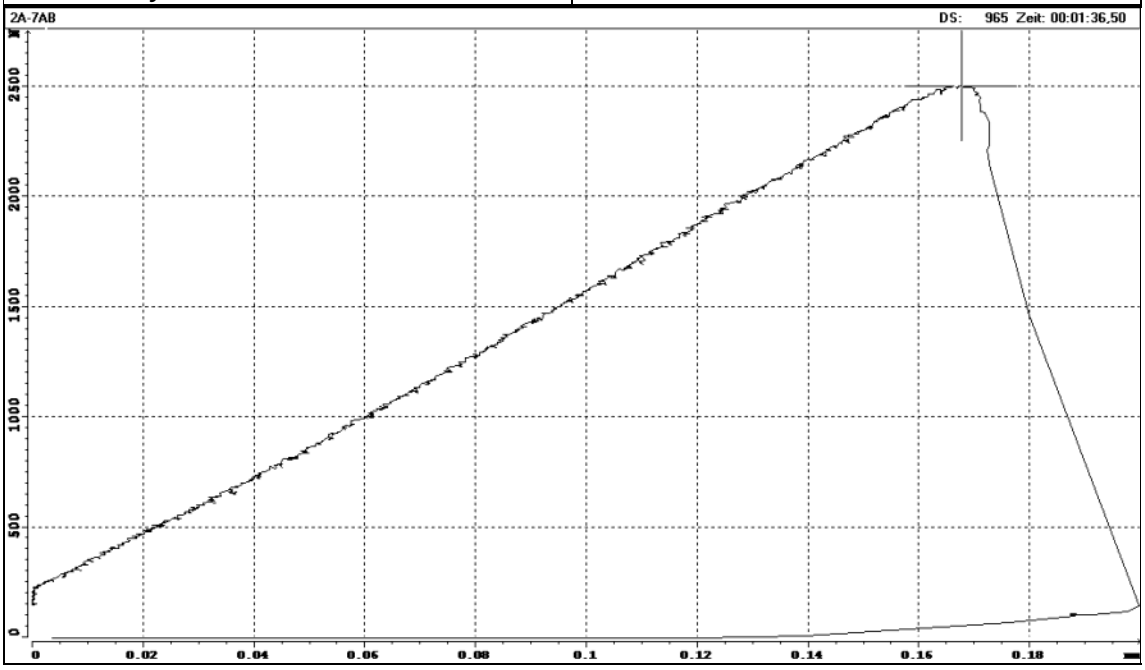

borehole:	KFM02A
sample - no.:	2A-7BC
mean depth, m:	594.38
diameter, mm:	50.8
initial crack length, mm:	6.9
max. Force, kN:	2.40
KIC, MN/m3/2:	2.09
date of testing:	23.07.04
operated by	F. Seebald, U. Weber
checked by	U. Weber

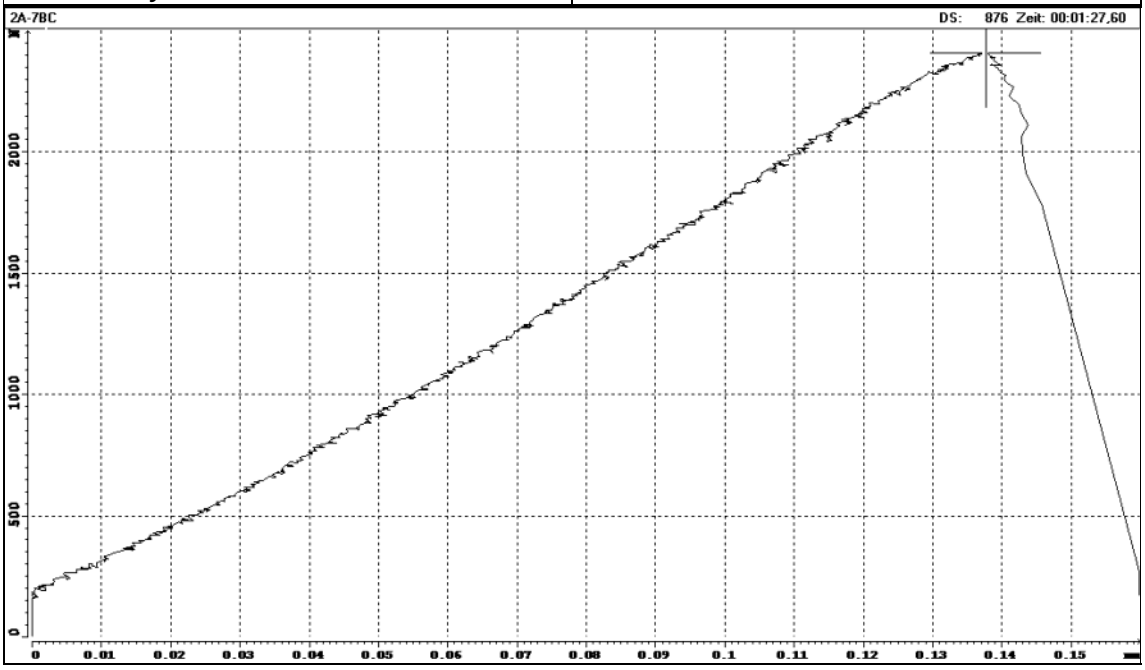

borehole:	KFM02A
sample - no.:	2A-8AB
mean depth, m:	602.92
diameter, mm:	51.0
initial crack length, mm:	6.7
max. Force, kN:	2.53
KIC, MN/m3/2:	2.15
date of testing:	23.07.04
operated by	F. Seebald, U. Weber
checked by	U. Weber

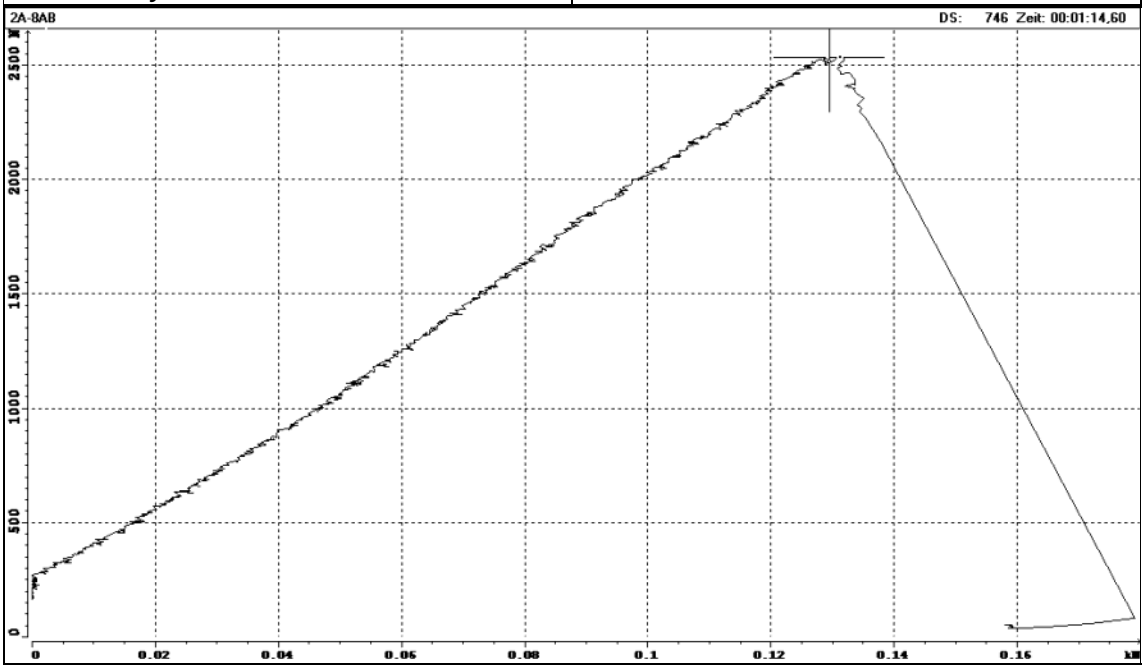

borehole:	KFM02A
sample - no.:	2A-8BC
mean depth, m:	602.92
diameter, mm:	51.0
initial crack length, mm:	7.3
max. Force, kN:	2.59
KIC, MN/m3/2:	2.29
date of testing:	23.07.04
operated by	F. Seebald, U. Weber
checked by	U. Weber

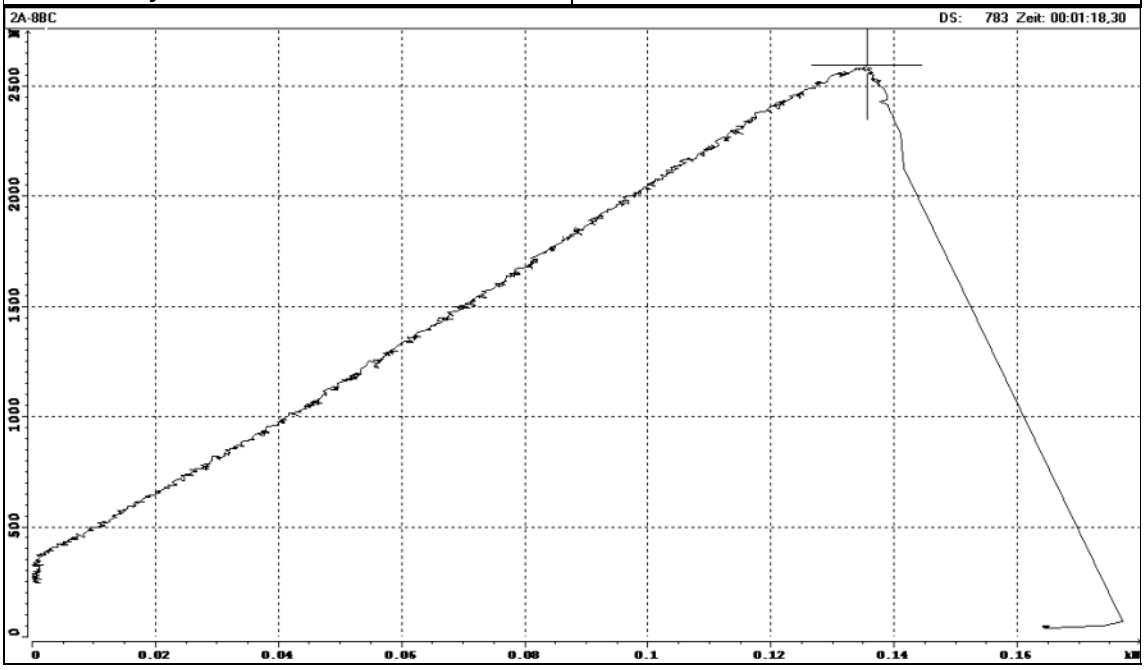

borehole:	KFM02A
sample - no.:	2A-9AB
mean depth, m:	699.83
diameter, mm:	50.8
initial crack length, mm:	7.0
max. Force, kN:	2.53
KIC, MN/m3/2:	2.21
date of testing:	23.07.04
operated by	F. Seebald, U. Weber
checked by	U. Weber

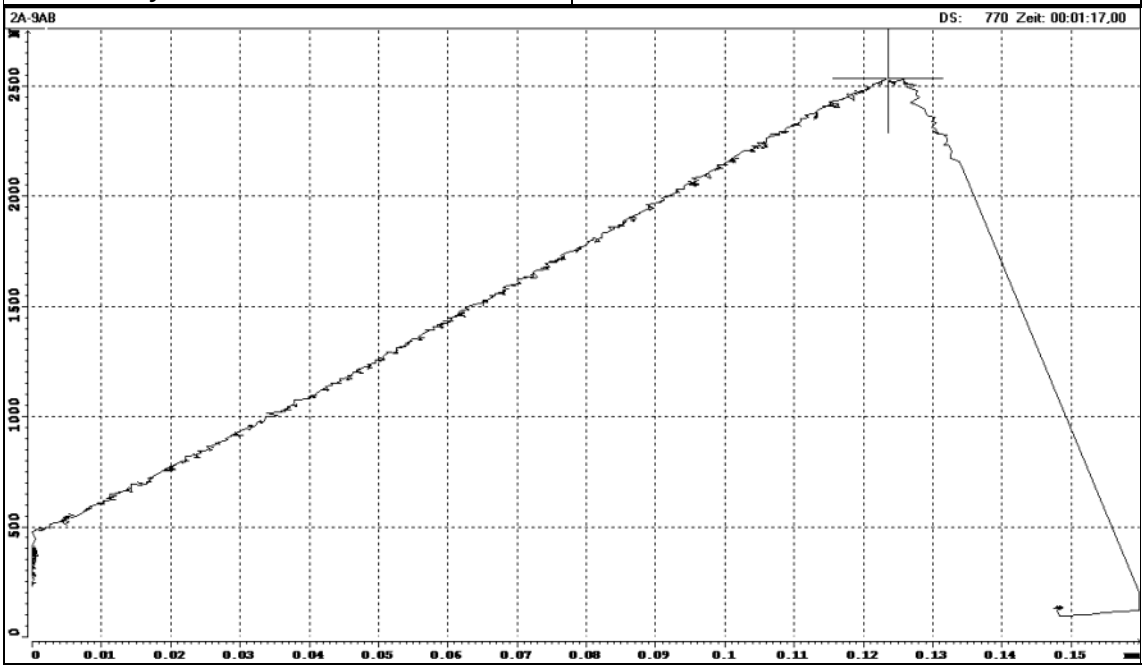

borehole:	KFM02A
sample - no.:	2A-9BC
mean depth, m:	699.83
diameter, mm:	50.8
initial crack length, mm:	7.0
max. Force, kN:	2.47
KIC, MN/m3/2:	2.16
date of testing:	23.07.04
operated by	F. Seebald, U. Weber
checked by	U. Weber

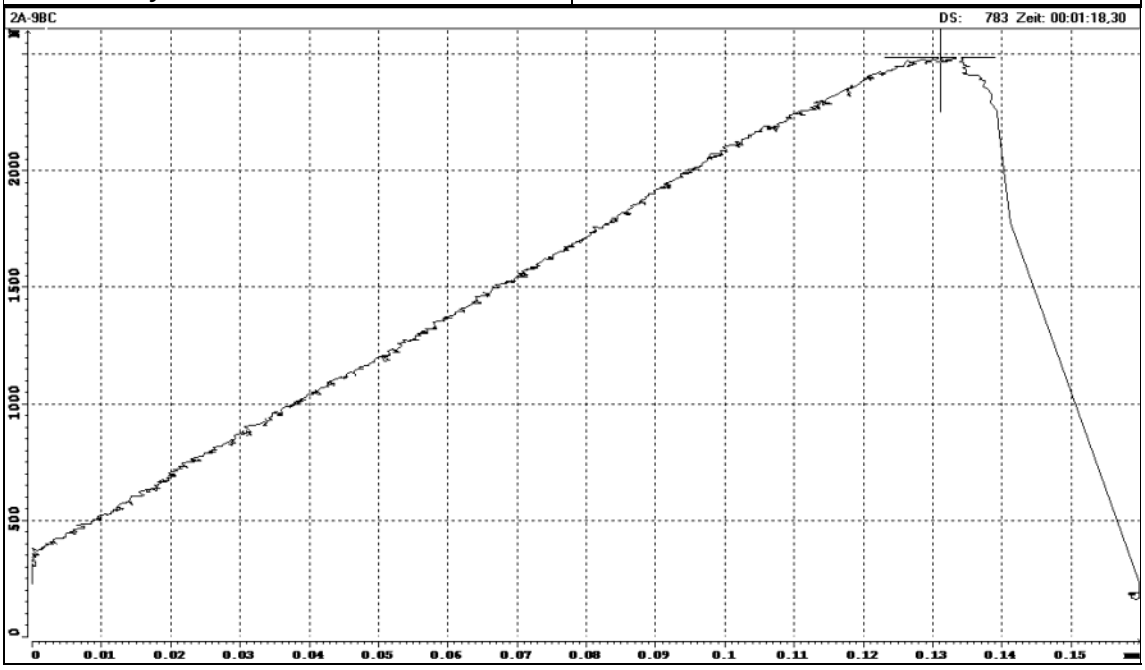

borehole:	KFM02A
sample - no.:	2A-10AB
mean depth, m:	702.82
diameter, mm:	50.8
initial crack length, mm:	6.8
max. Force, kN:	2.46
KIC, MN/m3/2:	2.12
date of testing:	23.07.04
operated by	F. Seebald, U. Weber
checked by	U. Weber

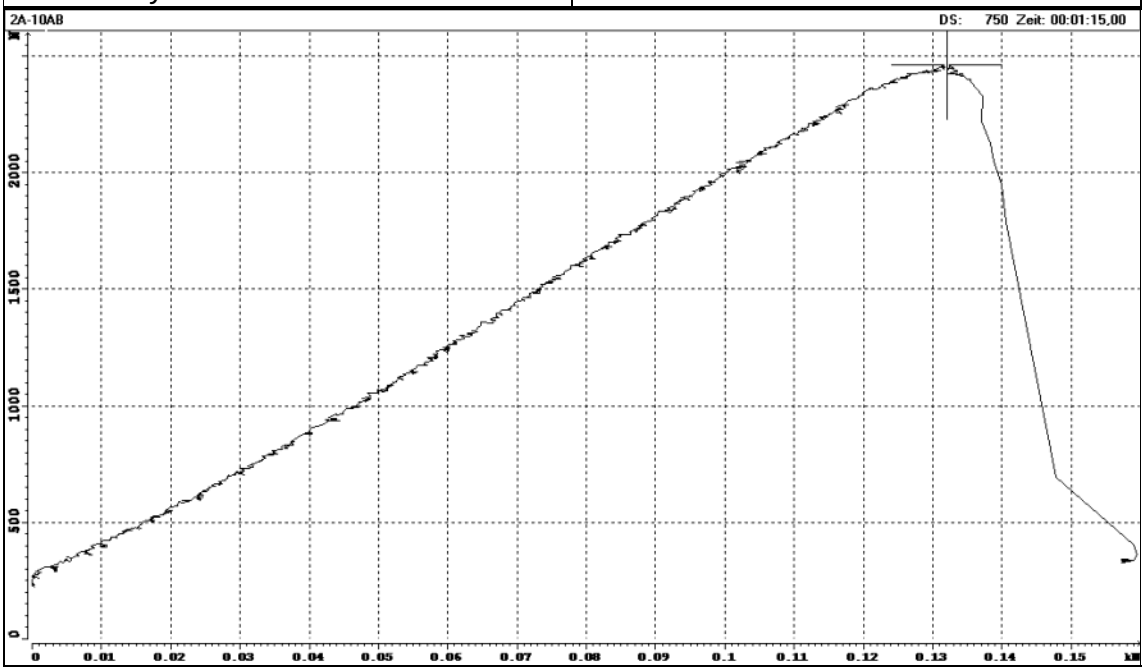

borehole:	KFM02A
sample - no.:	2A-10BC
mean depth, m:	702.82
diameter, mm:	50.8
initial crack length, mm:	7.0
max. Force, kN:	2.41
KIC, MN/m3/2:	2.11
date of testing:	23.07.04
operated by	F. Seebald, U. Weber
checked by	U. Weber

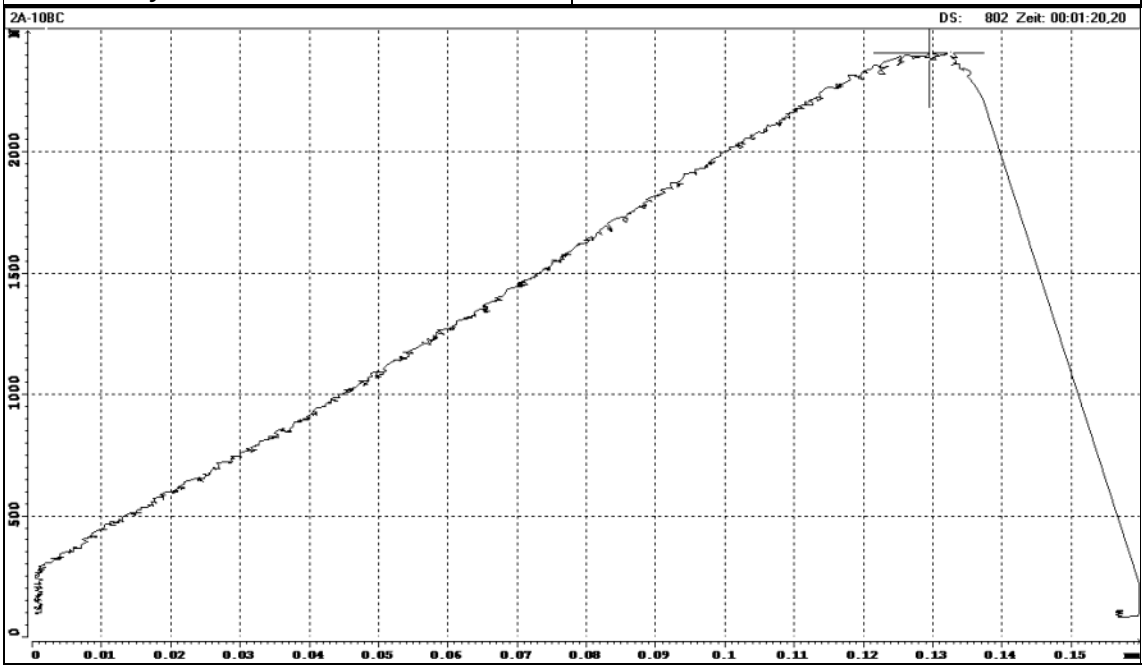

borehole:	KFM04A
sample - no.:	4A-1AB
mean depth, m:	192.28
diameter, mm:	50.8
initial crack length, mm:	6.7
max. Force, kN:	2.62
KIC, MN/m3/2:	2.25
date of testing:	23.07.04
operated by	F. Seebald, U. Weber
checked by	U. Weber

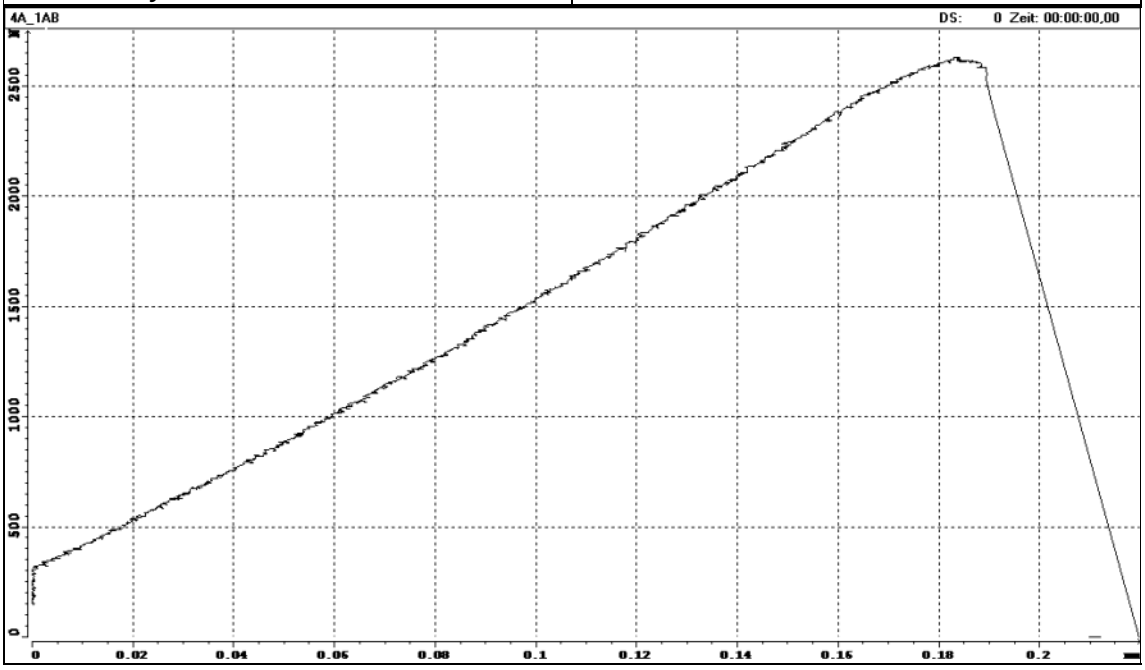

borehole:	KFM04A
sample - no.:	4A-1BC
mean depth, m:	192.28
diameter, mm:	50.8
initial crack length, mm:	6.6
max. Force, kN:	2.61
KIC, MN/m3/2:	2.22
date of testing:	23.07.04
operated by	F. Seebald, U. Weber
checked by	U. Weber

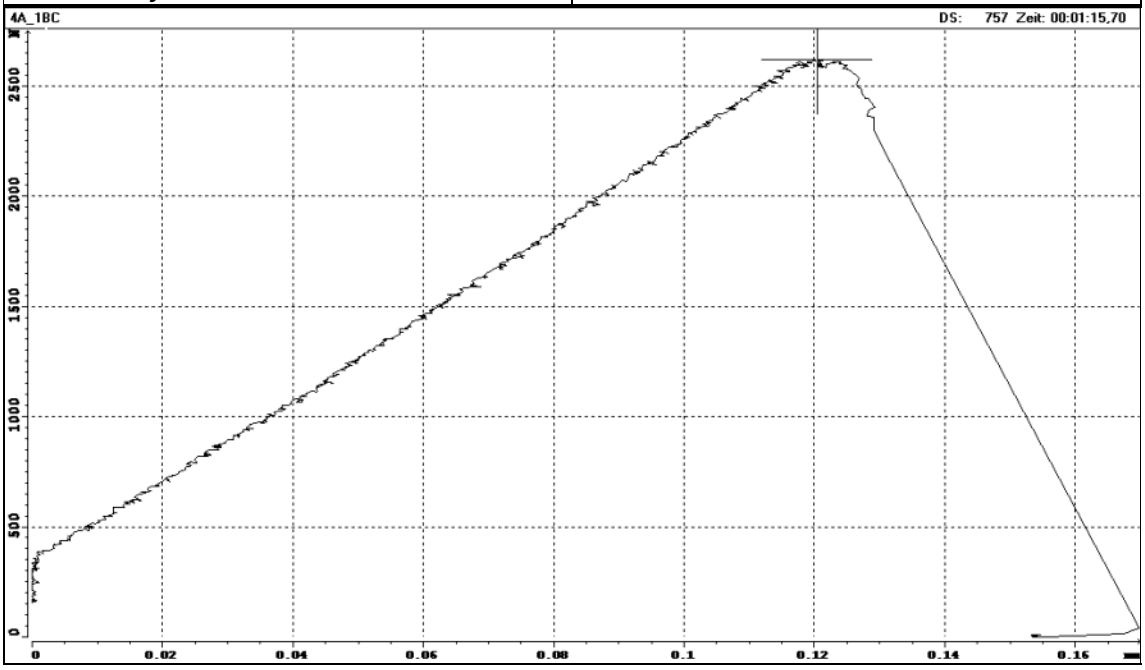

borehole:	KFM04A
sample - no.:	4A-2AB
mean depth, m:	192.61
diameter, mm:	50.8
initial crack length, mm:	6.9
max. Force, kN:	2.73
KIC, MN/m3/2:	2.37
date of testing:	23.07.04
operated by	F. Seebald, U. Weber
checked by	U. Weber

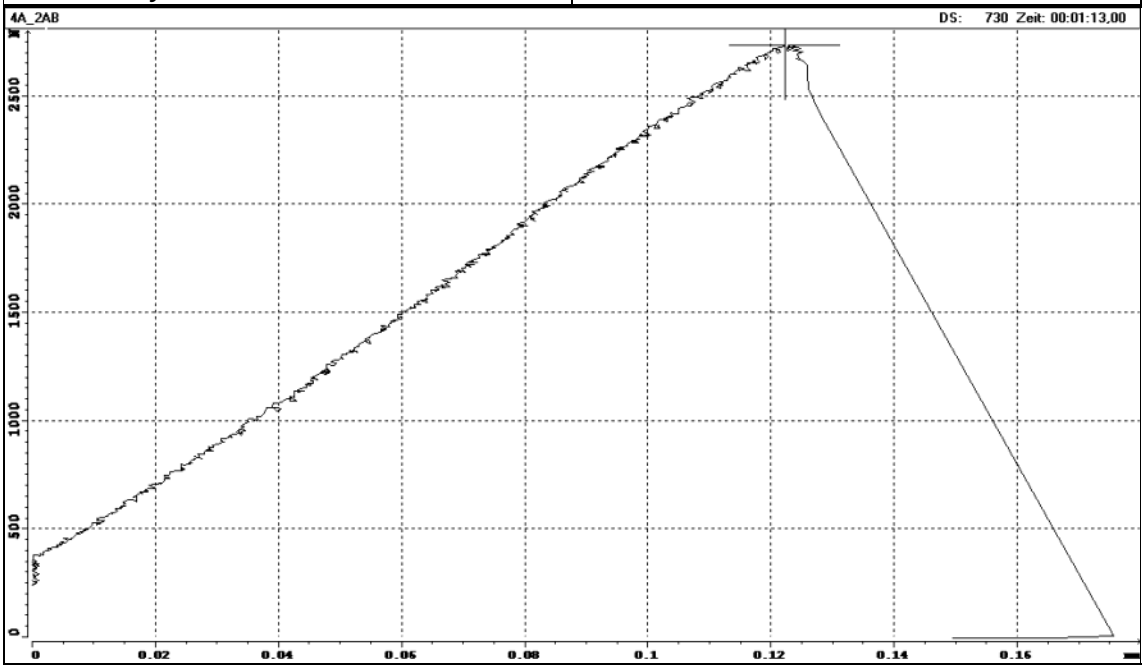

borehole:	KFM04A
sample - no.:	4A-2BC
mean depth, m:	192.61
diameter, mm:	50.7
initial crack length, mm:	7.0
max. Force, kN:	2.64
KIC, MN/m3/2:	2.32
date of testing:	23.07.04
operated by	F. Seebald, U. Weber
checked by	U. Weber

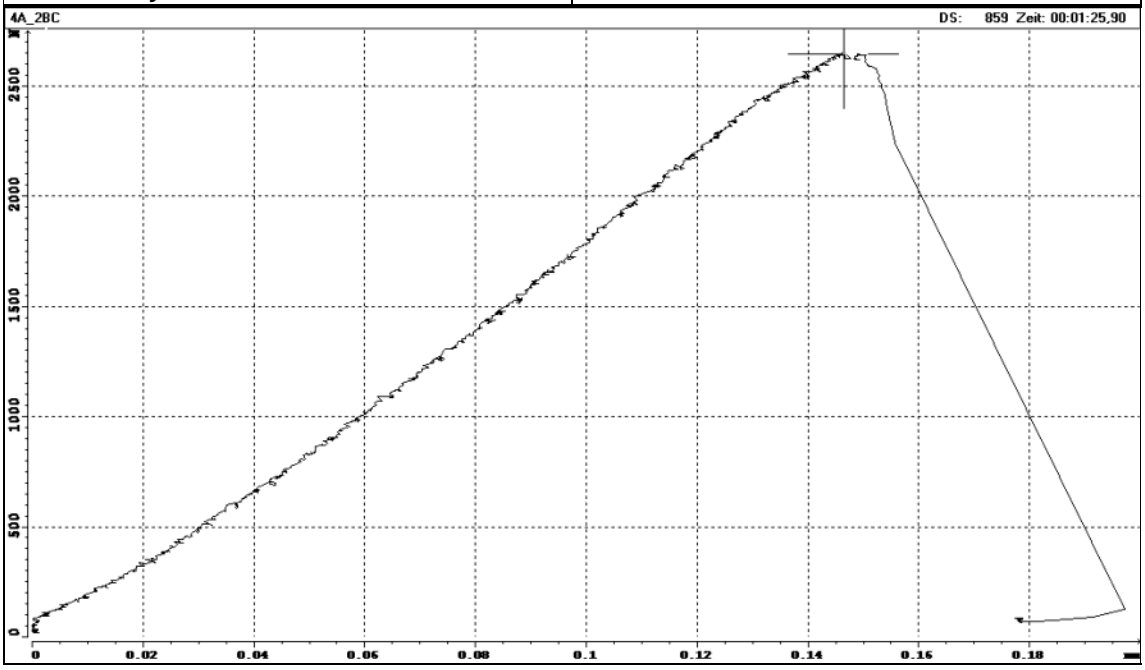

borehole:	KFM04A
sample - no.:	4A-3AB
mean depth, m:	260.31
diameter, mm:	50.7
initial crack length, mm:	6.7
max. Force, kN:	2.55
KIC, MN/m3/2:	2.24
date of testing:	23.07.04
operated by	F. Seebald, U. Weber
checked by	U. Weber

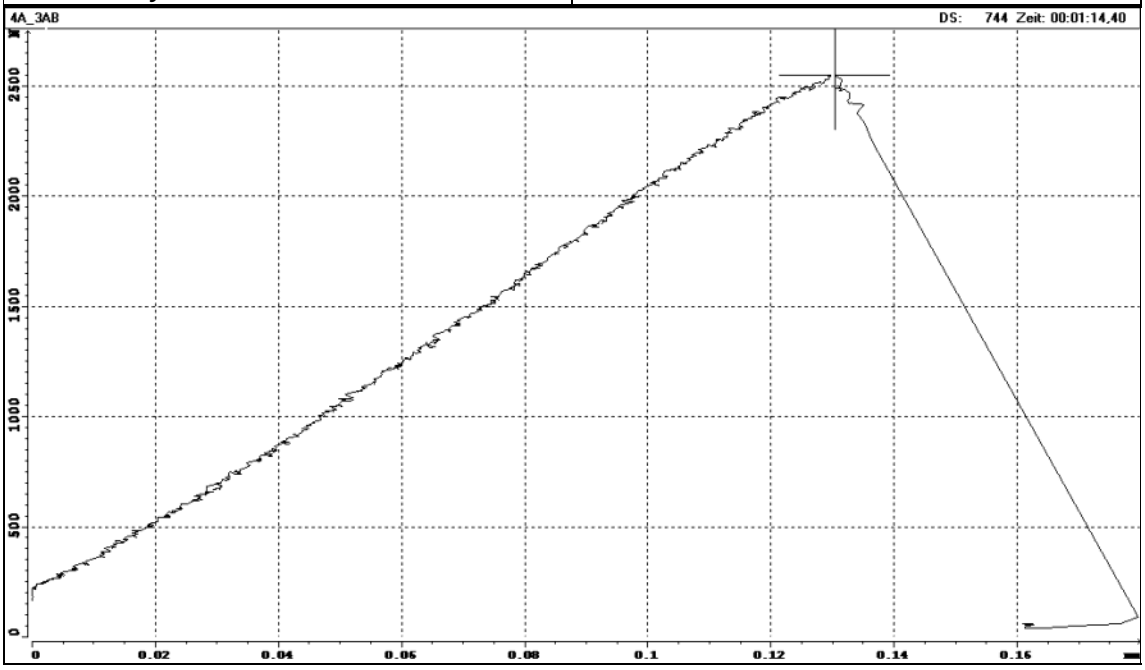

borehole:	KFM04A
sample - no.:	4A-3BC
mean depth, m:	260.31
diameter, mm:	50.7
initial crack length, mm:	0
max. Force, kN:	2.68
KIC, MN/m3/2:	1.43
date of testing:	23.07.04
operated by	F. Seebald, U. Weber
checked by	U. Weber

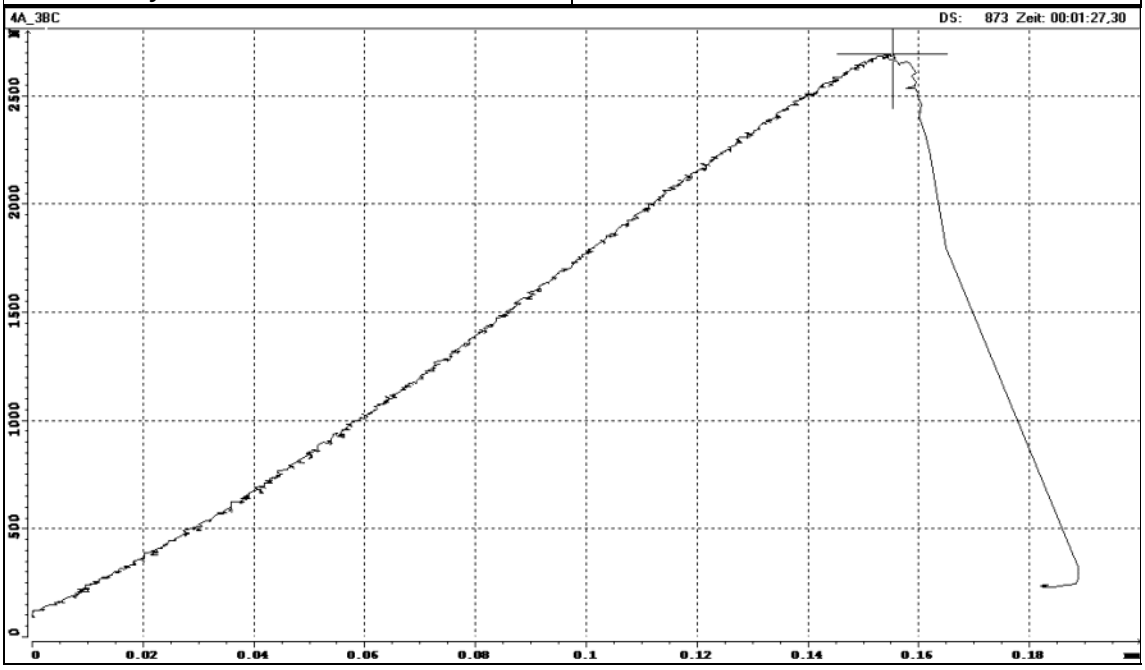

borehole:	KFM04A
sample - no.:	4A-4AB
mean depth, m:	527.63
diameter, mm:	50.7
initial crack length, mm:	6.6
max. Force, kN:	2.10
KIC, MN/m3/2:	1.80
date of testing:	23.07.04
operated by	F. Seebald, U. Weber
checked by	U. Weber

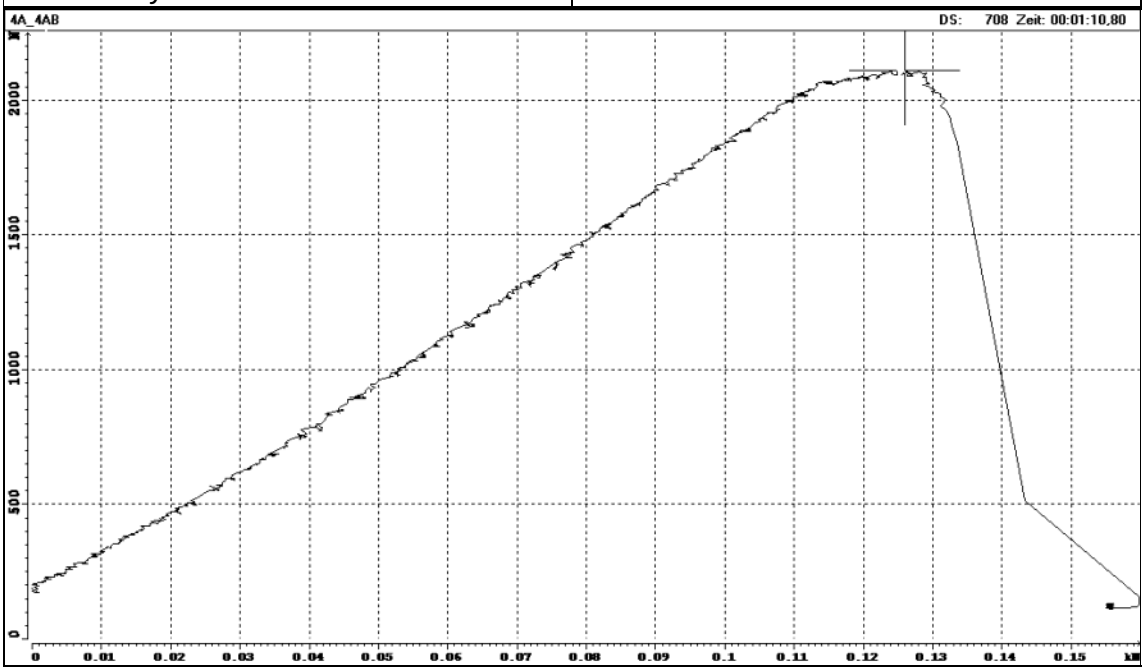

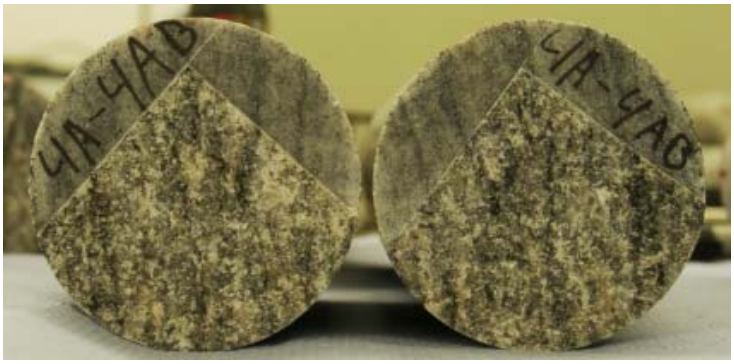

borehole:	KFM04A
sample - no.:	4A-4BC
mean depth, m:	527.63
diameter, mm:	50.6
initial crack length, mm:	7.2
max. Force, kN:	2.14
KIC, MN/m3/2:	1.91
date of testing:	23.07.04
operated by	F. Seebald, U. Weber
checked by	U. Weber

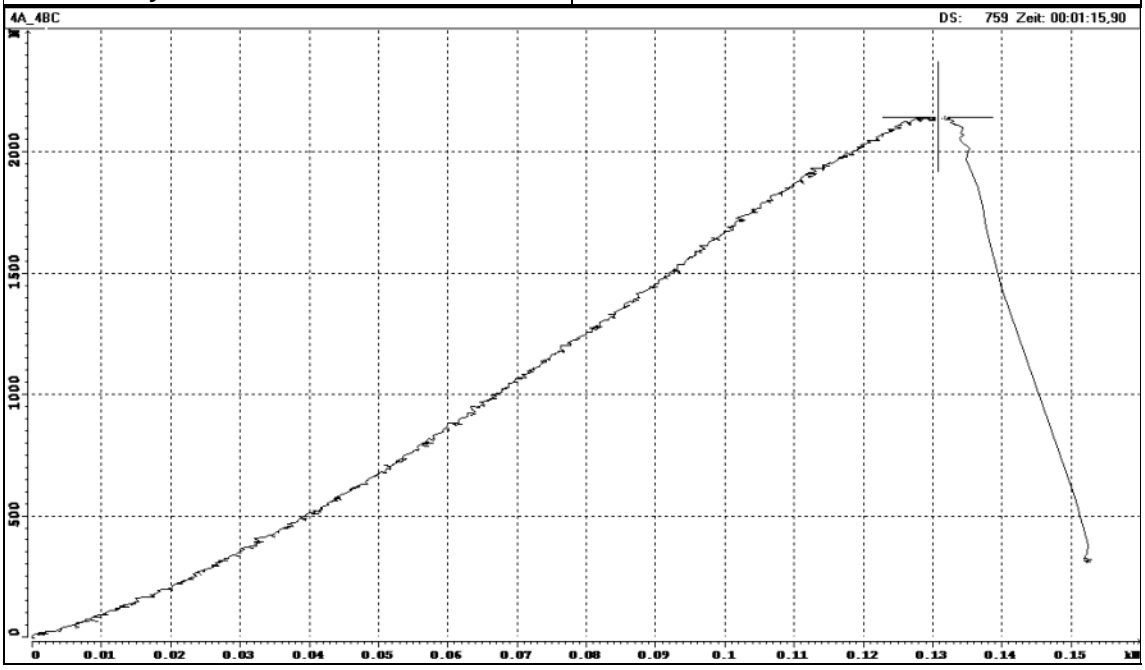

borehole:	KFM04A
sample - no.:	4A-5AB
mean depth, m:	527.97
diameter, mm:	50.6
initial crack length, mm:	7.2
max. Force, kN:	2.24
KIC, MN/m3/2:	2.00
date of testing:	23.07.04
operated by	F. Seebald, U. Weber
checked by	U. Weber

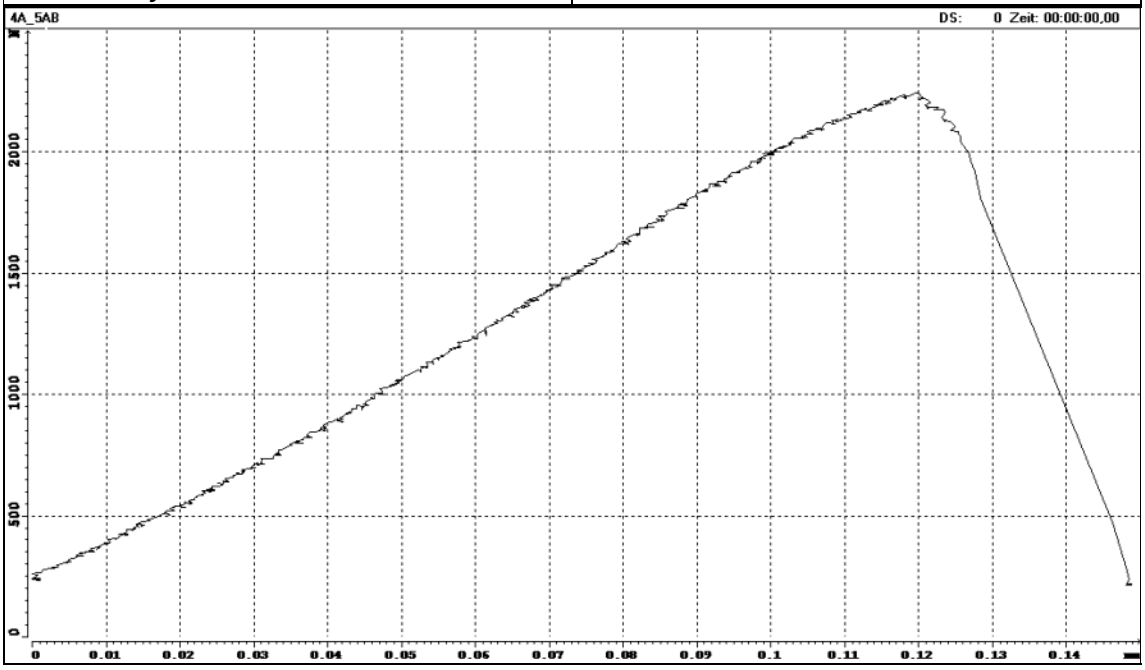

borehole:	KFM04A
sample - no.:	4A-5BC
mean depth, m:	527.97
diameter, mm:	50.6
initial crack length, mm:	7.0
max. Force, kN:	1.99
KIC, MN/m3/2:	1.75
date of testing:	23.07.04
operated by	F. Seebald, U. Weber
checked by	U. Weber

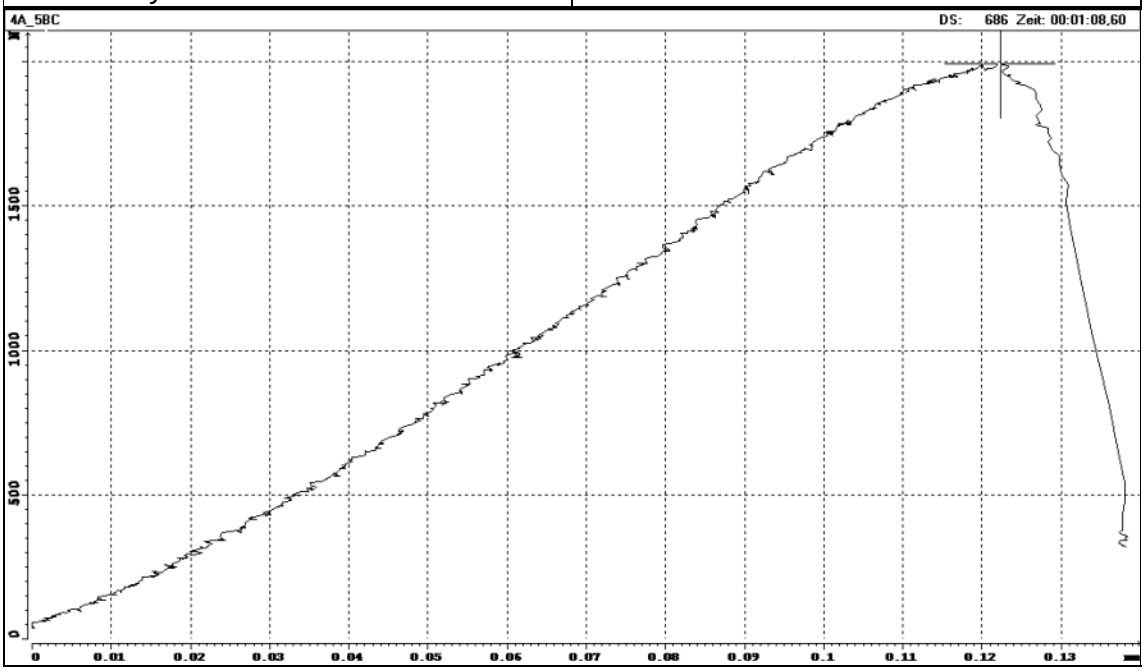

borehole:	KFM04A
sample - no.:	4A-6AB
mean depth, m:	528.38
diameter, mm:	50.6
initial crack length, mm:	7.2
max. Force, kN:	2.30
KIC, MN/m3/2:	2.05
date of testing:	23.07.04
operated by	F. Seebald, U. Weber
checked by	U. Weber

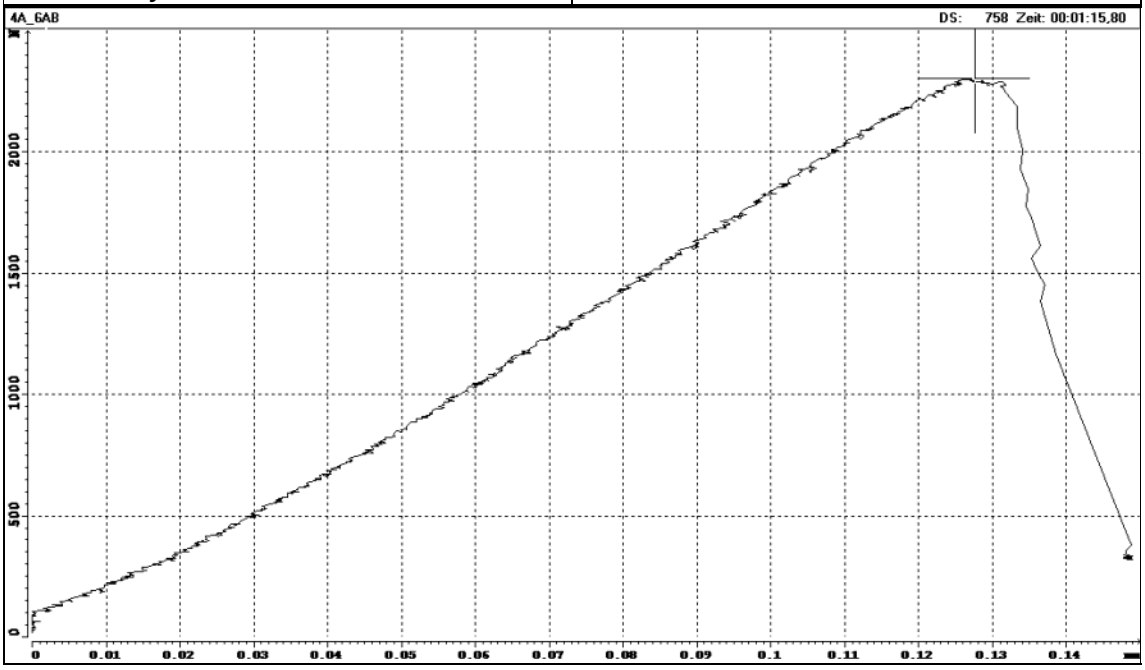

borehole:	KFM04A
sample - no.:	4A-6BC
mean depth, m:	528.38
diameter, mm:	50.7
initial crack length, mm:	7.4
max. Force, kN:	2.10
KIC, MN/m3/2:	1.89
date of testing:	23.07.04
operated by	F. Seebald, U. Weber
checked by	U. Weber

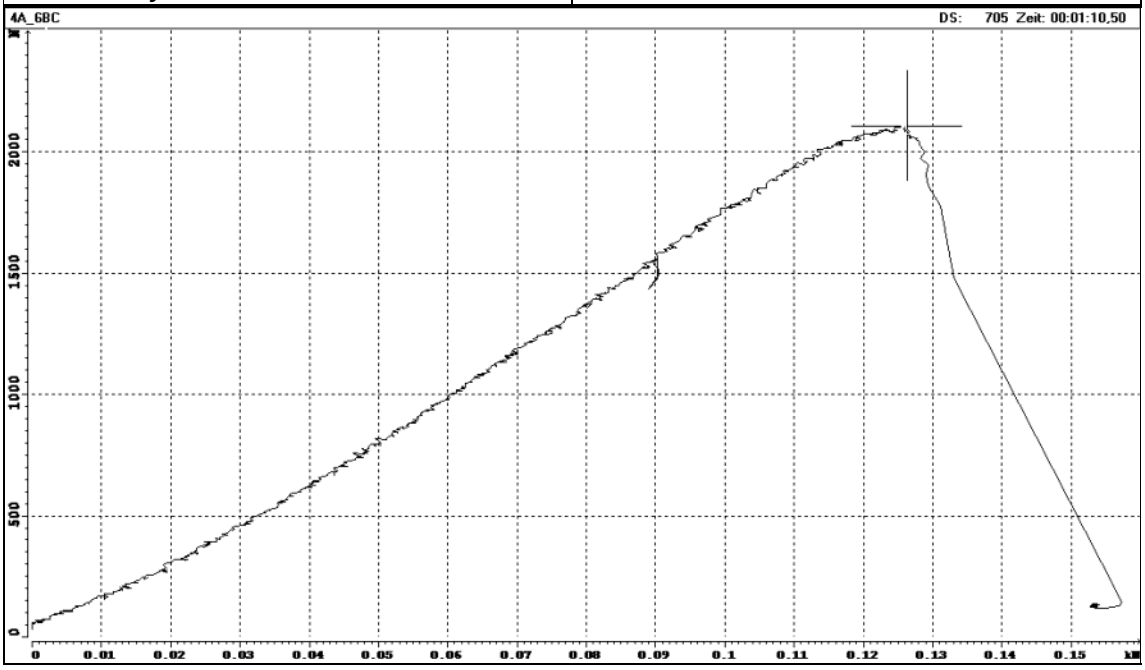

borehole:	KFM04A
sample - no.:	4A-7AB
mean depth, m:	528.79
diameter, mm:	50.6
initial crack length, mm:	7.2
max. Force, kN:	2.41
KIC, MN/m3/2:	2.15
date of testing:	23.07.04
operated by	F. Seebald, U. Weber
checked by	U. Weber

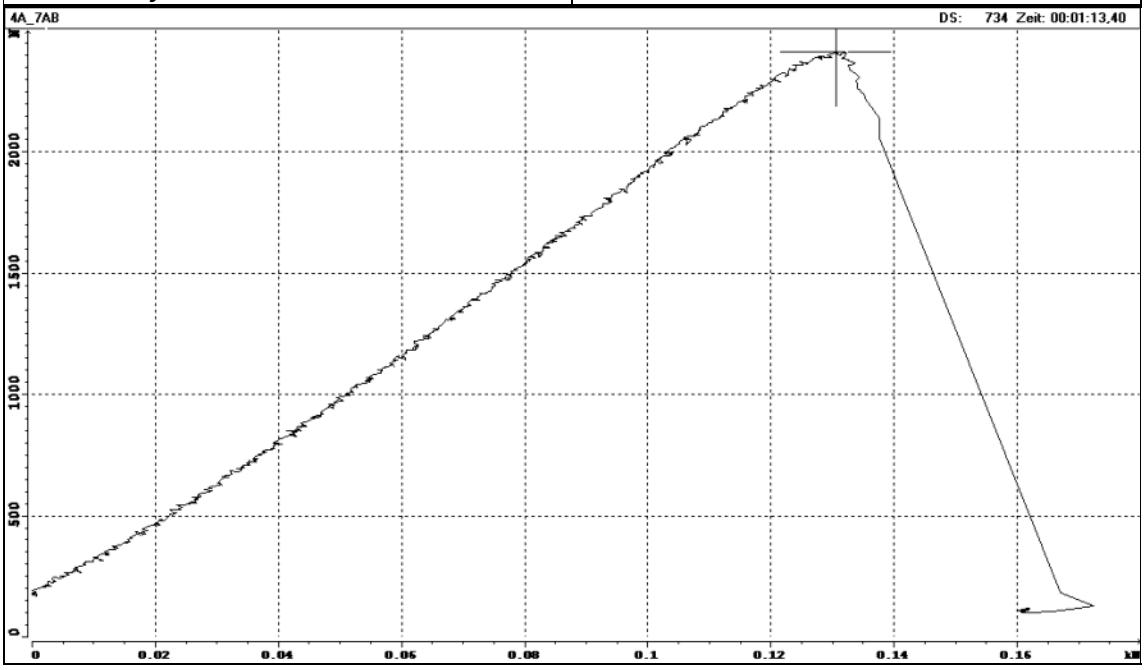

borehole:	KFM04A
sample - no.:	4A-7BC
mean depth, m:	528.79
diameter, mm:	50.7
initial crack length, mm:	7.0
max. Force, kN:	2.19
KIC, MN/m3/2:	1.92
date of testing:	23.07.04
operated by	F. Seebald, U. Weber
checked by	U. Weber

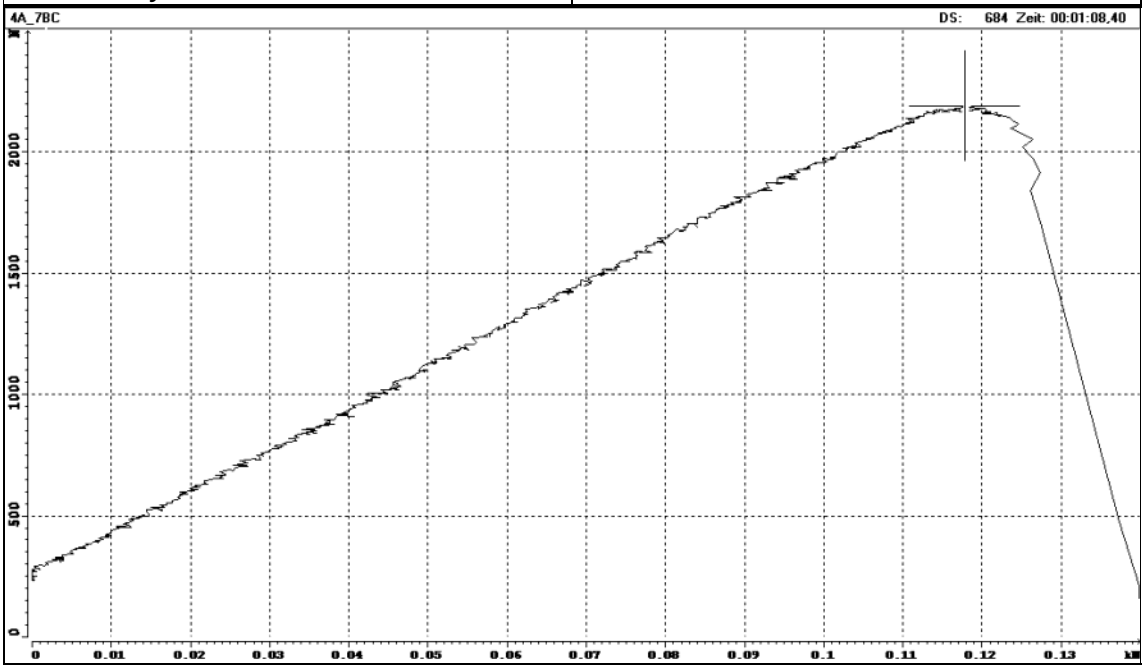

borehole:	KFM04A
sample - no.:	4A-8AB
mean depth, m:	529.13
diameter, mm:	50.7
initial crack length, mm:	7.0
max. Force, kN:	2.12
KIC, MN/m3/2:	1.86
date of testing:	23.07.04
operated by	F. Seebald, U. Weber
checked by	U. Weber

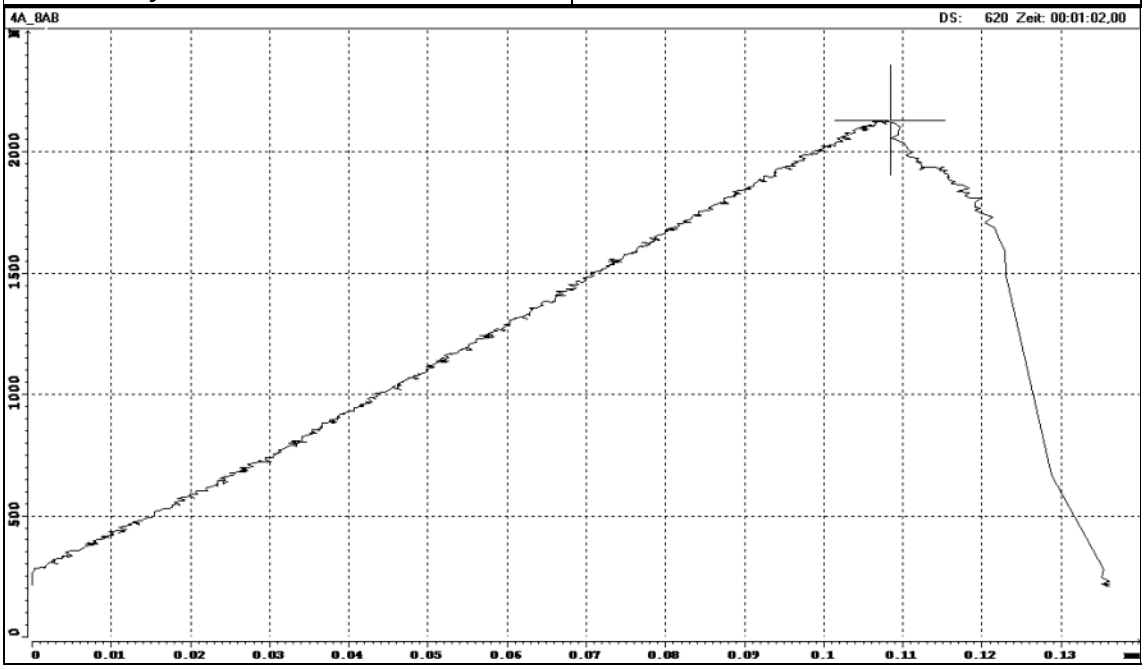

borehole:	KFM04A
sample - no.:	4A-8BC
mean depth, m:	529.13
diameter, mm:	50.7
initial crack length, mm:	6.7
max. Force, kN:	1.81
KIC, MN/m3/2:	1.56
date of testing:	23.07.04
operated by	F. Seebald, U. Weber
checked by	U. Weber

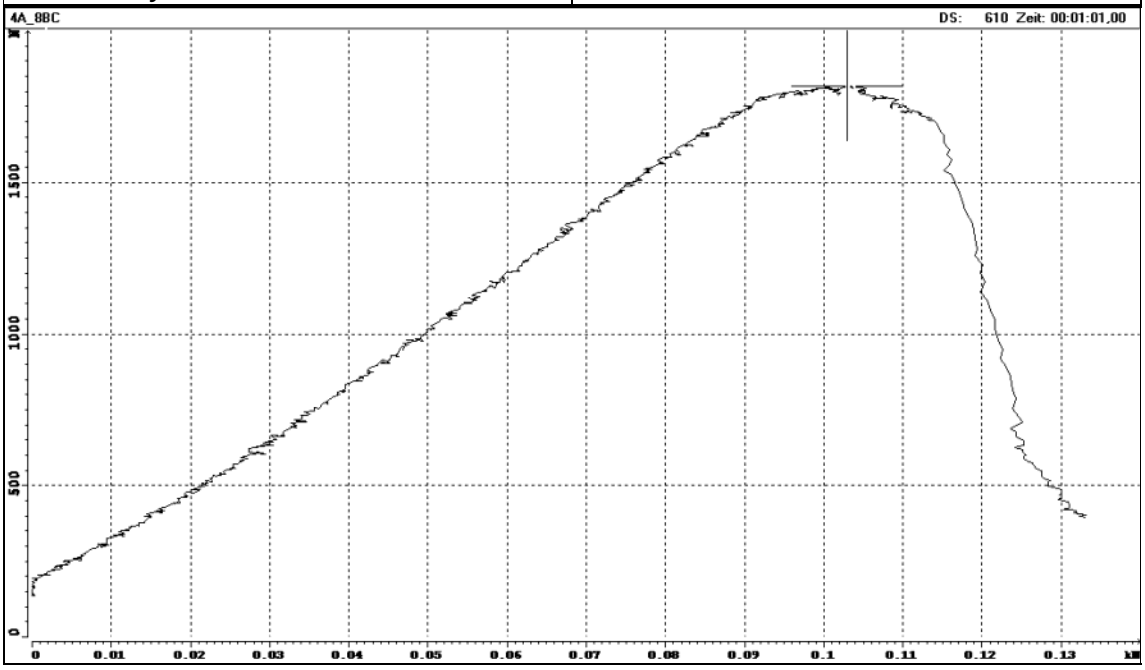

borehole:	KFM04A
sample - no.:	4A-9AB
mean depth, m:	529.47
diameter, mm:	50.7
initial crack length, mm:	6.9
max. Force, kN:	2.14
KIC, MN/m3/2:	1.87
date of testing:	23.07.04
operated by	F. Seebald, U. Weber
checked by	U. Weber

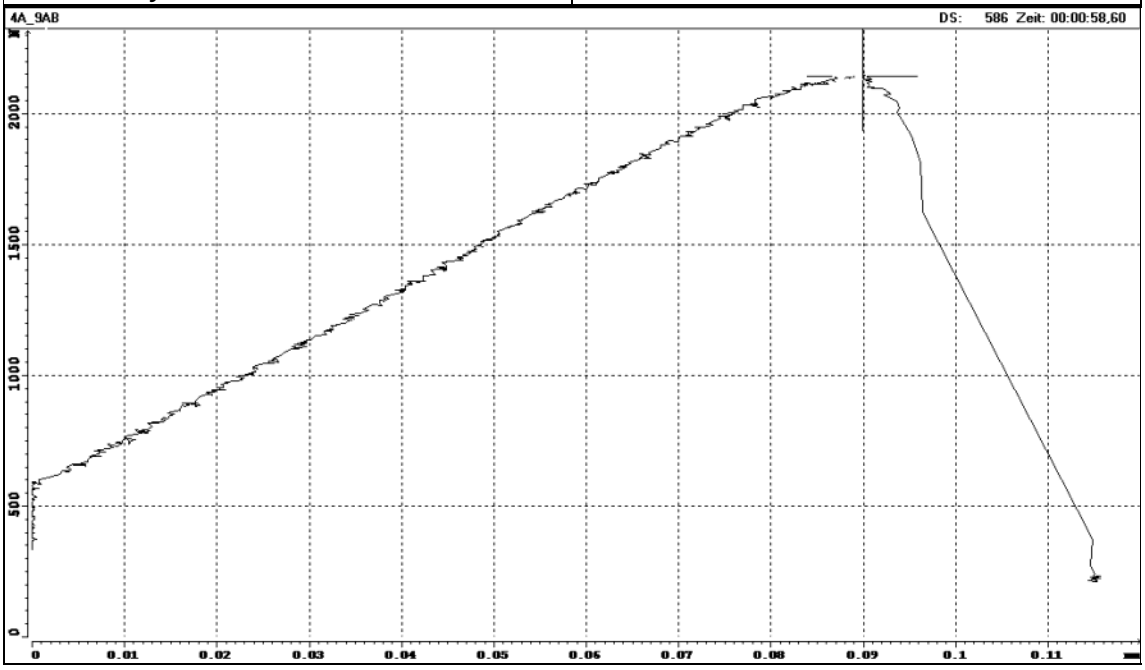

borehole:	KFM04A
sample - no.:	4A-9BC
mean depth, m:	529.47
diameter, mm:	50.8
initial crack length, mm:	7.0
max. Force, kN:	2.07
KIC, MN/m$^{3/2}$:	1.81
date of testing:	23.07.04
operated by	F. Seebald, U. Weber
checked by	U. Weber

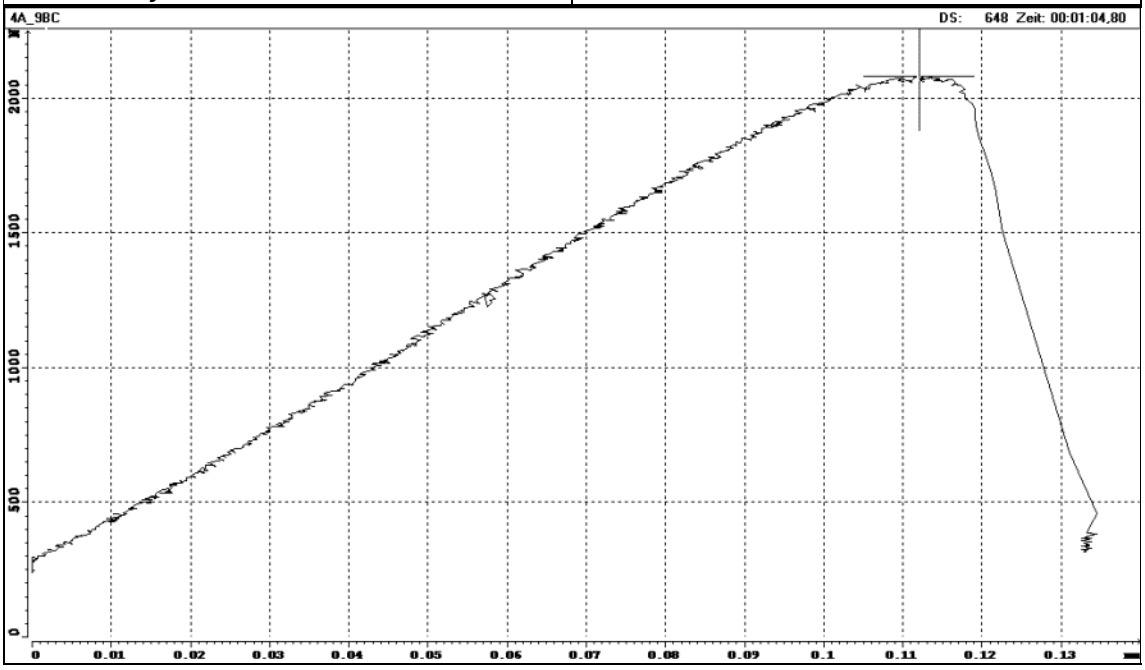

Appendix D

Records of hydrofrac tests on mini-samples

Sample no.: 1A-1A

operator	Schreiner/Weber/Witthaus
date	14.07.04 12:15-12:45

mean depth, m	423.17
axial load σ_1, MPa	20.82
confining pressure σ_3, MPa	18.21
breakdown pressure p_c, MPa	52.01
injection fluid	TELLUS 32
injection rate, ml s^{-1}	1
remarks	axial fractured

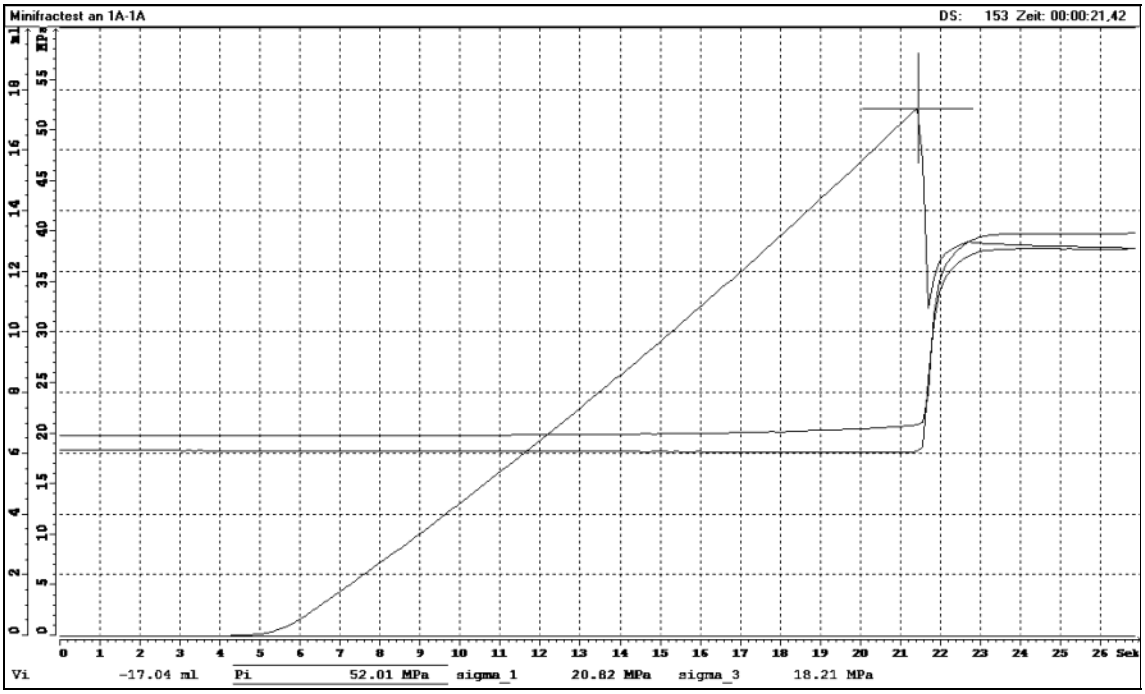

Sample no.: 1A-1C

operator	Schreiner/Weber/Witthaus
date	14.07.04 13:15-13:30

mean depth, m	423.17
axial load σ_1, MPa	21.29
confining pressure σ_3, MPa	14.14
breakdown pressure p_c, MPa	46.25
injection fluid	TELLUS32
injection rate, ml s^{-1}	1
remarks	axial fractured

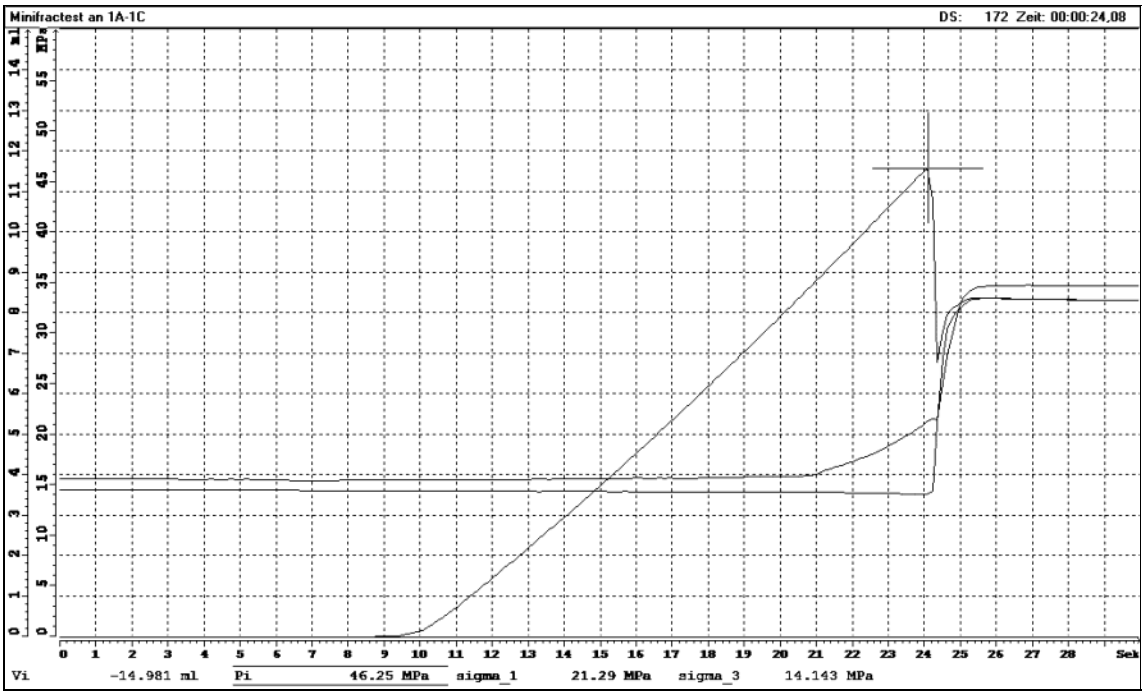

Sample no.: 1A-2B

operator	Weber/Witthaus
date	14.07.04 09:30-09:50

mean depth, m	424.83
axial load σ_1, MPa	23.88
confining pressure σ_3, MPa	10.02
breakdown pressure p_c, MPa	44.13
injection fluid	TELLUS32
injection rate, ml s^{-1}	1
remarks	axial fractured

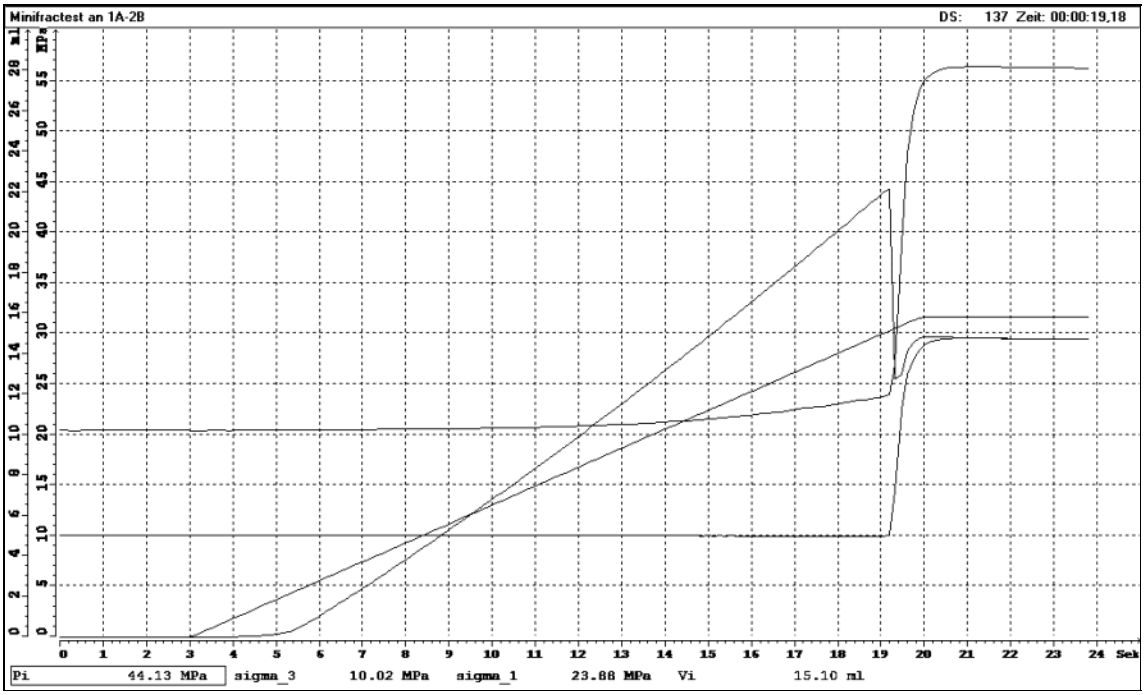

Sample no.: 1A-2C

operator	Schreiner/Weber/Witthaus
date	14.07.04 11:15-11:30

mean depth, m	424.83
axial load σ_1, MPa	13.18
confining pressure σ_3, MPa	3.96
breakdown pressure p_c, MPa	34.11
injection fluid	TELLUS32
injection rate, ml s^{-1}	1
remarks	axial fractured

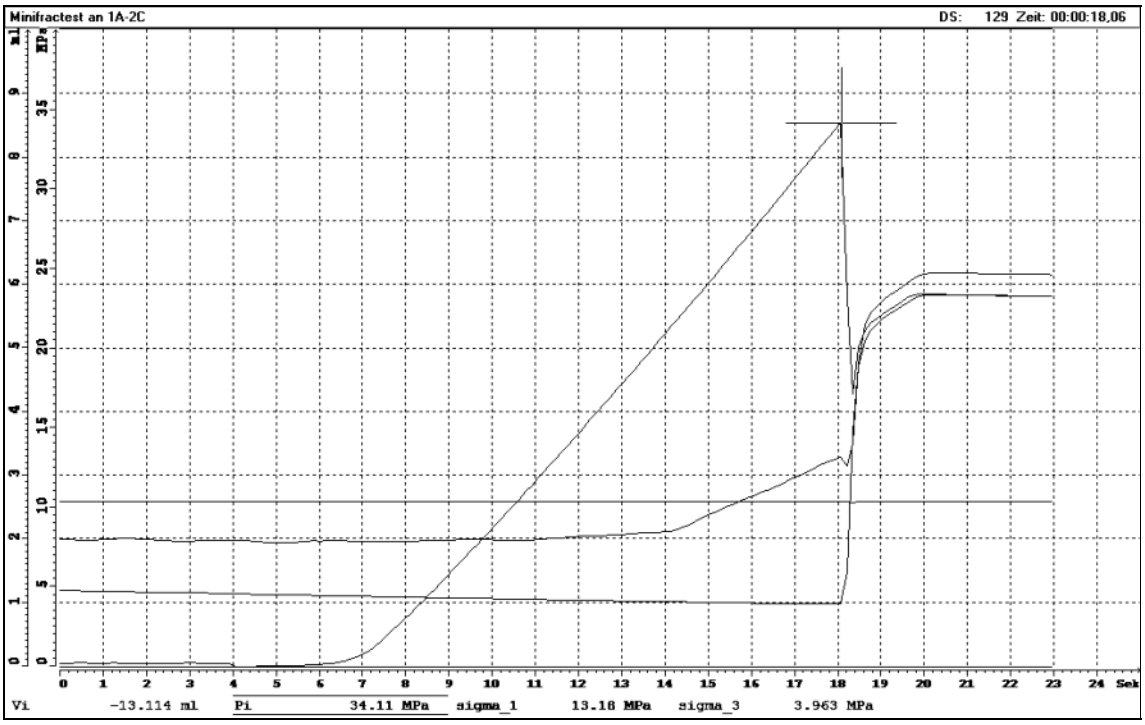

Sample no.: 1A-3A

operator	Vogt
date	24.08.04 10:30-10:40

mean depth, m	428.17
axial load σ_1, MPa	37.20
confining pressure σ_3, MPa	29.98
breakdown pressure p_c, MPa	66.28
injection fluid	TELLUS32
injection rate, ml s^{-1}	1
remarks	axial fractured

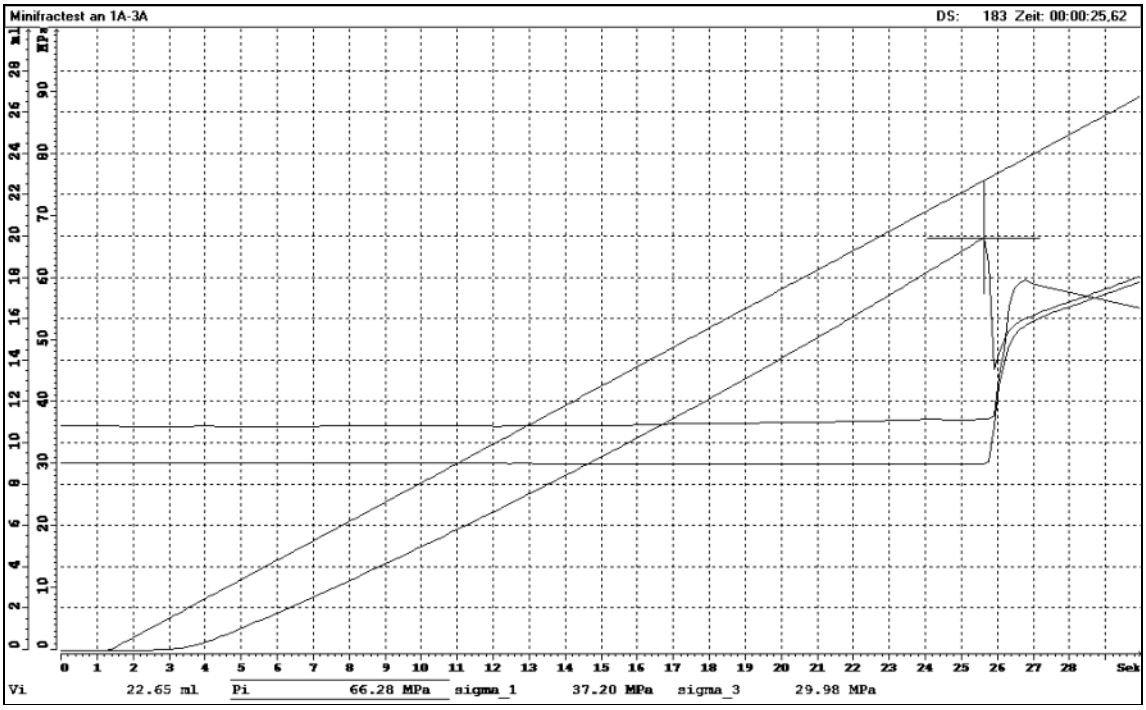

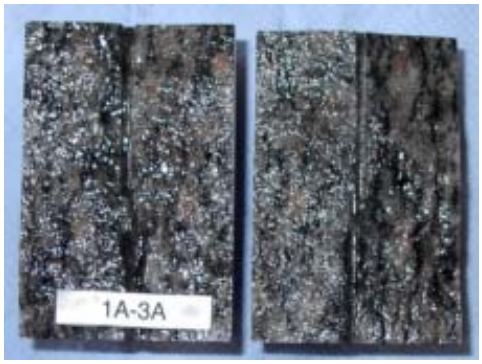

Sample no.: 1A-3C

operator	Schreiner/Vogt
date	24.08.04 11:30-11:40

mean depth, m	428.17
axial load σ_1, MPa	30.44
confining pressure σ_3, MPa	25.54
breakdown pressure p_c, MPa	63.95
injection fluid	TELLUS32
injection rate, ml s^{-1}	1
remarks	axial and inclined fractured

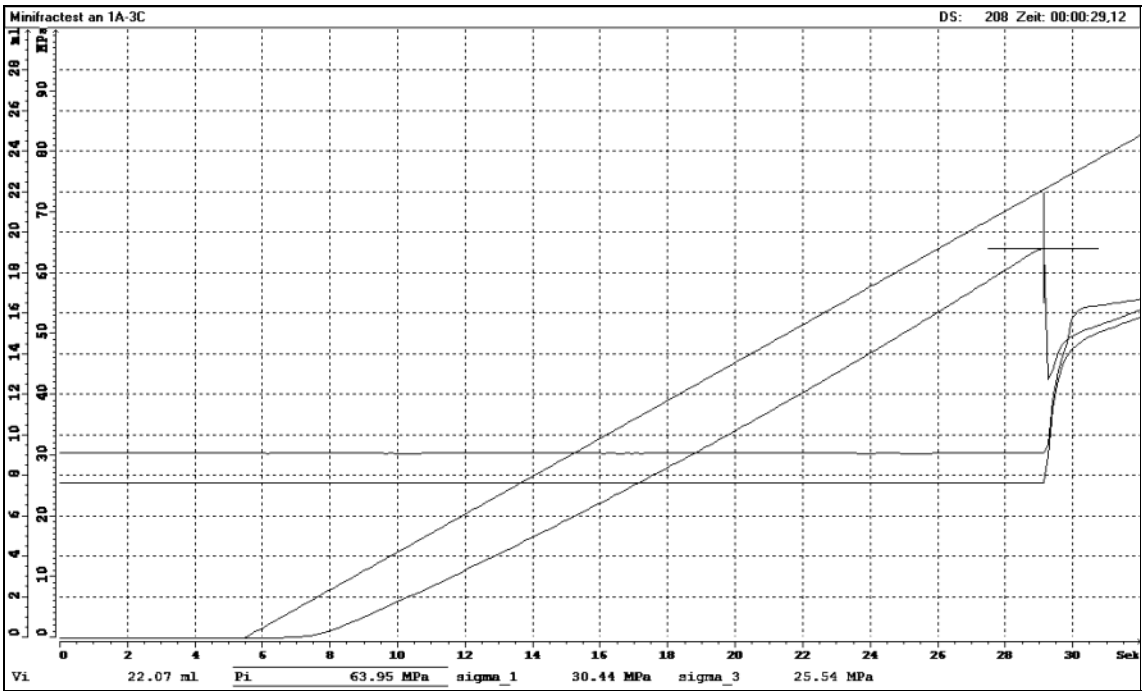

Sample no.: 1A-4A

operator	Vogt
date	24.08.04 13:50-14:10

mean depth, m	484.59
axial load σ_1, MPa	34.59
confining pressure σ_3, MPa	22.58
breakdown pressure p_c, MPa	56.46
injection fluid	TELLUS32
injection rate, ml s^{-1}	1
remarks	axial fractured

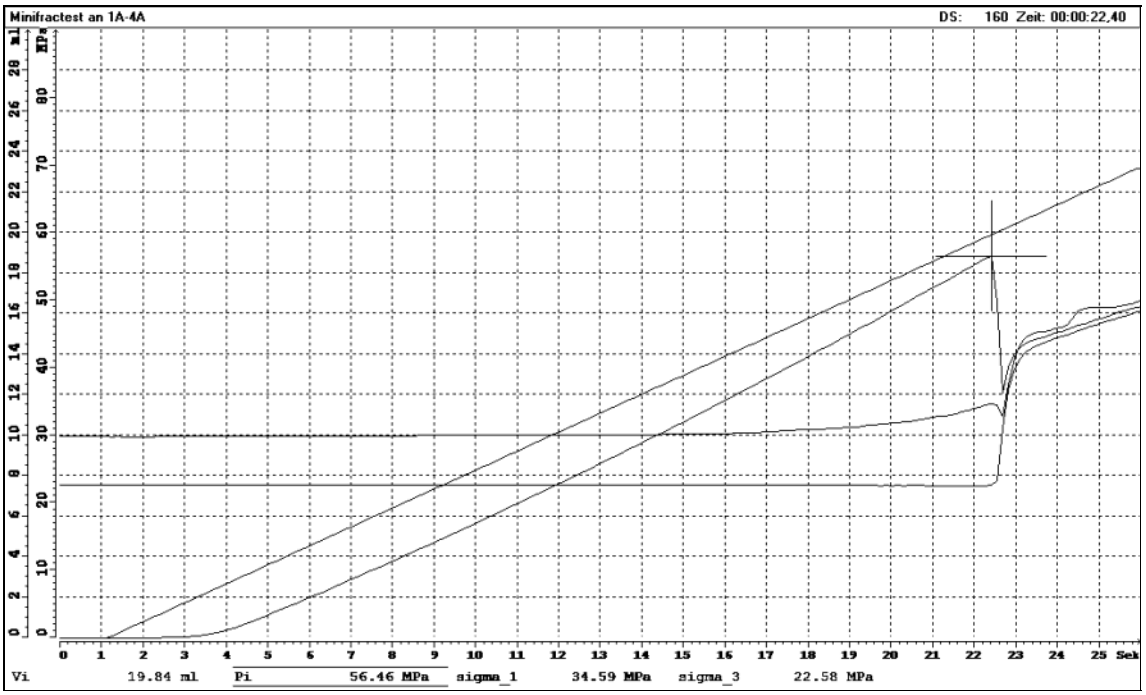

Sample no.: 1A-4C

operator	Schreiner/Vogt
date	24.08.04 14:20-15:10

mean depth, m	484.59
axial load σ_1, MPa	25.18
confining pressure σ_3, MPa	11.50
breakdown pressure p_c, MPa	39.87
injection fluid	TELLUS32
injection rate, ml s^{-1}	1
remarks	inclined fractured

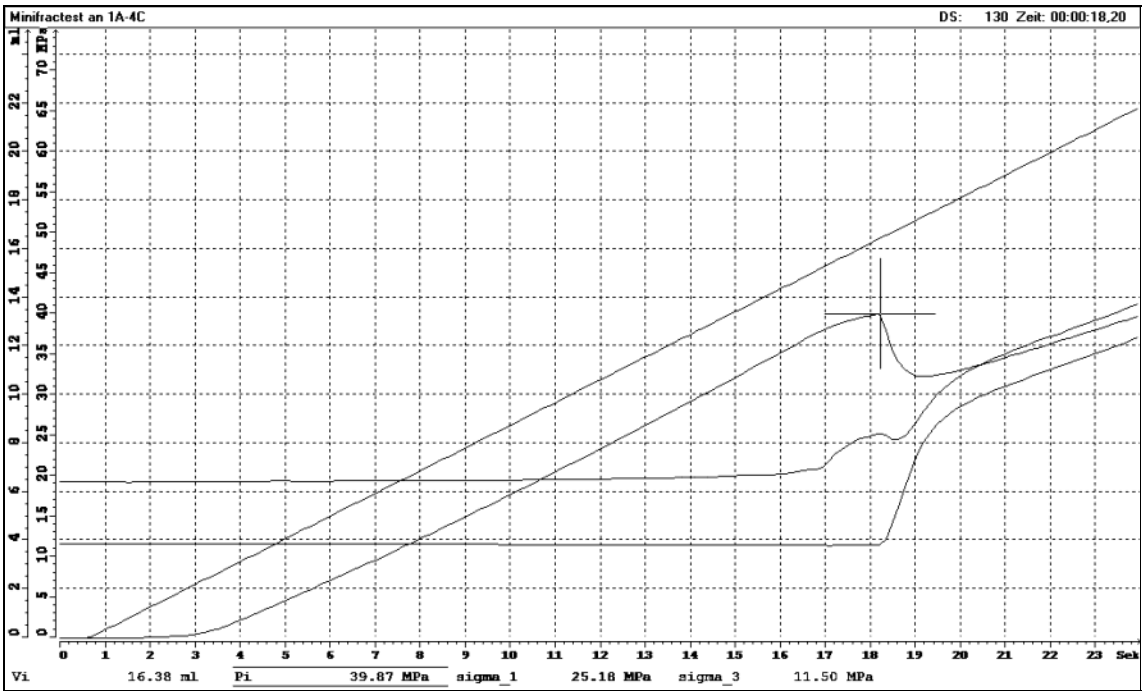

Sample no.: 1A-5A

operator	Küperkoch/Schreiner/Vogt
date	24.08.04 15:30-15:40

mean depth, m	489.95
axial load σ_1, MPa	28.37
confining pressure σ_3, MPa	22.23
breakdown pressure p_c, MPa	50.51
injection fluid	TELLUS32
injection rate, ml s^{-1}	1
remarks	axial fractured

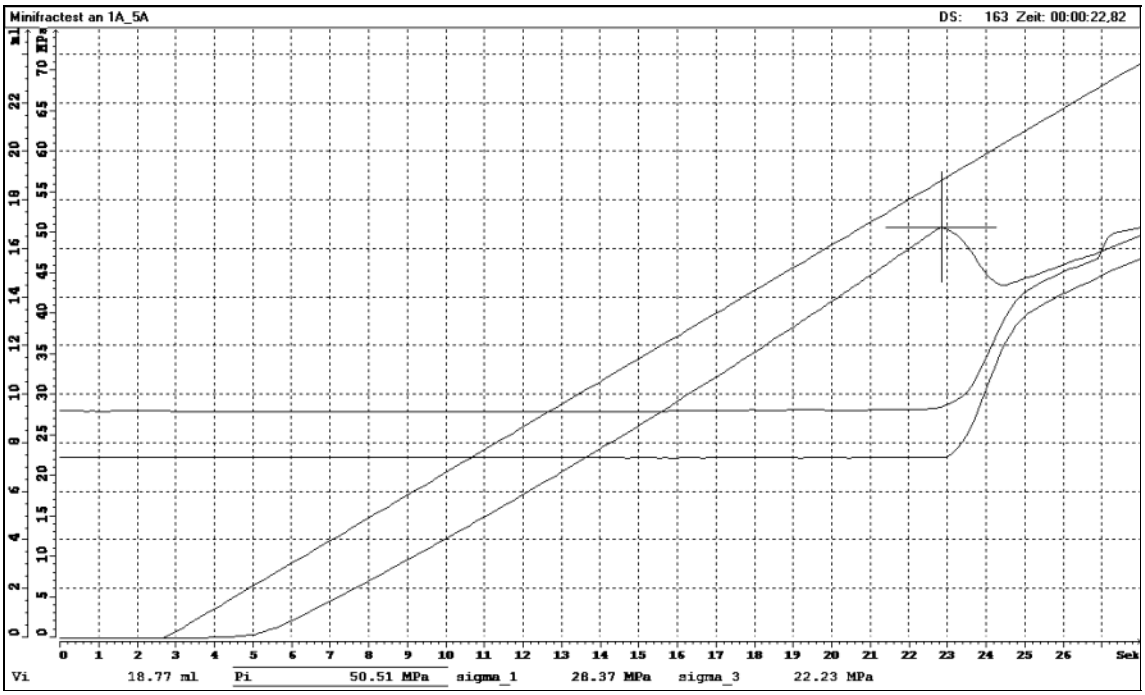

Sample no.: 1A-5C

operator	Küperkoch
date	25.08.04 09:20-09:30

mean depth, m	489.95
axial load σ_1, MPa	35.71
confining pressure σ_3, MPa	24.68
breakdown pressure p_c, MPa	66.34
injection fluid	TELLUS32
injection rate, ml s^{-1}	1
remarks	axial and inclined fractured

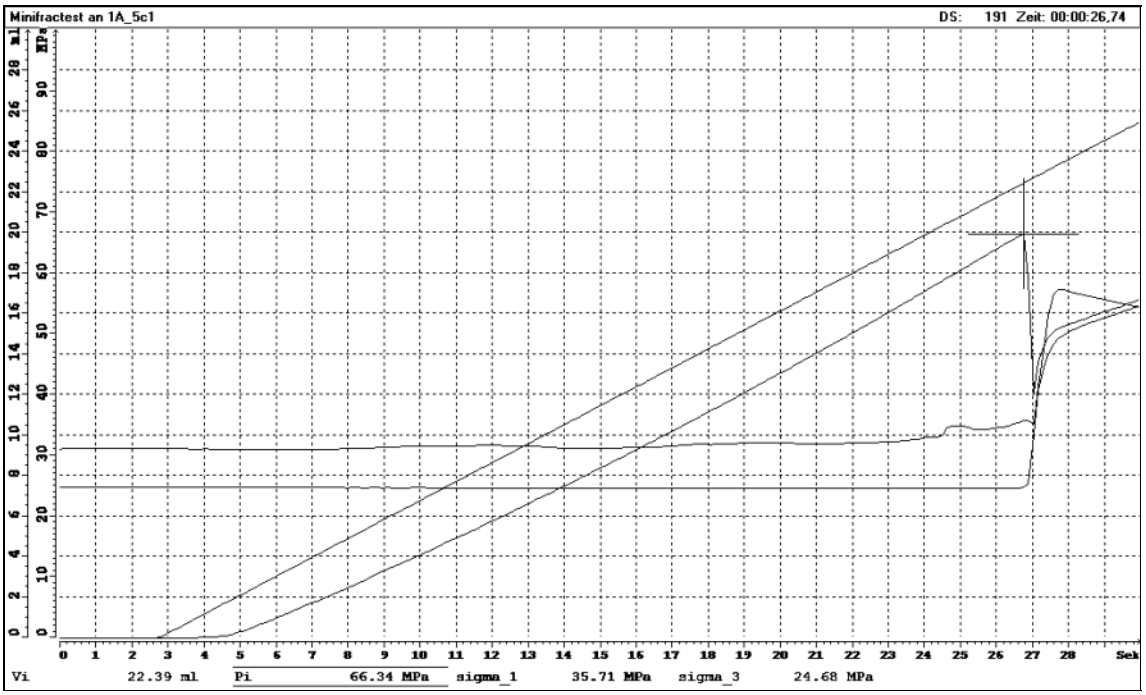

Sample no.: 1A-6A

operator	Küperkoch/Schreiner
date	25.08.04 10:10-10:20

mean depth, m	504.69
axial load σ_1, MPa	29.39
confining pressure σ_3, MPa	23.89
breakdown pressure p_c, MPa	62.71
injection fluid	TELLUS32
injection rate, ml s^{-1}	1
remarks	axial fractured

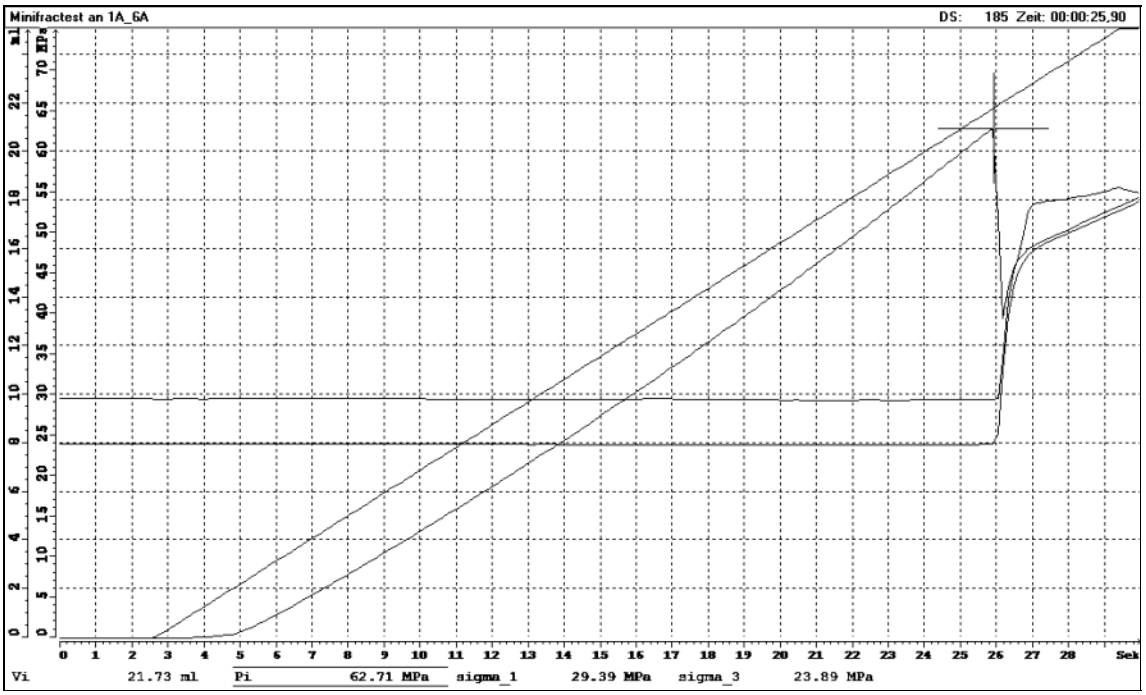

Sample no.: 1A-6C

operator	Küperkoch/Schreiner
date	25.08.04 11:00-11:10

mean depth, m	504.69
axial load σ_1, MPa	31.06
confining pressure σ_3, MPa	26.82
breakdown pressure p_c, MPa	68.32
injection fluid	TELLUS32
injection rate, ml s^{-1}	1
remarks	axial fractured

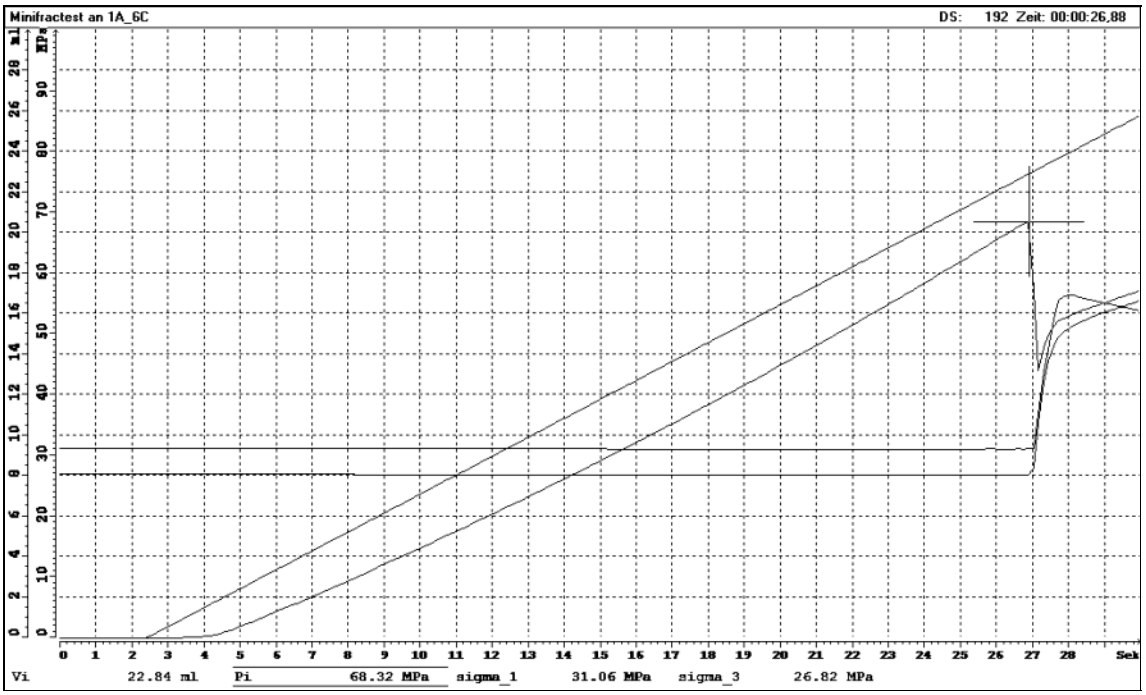

Sample no.: 1A-7A

operator	Küperkoch/Schreiner
date	25.08.04 12:00-12:10

mean depth, m	688.13
axial load σ_1, MPa	37.64
confining pressure σ_3, MPa	28.82
breakdown pressure p_c, MPa	57.24
injection fluid	TELLUS32
injection rate, ml s^{-1}	1
remarks	axial fractured

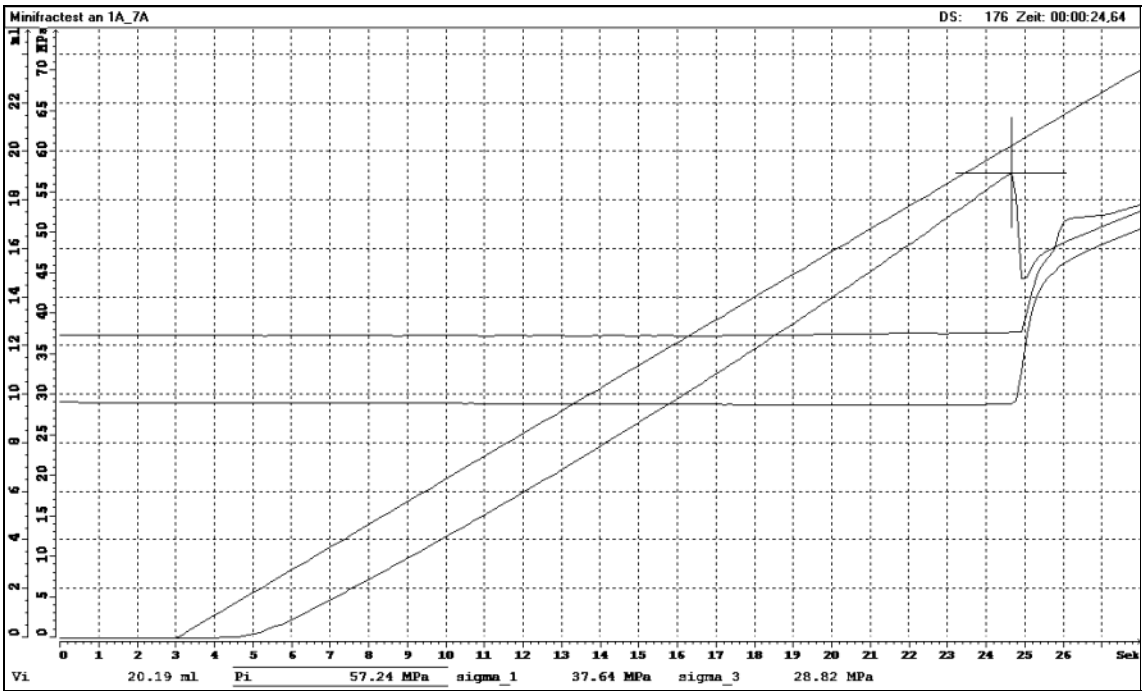

Sample no.: 1A-7C

operator	Küperkoch
date	26.08.04 09:10-09:20

mean depth, m	688.13
axial load σ_1, MPa	14.55
confining pressure σ_3, MPa	8.28
breakdown pressure p_c, MPa	32.12
injection fluid	TELLUS32
injection rate, ml s^{-1}	1
remarks	axial fractured

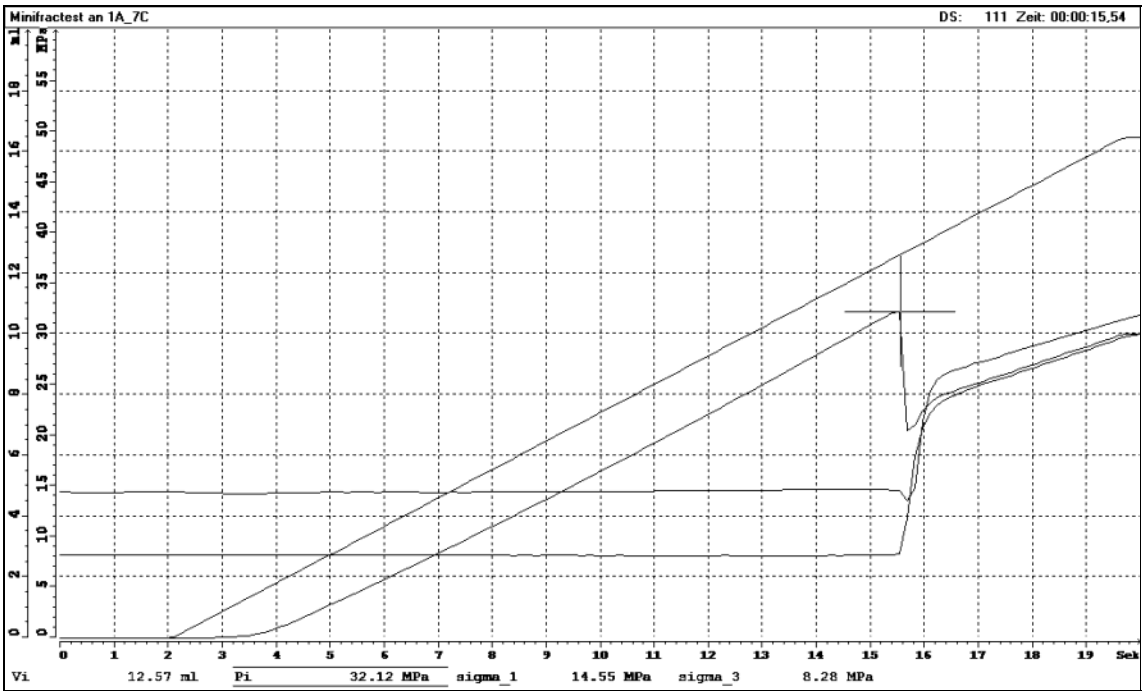

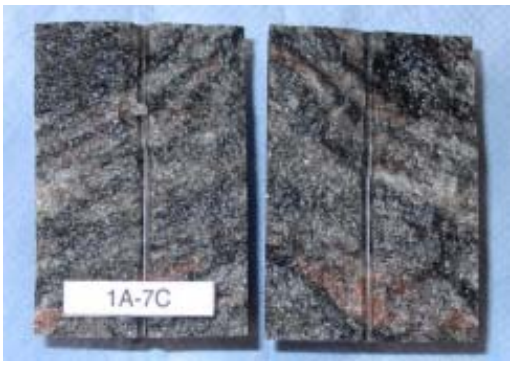

Sample no.: 1A-8A

operator	Küperkoch/Schreiner
date	25.08.04 12:20-12:30

mean depth, m	950.0
axial load σ_1, MPa	24.28
confining pressure σ_3, MPa	20.80
breakdown pressure p_c, MPa	62.61
injection fluid	TELLUS32
injection rate, ml s^{-1}	1
remarks	axial fractured

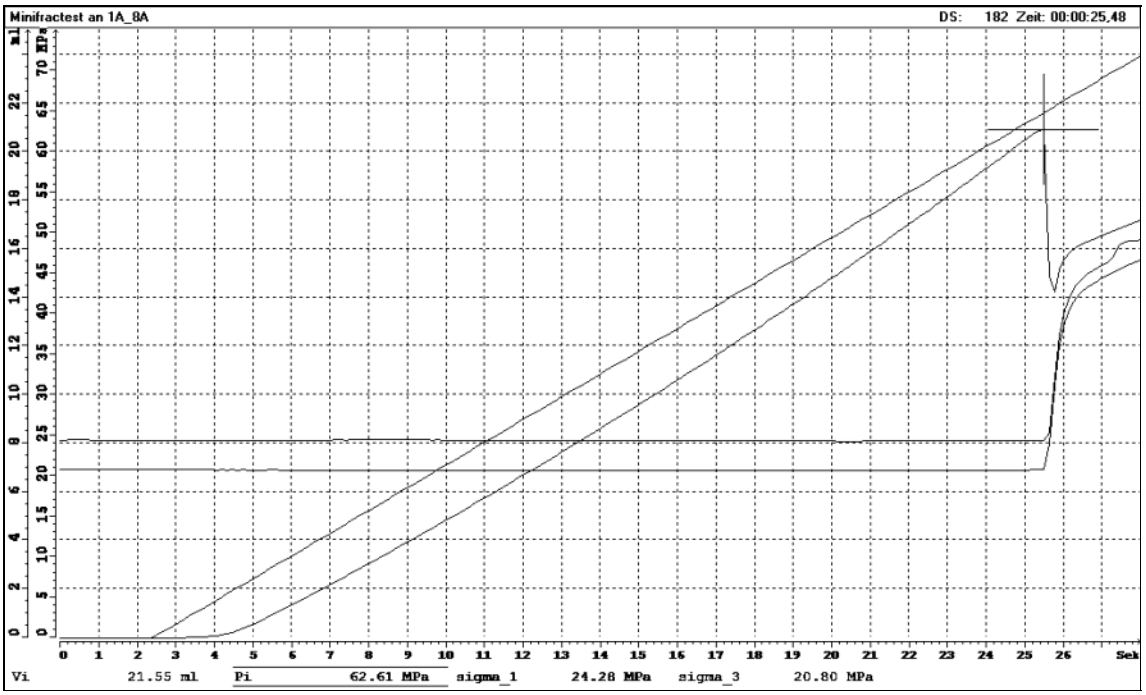

Sample no.: 1A-8C

operator	Küperkoch/Schreiner
date	25.08.04 12:50-13:00

mean depth, m	950.0
axial load σ_1, MPa	30.94
confining pressure σ_3, MPa	21.63
breakdown pressure p_c, MPa	64.36
injection fluid	TELLUS32
injection rate, ml s^{-1}	1
remarks	axial fractured

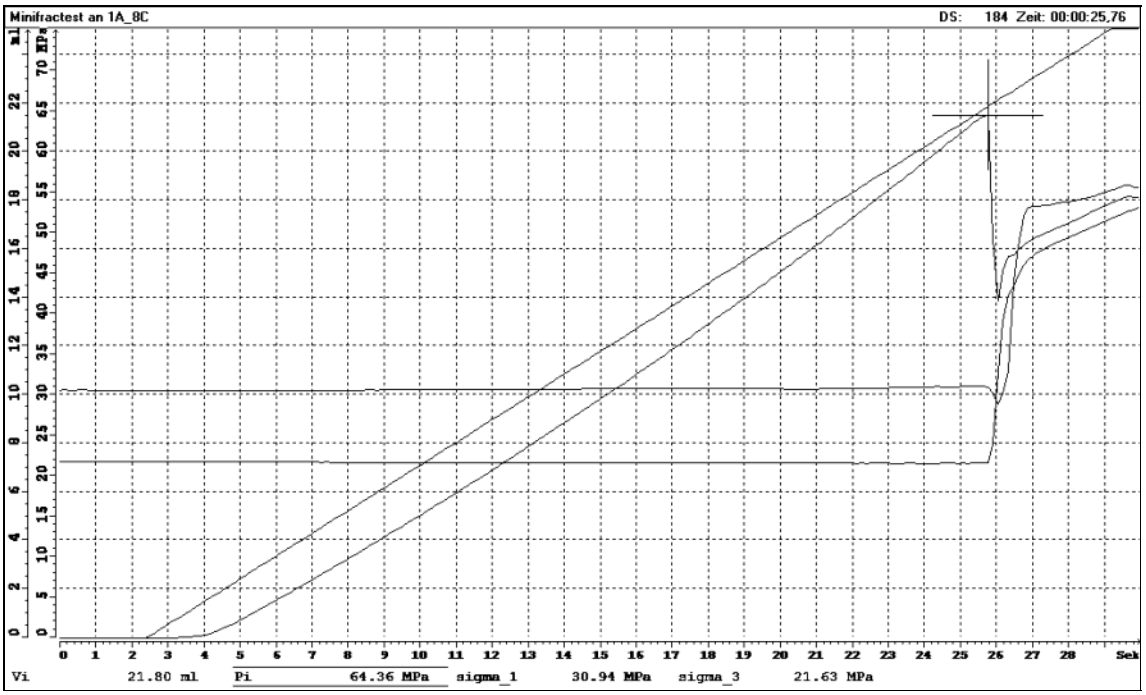

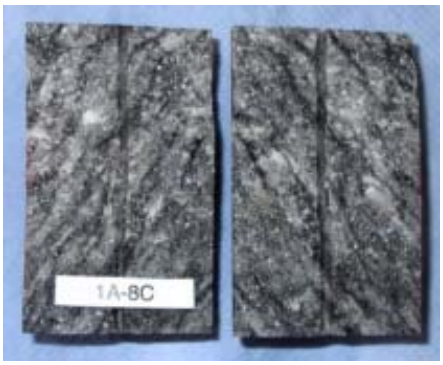

Sample no.: 1A-9A

operator	Küperkoch/Schreiner
date	25.08.04 13:20-13:40

mean depth, m	971.57
axial load σ_1, MPa	24.06
confining pressure σ_3, MPa	17.94
breakdown pressure p_c, MPa	57.73
injection fluid	TELLUS32
injection rate, ml s^{-1}	1
remarks	axial fractured

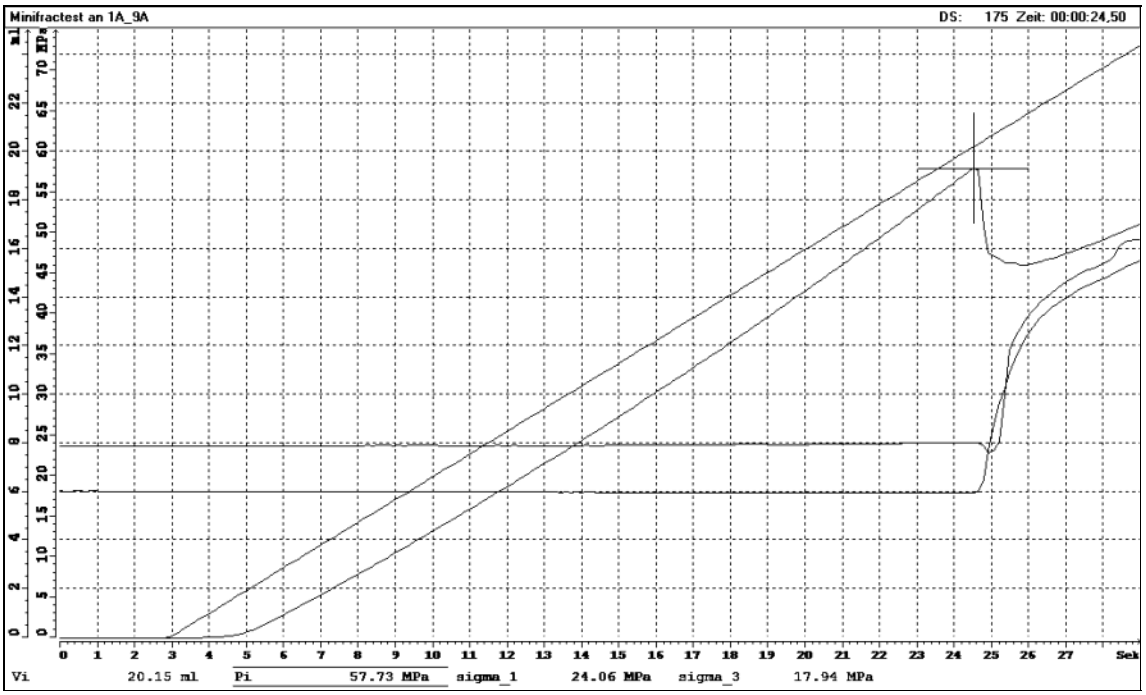

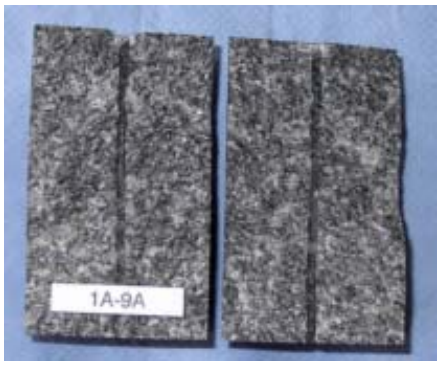

Sample no.: 1A-9C

operator	Küperkoch
date	25.08.04 14:50-15:00

mean depth, m	971.57
axial load σ_1, MPa	16.11
confining pressure σ_3, MPa	12.49
breakdown pressure p_c, MPa	42.08
injection fluid	TELLUS32
injection rate, ml s^{-1}	1
remarks	axial fractured

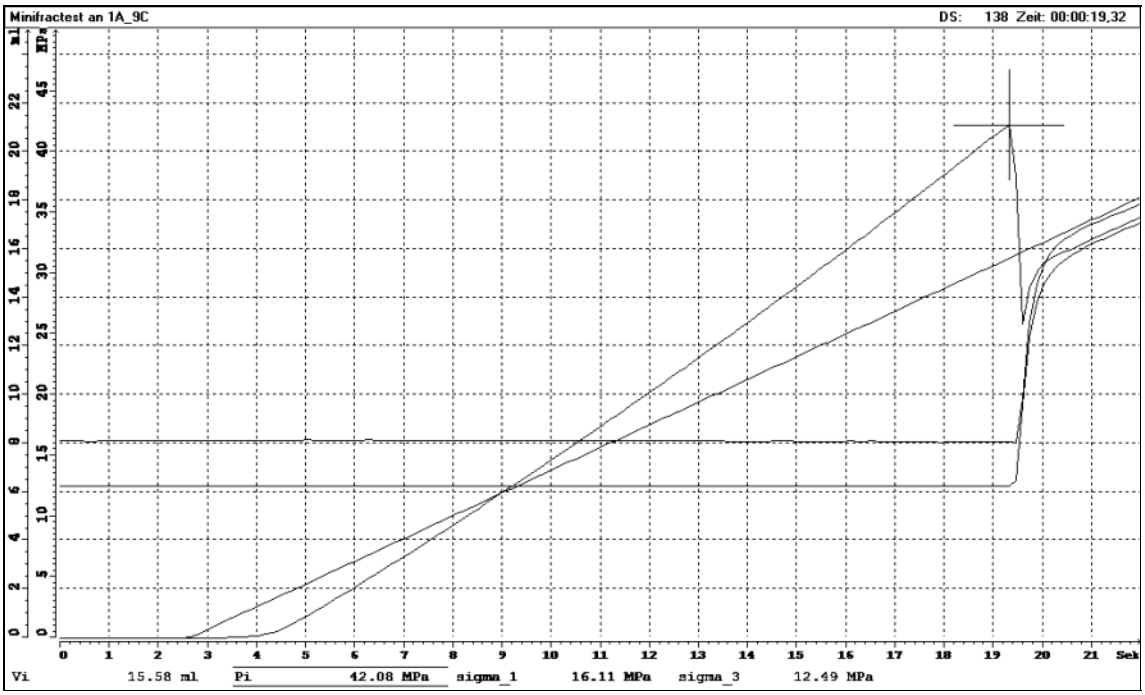

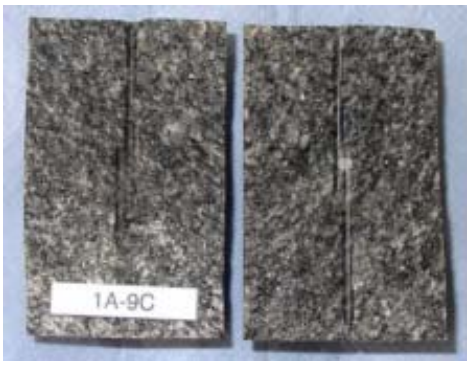

Sample no.: 1A-10A

operator	Küperkoch/Schreiner
date	25.08.04 15:20-15:30

mean depth, m	978.53
axial load σ_1, MPa	18.82
confining pressure σ_3, MPa	16.45
breakdown pressure p_c, MPa	69.07
injection fluid	TELLUS32
injection rate, ml s^{-1}	1
remarks	axial fractured

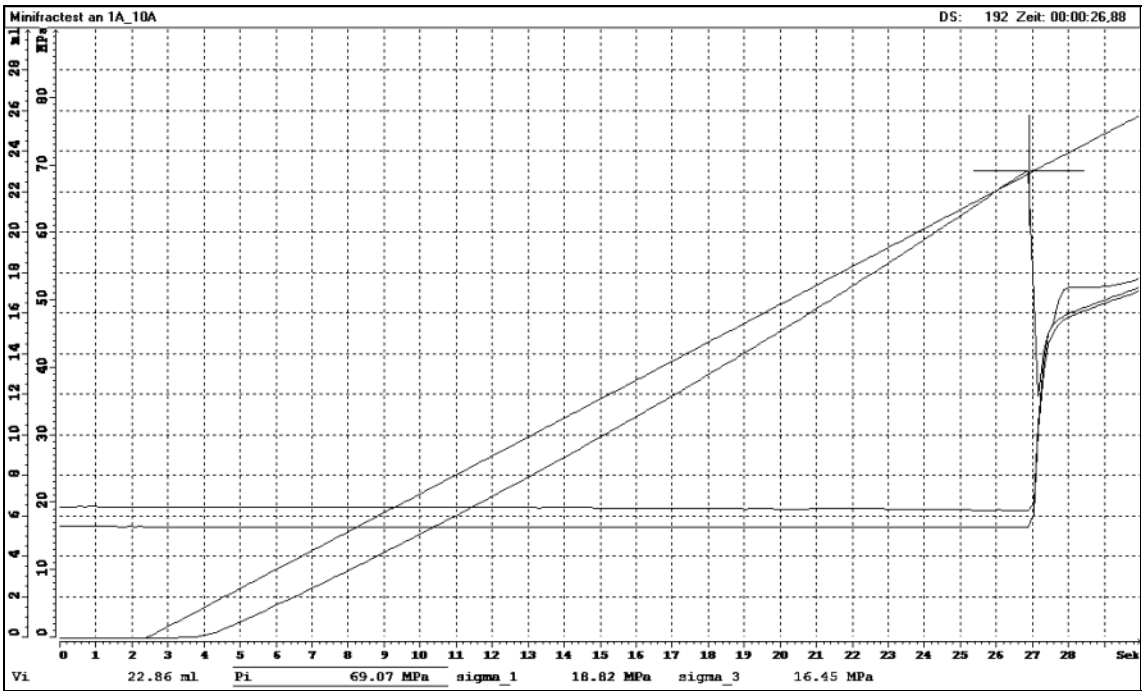

Sample no.: 1A-10C

operator	Küperkoch/Schreiner
date	25.08.04 15:50-16:00

mean depth, m	978.53
axial load σ_1, MPa	19.23
confining pressure σ_3, MPa	15.97
breakdown pressure p_c, MPa	49.35
injection fluid	TELLUS32
injection rate, ml s^{-1}	1
remarks	axial fractured

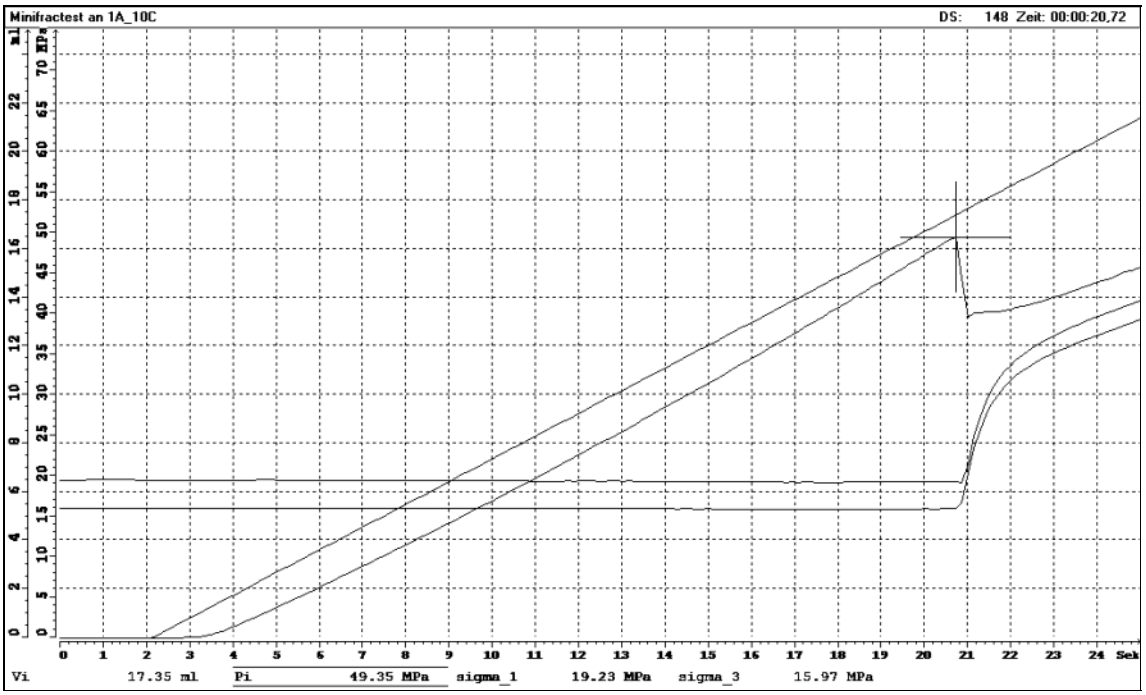

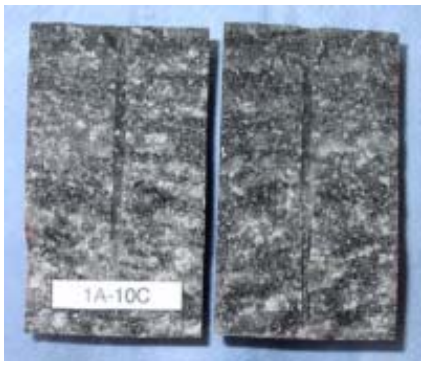

Sample no.: 1B-1A

operator	Vogt/Witthaus
date	09.08.04 09:00-09:10

mean depth, m	421.03
axial load σ_1, MPa	31.41
confining pressure σ_3, MPa	29.75
breakdown pressure p_c, MPa	42.88
injection fluid	TELLUS32
injection rate, ml s^{-1}	1
remarks	axial fractured, Refrac?

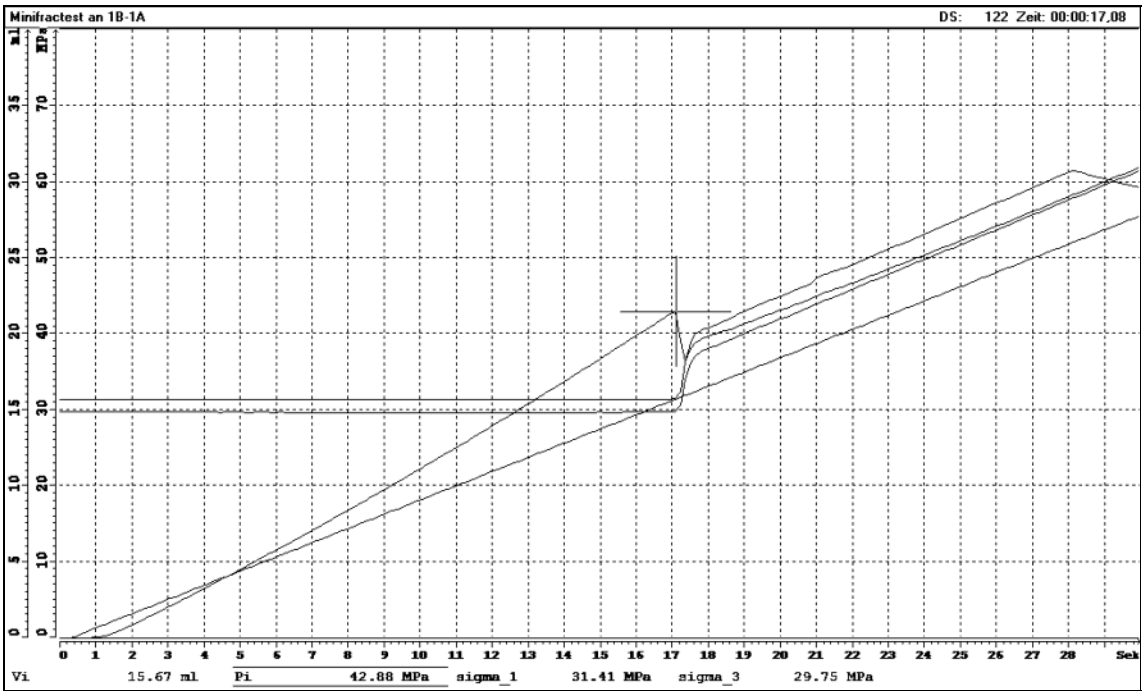

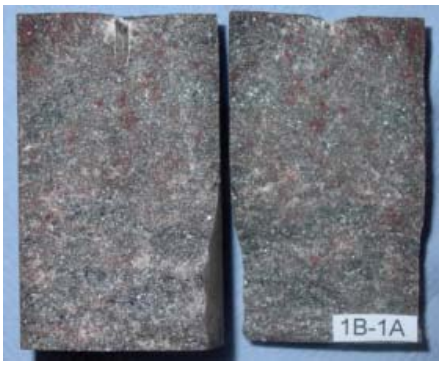

Sample no.: 1B-1C

operator	Vogt/Witthaus
date	09.08.04 10:10-10:20

mean depth, m	421.03
axial load σ_1, MPa	11.49
confining pressure σ_3, MPa	7.55
breakdown pressure p_c, MPa	24.22
injection fluid	TELLUS32
injection rate, ml s^{-1}	1
remarks	axial and inclined fractured

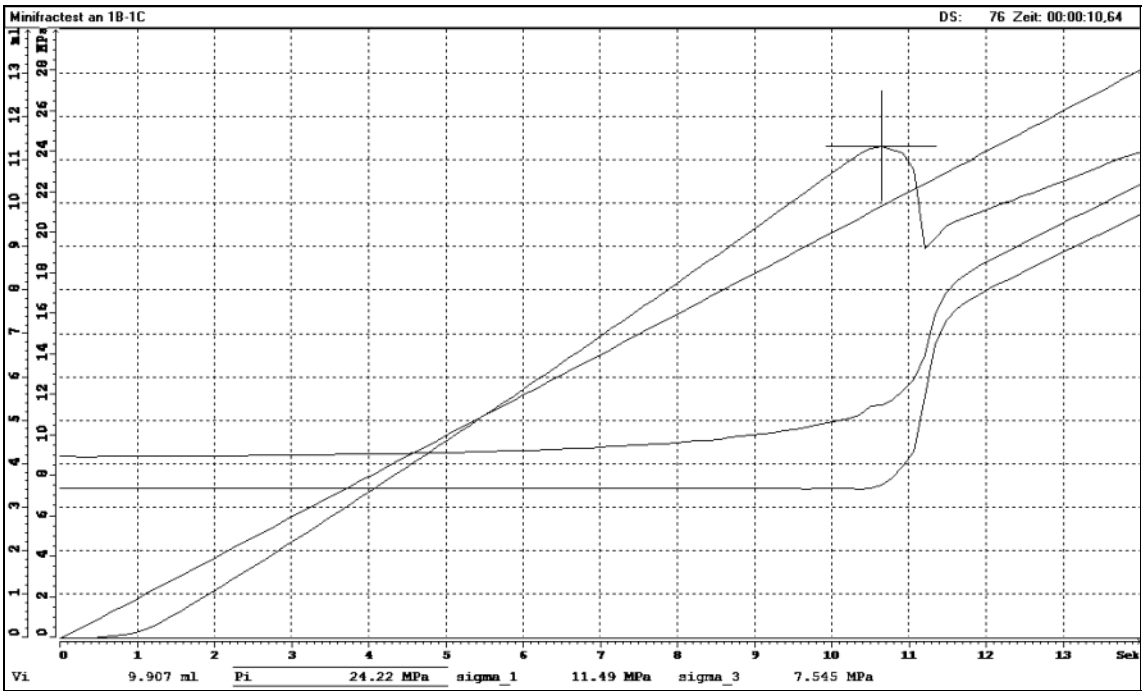

Sample no.: 1B-2A

operator	Vogt/Witthaus
date	09.08.04 15:10-15:20

mean depth, m	421.60
axial load σ_1, MPa	13.86
confining pressure σ_3, MPa	10.21
breakdown pressure p_c, MPa	50.93
injection fluid	TELLUS32
injection rate, ml s^{-1}	1
remarks	axial fractured

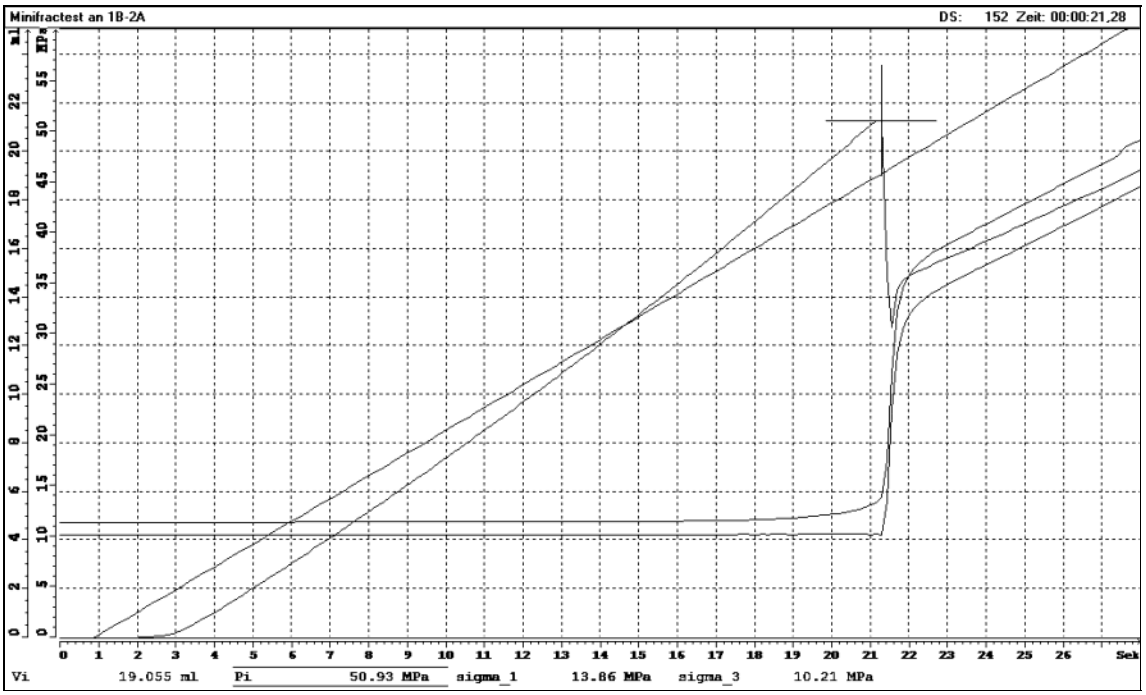

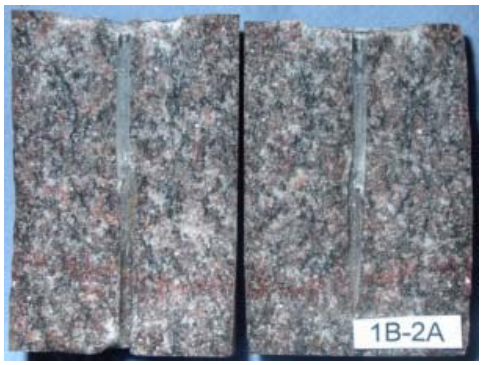

Sample no.: 1B-2C

operator	Küperkoch/Vogt/Witthaus
date	10.08.04 11:10-11:30

mean depth, m	421.60
axial load σ_1, MPa	29.85
confining pressure σ_3, MPa	23.41
breakdown pressure p_c, MPa	56.39
injection fluid	TELLUS32
injection rate, ml s^{-1}	1
remarks	inclined fractured

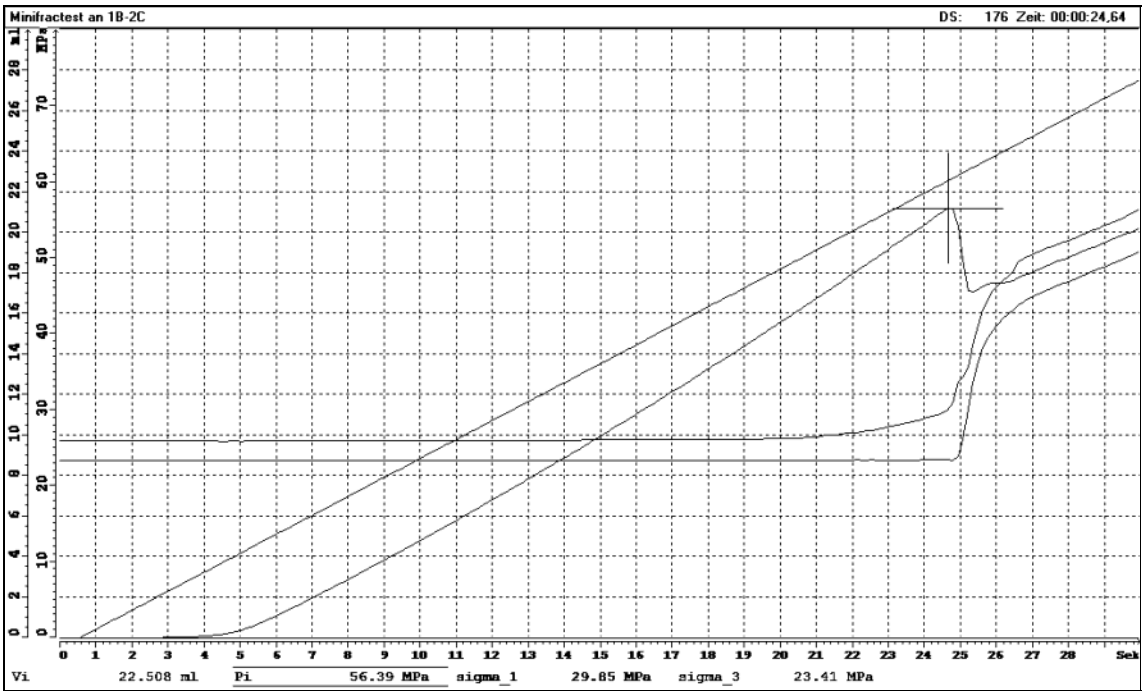

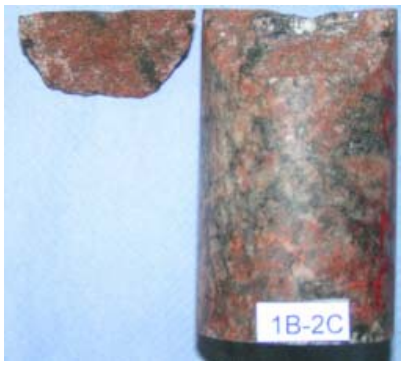

Sample no.: 1B-3A

operator	Küperkoch/Vogt/Witthaus
date	10.08.04 13:10-13:20

mean depth, m	428.09
axial load σ_1, MPa	13.85
confining pressure σ_3, MPa	8.37
breakdown pressure p_c, MPa	28.03
injection fluid	TELLUS32
injection rate, ml s^{-1}	1
remarks	axial fractured

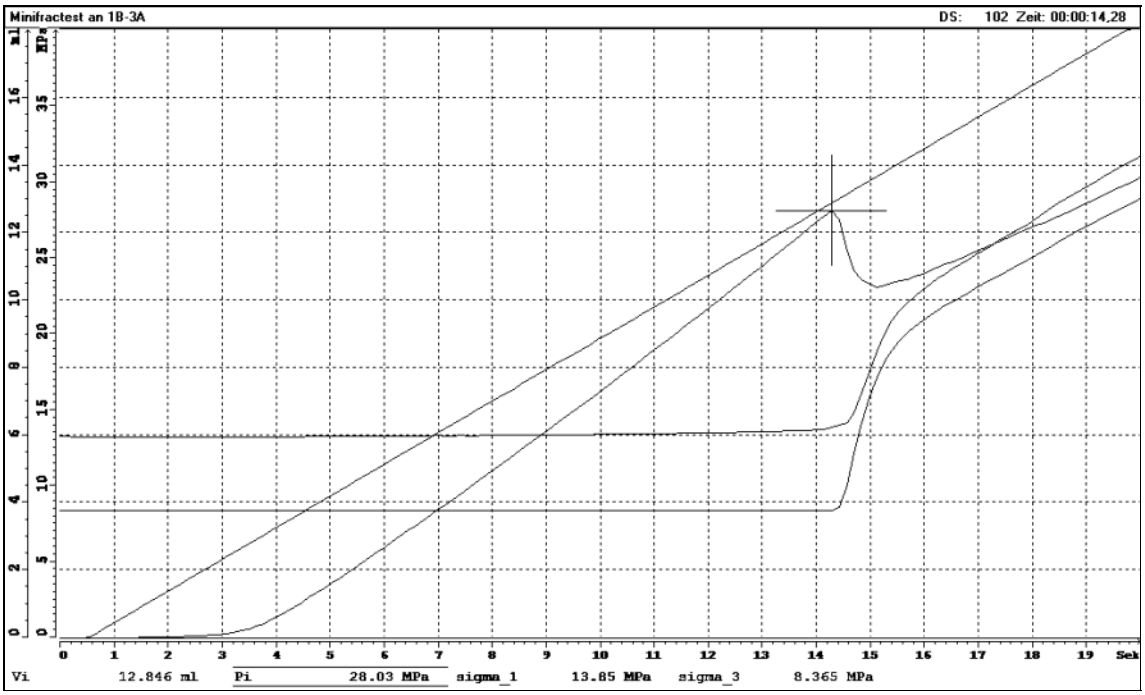

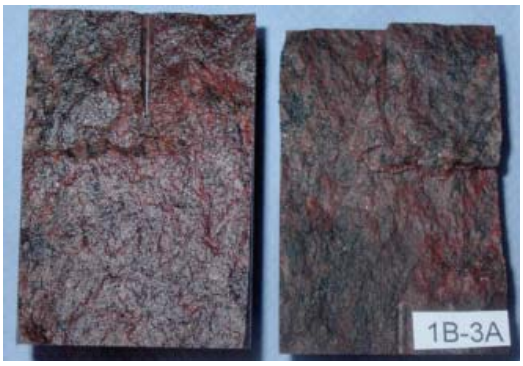

Sample no.: 1B-3C

operator	Küperkoch/Vogt/Witthaus
date	10.08.04 14:10-14:20

mean depth, m	428.09
axial load σ_1, MPa	36.26
confining pressure σ_3, MPa	28.18
breakdown pressure p_c, MPa	59.40
injection fluid	TELLUS32
injection rate, ml s^{-1}	1
remarks	axial fractured

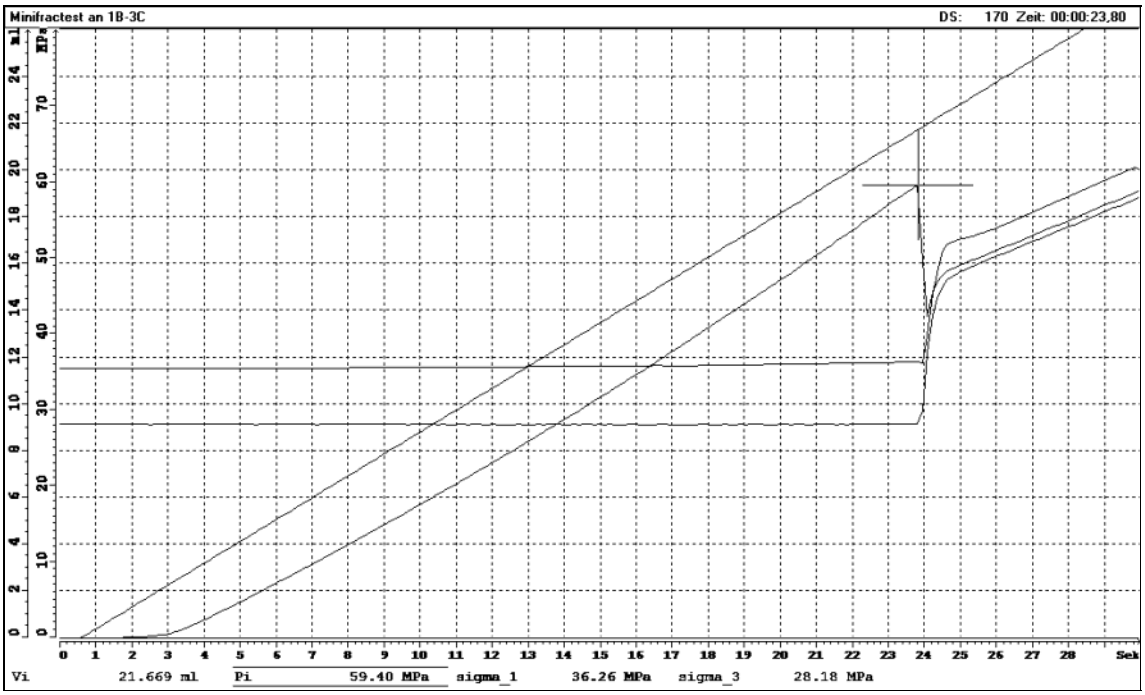

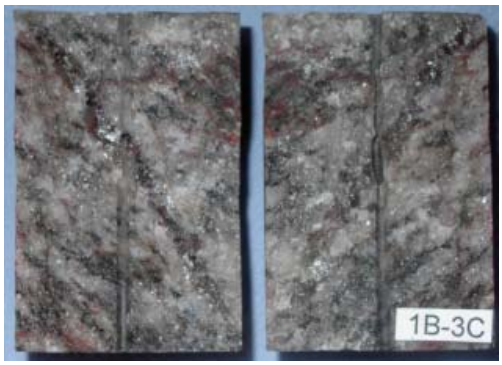

Sample no.: 1B-4A

operator	Vogt/Witthaus
date	09.08.04 14:20-14:30

mean depth, m	429.97
axial load σ_1, MPa	22.43
confining pressure σ_3, MPa	16.12
breakdown pressure p_c, MPa	40.84
injection fluid	TELLUS32
injection rate, ml s^{-1}	1
remarks	axial fractured

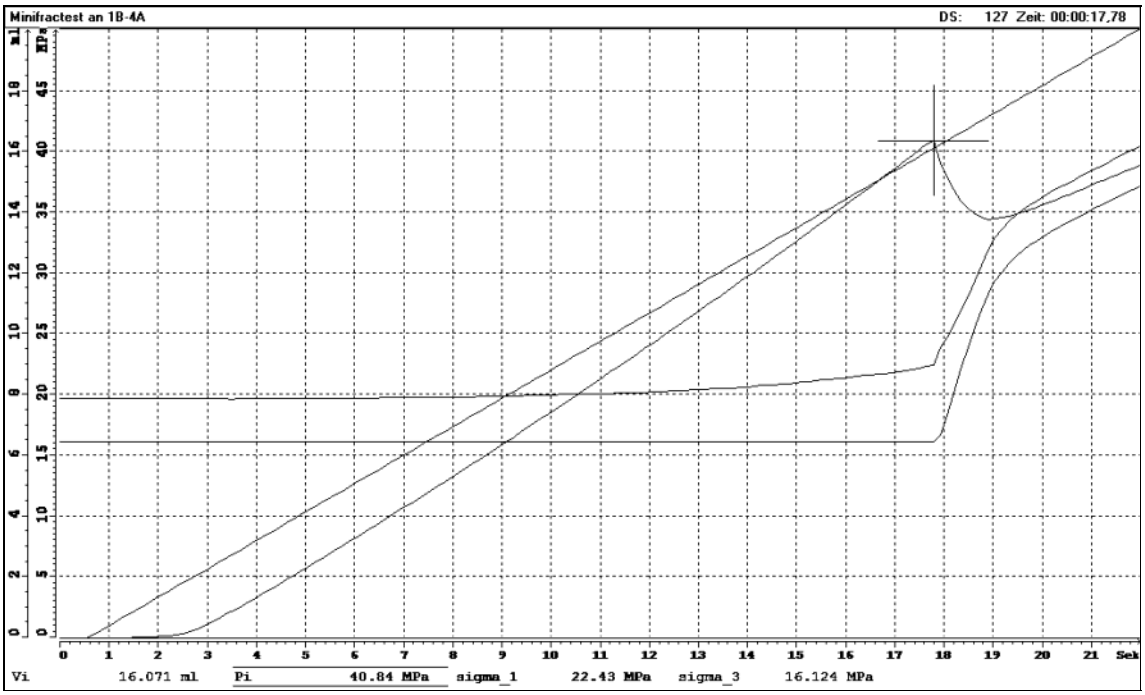

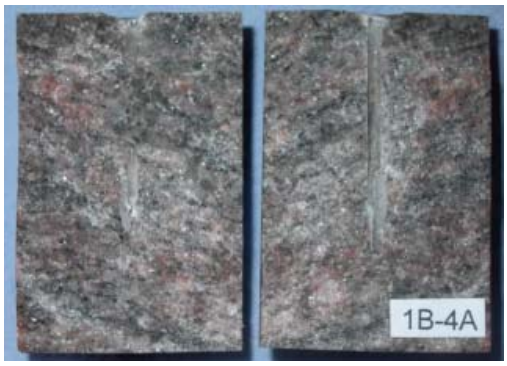

Sample no.: 1B-4C

operator	Vogt/Witthaus
date	10.08.04 14:20-14:30

mean depth, m	429.97
axial load σ_1, MPa	40.89
confining pressure σ_3, MPa	29.96
breakdown pressure p_c, MPa	132.42
injection fluid	TELLUS32
injection rate, ml s^{-1}	1
remarks	sealing in injection line, axial fractured

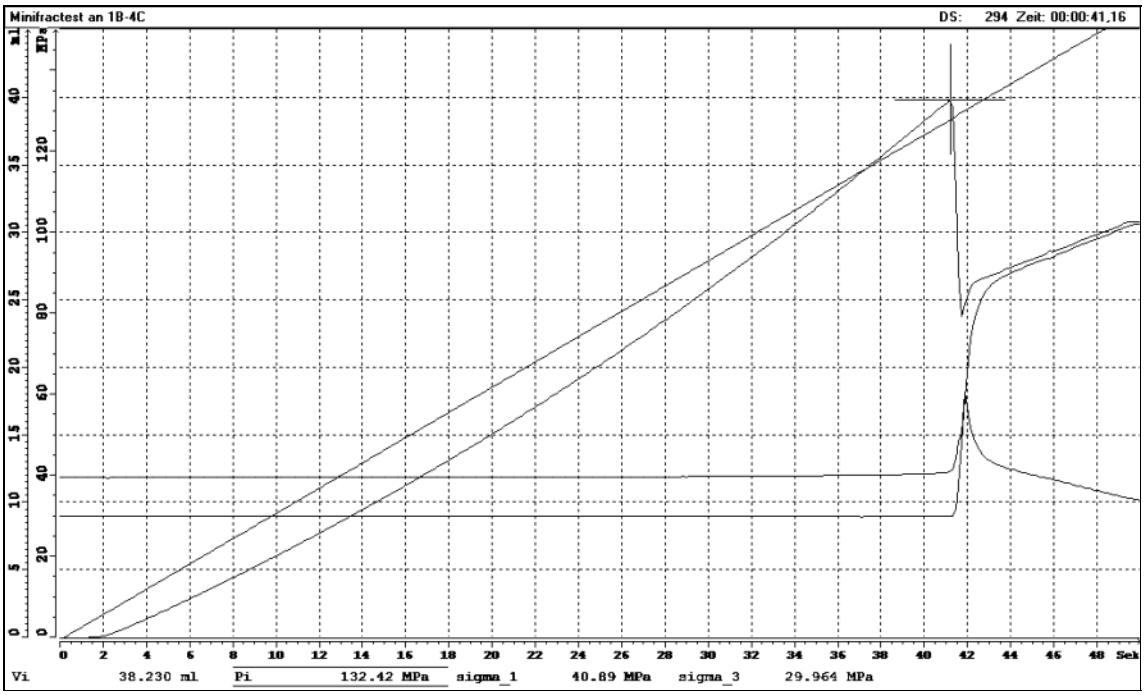

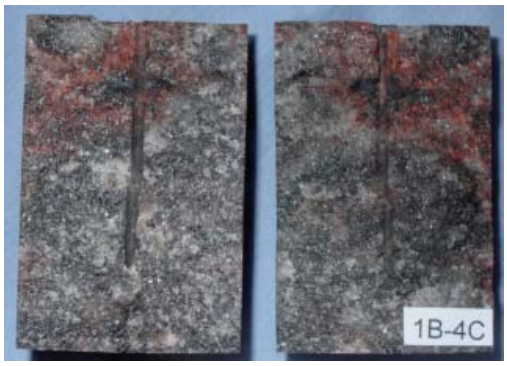

Sample no.: 1B-5A

operator	Küperkoch/Vogt/Witthaus
date	10.08.04 15:00-15:20

mean depth, m	430.43
axial load σ_1, MPa	32.41
confining pressure σ_3, MPa	25.42
breakdown pressure p_c, MPa	81.55
injection fluid	TELLUS32
injection rate, ml s^{-1}	1
remarks	axial and inclined fractured

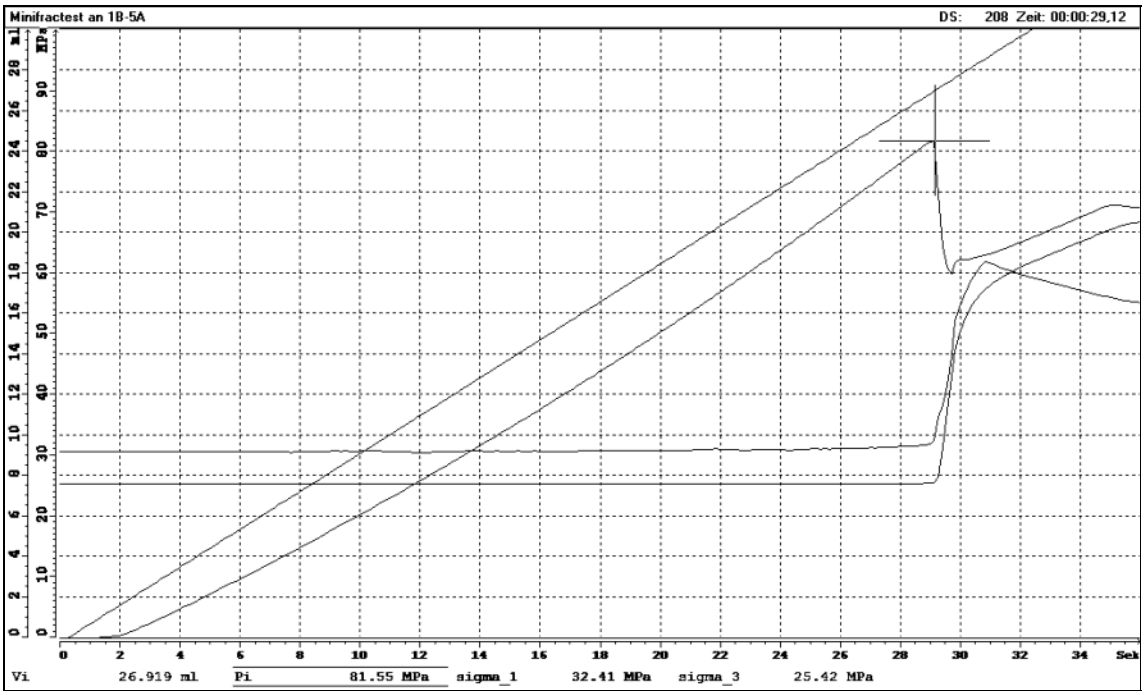

Sample no.: 1B-5C

operator	Küperkoch/Vogt/Witthaus
date	10.08.04 09:10-09:30

mean depth, m	430.43
axial load σ_1, MPa	10.97
confining pressure σ_3, MPa	5.62
breakdown pressure p_c, MPa	51.54
injection fluid	TELLUS32
injection rate, ml s^{-1}	1
remarks	axial fractured

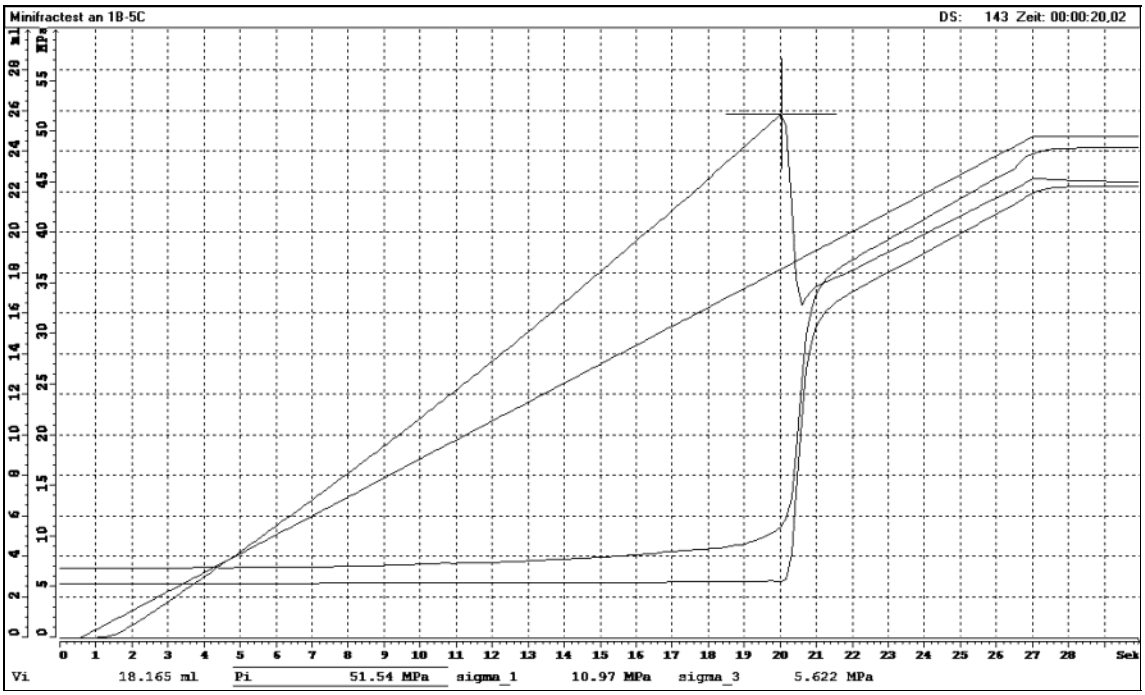

Sample no.: 1B-6A

operator	Küperkoch/Vogt/Witthaus
date	10.08.04 10:10-10:30

mean depth, m	455.13
axial load σ_1, MPa	55.52
confining pressure σ_3, MPa	25.02
breakdown pressure p_c, MPa	72.63
injection fluid	TELLUS32
injection rate, ml s^{-1}	1
remarks	axial and inclined fractured

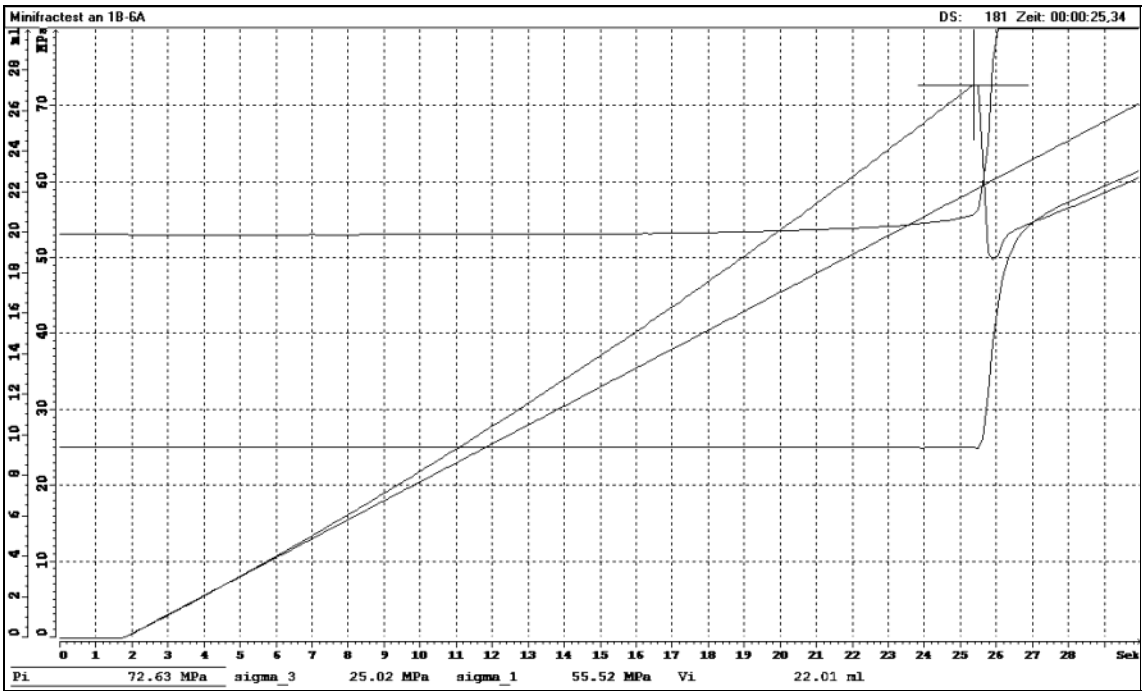

Sample no.: 1B-6C

operator	Küperkoch/Vogt/Witthaus
date	10.08.04 16:00-16:20

mean depth, m	455.13
axial load σ_1, MPa	15.36
confining pressure σ_3, MPa	12.24
breakdown pressure p_c, MPa	42.06
injection fluid	TELLUS32
injection rate, ml s^{-1}	1
remarks	axial fractured

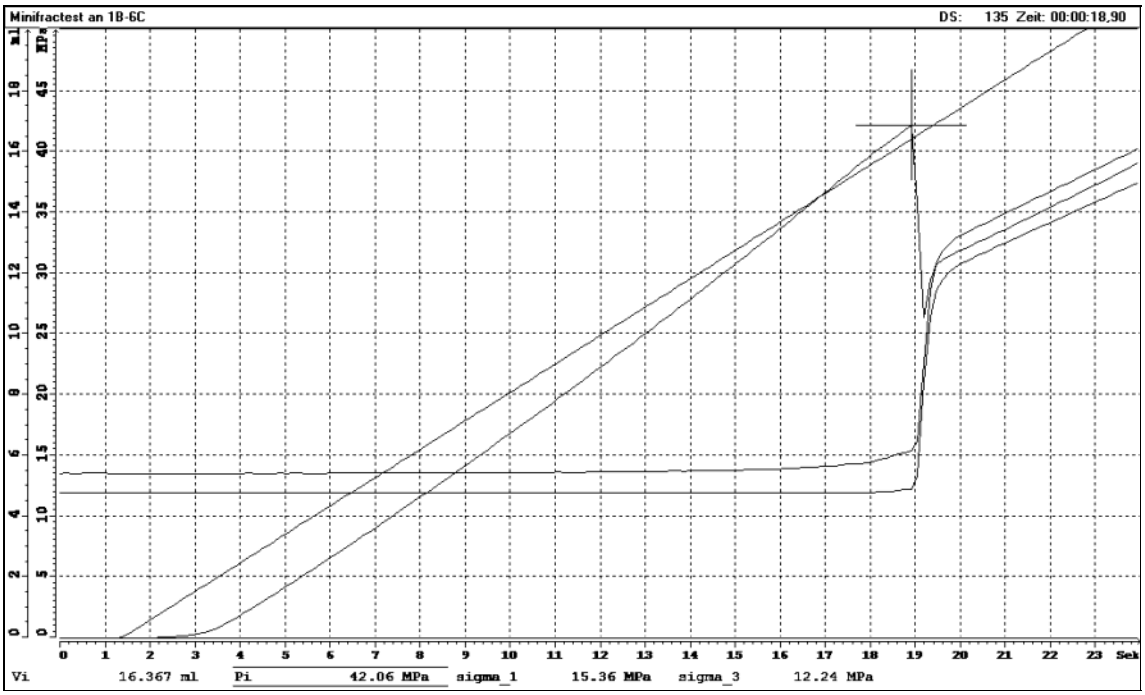

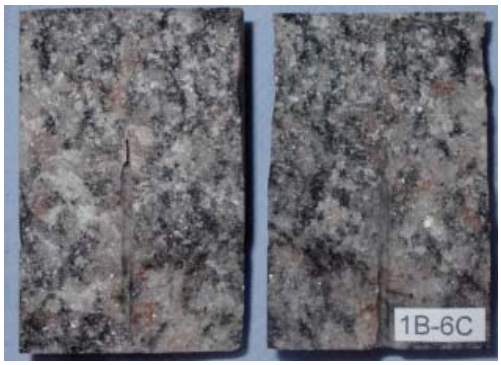

Sample no.: 1B-7A

operator	Küperkoch/Vogt/Witthaus
date	10.08.04 15:30-15:40

mean depth, m	456.20
axial load σ_1, MPa	22.33
confining pressure σ_3, MPa	16.92
breakdown pressure p_c, MPa	50.81
injection fluid	TELLUS32
injection rate, ml s^{-1}	1
remarks	axial fractured

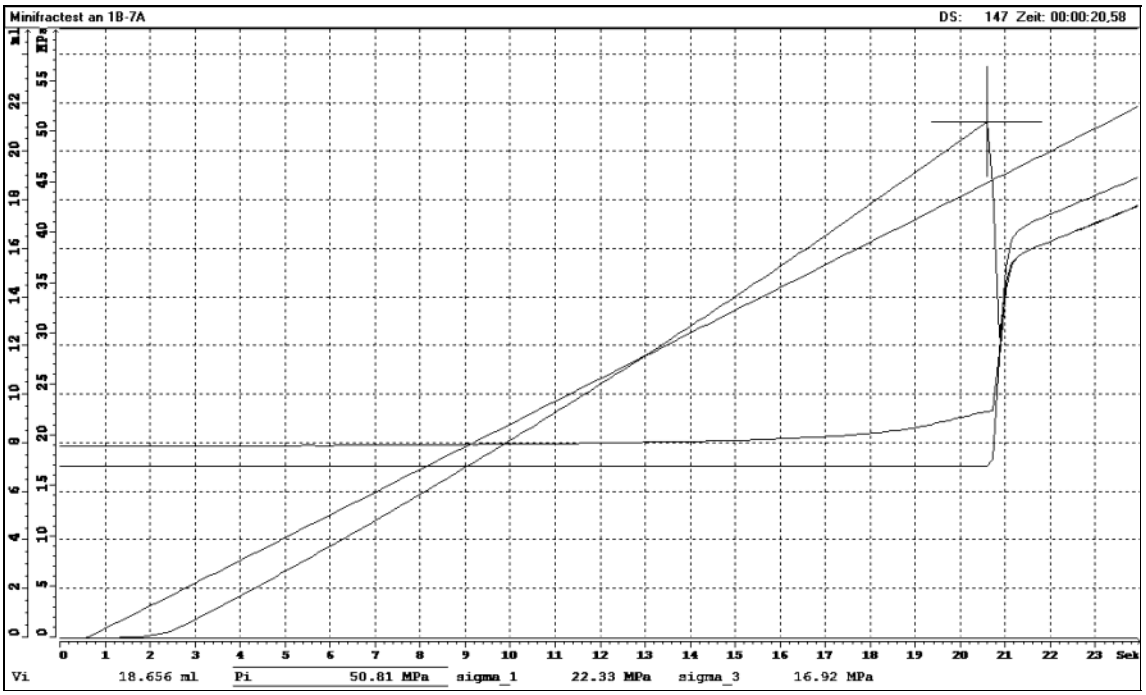

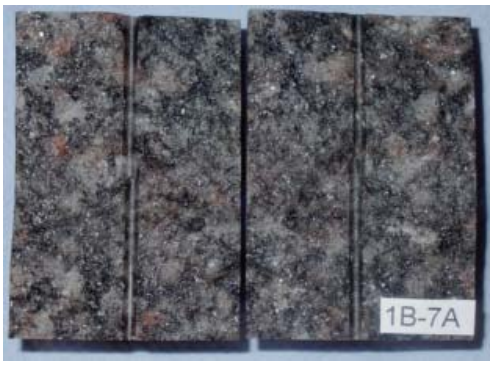

Sample no.: 1B-7C

operator	Vogt/Witthaus
date	10.08.04 15:40-16:00

mean depth, m	456.20
axial load σ_1, MPa	21.70
confining pressure σ_3, MPa	20.16
breakdown pressure p_c, MPa	30.74
injection fluid	TELLUS32
injection rate, ml s^{-1}	1
remarks	inclined fractured

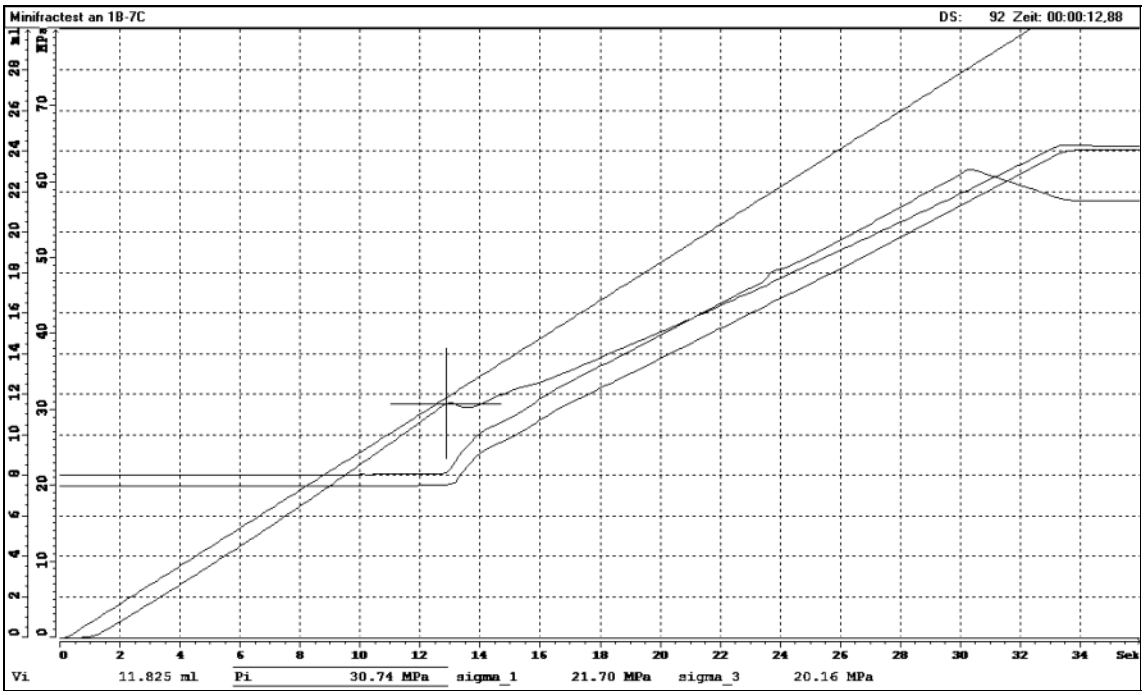

Sample no.: 2A-1A

operator	Küperkoch/Vogt/Witthaus
date	11.08.04 09:30-09:50

mean depth, m	220.84
axial load σ_1, MPa	22.85
confining pressure σ_3, MPa	20.07
breakdown pressure p_c, MPa	53.67
injection fluid	TELLUS32
injection rate, ml s^{-1}	1
remarks	axial fractured, Refrac?

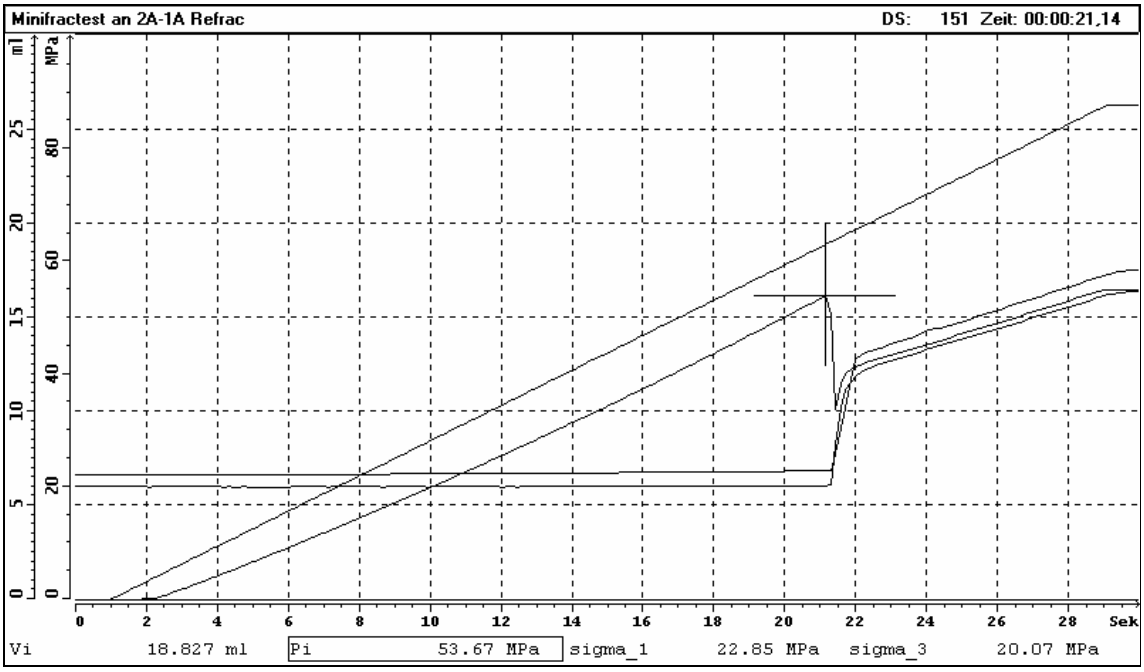

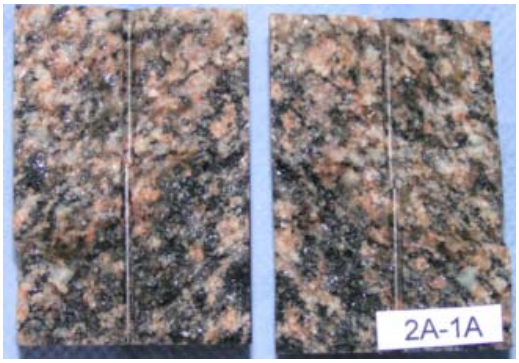

Sample no.: 2A-1C

operator	Küperkoch/Vogt/Witthaus
date	11.08.04 10:30-10:50

mean depth, m	220.84
axial load σ_1, MPa	15.46
confining pressure σ_3, MPa	10.04
breakdown pressure p_c, MPa	43.36
injection fluid	TELLUS32
injection rate, ml s^{-1}	1
remarks	axial fractured

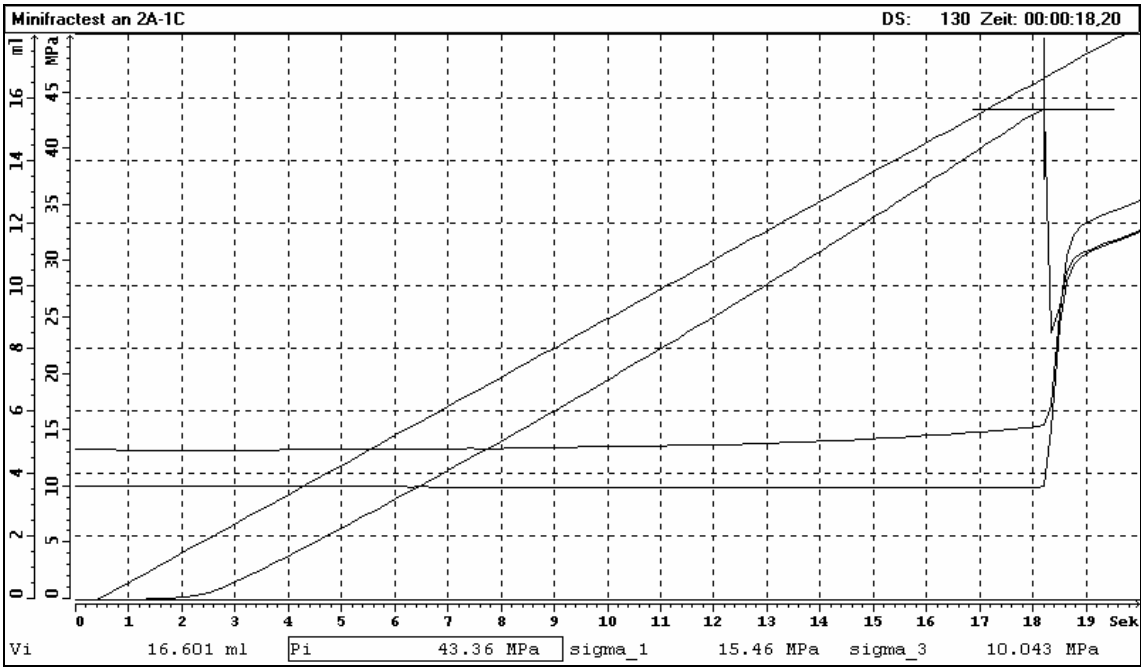

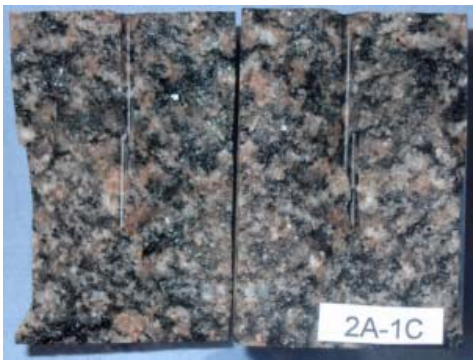

Sample no.: 2A-2A

operator	Küperkoch/Vogt/Witthaus
date	11.08.04 11:30-11:50

mean depth, m	226.04
axial load σ_1, MPa	34.87
confining pressure σ_3, MPa	30.51
breakdown pressure p_c, MPa	44.98
injection fluid	TELLUS32
injection rate, ml s^{-1}	1
remarks	axial fractured, Refrac?

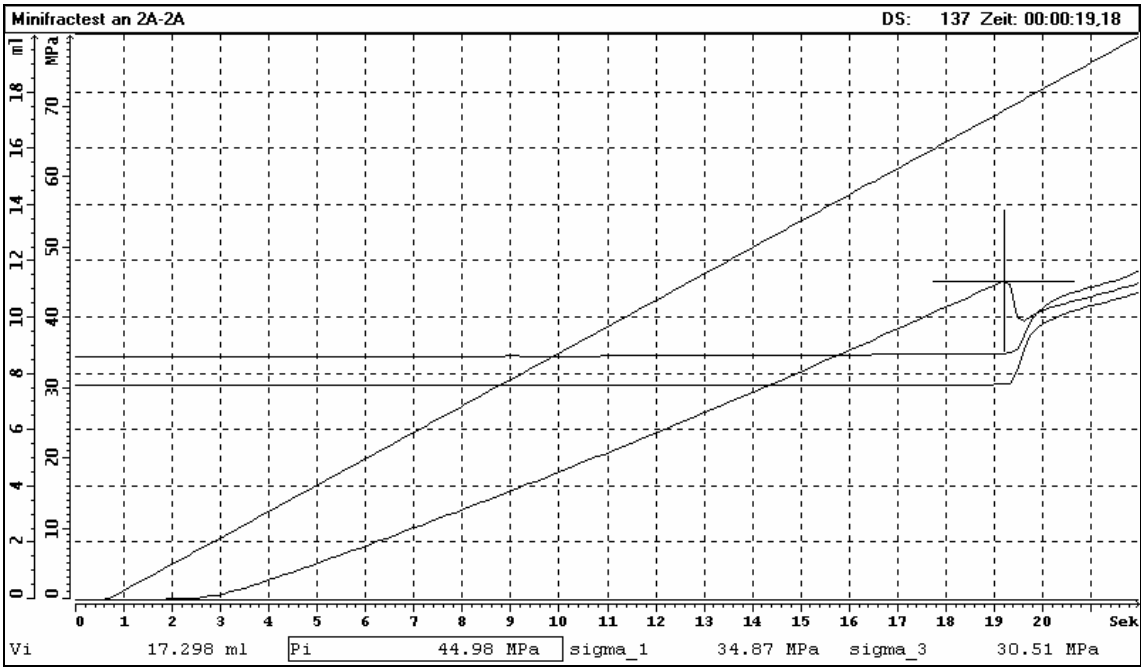

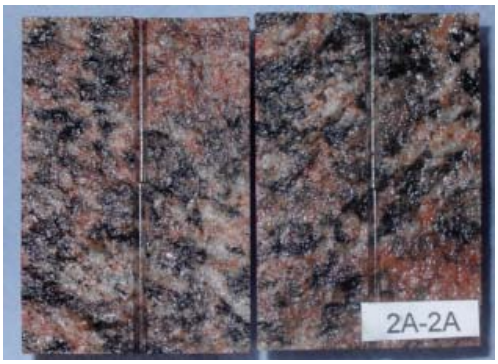

Sample no.: 2A-2C

operator	Vogt/Witthaus
date	11.08.04 13:30-13:50

mean depth, m	226.04
axial load σ_1, MPa	29.70
confining pressure σ_3, MPa	25.01
breakdown pressure p_c, MPa	61.56
injection fluid	TELLUS32
injection rate, ml s^{-1}	1
remarks	axial fractured

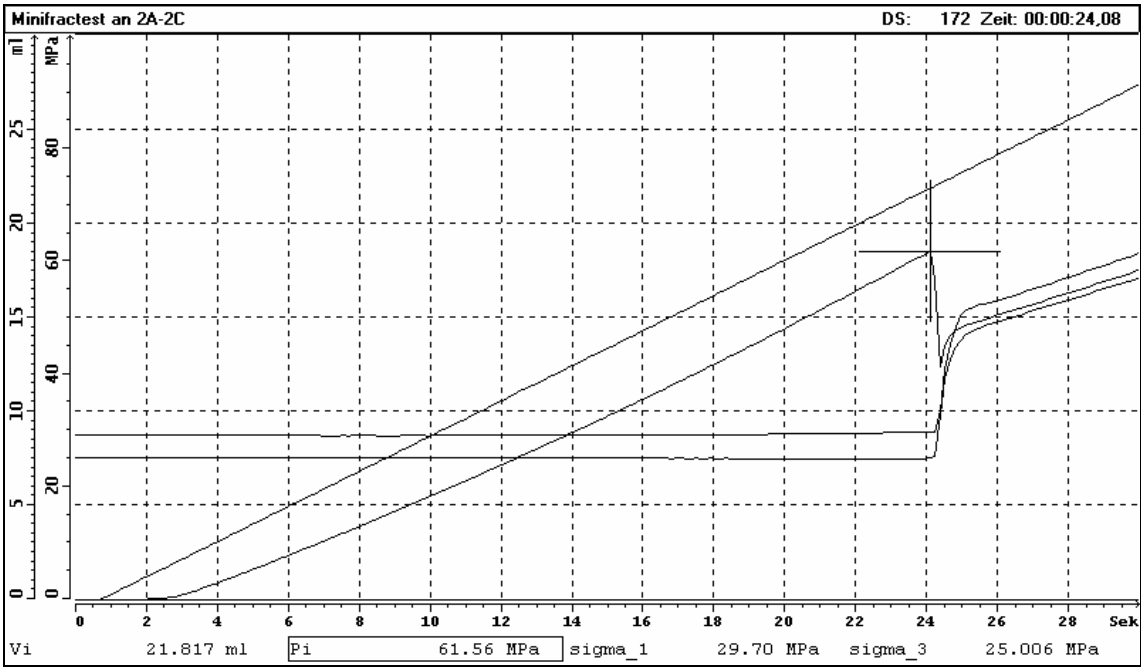

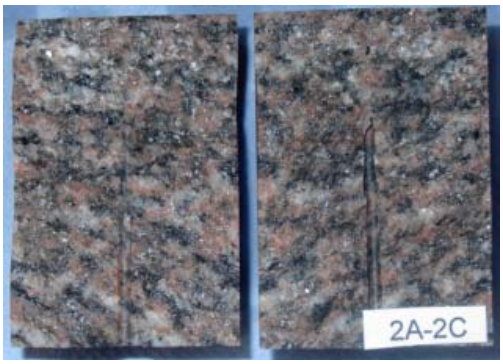

Sample no.: 2A-3A

operator	Vogt/Witthaus
date	11.08.04 14:30-14:50

mean depth, m	396.04
axial load σ_1, MPa	45.00
confining pressure σ_3, MPa	17.74
breakdown pressure p_c, MPa	44.99
injection fluid	TELLUS32
injection rate, ml s^{-1}	1
remarks	axial fractured

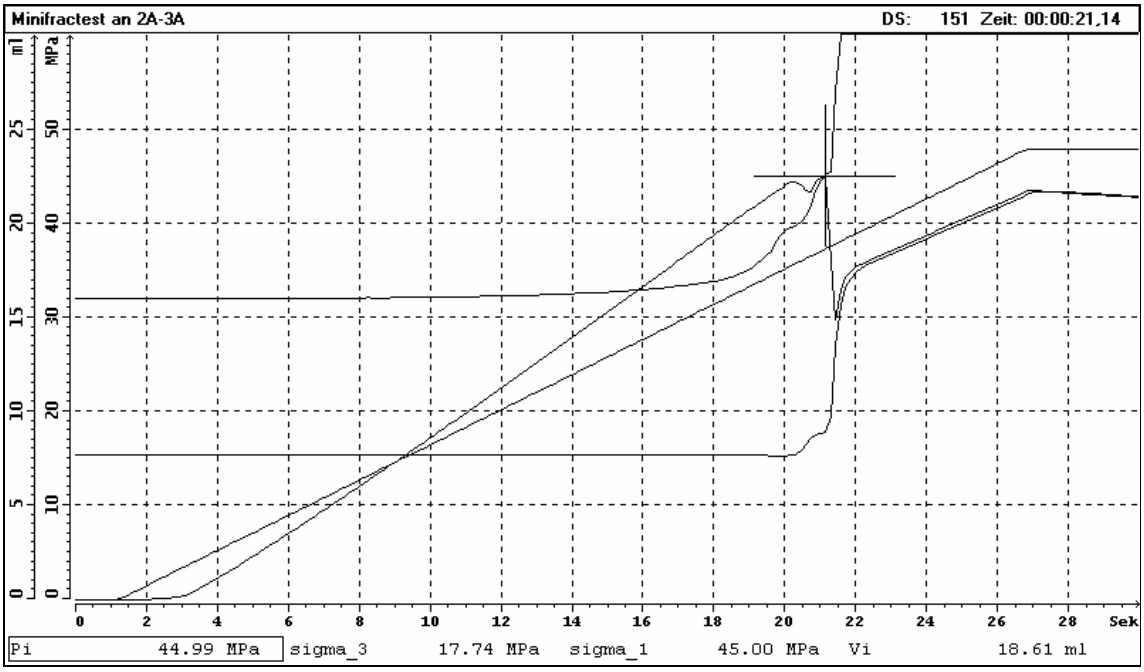

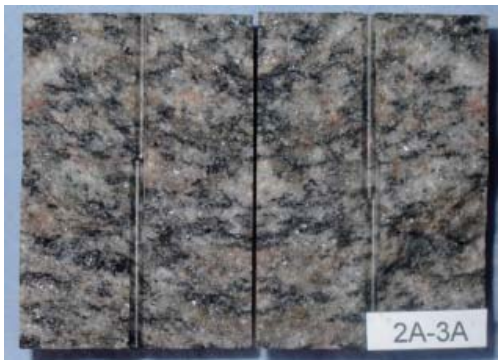

Sample no.: 2A-3C

operator	Küperkoch/Vogt
date	11.08.04 15:30-15:50

mean depth, m	386.04
axial load σ_1, MPa	23.11
confining pressure σ_3, MPa	17.38
breakdown pressure p_c, MPa	50.34
injection fluid	TELLUS32
injection rate, ml s^{-1}	1
remarks	axial fractured

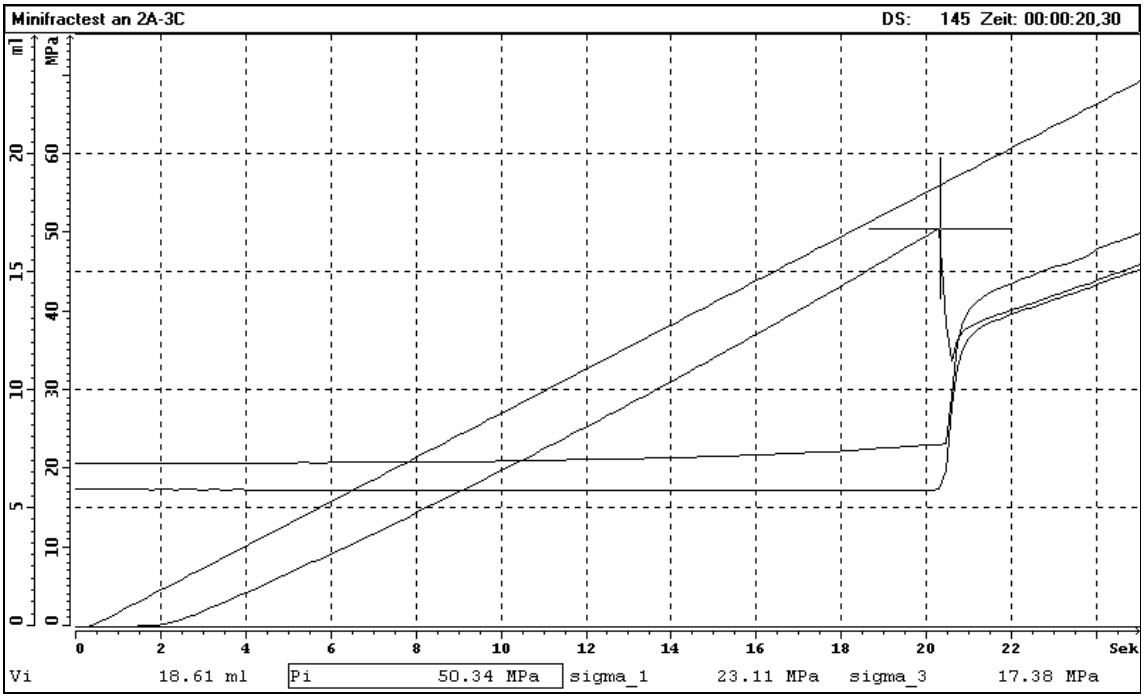

Sample no.: 2A-4A

operator	Vogt
date	13.08.04 09:30-10:30

mean depth, m	414.07
axial load σ_1, MPa	49.49
confining pressure σ_3, MPa	29.52
breakdown pressure p_c, MPa	79.64
injection fluid	TELLUS32
injection rate, ml s^{-1}	1
remarks	axial fractured

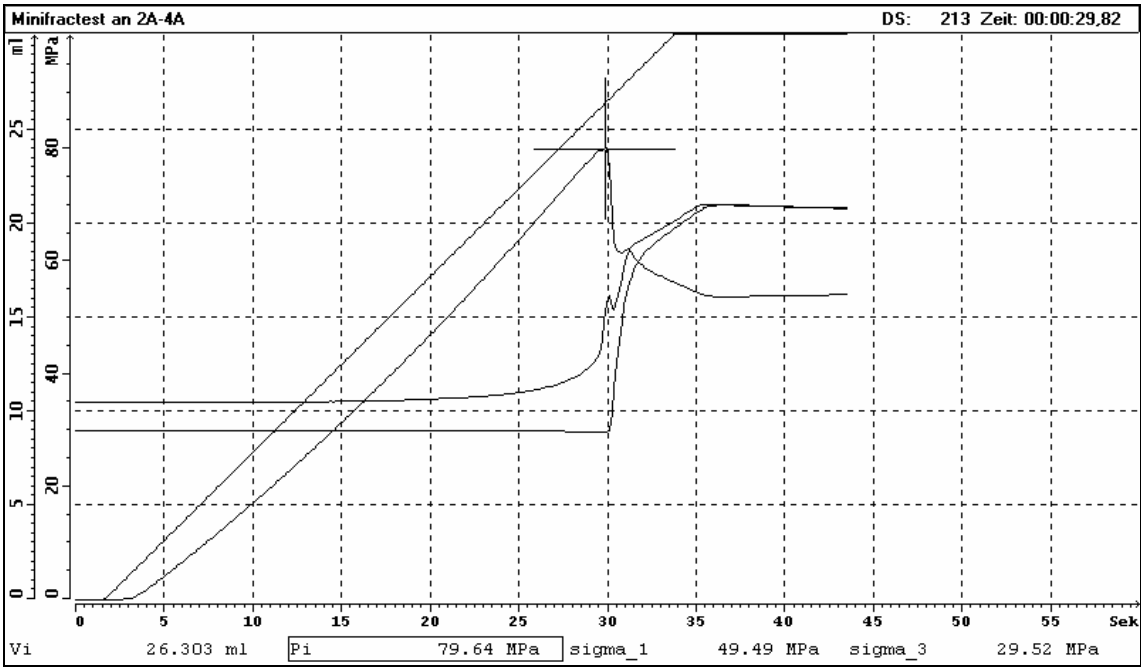

Sample no.: 2A-4C

operator	Vogt
date	13.08.04 12:30-12:40

mean depth, m	414.07
axial load σ_1, MPa	28.76
confining pressure σ_3, MPa	22.49
breakdown pressure p_c, MPa	58.15
injection fluid	TELLUS32
injection rate, ml s^{-1}	1
remarks	axial fractured

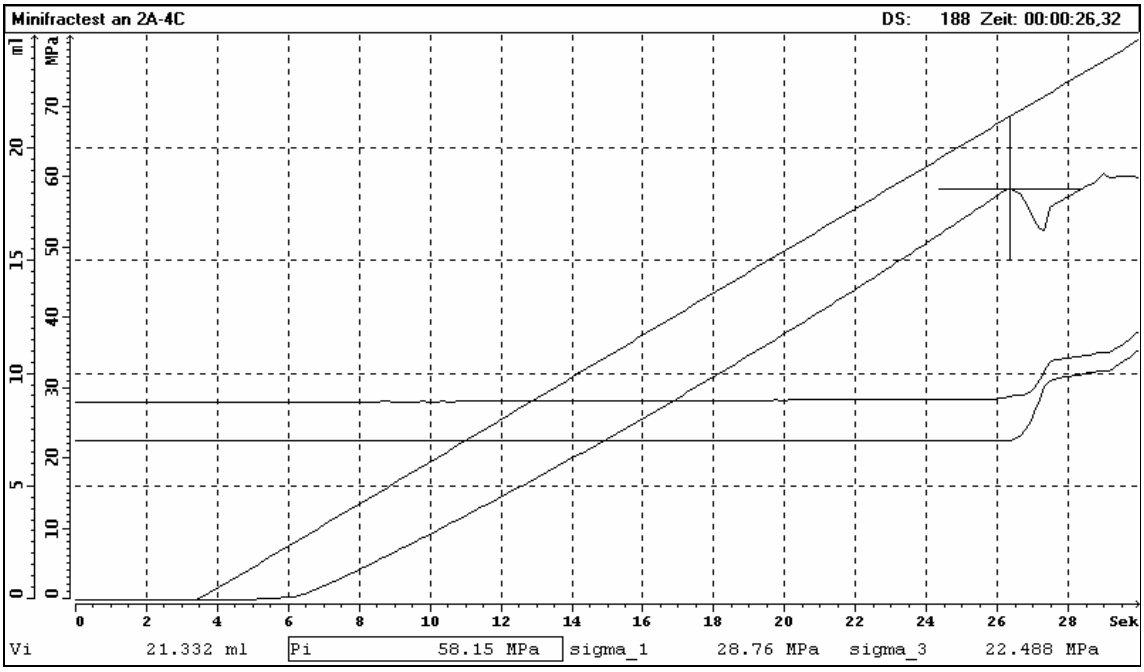

Sample no.: 2A-5A

operator	Vogt
date	16.08.04 14:50-15:00

mean depth, m	451.32
axial load σ_1, MPa	12.08
confining pressure σ_3, MPa	7.64
breakdown pressure p_c, MPa	39.20
injection fluid	TELLUS32
injection rate, ml s^{-1}	1
remarks	axial fractured

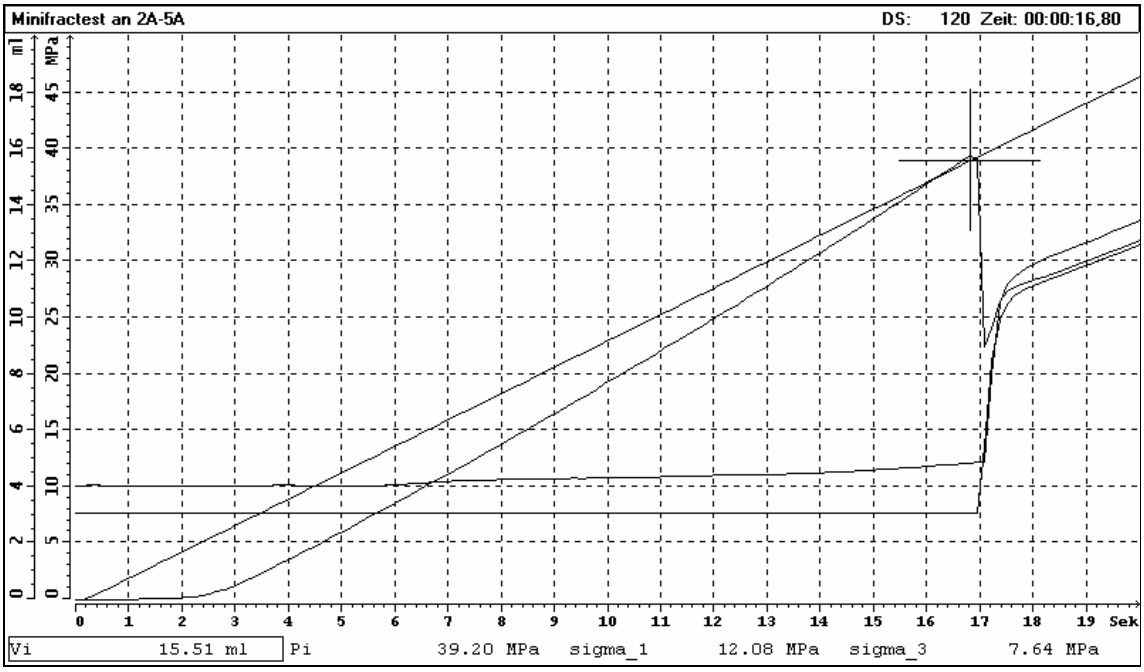

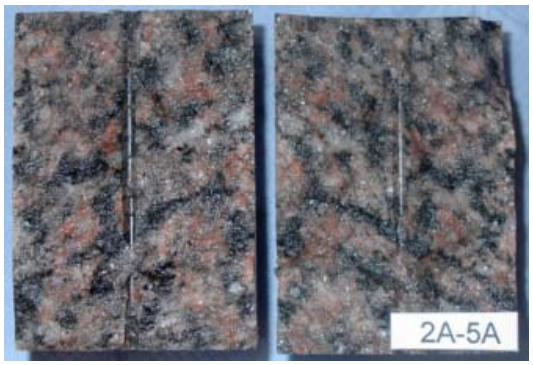

Sample no.: 2A-5C

operator	Vogt
date	16.08.04 15:30-15:50

mean depth, m	451.32
axial load σ_1, MPa	11.37
confining pressure σ_3, MPa	5.60
breakdown pressure p_c, MPa	29.34
injection fluid	TELLUS32
injection rate, ml s^{-1}	1
remarks	axial fractured

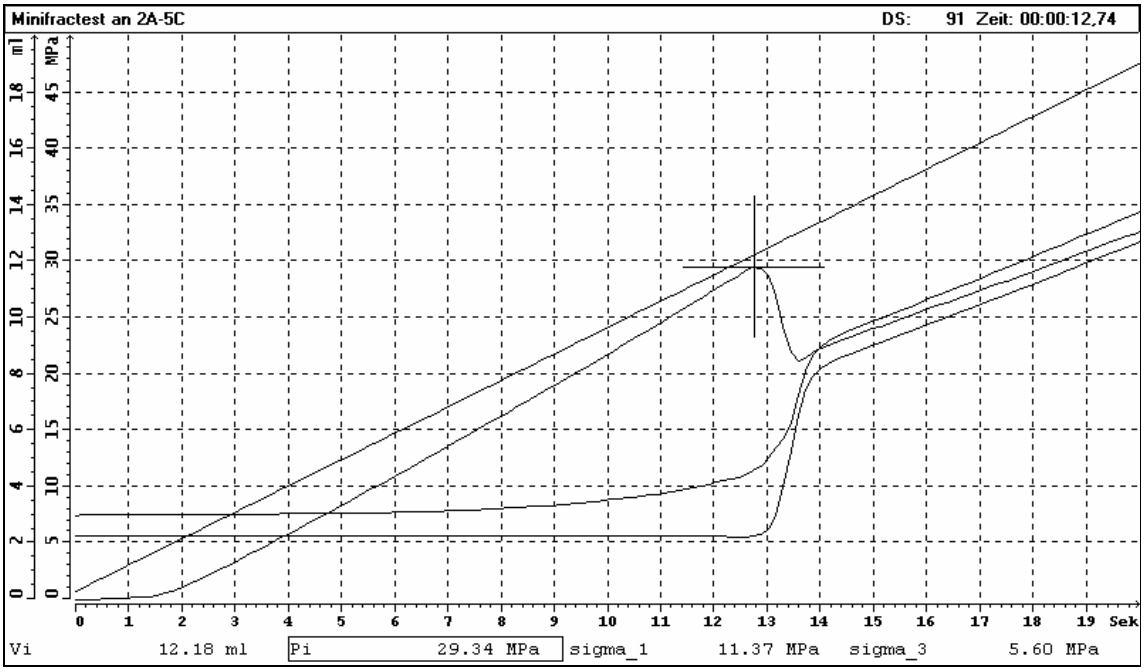

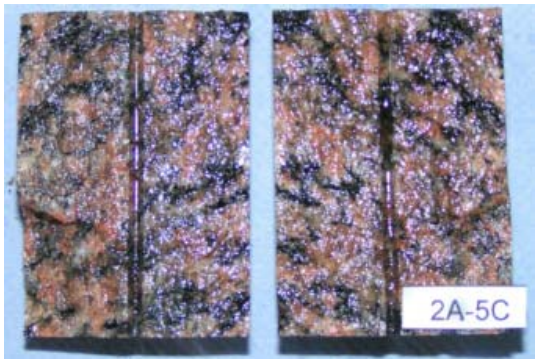

Sample no.: 2A-6A

operator	Vogt
date	16.08.04 16:20-16:30

mean depth, m	554.39
axial load σ_1, MPa	19.25
confining pressure σ_3, MPa	6.42
breakdown pressure p_c, MPa	35.62
injection fluid	TELLUS32
injection rate, ml s^{-1}	1
remarks	axial fractured

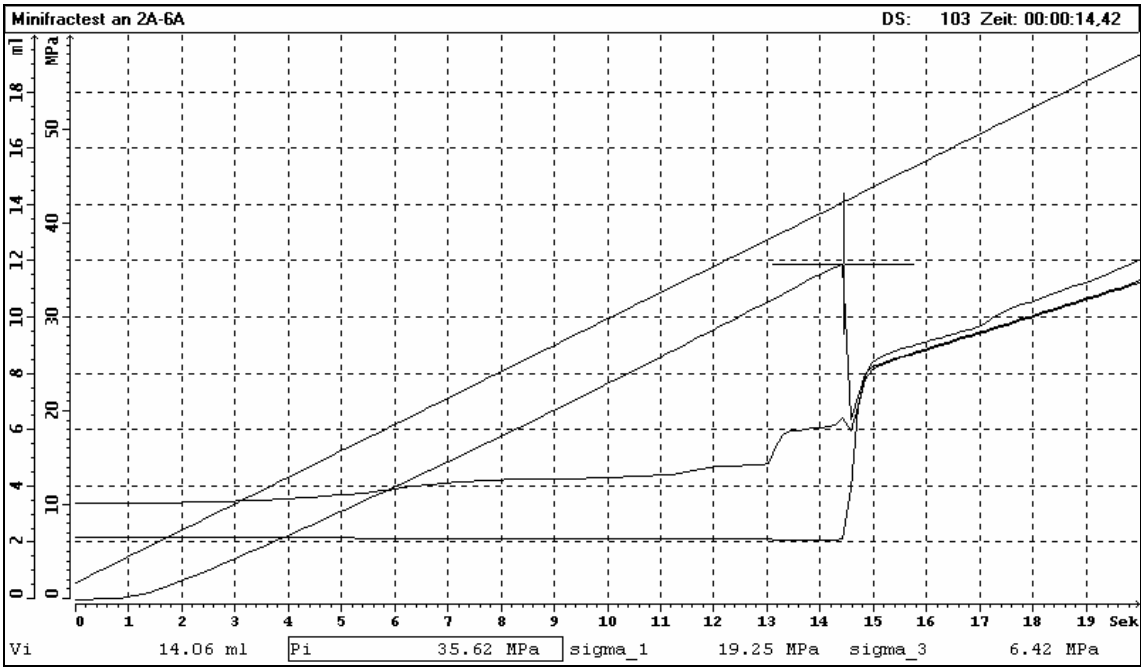

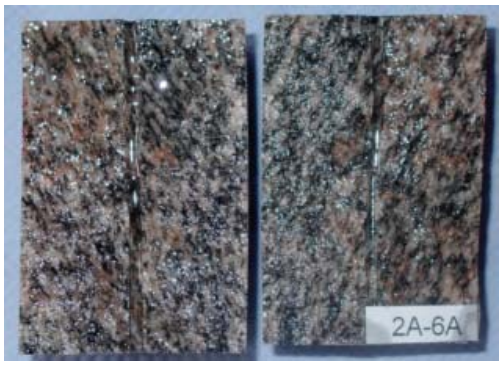

Sample no.: 2A-6C

operator	Schreiner/Vogt
date	17.08.04 10:10-10:30

mean depth, m	554.39
axial load σ_1, MPa	36.22
confining pressure σ_3, MPa	28.67
breakdown pressure p_c, MPa	77.43
injection fluid	TELLUS32
injection rate, ml s^{-1}	1
remarks	axial fractured

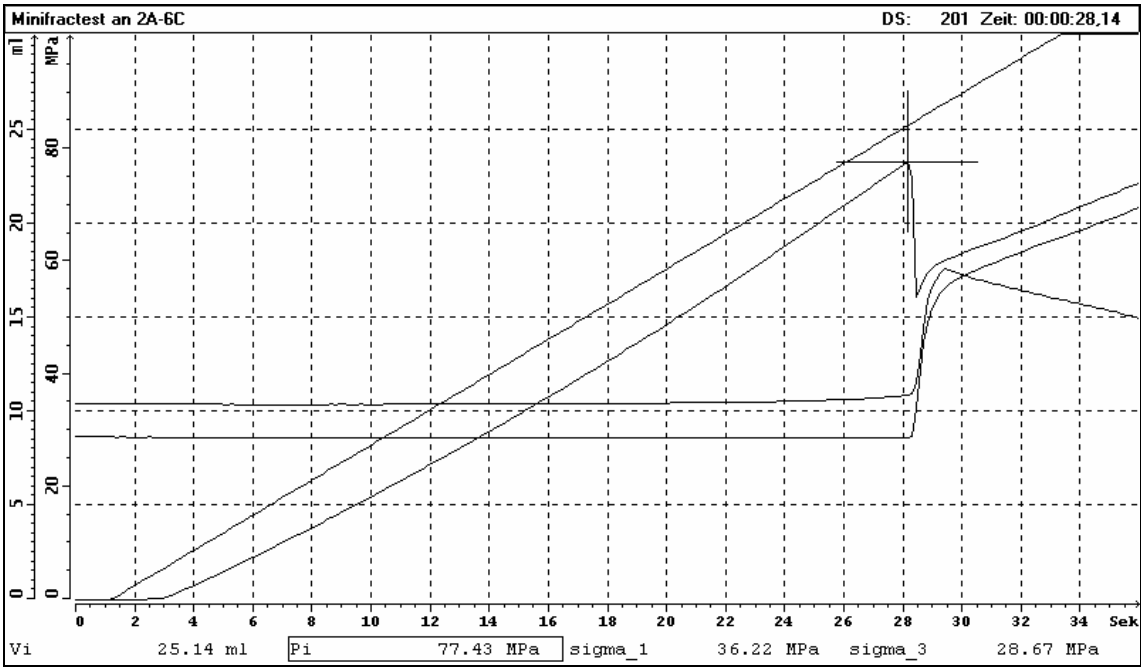

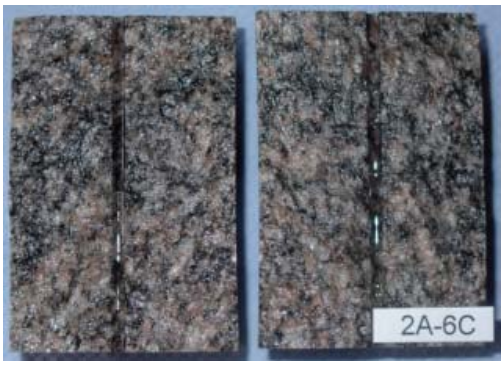

Sample no.: 2A-7A

operator	Schreiner/Vogt
date	23.08.04 15:50-16:10

mean depth, m	594.38
axial load σ_1, MPa	40.23
confining pressure σ_3, MPa	29.39
breakdown pressure p_c, MPa	60.80
injection fluid	TELLUS32
injection rate, ml s^{-1}	1
remarks	axial and inclined fractured

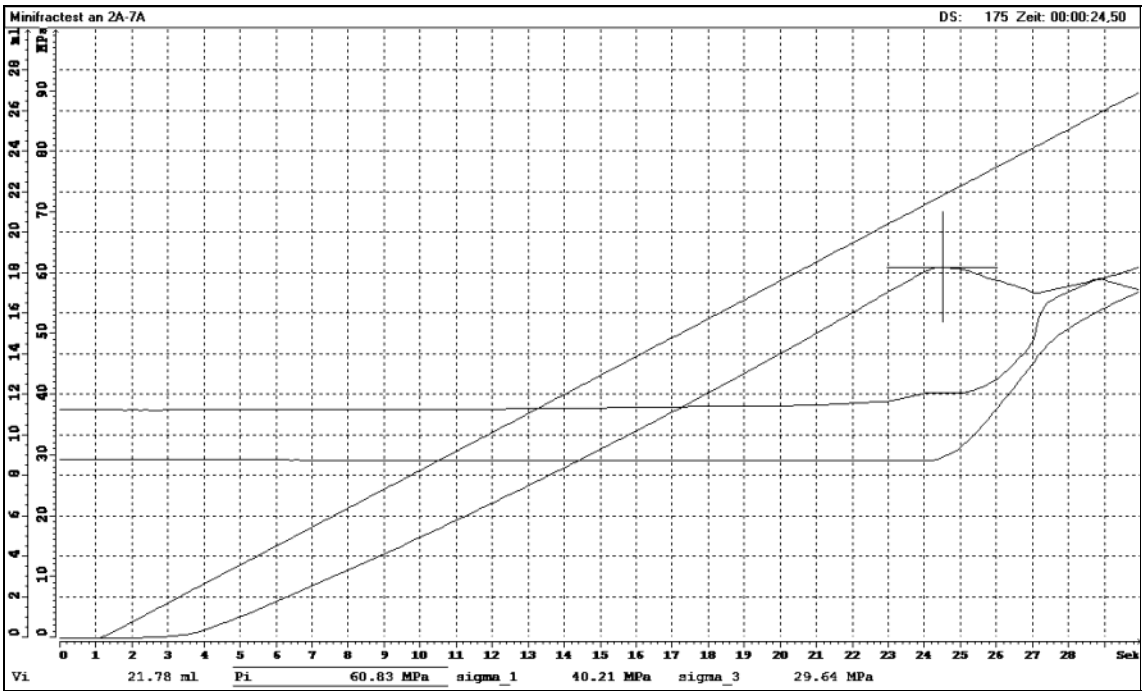

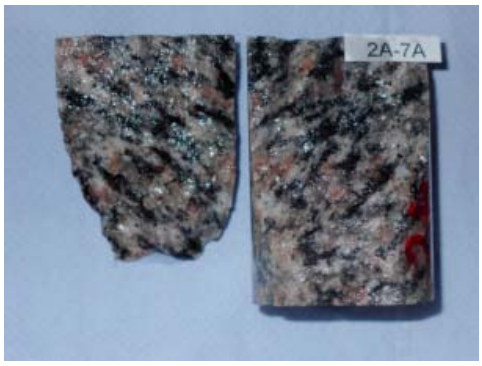

Sample no.: 2A-7C

operator	Schreiner/Vogt
date	23.08.04 14:30-14:50

mean depth, m	594.38
axial load σ_1, MPa	23.05
confining pressure σ_3, MPa	15.38
breakdown pressure p_c, MPa	47.14
injection fluid	TELLUS32
injection rate, ml s^{-1}	1
remarks	axial fractured

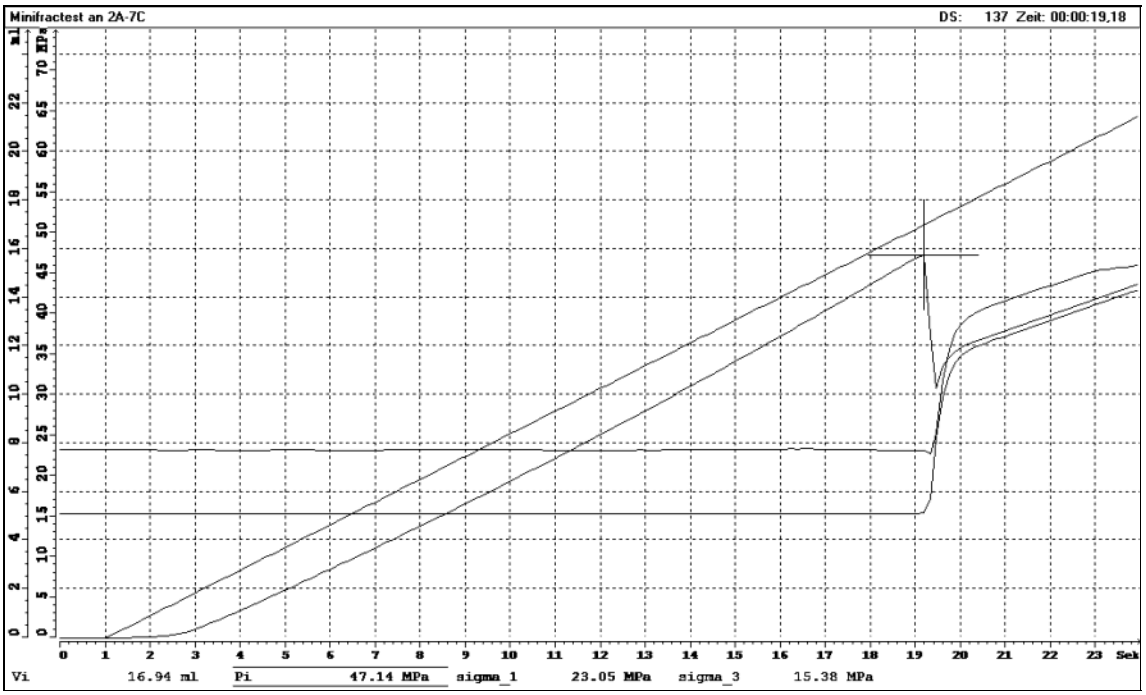

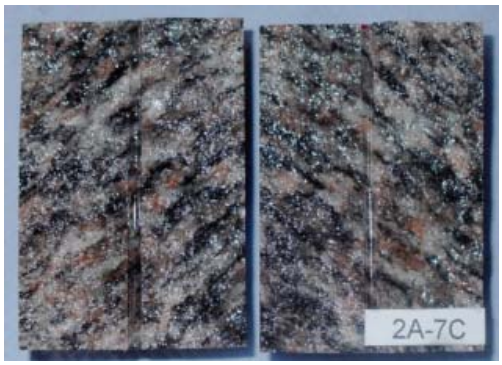

Sample no.: 2A-8A

operator	Vogt
date	23.08.04 16:40-16:50

mean depth, m	602.92
axial load σ_1, MPa	23.41
confining pressure σ_3, MPa	18.78
breakdown pressure p_c, MPa	54.29
injection fluid	TELLUS32
injection rate, ml s^{-1}	1
remarks	axial fractured

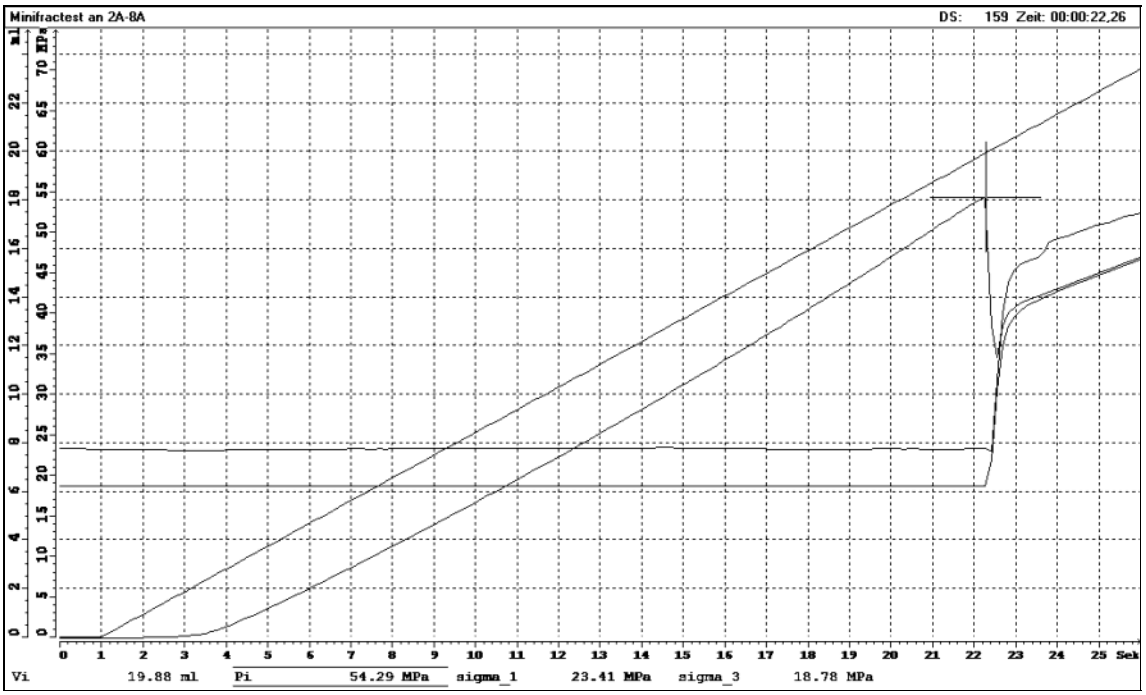

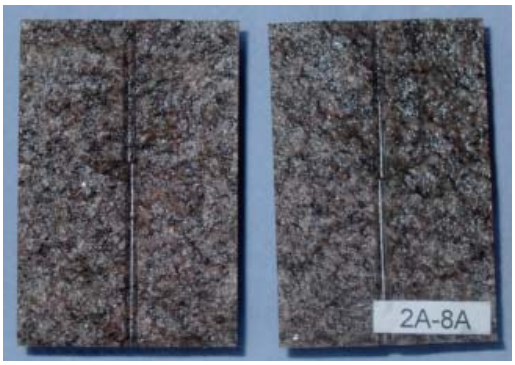

Sample no.: 2A-8C

operator	Vogt
date	16.08.04 13:20-13:30

mean depth, m	602.92
axial load σ_1, MPa	38.59
confining pressure σ_3, MPa	27.33
breakdown pressure p_c, MPa	64.95
injection fluid	TELLUS32
injection rate, ml s^{-1}	1
remarks	axial fractured

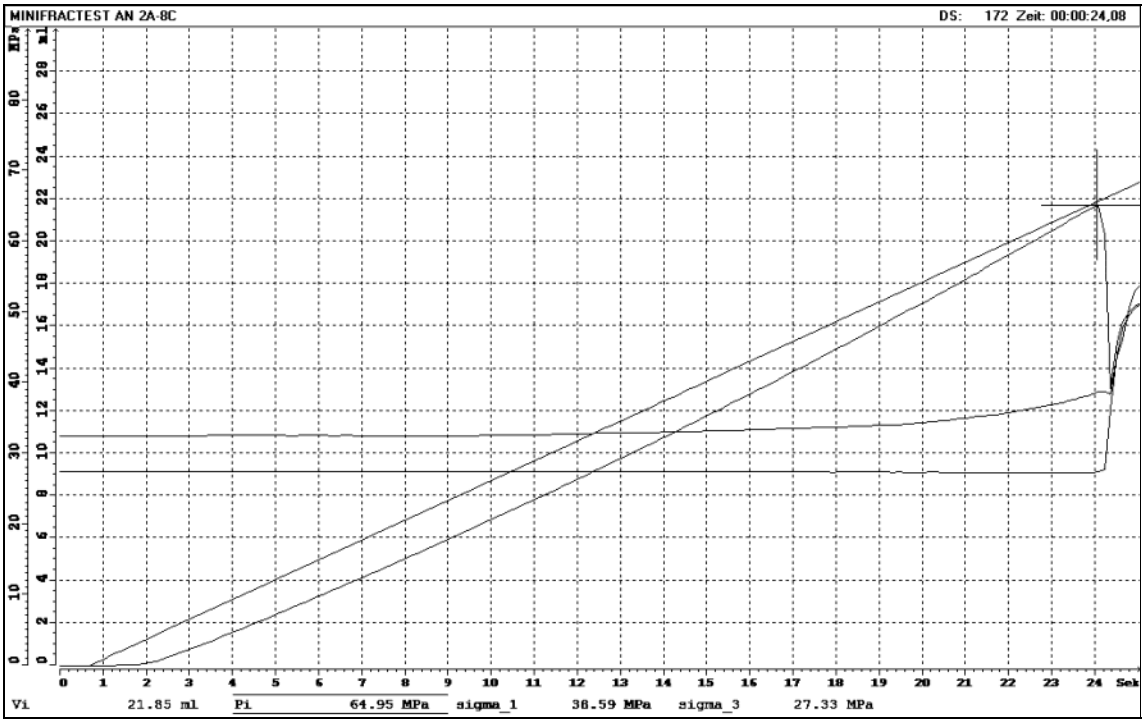

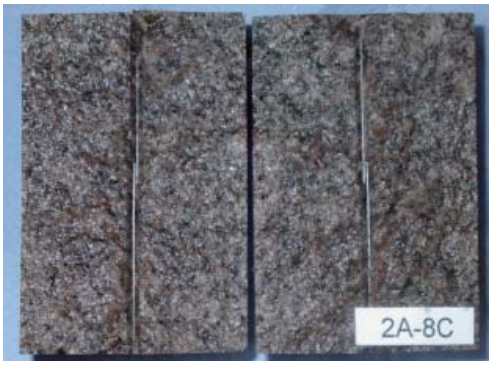

Sample no.: 2A-9A

operator	Vogt
date	16.08.04 11:10-11:30

mean depth, m	699.83
axial load σ_1, MPa	20.55
confining pressure σ_3, MPa	12.42
breakdown pressure p_c, MPa	40.98
injection fluid	TELLUS32
injection rate, ml s^{-1}	1
remarks	axial fractured

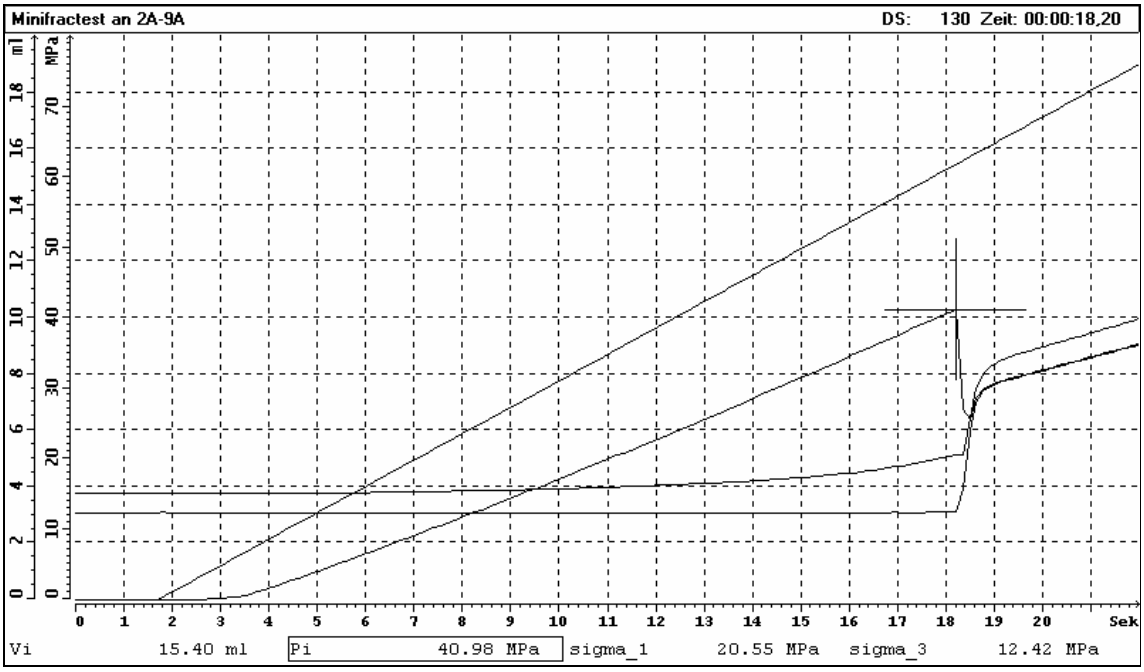

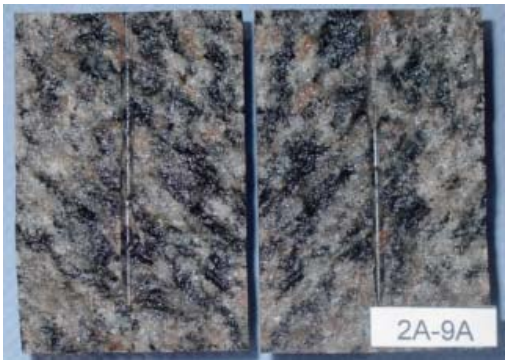

Sample no.: 2A-9C

operator	Vogt
date	23.08.04 15:00-15:20

mean depth, m	699.83
axial load σ_1, MPa	19.07
confining pressure σ_3, MPa	13.71
breakdown pressure p_c, MPa	44.34
injection fluid	TELLUS32
injection rate, ml s^{-1}	1
remarks	axial fractured

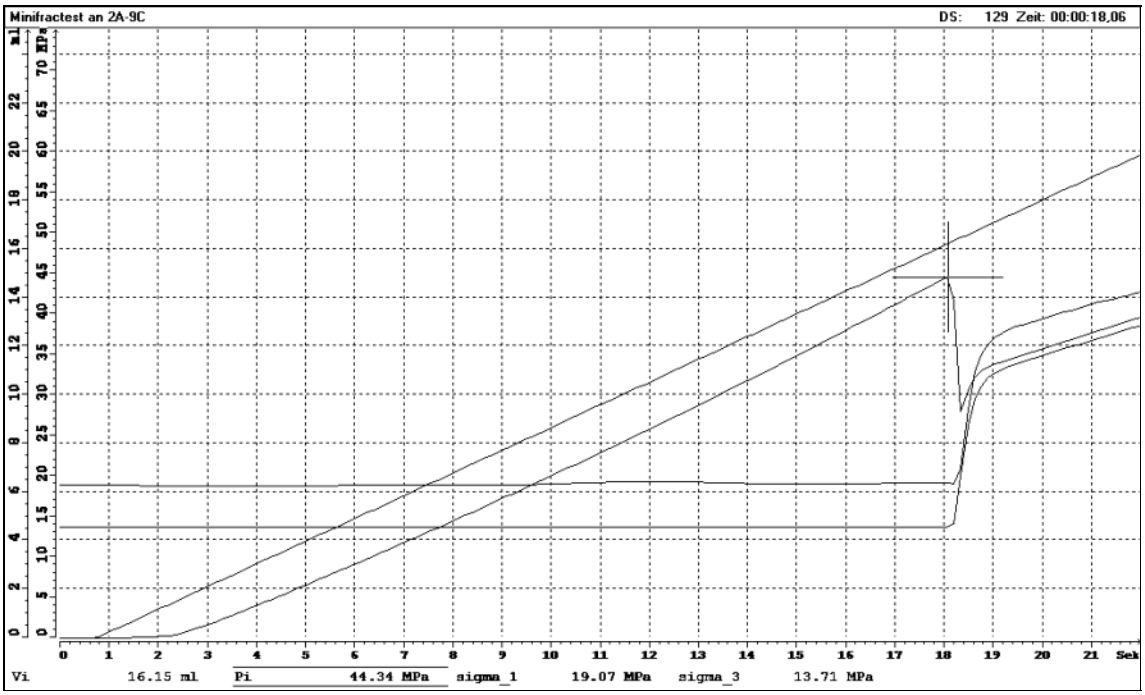

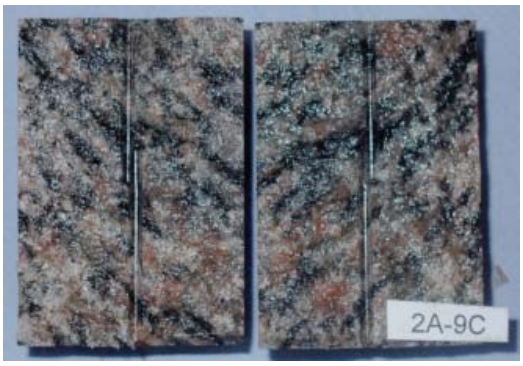

Sample no.: 2A-10A

operator	Vogt
date	16.08.04 14:10-14:30

mean depth, m	702.82
axial load σ_1, MPa	31.94
confining pressure σ_3, MPa	29.84
breakdown pressure p_c, MPa	54.40
injection fluid	TELLUS32
injection rate, ml s^{-1}	1
remarks	axial fractured, Refrac?

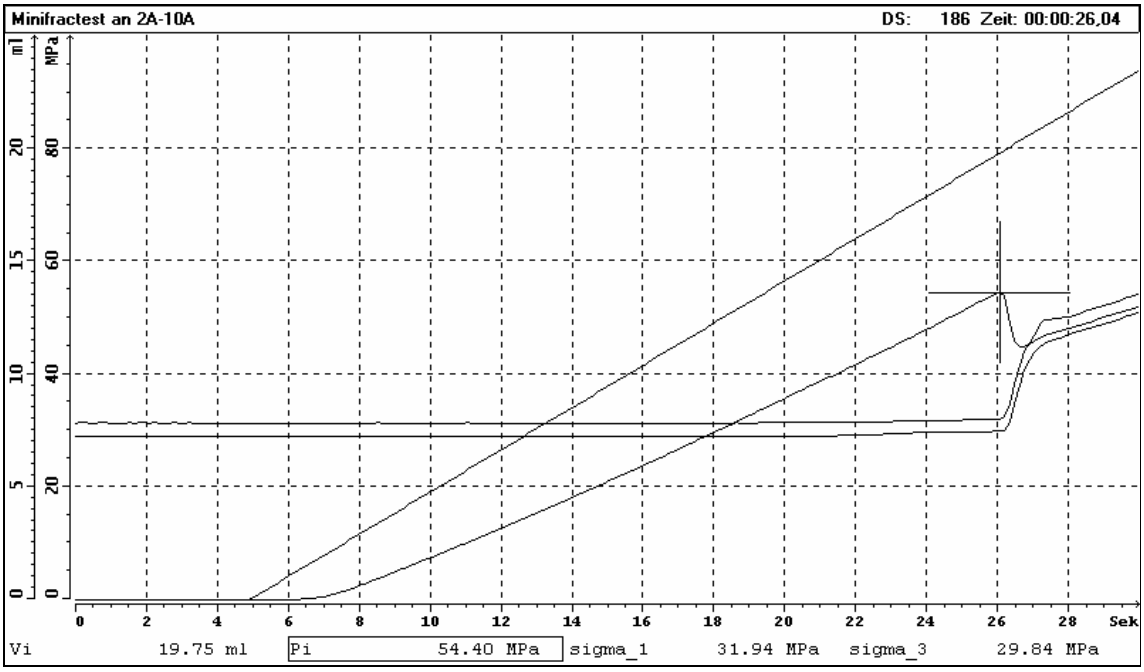

Sample no.: 4A-1A

operator	Küperkoch
date	27.08.04 09:30-09:50

mean depth, m	192.28
axial load σ_1, MPa	22.91
confining pressure σ_3, MPa	19.80
breakdown pressure p_c, MPa	57.57
injection fluid	TELLUS32
injection rate, ml s^{-1}	1
remarks	axial fractured

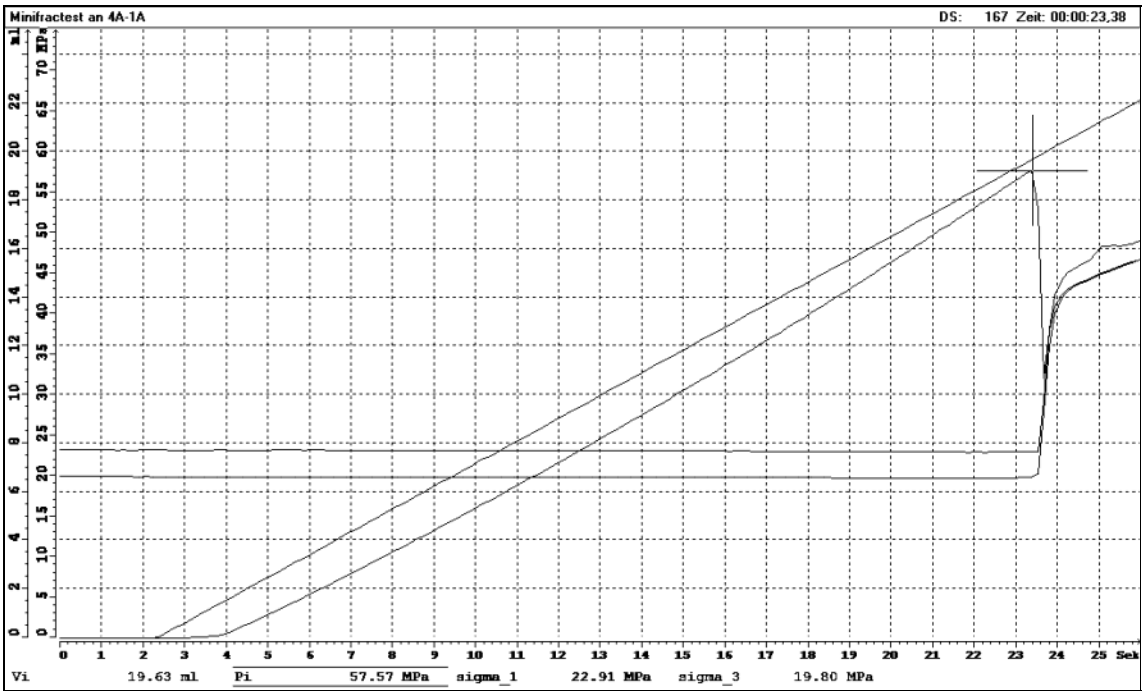

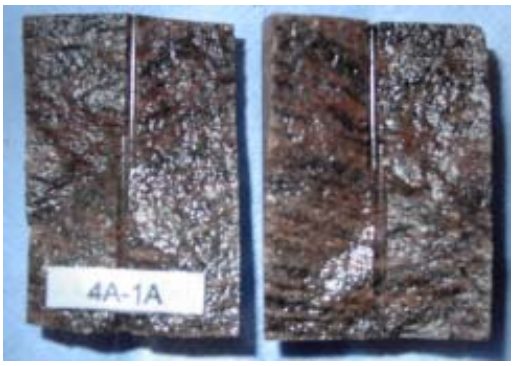

Sample no.: 4A-1C

operator	Küperkoch
date	30.08.04 09:00-09:20

mean depth, m	192.28
axial load σ_1, MPa	48.80
confining pressure σ_3, MPa	24.19
breakdown pressure p_c, MPa	68.36
injection fluid	TELLUS32
injection rate, ml s^{-1}	1
remarks	axial and inclined fractured

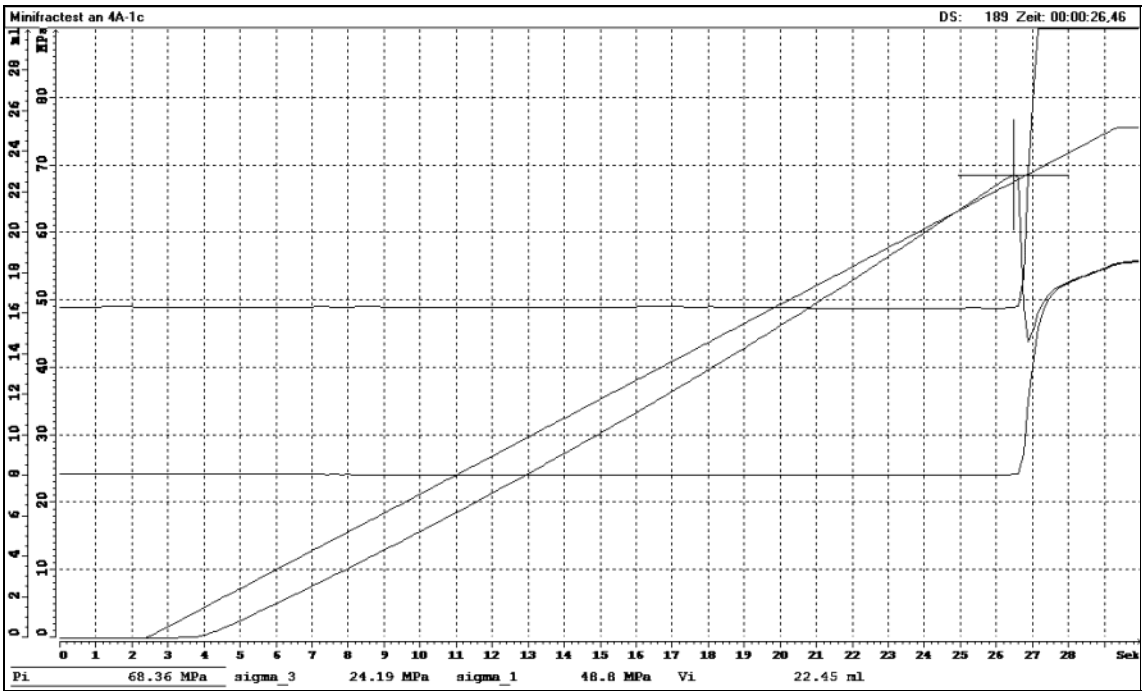

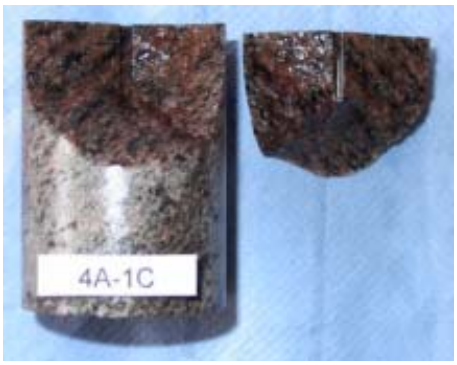

Sample no.: 4A-2A

operator	Küperkoch
date	30.08.04 11:10-11:20

mean depth, m	192.61
axial load σ_1, MPa	26.95
confining pressure σ_3, MPa	22.19
breakdown pressure p_c, MPa	63.64
injection fluid	TELLUS32
injection rate, ml s^{-1}	1
remarks	axial fractured

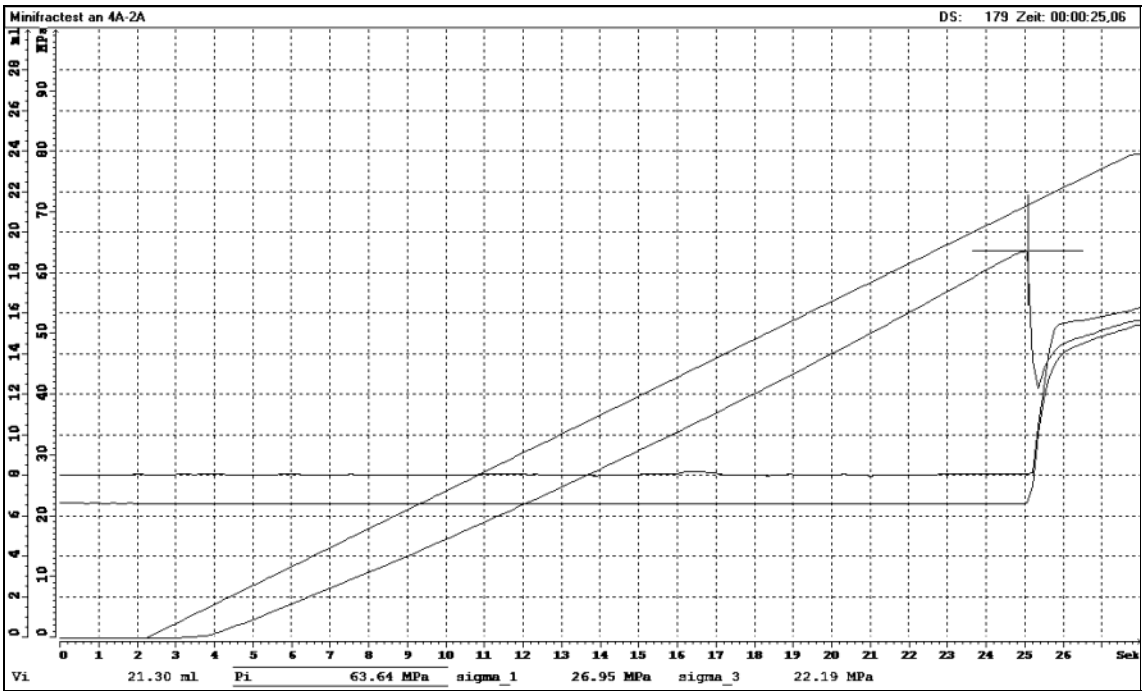

Sample no.: 4A-2C

operator	Küperkoch
date	30.08.04 11:45-11:55

mean depth, m	192.61
axial load σ_1, MPa	25.66
confining pressure σ_3, MPa	17.87
breakdown pressure p_c, MPa	57.07
injection fluid	TELLUS32
injection rate, ml s^{-1}	1
remarks	axial fractured

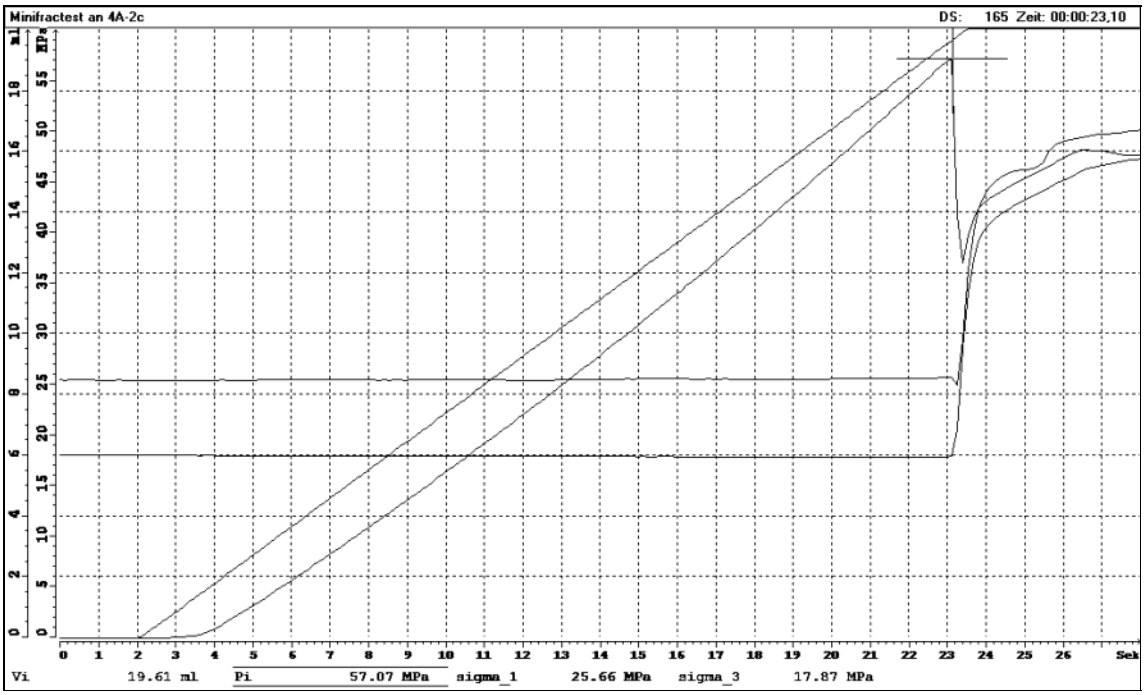

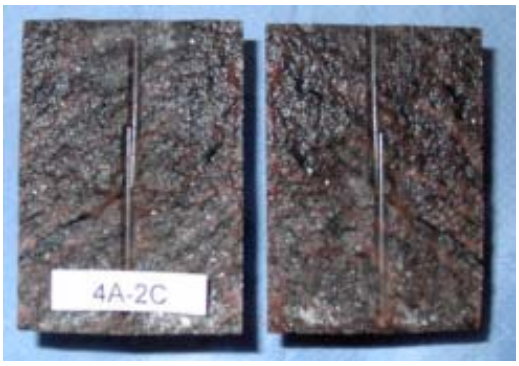

Sample no.: 4A-3A

operator	Küperkoch/Vogt
date	30.08.04 13:05-13:25

mean depth, m	260.31
axial load σ_1, MPa	34.83
confining pressure σ_3, MPa	25.95
breakdown pressure p_c, MPa	69.55
injection fluid	TELLUS32
injection rate, ml s^{-1}	1
remarks	axial fractured

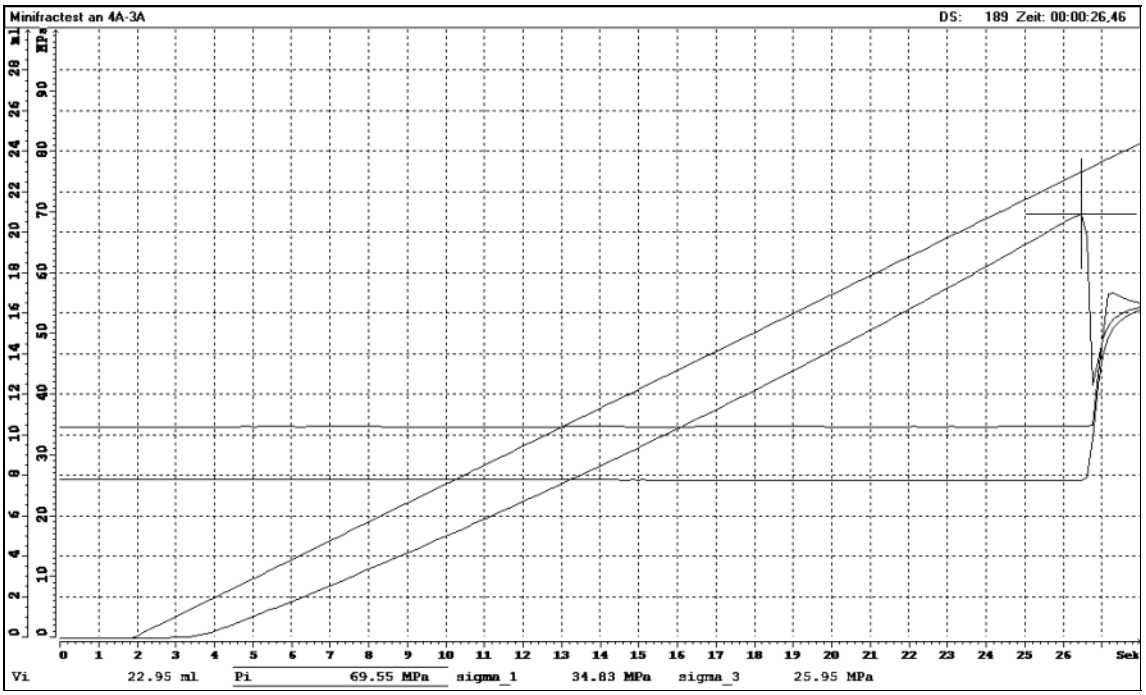

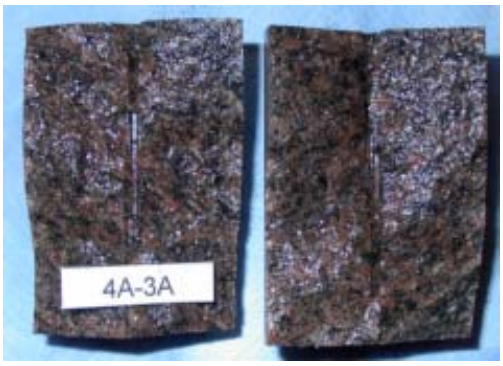

Sample no.: 4A-3C

operator	Küperkoch/Vogt
date	30.08.04 13:30-13:40

mean depth, m	260.31
axial load σ_1, MPa	21.50
confining pressure σ_3, MPa	16.02
breakdown pressure p_c, MPa	57.41
injection fluid	TELLUS32
injection rate, ml s^{-1}	1
remarks	axial fractured

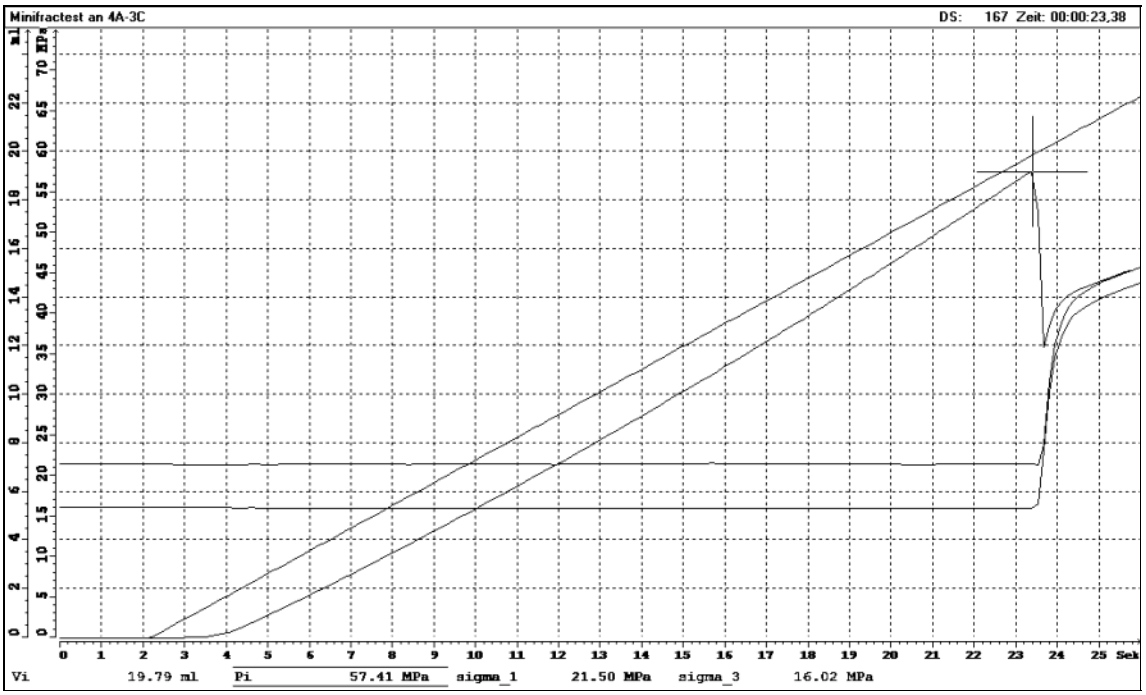

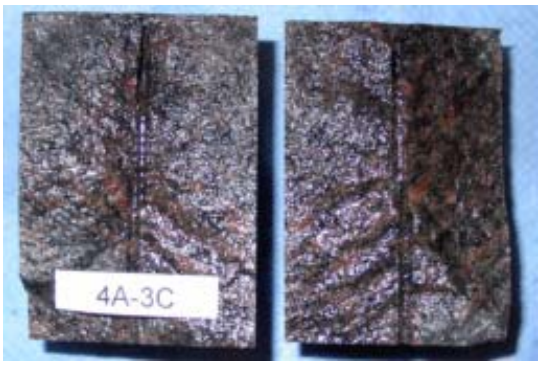

Sample no.: 4A-4A

operator	Küperkoch
date	27.08.04 11:50-12:10

mean depth, m	527.63
axial load σ_1, MPa	61.09
confining pressure σ_3, MPa	28.30
breakdown pressure p_c, MPa	72.71
injection fluid	TELLUS32
injection rate, ml s^{-1}	1
remarks	axial and inclined fractured

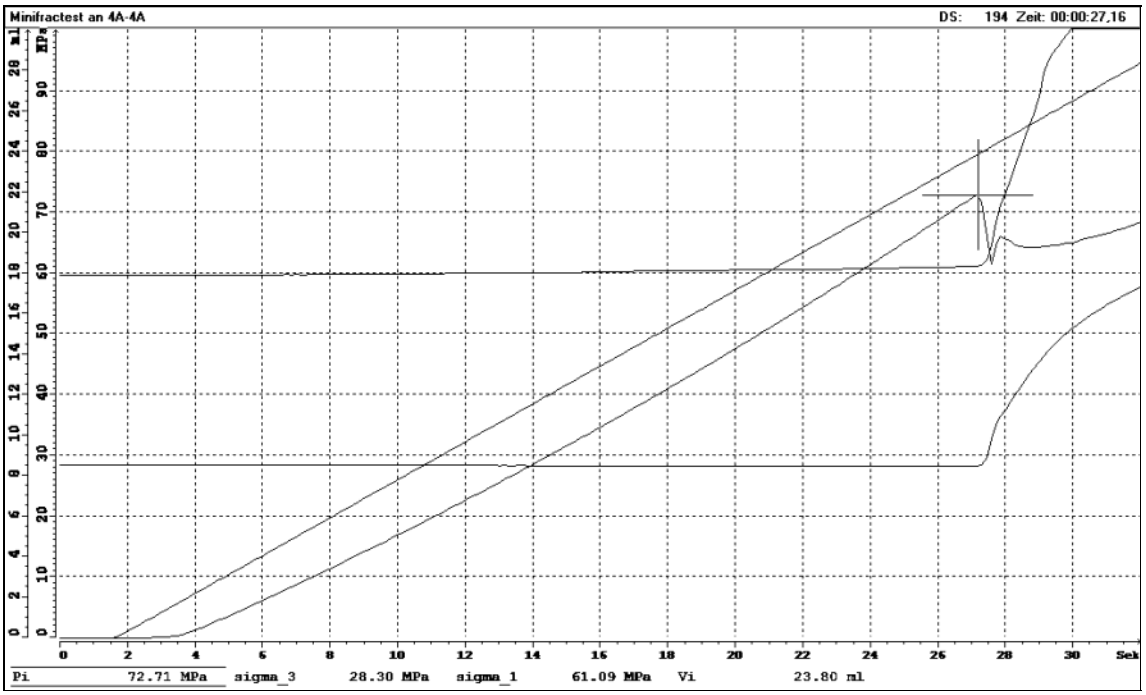

Sample no.: 4A-4C

operator	Küperkoch/Vogt
date	30.08.04 14:10-14:20

mean depth, m	527.63
axial load σ_1, MPa	27.40
confining pressure σ_3, MPa	14.66
breakdown pressure p_c, MPa	66.69
injection fluid	TELLUS32
injection rate, ml s^{-1}	1
remarks	axial fractured

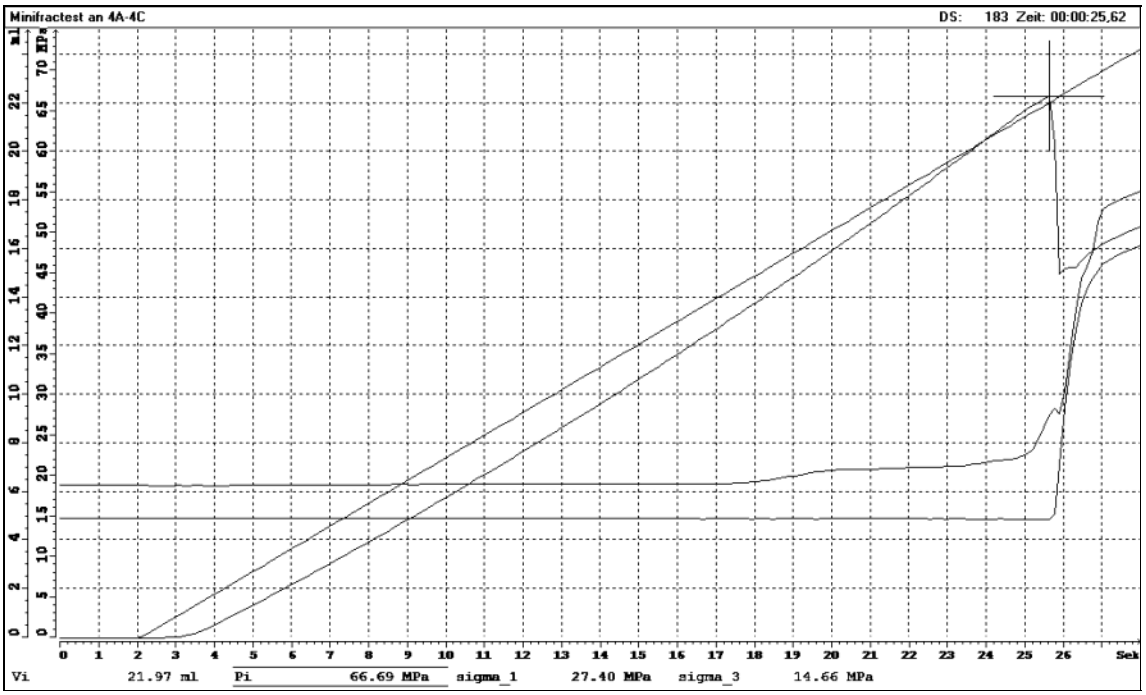

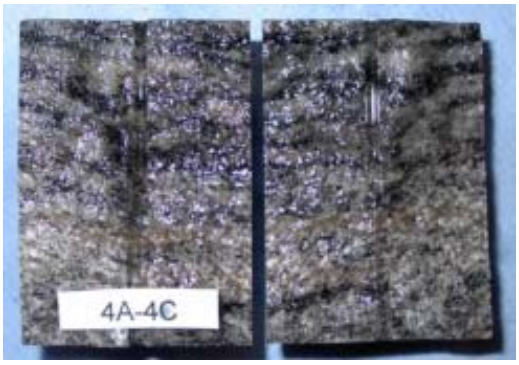

Sample no.: 4A-5A

operator	Küperkoch/Vogt
date	30.08.04 14:30-14:40

mean depth, m	527.97
axial load σ_1, MPa	29.11
confining pressure σ_3, MPa	12.06
breakdown pressure p_c, MPa	43.05
injection fluid	TELLUS32
injection rate, ml s^{-1}	1
remarks	axial fractured

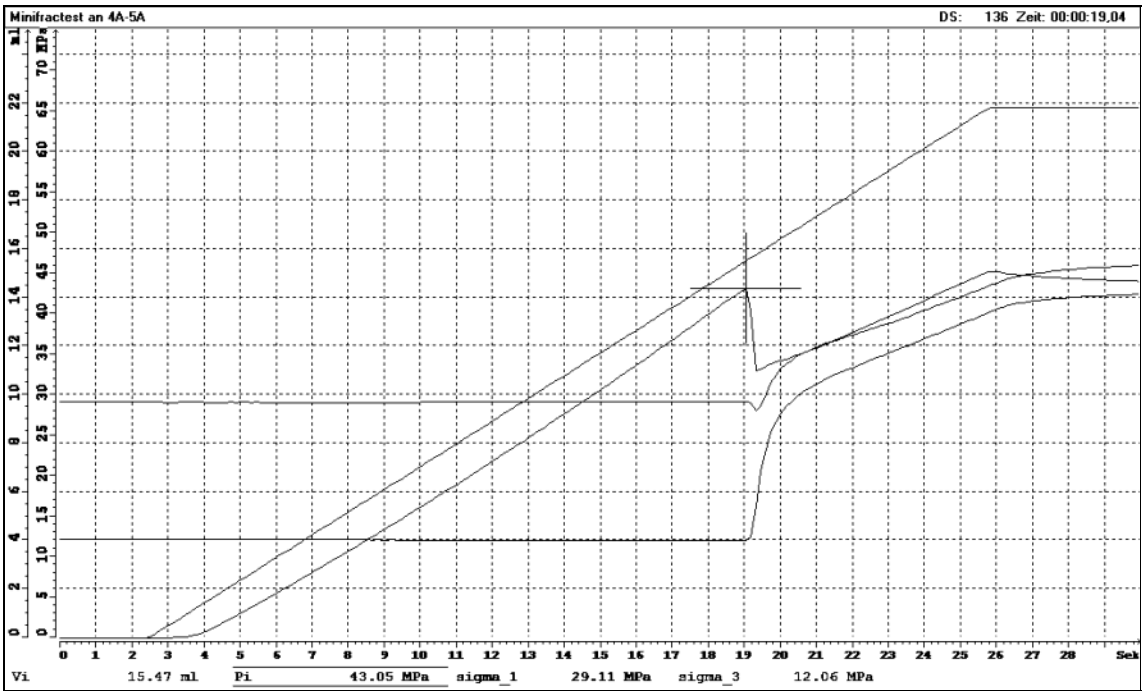

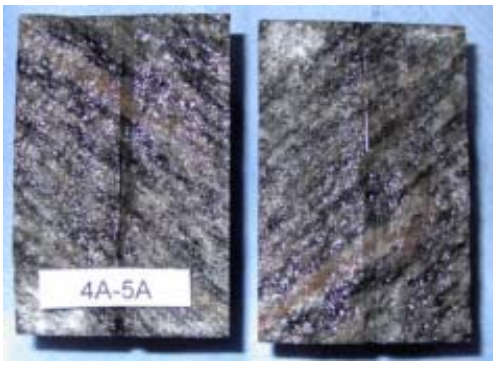

Sample no.: 4A-5C

operator	Küperkoch/Vogt
date	30.08.04 15:30-15:40

mean depth, m	527.97
axial load σ_1, MPa	18.35
confining pressure σ_3, MPa	9.80
breakdown pressure p_c, MPa	43.68
injection fluid	TELLUS32
injection rate, ml s^{-1}	1
remarks	axial fractured

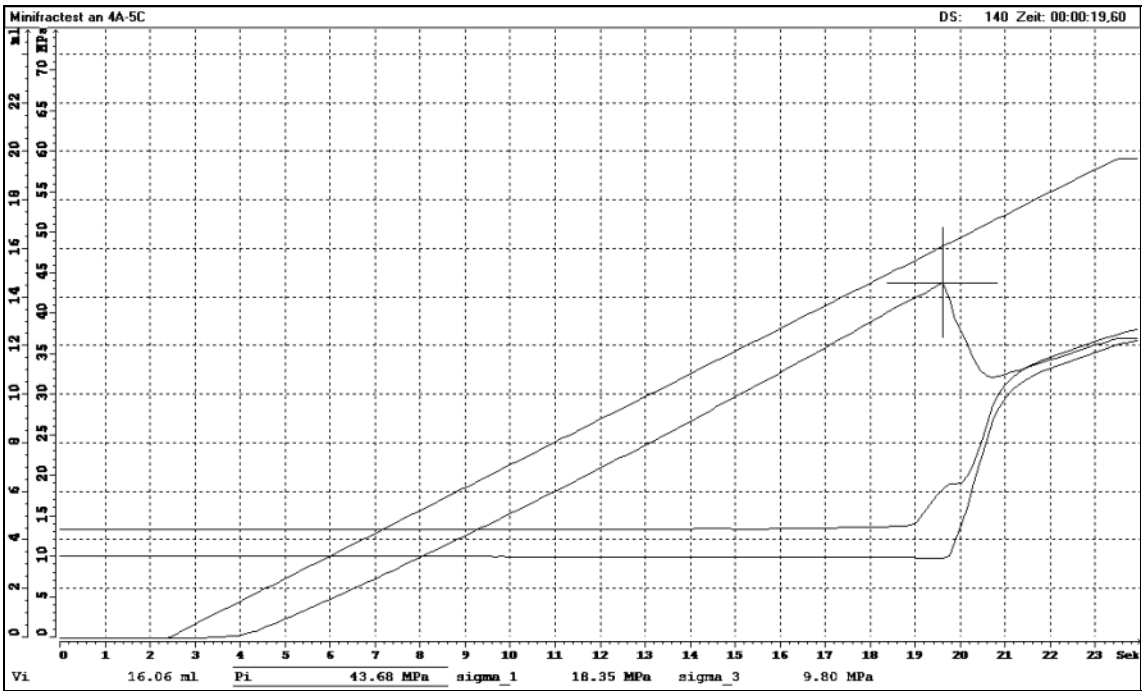

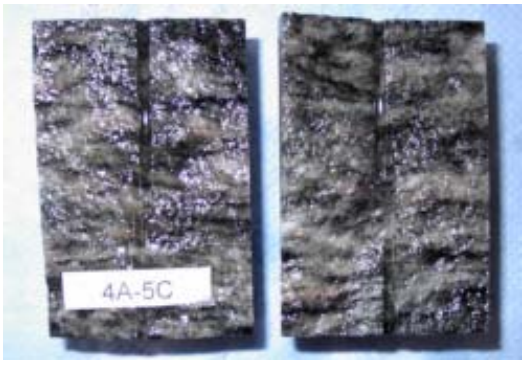

Sample no.: 4A-6A

operator	Küperkoch/Vogt
date	30.08.04 15:40-15:50

mean depth, m	528.38
axial load σ_1, MPa	61.09
confining pressure σ_3, MPa	28.30
breakdown pressure p_c, MPa	72.71
injection fluid	TELLUS32
injection rate, ml s^{-1}	1
remarks	axial and inclined fractured

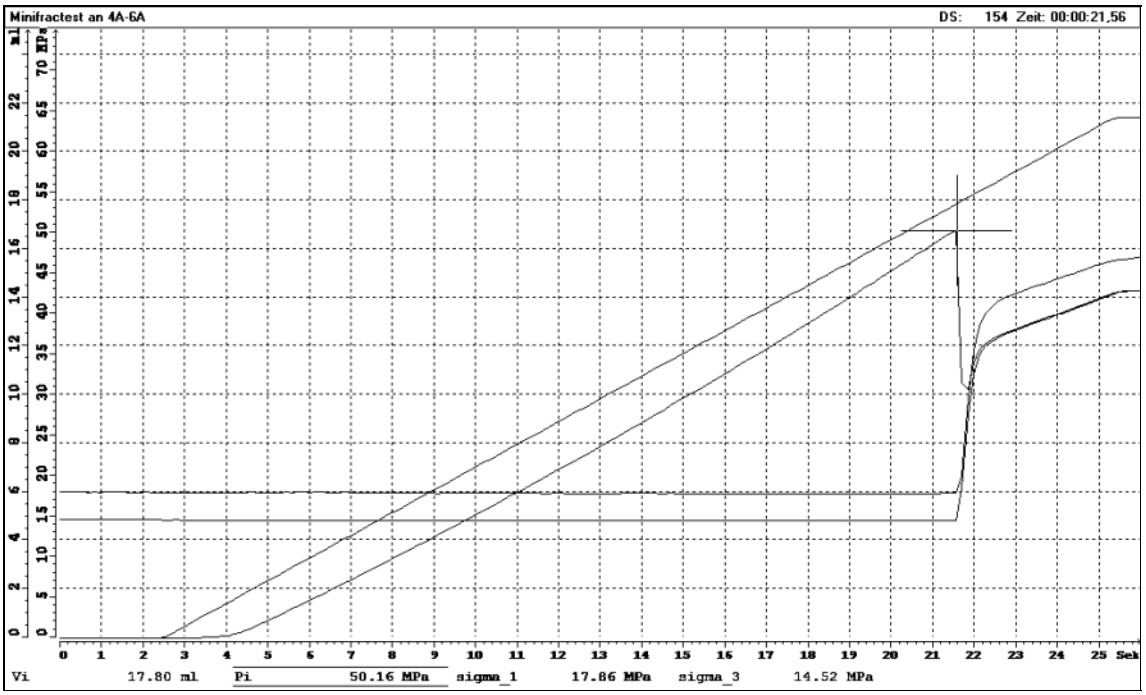

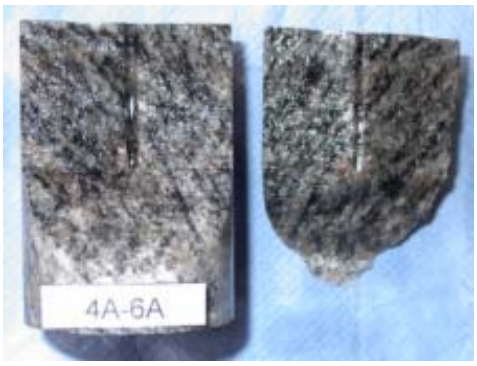

Sample no.: 4A-6C

operator	Küperkoch/Schreiner/Vogt
date	30.08.04 16:10-16:20

mean depth, m	528.38
axial load σ_1, MPa	34.46
confining pressure σ_3, MPa	29.84
breakdown pressure p_c, MPa	73.02
injection fluid	TELLUS32
injection rate, ml s^{-1}	1
remarks	axial fractured

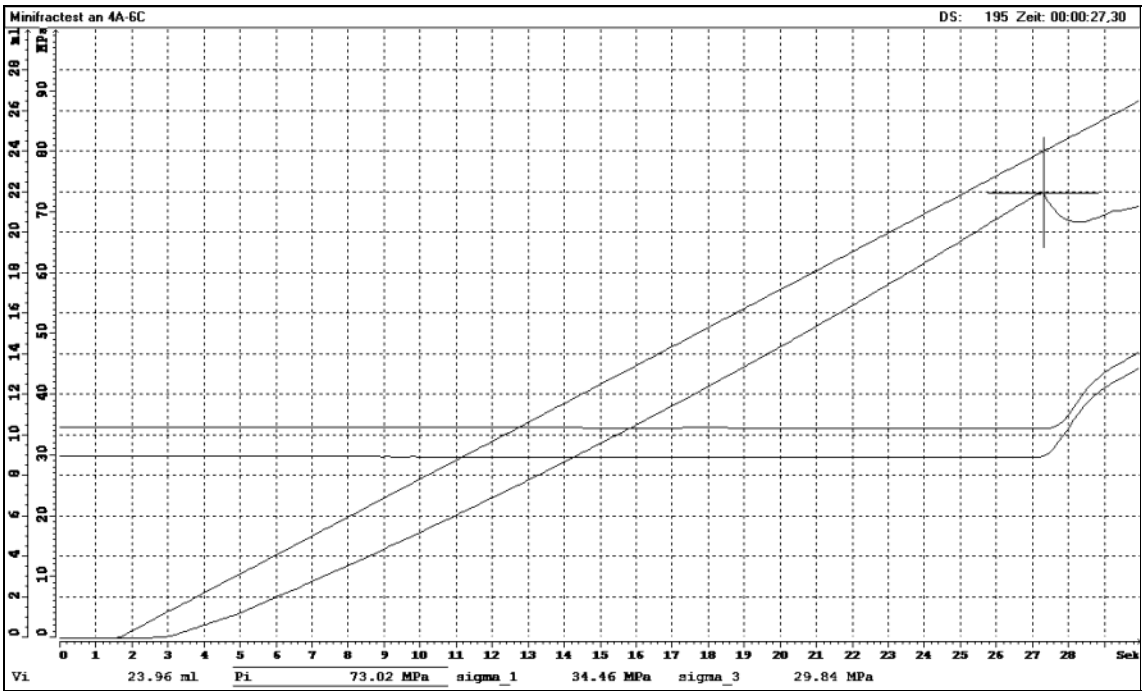

Sample no.: 4A-7A

operator	Küperkoch/Schreiner/Vogt
date	30.08.04 16:55-16:10

mean depth, m	528.79
axial load σ_1, MPa	14.34
confining pressure σ_3, MPa	8.43
breakdown pressure p_c, MPa	35.31
injection fluid	TELLUS32
injection rate, ml s^{-1}	1
remarks	axial fractured

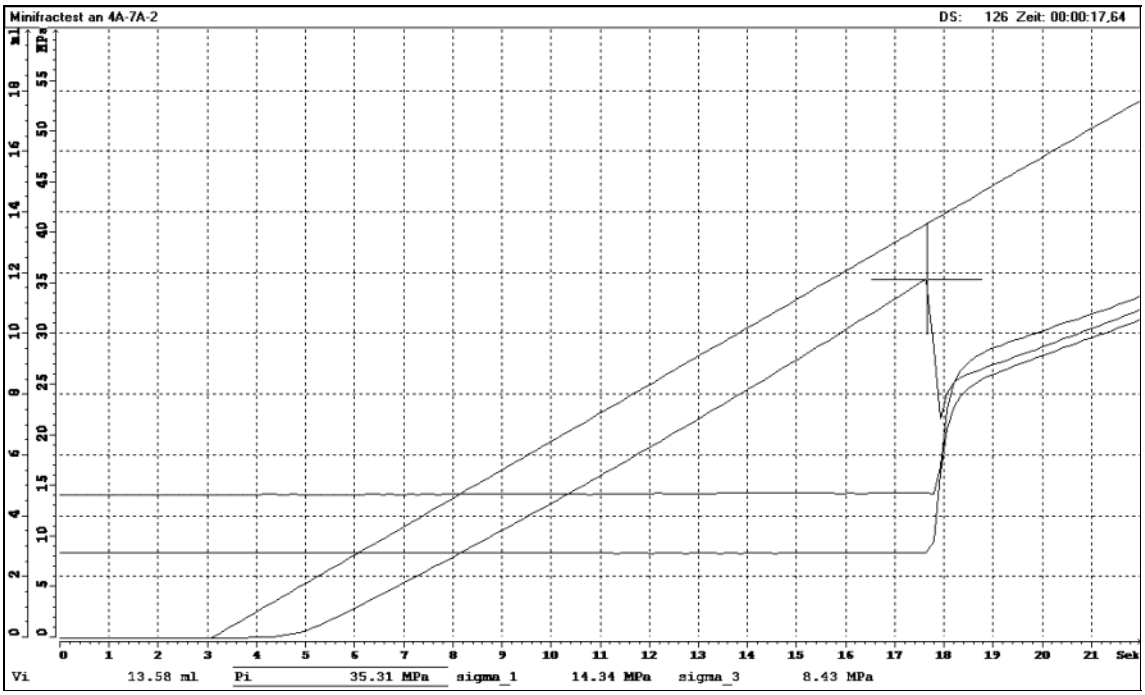

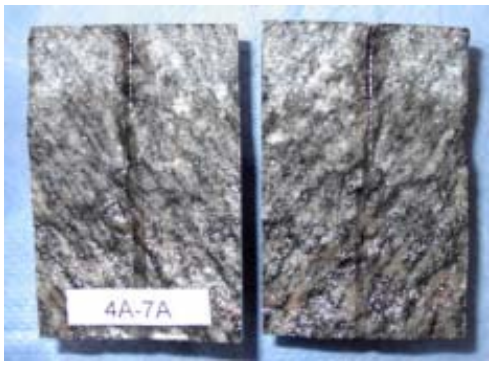

Sample no.: 4A-7C

operator	Küperkoch/Vogt
date	31.08.04 09:40-10:00

mean depth, m	528.79
axial load σ_1, MPa	16.79
confining pressure σ_3, MPa	6.85
breakdown pressure p_c, MPa	36.41
injection fluid	TELLUS32
injection rate, ml s^{-1}	1
remarks	axial fractured

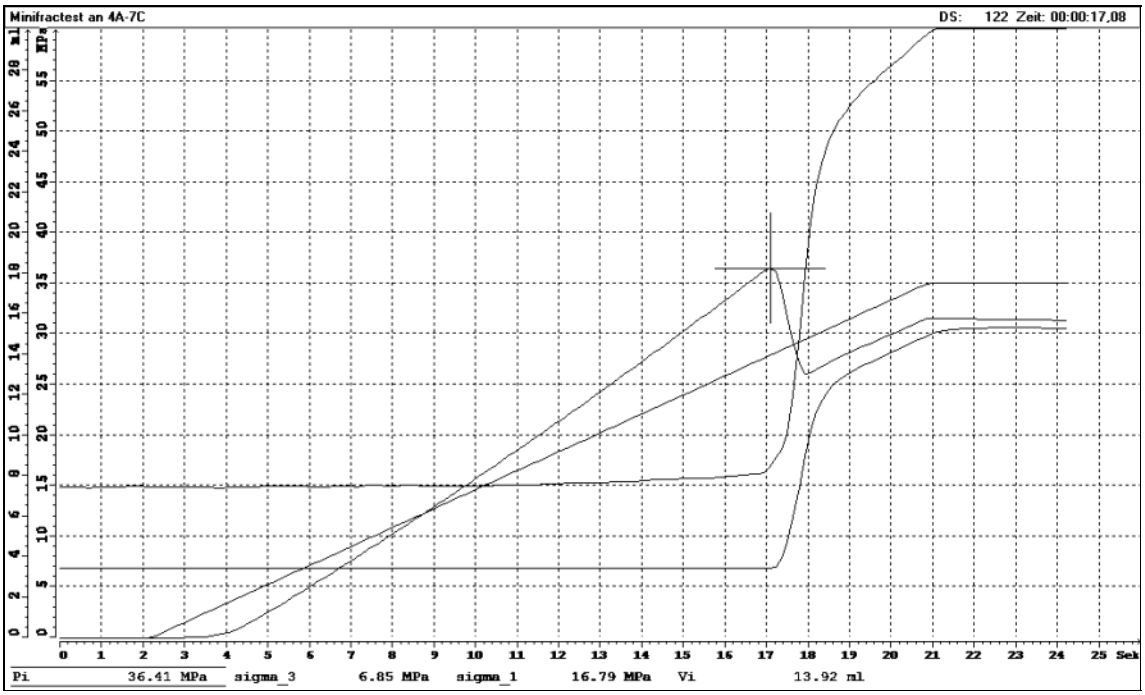

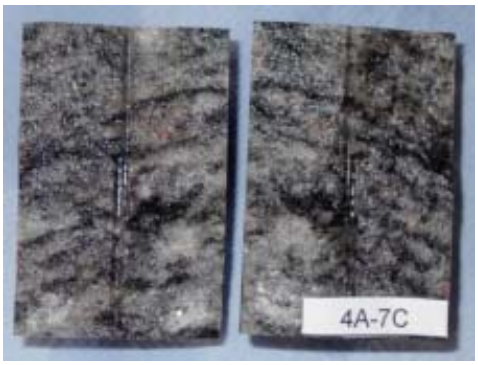

Sample no.: 4A-8A

operator	Küperkoch
date	27.08.04 10:10-10:20

mean depth, m	529.13
axial load σ_1, MPa	23.45
confining pressure σ_3, MPa	20.09
breakdown pressure p_c, MPa	51.21
injection fluid	TELLUS32
injection rate, ml s^{-1}	1
remarks	axial and inclined fractured

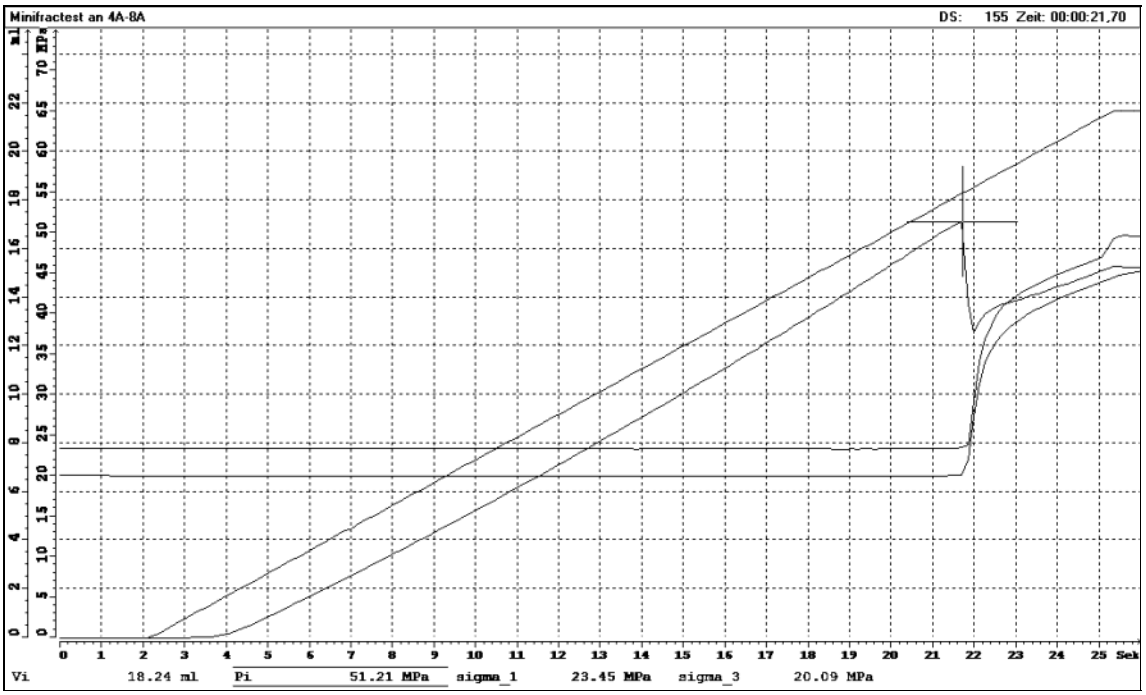

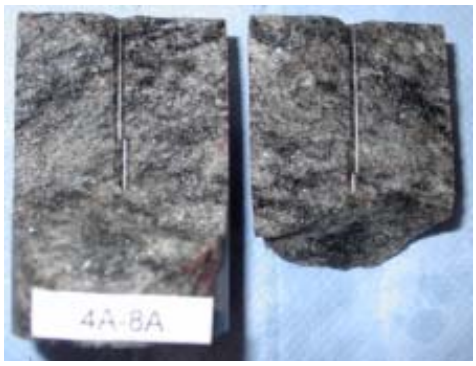

Sample no.: 4A-8C

operator	Küperkoch/Vogt
date	31.08.04 10:00-10:10

mean depth, m	529.13
axial load σ_1, MPa	35.98
confining pressure σ_3, MPa	32.81
breakdown pressure p_c, MPa	75.26
injection fluid	TELLUS32
injection rate, ml s^{-1}	1
remarks	axial fractured

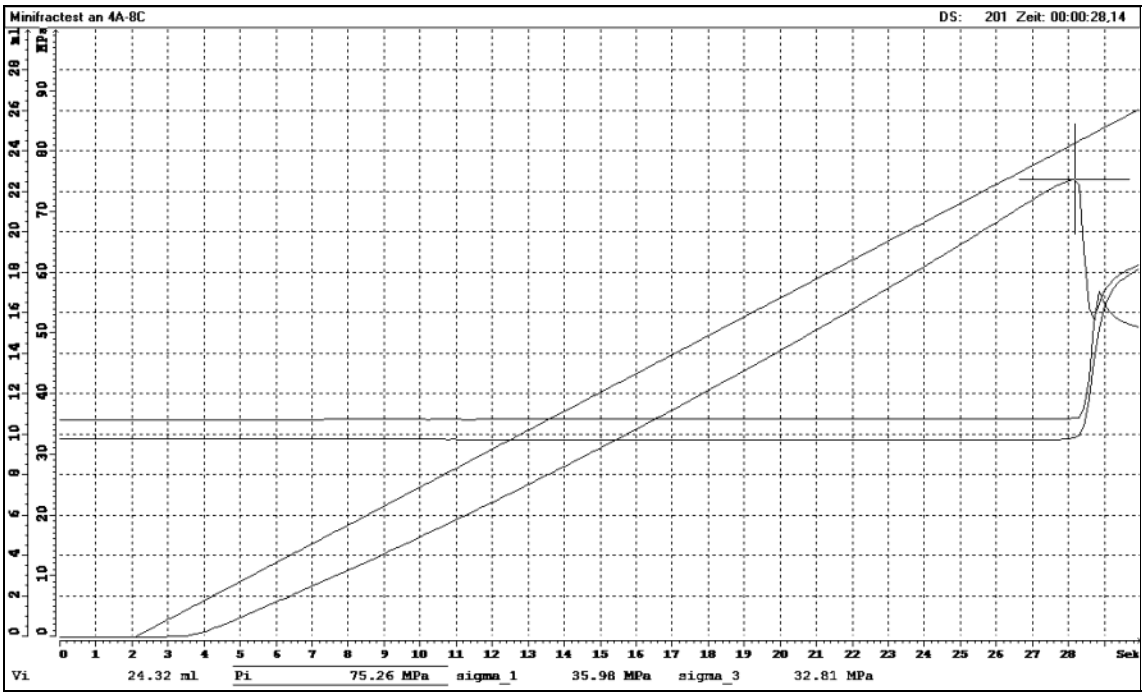

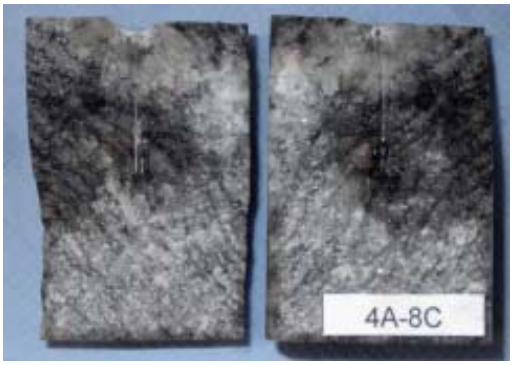

Sample no.: 4A-9A

operator	Küperkoch/Vogt
date	31.08.04 10:10-10:20

mean depth, m	529.47
axial load σ_1, MPa	23.75
confining pressure σ_3, MPa	20.56
breakdown pressure p_c, MPa	59.33
injection fluid	TELLUS32
injection rate, ml s^{-1}	1
remarks	axial fractured

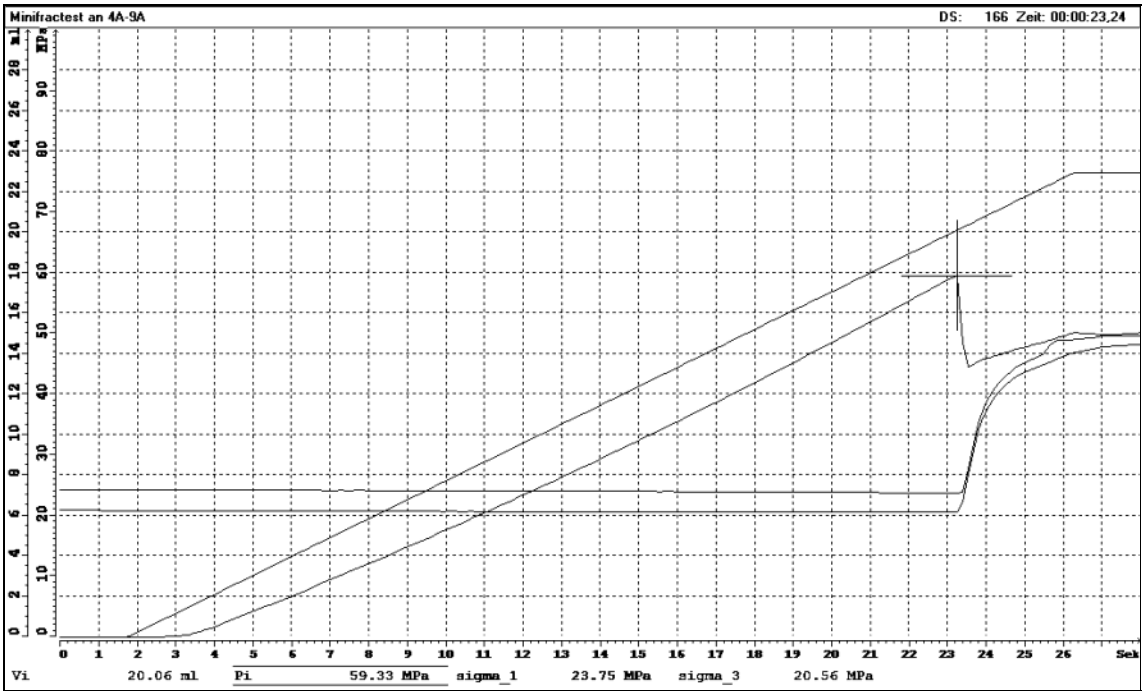

Sample no.: 4A-9C

operator	Küperkoch/Vogt
date	31.08.04 10:30-10:40

mean depth, m	529.47
axial load σ_1, MPa	16.20
confining pressure σ_3, MPa	13.45
breakdown pressure p_c, MPa	49.64
injection fluid	TELLUS32
injection rate, ml s^{-1}	1
remarks	axial and inclined fractured